Geocell – Sand Mattress Overlying Soft Clay Subgrade: Behaviour under Circular Loading

A Thesis Submitted
in Partial Fulfillment of the Requirements
for the Degree of

DOCTOR OF PHILOSOPHY

by

MINAXI RAI

Department of Civil Engineering
Indian Institute of Technology Guwahati
Guwahati – 781039, Assam, INDIA

January, 2010

CERTIFICATE

This is to certify that the thesis entitled **"Geocell-sand Mattress Overlying Soft Clay Subgrade: Behaviour under Circular Loading"** submitted by **Minaxi Rai** Roll No. 04610404 to the Indian Institute of Technology Guwahati, for the award of the degree of Doctor of Philosophy in Civil Engineering is a record of bonafide research work carried out by her under our supervision and guidance. The thesis work, in our opinion, has reached the requisite standard fulfilling the requirement for the degree of Doctor of Philosophy.

The results contained in this thesis have not been submitted in part or full to any other University or Institute for award of any degree or diploma.

Dr. Sujit Kumar Dash
Associate Professor
Department of Civil Engineering
Indian Institute of Technology Guwahati
Guwahati -781039, INDIA.

Date:

Dr. Teiborlang Lyngdoh Ryntathiang
Assistant Professor
Department of Civil Engineering
Indian Institute of Technology Guwahati
Guwahati -781039, INDIA.

Date:

STATEMENT

I do hereby declare that the matter embodied in this thesis is the result of investigations carried out by me in the Department of Civil Engineering, Indian Institute of Technology Guwahati, Guwahati, Assam, India.

In keeping with the general practice of reporting scientific observations, due acknowledgements have been made wherever the work described is based on the findings of other investigators.

Guwahati 781039

Date: (Minaxi Rai)

ACKNOWLEDGEMENTS

Throughout my thesis work, I have been associated with people whose contribution in assorted ways to the research and the making of this thesis deserve special mention. It is a pleasure to convey my gratitude to them all in my humble acknowledgment. I am deeply indebted to my supervisors Dr. S.K. Dash and Dr. T.R. Lyngdoh whose help, expert advice and encouragement helped me in all the time of research work and writing of this thesis. Their constant inspiration and guidance kept me focused and motivated. I would like to thank my Doctoral Committee members, Dr. S. Talukdar, Dr. K. D. Singh and Dr. D. Chakraborty for sparing their valuable time in reviewing my work.

I thank the former Heads of the Department, Dr. S. Talukdar, Dr. Anjan Dutta and the present Head of the Department, Dr. S.K. Deb for the facilities provided for conducting the research. I am also thankful to the scientific officers of Civil Engineering Department; Mr. K. Pallav and Mr. A. Borsaikia for extending all possible support. I gratefully acknowledge the unstinted help provided by Mr. Hari Ram Upadhyaya, Md. Bazal Hoque and Mr. Upen Gohain during all phases of my research work. Furthermore, I would like to thank the office staff of Civil Engineering Department for their support in administrative works.

My time at IITG was made enjoyable in large part due to many friends who became a part of my life - Ajanta, Albino, Alka, Chhabi, Cosmika, Dipti, Ines, Jasmini, Lipika, Trupti, Madhusmita, Monikankana, Monowar, Mukul da, Roshni, Rupak, Sandip, Shyam, Sumitra, Tanuja, Uday and Zela. I was touched by their friendly affection, timely help, and moral support during my stay at the institute. I especially owe Kamal a lot for keeping the faith and not letting me turn back. My sincere and heartfelt thanks to Jyotsna, Dipti, Kamal and their family for being the surrogate family during my stay at Guwahati.

I feel a lasting gratitude towards my school and graduation friends (Anisha, Arbin, Balli, Meena, Richard, Surender, Pawan, Vivek-Chhaya) who always kept me in their prayers.

It is not possible to express in words the inspirations from my grandmother, my parents, and Nikesh whose invaluable love, endless patience and unstinted support has brought me to this position. The concern and love of my relatives, cousins and family friends are highly appreciated. It is my grandfather who was my first teacher and it is to him that this thesis is dedicated. Lastly, I offer my regards to all of those who supported me in any respect during the completion of the project.

Minaxi

ABSTRACT

The soft soil often poses design, construction and maintenance hazards to civil engineering structures, so any development activities on such areas are generally avoided. However, the advancement of technology has led to the emergence of numerous ground improvement techniques that render such sites suitable for constructional purposes. Among others, soil reinforcement technique is a viable alternative to enhance the strength of the soft soils. The latest adaptation of this technique involves the use of geocell mattress which is a three dimensional, polymeric, honeycomb like structure interconnected at joints. The geocells provide an all round confinement to the material by virtue of their interconnected cells and prevent their lateral spreading on the application of load, thus resulting in a much stiffer material with higher load carrying capacity. Available literature on geocell reinforcement indicates that substantial improvement in performance can be obtained with the provision of geocell reinforced sand mattress over soft clay subgrade. However, the influence of various key parameters on the overall performance and behaviour of geocell-sand mattress reinforced clay subgrade system are not well understood.

Under the present investigation, a detailed parametric study through a series of experiments has been carried out to develop an understanding of the behaviour of the soft clay subgrade supported geocell-sand mattress system under circular loading. The influence of various parameters pertaining to geocell-soil configuration such as depth of placement of geocell mattress from the base of the footing, pattern of formation of geocells, pocket size of geocells, height of geocell mattress and relative density of the infill sand in geocells have been studied extensively in a systematic manner. Tests have also been carried out with an additional layer of geogrid placed at the base of the geocell mattress. The influences of the height of geocell mattress, pocket size of geocells and

relative density of infill sand on the overall performance of the geocell-geogrid composite system have been evaluated.

The results of the model load tests show that the stiffness and the load carrying capacity of the clay subgrade improve substantially with the provision of geocell reinforcement. The load carrying capacity of the reinforced foundation bed is found to be influenced by the depth of placement of geocell mattress, pocket size of geocells, height of geocell mattress and relative density of infill sand in geocells. Based on the analysis of the test data, the critical values of the geocell-sand mattress giving maximum beneficial effect are determined. The heaving on the fill surface is found to reduce due to increased confinement provided by the geocell reinforcement to the infill sand. The reduction is relatively more with geocell mattress of higher height and of smaller pocket sizes. An additional geogrid layer at the base of the geocell mattress further enhances the load carrying capacity of the foundation bed. The beneficial effect of the basal geogrid layer is, however, dependent on the pocket size of geocells, height of geocell mattress and relative density of the infill sand.

Multiple-variable regression analysis has been performed on the experimental data to develop models in order to predict the bearing capacity of the reinforced foundation bed as a function of various parameters that influence the bearing capacity. Dimensional analysis is carried out in an attempt to transfer the results of the model tests to the actual field conditions. It was found that, for the present test data to be valid in prototype case, the strength of the reinforcement in the prototype reinforced soil foundation bed should be N^2 times the strength of the reinforcement used in the model test, where N is the model scale.

Keywords: Bearing capacity, geocell reinforcement, model test, circular footing, reinforced sand, soft clay subgrade

Contents

TABLE OF CONTENTS

Table of Contents (continued) **Page**

Table of Contents (continued) **Page**

भारतीय प्रौद्योगिकी संस्थान गुवाहाटी
Indian Institute of Technology Guwahati

LIST OF TABLES

List of tables (continued) **Page**

List of tables (continued) **Page**

भारतीय प्रौद्योगिकी संस्थान गुवाहाटी
Indian Institute of Technology Guwahati

LIST OF FIGURES

List of Figures (continued) **Page**

List of Figures (continued) **Page**

List of Figures (continued) **Page**

List of Figures (continued) **Page**

List of Figures (continued) **Page**

List of Figures (continued) **Page**

List of Figures (continued)

Page

List of Figures (continued)

List of Figures (continued) **Page**

List of Figures (continued) **Page**

List of Figures (continued) **Page**

List of Figures (continued) **Page**

Figures (continued) **Page**

List of Figures (continued) **Page**

LIST OF PHOTOGRAPHS

भारतीय प्रौद्योगिकी संस्थान गुवाहाटी
Indian Institute of Technology Guwahati

GLOSSARY

Basal geogrid	geogrid provided at the base of the geocell layer
Bodkin	plastic strip used to connect geogrids in a geocell structure
Fill soil	soil filled in the geocell pockets
Pocket size	equivalent diameter of the geocell pockets

भारतीय प्रौद्योगिकी संस्थान गुवाहाटी
Indian Institute of Technology Guwahati

ABBREVIATIONS

ANOVA	Analysis of variance
ASTM	American Society for Testing and Materials
IF	Improvement Factor
BX	Biaxial geogrid
BPR	Bearing pressure ratio
CL	Clay with low plasticity
HPDE	High Density Polyethylene
SP	Poorly graded sand
USCS	Unified Soil Classification System

भारतीय प्रौद्योगिकी संस्थान गुवाहाटी
Indian Institute of Technology Guwahati

NOTATION

English Symbols

b	width of the geocell mattress
c_u	cohesive strength of the soil
C_c	coefficient of curvature
C_u	coefficient of uniformity
d	equivalent diameter of geocell pockets
df	degree of freedom
D	diameter of the footing
D_{10}	grain size corresponding to 10% finer
D_{30}	grain size corresponding to 30% finer
D_{50}	grain size corresponding to 50% finer
D_{60}	grain size corresponding to 60% finer
Dg	dial gauge
E_s	standard error
f	friction angle
G	shear modulus of soil
h	height of geocell mattress
H	height of sand layer
IF_s	improvement factor due to sand layer
IF_{gc}	improvement factor due to geocell reinforcement
IF_{bg}	improvement factor due to geocell reinforcement and additional basal geogrid
ID	relative density of sand
N	model scale
q_o	footing pressure on unreinforced clay subgrade
q_s	footing pressure on sand layer overlying soft clay subgrade
q_{gc}	footing pressure on geocell reinforcement bed
q_{bg}	footing pressure with additional basal geogrid
R^2	multiple coefficient of determination
R_a^2	adjusted value of R^2

s	footing settlement
S_r	degree of saturation
S_t	stiffness of reinforcement
u	depth to the top of reinforcement layer
x	distance from center of footing

Greek Symbols

δ_s	interfacial friction angle between geogrid and sand
δ	surface deformation (settlement/heave)
ϕ	angle of internal friction of the soil
σ_n	normal stress
σ_1	major principal stress
σ_3	minor principal stress (confining pressure)
ψ	dilation angle
γ	Unit weight of soil
γ_{dmax}	Maximum dry density
γ_{dmin}	Minimum dry density

CHAPTER 1

INTRODUCTION

1.1 BACKGROUND

The soft soil often poses design, construction and maintenance hazards to civil engineering structures founded on them. Problems may arise during the construction stage due to the inability of the soft soil to provide adequate support to the construction equipments. Post construction, the excessive settlement and insufficient bearing capacity of the soft subgrade may lead to loss of stability of the overlying structures. Rutting of pavements (Photo 1.1), rotational slip failure of embankments, cracking and differential settlement of buildings are some of the failures associated with construction of structures on soft soils.

Photo 1.1 Pavement failure due to weak subgrade

Various approaches adopted to mitigate the problems caused due to soft subgrade include provision of piled foundation, excavation and replacement with good quality soil, preloading with vertical drains, stone columns etc. The choice of the appropriate improvement method to be adopted for a particular site is governed mostly by technical, economical and ecological feasibility. Sometimes they may be the only alternative available. Therefore, there is still a huge scope for innovation in this area. Soil reinforcing technique is widely gaining acceptance as a viable alternative to other ground improvement techniques. The concept of earth reinforcement is not a new technique entirely. Man, has since centuries used various forms of soil reinforcement like bamboo, logs, timber planks to support roads and small embankments on soft soils. Many ancient structures incorporated natural materials like straw, reed and branches to reinforce the soil for construction of stable structures. However, the advent to systematic world-wide research in this area is attributed to Henri Vidal (1969), a pioneer on 'Reinforced Earth' technique. He is credited to have coined the term 'Reinforced Earth', a general term used nowadays to describe all forms of earth reinforcement. Over the years, there has been a significant increase in the use of reinforced soil technique as a preferred solution for many civil engineering problems. The cost effectiveness and versatility of the reinforced soil provides it a distinct advantage over alternative construction methods. Besides, the ease and speed of construction contribute in reducing the overall cost. The technology has made possible the use of problematic areas which were earlier deemed not suitable for constructional purposes. The use of these areas for infrastructural development would invariably give a huge boost in terms of both the economy and landuse. For several years, metal strips were used as a reinforcing material. However, the discovery and production of synthetic polymers or geosynthetics has added a completely new dimension to the soil reinforcing techniques. The flexible construction methods, reduced construction time and

competitive costs have made it an attractive alternative for the construction of foundation beds for pavements and heavy structures on soft soils, retaining walls, embankments, etc. The latest adaptation of this technique involves the use of geocell mattress, which is a three dimensional, polymeric, honeycomb like structure interconnected at joints.

A commercially available geocell structure is shown in Fig. 1.1. These types of geocells are made from strips of polymer sheets, ultrasonically welded together to form a mattress of interconnected cells. The geocell mattress is expanded at the site and filled with granular material as shown in Photo 1.2. They are mostly used for strengthening of road bases or heavy container yards, slope protection, river bank protection and retaining walls.

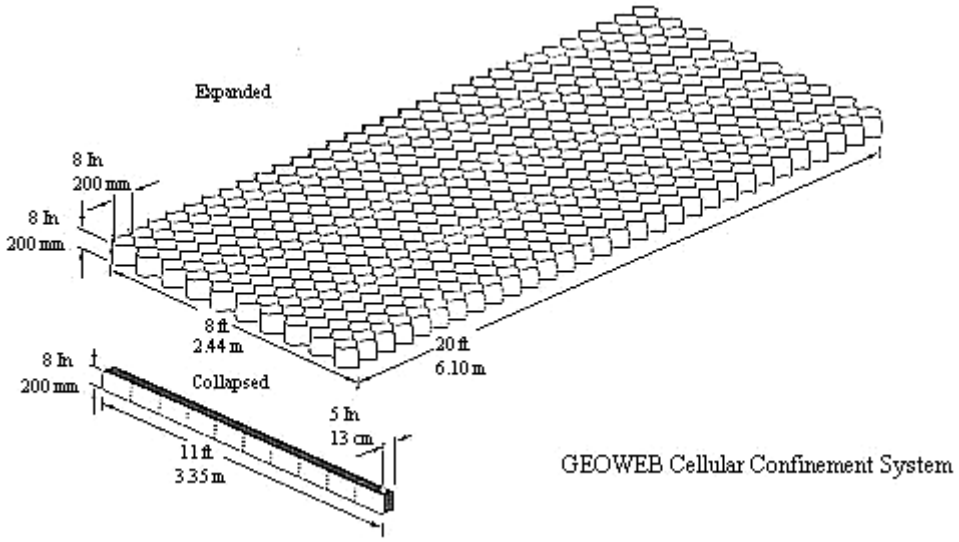

Fig. 1.1 Structure of a commercially available geocell (Bathurst and Knight, 1998)

Photo 1.2 Installation of geocell in the field (Emersleben and Meyer, 2008)

To enable constructions of embankments and roadways, foundations of liquid storage tanks and parking lots over deep deposits of extremely soft soil, a much deeper geocell mattress is required. The geocells for these purposes are assembled at the site from strips of geogrids cut to required size. The construction methodology is further described in the following section.

1.2 CONSTRUCTION OF GEOCELL FOUNDATION MATTRESS

Prior to construction of geocell mattress in the field, the site is cleared of all obstructions and the ground is leveled. The basal geogrid layer is unrolled onto the leveled ground in such a way that a minimum overlap of around 300 mm is maintained between adjacent rolls of basal geogrid layers. The overlaps are preferred over stitching to reduce construction time. Sheets of geogrids of required size are cut from long rolls to construct the three dimensional structure. After the laying of basal geogrid, a sheet of geogrid is laid in a transverse direction with one of its end stitched to the basal geogrid. The sheet is then rotated about the stitched edge to bring it to a vertical position and temporarily

tensioned using timber posts (Fig. 1.2). Similarly, a number of transverse sheets covering the entire area are laid out. The cellular structure is formed by placing another geogrid sheet between the two transverse sheets and connecting it to the transverse sheet using hooked steel bars or polypropylene 'bodkin joints' as shown in Fig. 1.3. The bodkin joint is formed by pulling the strands of transverse geogrid up through the diagonal geogrid and slipping a dowel through the loop created (Simac, 1990; Carroll Jr. and Curtis, 1990). The published pictorial views of bodkin joints (Simac, 1990; Carroll Jr. and Curtis, 1990) are depicted in Fig. 1.4 and Fig. 1.5. The construction of a typical geocell layer in the field is shown in Photo 1.3 and Photo 1.4.

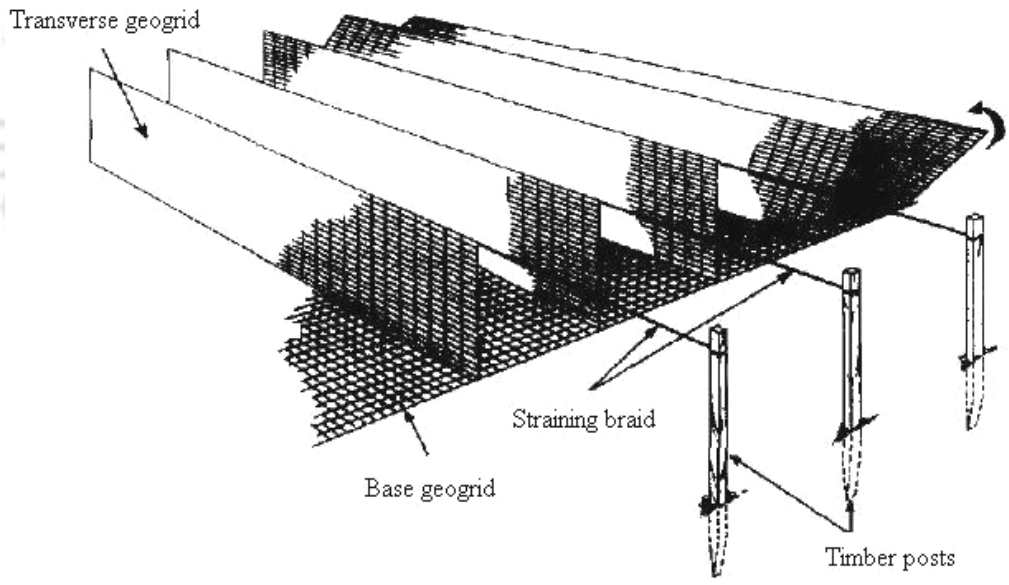

Fig. 1.2 Fabrication of geocell mattress (Bush et al., 1990)

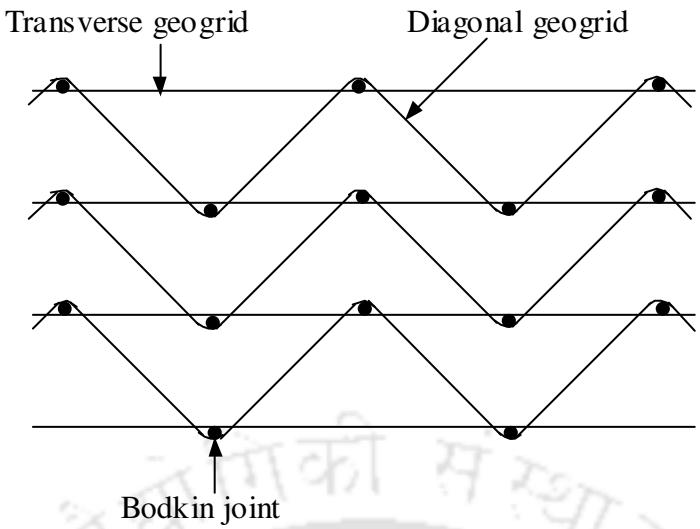

Fig. 1.3 Plan view of geocell mattress showing connections (Bush et al., 1990)

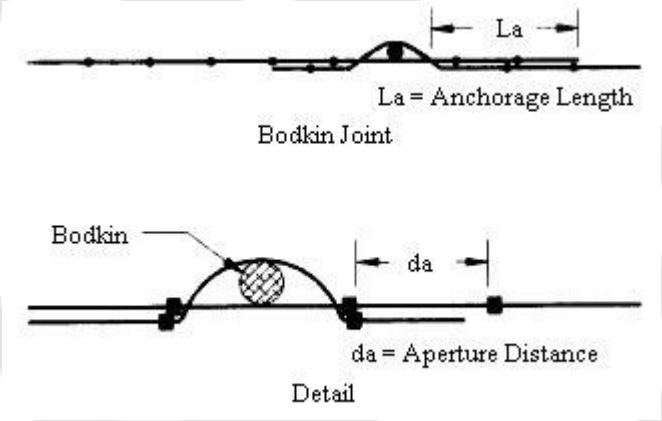

Fig. 1.4 Bodkin joint (Simac, 1990)

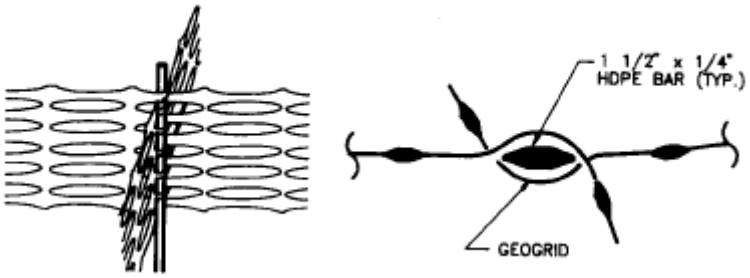

Fig. 1.5 Bodkin joint details (Carroll Jr. and Curtis, 1990)

Photo 1.3 Construction of geocell mattress in progress

Photo 1.4 Construction of geocell mattress nearing completion (Kawalec et al., 2006)

Filling of the cells can commence once sufficient number of cells are formed. Free draining granular materials are generally used as an infill for the geocell mattress. Materials are filled into the cells, taking care to fill the first two rows of cells to half of its height and then the first row to its full height. This filling sequence is continued, always

ensuring that no cell is filled to full height before the adjacent cell is atleast half filled. This technique is normally adopted to avoid any distortion of the cellular structure. It is suggested to place a minimum fill of about 75 mm over the geocell mattress to act as a cover and thus to prevent the damage of the vertical cell walls.

1.3 MECHANISM OF GEOCELL REINFORCEMENT

The geocell reinforcement, due to its three dimensional configuration provides an all-round confinement to the infill soil (Fig. 1.6) that prevents the lateral spreading of the soil. This results in a stable and strong composite structure which redistributes the additional pressure acting on the structure to a wider area thereby reducing the pressure on the underlying soft soil. On the application of load, the footing induces pressure in each cell of the geocell. This pressure is restricted by the passive resistance offered by the soil in the cells, cell walls and joints. Such a resistance would lead to a triaxial state of confinement to the soil and hence result in an increase in shear strength. In addition to this, the geocell walls intersect the potential failure planes and their rigidity forces them to pass vertically deeper into the soil leading to higher load carrying capacity.

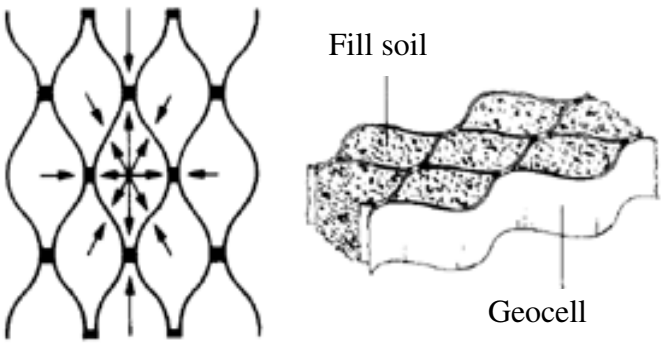

Fig. 1.6 Soil confinement by geocell reinforcement

1.4 OBJECTIVE OF THE PRESENT STUDY

The objective of the present study is to develop an understanding of the performance and behaviour of geocell-sand mattress reinforced soft clay subgrade, under circular loading.

1.5 ORGANISATION OF THE THESIS

In Chapter 2 an extensive literature review relevant to the present study is presented and consequently the scope of work has been brought out. Chapter 3 describes the materials used and their characterization, details of model test setup, planning of experimental programme and the test procedure. Chapters 4, 5 and 6 present and discuss the details of results obtained from the load tests. Chapter 4 presents and discusses the results of the tests done on soft clay subgrade alone and on sand layer overlying soft clay subgrade. The influence of relative density and height of the sand layer are investigated and presented in this chapter. In Chapter 5, results of the tests carried out with geocell reinforcement are presented. The influence of various parameters such as patterns of formation, depth of placement from the base of the footing, pocket size, height of geocell mattress and the relative density of infill sand on the overall performance of the reinforced structure are presented. Chapter 6 discusses the results of the load tests done using a layer of planar reinforcement (basal geogrid) along with the geocell mattress over soft clay subgrade. The influence of the basal geogrid is brought out in this chapter. Details of multiple regression analysis performed on the experimental data and dimensional analysis which bring out the scale effects are presented in Chapter 7. Chapter 8 summarizes the results obtained and major conclusions drawn from this research work.

भारतीय प्रौद्योगिकी संस्थान गुवाहाटी
Indian Institute of Technology Guwahati

CHAPTER 2

REVIEW OF LITERATURE AND SCOPE OF THE PRESENT STUDY

2.1 INTRODUCTION

This chapter presents a review of the previous research works done by various investigators in the area of reinforced earth beds. It has been divided into two main sections dealing with planar reinforcement and geocell reinforcement separately. The literatures in each of these sections have further been summarized under various heads depending on the test conditions.

2.2 STUDIES WITH PLANAR REINFORCEMENT

2.2.1 Sand bed reinforced with horizontal tensile reinforcement

Binquet and Lee (1975) conducted a series of model tests on strip footing placed on sand reinforced with aluminum foils of 0.013 mm thickness and 13 mm width. Three types of foundation conditions were varied in the study: (i) a deep homogeneous sand bed, (ii) sand above deep extensive layer of soft soil and (iii) sand above a deep finite pocket of soft material. The vertical spacing between the reinforcement layers were kept constant at one-third of the footing width for all the tests. The depth to the first reinforcement layer from the base of the footing was kept at one-third of the footing width for most tests except for one series where it was varied between 0.33 to 1.67 times the width of the footing. It was observed that the stiffness as well as the strength of the foundation bed increases with the increase in the number of reinforcing layers. They found that in order to achieve significant improvement in bearing capacity, the reinforcements should be placed between 1.3 to 2 times the footing width, from the base of the footing. This is in

agreement with the bearing capacity theories which state that the failure surface below strip footings extends to about 1.5 to 2 times the footing width. They also observed that by placing the first layer at a depth of 0.3 times the footing width, the performance improvement is maximum. Also they observed that, with the provision of planar reinforcement layers, the bearing capacity of the sand bed could be improved by a factor ranging from 2 to 4.

Akinmusuru and Akinbolade (1981) performed laboratory model tests where they studied the influence of vertical and horizontal spacing of reinforcement, depth to top reinforcement layer and the number of layers of reinforcement on the load carrying capacity of the reinforced soil beds. A locally available flat strips of rope fibre material called 'iko' having dimensions 1000 mm × 100 mm × 0.03 mm was used as the reinforcing material. The length of the reinforcement was kept constant at 10 times the footing width for all of the tests. Based on the results of the tests that they carried out, the maximum improvement in bearing capacity was observed when the top layer of reinforcement was placed at a depth of 0.5 times the footing width, below the footing. They also observed that there is a decrease in the performance when the top reinforcement layer was placed at a distance of less than 0.5 times the footing width which was attributed to the small overburden that could not effectively impart adequate pullout capacity to the reinforcement layers leading to early failure. The improvement in bearing capacity was found to be negligible beyond an influence depth of 1.75 times the footing width. For both horizontal and vertical spacing, the bearing capacity upto a spacing of 0.5 times the footing width was almost the same; beyond which, due to the block action, there was a drop in the bearing capacity. The maximum improvement in bearing capacity was found to be 2.9 times the ultimate capacity of the unreinforced sand.

Fragaszy and Lawton (1984) investigated the influence of soil density and reinforcing strip length on the load-settlement behaviour of the reinforced sand. The model footing used was a rectangular steel plate and the reinforcing material was aluminum strips of 25.4 mm width and 0.0254 mm depth. The performance improvement was quantified through the factor bearing capacity ratio (BCR) which is defined as the ratio of footing pressure with reinforcement at a given settlement to footing pressure without reinforcement at the same settlement. The test results showed that when the BCR was calculated at a settlement ratio of 10% of the footing width, there was no effect of soil density. However, when the BCR was calculated at a settlement ratio of 4%, there was an improvement in bearing capacity with the increase in the density of the sand. The increase in the length of the reinforcement beyond 7 times the footing width resulted in only marginal improvement in the bearing capacity.

Guido et al. (1986) conducted laboratory model tests where they compared the performance of geogrid and geotextile reinforced earth slabs. A square footing of side 305 mm width was used in the tests. The parameters investigated were: depth below footing to the first reinforcement layer; vertical spacing of the reinforcement layers; number of reinforcement layers; width of the square sheet of reinforcement and its tensile strength. They observed that the geogrid performed better than the geotextiles due to better interlocking of soil particles within the geogrid apertures. The improvement was observed to increase with reduction in the aperture size. The bearing capacity of the soil bed was found to increase by a factor of about 2.8 times with the inclusion of the geogrids.

Huang and Tatsuoka (1990) carried out a series of plain strain model tests on sandy ground reinforced with planar tensile material. The influence of length, pattern, rigidity and rupture strength of the reinforcement were studied systematically. It was observed

that by reinforcing the soil in the zone immediately below the footing with reinforcement layers of length just equal to the width of footing, a visible increase in bearing capacity could be obtained. They identified two mechanisms which describe the increase in bearing capacity of a reinforced soil bed – deep footing mechanism and wide slab mechanism. The reinforced zone behaved as part of a deep footing when densely reinforced. The effect of restraining the potential tensile strains was found to be largest beneath the footing and the reinforcement larger than the width of footing only contributed in a secondary manner. The effective length of the reinforcement beyond which negligible change in strain fields was noticed was 2 times the footing width. They also found that the influence of stiffness of the reinforcement was negligible unless the reinforcement failed by rupture.

Khing et al. (1993) conducted laboratory model tests on strip foundation supported by sand layer reinforced with layers of geogrid. The parameters evaluated were the location of the top layer of the reinforcement measured from the bottom of the foundation, the depth of the reinforcement zone, number of reinforcement layers and the width of each reinforcement layer. The maximum improvement in bearing capacity was obtained when the ratio of the depth of first reinforcing layer to the foundation width was less than 1 (one). It was reported that reinforcements placed below the foundation at a depth of more than 2.25 times the foundation width did not contribute to any increase in bearing capacity. The minimum width of the geogrid layers to achieve maximum benefit was found to be 6 times the width of the foundation. An increase in the BCR by a factor of 4 could be obtained by providing 6 layers of geogrids. The BCR calculated for a limited settlement ratio (i.e. at settlement of 25%, 50% and 75% of the ultimate settlement) was observed to be approximately 67-70% greater than the ultimate BCR. They also observed

that the calculation of BCR based on limited settlement rather than ultimate bearing capacity was more appropriate for the design of foundations.

Omar et al. (1993) investigated the influence of width to length ratios of rectangular foundations supported by geogrid-reinforced sand on the ultimate bearing capacity. Four different model footings with varying width to length ratios were used. The results indicated that the critical depth of reinforcement decreases with the increase in the ratio of width to length of the footing. They found the decrease to be 2 times the width of footing for strip footing and 1.2 times the width of footing for square footing. For a given optimum layout of the reinforcement, the maximum BCR was found to decrease with the increase in the ratio of width to length of the foundation. Based on the test data, empirical equations to calculate critical parameters of the reinforcement were proposed.

Das and Omar (1994) studied the effect of foundation width and relative density of sand on the bearing capacity of sand beds reinforced with geogrid. Six different sizes of strip footing of widths 50.8 mm, 76.2 mm, 101.6 mm, 127 mm, 152.4 mm and 177.8 mm with a constant length of 304.8 mm were studied. They observed that for a given relative density of sand, BCR decreased with the increase in the width of the foundation and reached an approximately constant value for widths of foundation greater than about 130-140 mm. For a given value of footing width, the magnitude of BCR increased with the decrease in the soil relative density.

Yetimoglu et al. (1994) investigated the performance of rectangular footing on single layer and multi layer geogrid reinforced sand beds. Model load tests as well as finite element simulations were carried out. The results indicated an optimum depth of placement of first geogrid reinforcement from the base of the footing to be at 0.3 times the width of footing for a single layer reinforced sand bed and 0.25 times the width of

footing when the sand was reinforced by multiple layers. They concluded that the maximum benefit was obtained when the vertical spacing between the reinforcements was 0.2 times the footing width. An increase in BCR was observed with the increase in reinforcement size upto 4.5 times the width of the footing and for reinforcement stiffness of about 1000 kN/m, beyond which further improvement was marginal.

Adams and Collin (1997) performed large scale model tests on geosynthetic reinforced soil foundation using four different sizes of square footing. The sand was reinforced by a biaxial geogrid and geoweb manufactured from extruded high density polyethylene sheets. The results indicated that the use of geosynthetics increased the ultimate bearing capacity of the footings on sand. The improvement in BCR was more significant when 3 layers of geogrid were used. They noticed that the maximum benefit was obtained when the top layer was within a depth of 0.25 times the footing width from the base of the footing. They also observed that when the sand was reinforced with single layer of geogrid, a higher improvement was found in case of densely compacted sand. The authors compared the performance of geogrids to geoweb based on the cost of the material per square meter. The investigators found that the 3 layered geogrid system performed better than geoweb. This difference was attributed to the difference in the mechanisms and the geometry of the two reinforcing materials.

2.2.2 Sand bed with horizontal tensile reinforcement underlain by clay

Love et al. (1987) carried out small scale model tests as well as analytical simulation to determine the effectiveness of geogrid reinforcement placed at the interface between granular fill and clay subgrade. The subgrade strength and the height of the fill were varied in the study and monotonic load was applied through a rigid footing under plain strain condition. Both analytical and experimental results indicated that the geogrid

reinforcement reduced the shear stresses transferred to the clay surface. The amount of reduction of stresses on top of the subgrade is dependent upon the strength of the subgrade and the thickness of the fill. The deformation of the subgrade and geogrid reinforcement was measured from photographs to establish the failure mechanism for the unreinforced and reinforced foundation bed. The observations indicate that for better performance at small deformations, a stiffer reinforcement would be preferable as they would effectively sustain the tension induced by the shear stresses. The membrane action of the reinforcement became significant only at large deformations.

Kim and Cho (1988) performed laboratory model tests on strip footing placed on sand bed underlain by weak clay. Reinforcement in the form of geotextile was placed at the sand-clay interface. The influence of the depth of the geotextile layer below the footing and the footing embedment ratio were investigated. They observed that there was an increase in bearing capacity of the footing with the decrease in the distance of the geotextile layer from the footing base. Similar response was observed with increase in the embedment depth of the footing. Maximum improvement due to geotextile reinforcement was obtained when the overlying sand layer thickness was kept between 0.5 to 1 times the width of the footing.

Khing et al. (1994) studied the load carrying capacity behaviour of a model strip foundation placed on a strong sand layer underlain by a weak clay foundation reinforced with a single layer of geogrid at the sand-clay interface. Two types of biaxial geogrids were used as the reinforcing material. The relative density of sand and the shear strength of clay were kept constant throughout the test program. The results indicate that to obtain maximum benefit from geogrid reinforcement, the height of the sand layer should be two-

third of the width of the foundation. The optimum width of the geogrid required to mobilize the maximum bearing capacity was found to be 6 times the footing width.

Das and Khing (1994) conducted laboratory model tests on a strip foundation supported on a strong sand layer underlain by a weak clay layer with a layer of geogrid at the sand-clay interface. The clay bed had a continuous rectangular void located immediately below and parallel to the centre line of the foundation. The thickness of the overlying sand was kept at optimum as obtained earlier by Khing et al. (1994). They observed that the performance improvement in terms of increase in the bearing capacity due to the geogrid reinforcement initially increased with the increase in the depth of the void from clay surface and reached a maximum value at a depth of about 0.8 times the footing width beyond which the performance improvement continued to decrease and reached a constant value at a depth of around 2.5 times the footing width.

Alawaji (2001) presented the results of laboratory model tests on circular foundation supported by geogrid reinforced sand layer overlying a collapsible soil. The reinforcing action was attributed to the interlock created between the grid and the sand particles. This interlock enables the grid to resist horizontal shear stress from the applied load thereby mobilizing the maximum bearing capacity of the subsoil. The increase in the stiffness of soil allows the vertical pressure to be distributed more evenly thus reducing the settlement in the process. To obtain maximum benefit from the inclusion of reinforcement, he recommended the placement depth of geogrid as 0.1 times the footing diameter (D) and a geogrid width of 4D. He concluded that using the reinforced sand bed instead of a thicker unreinforced sand bed reduces the cost of the subbase.

2.2.3 Clay bed with horizontal tensile reinforcement

Samatani and Sonpal (1989) carried out a series of load tests on metal strips reinforced compacted clay foundation. Their test results showed that the bearing capacity of the cohesive soils could be considerably increased by the introduction of metal strips. It was also observed that for a given density of reinforcement, increase in the length of reinforcement did not bring much increase to the bearing capacity. The extent of the failure as found by them was almost equal both for unreinforced soil and reinforced soil with different densities of reinforcement.

Mandal and Sah (1992) conducted laboratory model tests on square footings supported by geogrid reinforced clay. A single layer of geogrid was placed at different distance from the bottom of the footing. They observed that maximum BCR of about 1.36 was achieved when the geogrid was placed at a depth of 0.175 times the footing width from the bottom of the footing, beyond which it was found to decrease. They also observed that a maximum reduction of 45% in settlement occurred with the introduction of the geogrid at a distance of 0.25 times the footing width from the base of the foundation. The improvement in the bearing capacity of the reinforced foundation bed was attributed to the interlock at the soil-reinforcement interface.

Shin et al. (1993) performed laboratory model tests to evaluate the ultimate bearing capacity of a strip foundation placed on clay bed reinforced with layers of geogrids. The parameters evaluated were: the depth of the top layer of reinforcement below the footing, the width of the reinforcement and extent of geogrid reinforced zone. The test results showed that maximum benefit can be obtained when the first geogrid layer was placed at 0.4 times the footing width from the base of the foundation. The maximum width of the geogrid, beyond which there was very little increase in improvement was found to be 5

times the footing width and the depth of the reinforced zone for mobilization of the maximum bearing capacity was found to be 1.7 times the footing width.

2.3 STUDIES WITH GEOCELL REINFORCEMENT

2.3.1 Field Tests

Webster and Watkins (1977), Webster and Alford (1978) conducted full scale traffic field tests on rectangular aluminum grids filled with sand, placed over soft subgrade. A significantly higher load bearing capacity was observed in the reinforced case than with the compacted soil alone. The resilient grid deflections were less suggesting that the behaviour of the mattress resembled that of the slab. The performance of sand filled grid cells was found to be equal to a layer of crushed stone which is as much as 1.6 times thicker than the height of the cells. They found that under direct application of wheel load, the sand got displaced which lead to failure of the grid cells by buckling and bending. They also observed that when a cover of 2 inch gravel is provided over the sand filled cells, displacement of sand that lead to failure was prevented.

Johnson (1982) reported the use of geocell mattress at Greatham Creek Bridge, England. The mattress was placed under a 5 meter high embankment over soft estuarine silt which was 7 meter deep. The lateral strain reported was small and the vertical settlement was found to be reduced by 50%. The author attributed the reduction in settlement to the lateral restraint offered by the geocell material that prevents the material from spreading and hence reduces the stresses coming onto the soft subgrade.

De Garidel and Morel (1986) carried out field tests using reinforcement in the form of geotextile cells in soil subgrade. The geocells used had a cell width to depth ratio of 0.5 and 0.1. The reinforcing effect of the geocells was observed to be more at higher

displacement of the footing. They attributed this improvement to the soil densification that occurs at higher settlements, which in turn transfers the stresses more effectively and hence gives higher performance.

Robertson and Gilchrist (1987) reported the geocell mattress to be the most viable option for constructing a 4 meter high embankment over 4 meter deep soft silty clay having an average undrained shear strength of about 15 kPa. The cost comparison between the alternate options i.e. geocell mattress and the 'excavation and replacement' method, showed a cost saving of 31% in case of the former.

Bush et al. (1990) reported the construction of geocell foundation mattress supporting embankments over soft ground. The geocell mattress of 1 meter deep was fabricated directly on the soft soil making use of the geogrid and then filled with granular materials. The cellular structure was formed by placing a grid diagonally between two transverse diaphragms and connecting them with hooked steel bar. Apart from serving as foundation to support the embankment it also served as a drainage blanket for consolidation of the underlying soft soil. With this provision the bearing capacity of the weak soil was enhanced substantially and the differential settlement of the structure was remarkably reduced. This method was also found to be more cost effective than the traditional methods of constructions.

Khay and Perrier (1990) conducted laboratory and full scale tests to study the suitability of geocells in granular subgrade. Geocells of three different heights (i.e. 100 mm, 150 mm, 200 mm) having an aspect ratio (cell width to height ratio) of 0.5 were tested. It was observed that the reinforcement enhanced the trafficability of the pavement and reduced the settlement indicating that the geocell reinforced soil structure behaved as a composite slab.

Cowland and Wong (1993) took up a case study of a fully instrumented embankment of 10 meter height, supported by geocell mattress over soft clay deposit. The geocell mattress was fabricated, in the field, from polypropylene geogrid and filled with 25-mm down angular shaped rockfill. The performance of the embankment was monitored right from the construction stage by pneumatic piezometers, inclinometers, profile gauges, settlements plates, surface settlement markers and lateral movement blocks. They observed the lateral displacement to be in the order of 100 mm, which is relatively less, given the large height of the embankment and the soft soil below. They found the geocell mattress to undergo very little extension which suggests that the mattress behaved as a stiff raft foundation.

Gupta and Somnath (1994) used the concept of geocell in the construction of box culverts over marine clay deposits in New Bombay Area where the depth of the soft soil was more than 6 meters. The tubular gabions with their ends resting on hard moorum layer underlying the soft clay were constructed first. The geocell mattress was then constructed over the gabions. Thus the tubular gabions acted as granular piles and the geocell mattress as flexible pile cap, leading to substantial improvement in performance of the soft clay bed.

Koerner (1997) reported a case study wherein geocells made of high-density polyethylene (HPDE) strips were placed over soft subsoil surface and were filled with sand and compacted using a vibratory hand operated plate compactor. Subsequently, emulsified asphalt was sprayed on the top surface of geocell-sand mattress. The system supported tandem-axle truck loads of 230 kN for 10,000 passes with only slight rutting while subgrade without the geocell mattress system bogged down in deep ruts only after 10

passes. It is suggested that the enhanced performance is due to increased surcharge loading and higher density condition.

Forsman et al. (1998) reported a case study on the performance of geocell reinforced road over deep peat deposit. The geocells were constructed from Tensar SS30 and SR55 geogrids and the pockets were filled with light expanded clay aggregate. The performance of the test structure was monitored using vertical magnetic probe extensometers, horizontal hydrostatic profile gauges, settlement plates, horizontal extensometers and strain gauges. Plate load tests and falling weight deflectometer tests were conducted to measure the modulus of subgrade. The introduction of geocells was found to increase the bearing capacity and reduce the settlement of the structure. The differential settlement was reported to be negligible even after one and half years of construction.

Hendricker et al. (1998) reported the use of geocell mattress as a cover system for a hazardous waste site in South California. The site consisted of pits containing highly acidic organic compounds and oil based drilling muds. The geocells were fabricated from uniaxial geogrids and filled with sand. The geocell mattress provided better distribution of load unto the weak underlying layer by virtue of their stiffness. The chemical compatibility test results indicated that the geocell mattress had adequate stress resistance to the waste exposure.

2.3.2 Laboratory Model Tests

2.3.2.1 Sand bed reinforced with Geocells

Mitchell et al. (1979) carried out model tests on footings supported on sand beds reinforced with square shaped paper grid cells. This arrangement rested on a concrete floor so that it would be possible to back calculate the elastic modulus of the reinforced soil layer using the elastic theory solutions for homogeneous elastic layers overlying rigid

base. The diameter and height of the cell was varied over a wide range in order to study their influence. The test results indicate that geocell reinforcement can increase the elastic modulus of the soil layer by several folds. The provision of cover layer above the grid cells offered little improvement in terms of strength and modulus improvement but acted as a protective layer for the reinforcement.

Kazerani and Jamnejad (1987) performed laboratory scale load tests on geocells made of woven geotextiles placed over granular subgrade. The aspect ratio (width to depth ratio) of the cells was kept at unity. They observed that the stress-strain relationship is enhanced due to the confinement provided by the honeycombed structure. The hoop strength of the cell walls and the passive resistance offered by the adjacent cells contributed in increasing the stiffness and the load carrying capacity of the soil. They also observed that the resistance offered by the geocells to repeated loading increased considerably.

Shimizu and Inui (1990) carried out load tests on six-sided geotextile cell buried in loose sand bed. The test results indicate that even with single cell reinforcement the bearing capacity of soil bed can be increased substantially. For better performance, the geocell should have smaller width, larger height and higher stiffness. Through x-ray photography they observed that at relatively small settlement, the movement of the encapsulated soil was restricted by the cell wall. However at larger settlement the soil particles begin to pass under the cell, to the region outside, leading to a reduction in bearing capacity.

Dash et al. (2001a) conducted a series of laboratory model tests on strip footings supported on geocell reinforced sand beds. The various parameters studied were the height, width, pattern of formation, stiffness, pocket size, depth of placement of the geocell mattress and the density of the infill soil. With the provision of geocell reinforcement, failure was not observed even at a settlement equal to about 50% of

footing width and at a load as high as 8 times the ultimate capacity of the unreinforced one. They observed that a significant improvement in performance could be obtained with increase in geocell height upto 2 times the width of the footing, beyond which further improvement was marginal. The optimum aspect ratio (height to diameter ratio) of the geocell pockets which gives maximum improvement was found to be 1.67. They observed that geocell mattress with width 4 times the width of the footing intercepts almost whole of the rupture planes in the foundation soil. Also geocell mattress placed at a depth of 0.1 times the footing width below the footing gave maximum performance improvement. They found chevron pattern of formation of geocells to be more effective than the diamond pattern.

In continuation to the above study, Dash et al. (2001b) provided planar reinforcement along with the geocell reinforcement and the additional improvement in the bearing capacity of soil was evaluated. Three different series of tests with planar geogrid above the geocell mattress, planar geogrid below the geocell, planar geogrid and geotextile below geocell mattress were carried out. The results show that it is more beneficial to place the geogrid layer at the bottom as it provides additional improvement in terms of enhancement of bearing capacity and stability against rotation of the footing. They found that the beneficial effect of planar reinforcement decreases with increase in height of the geocell mattress as lower strains are mobilized in the basal reinforcement. The contribution to bearing capacity improvement was found to be negligible when the planar geogrid was placed above the geocell mattress. When geotextile layer was placed in between the geocell mattress and the basal geogrid layer, the overall performance reduced due to interception of interlocking of soil with the apertures of the geogrid.

Dash et al. (2003a) studied the behaviour of circular footing supported by geocell reinforced sand beds. The test results indicate that a substantial improvement in performance in terms of initial stiffness and ultimate bearing capacity of the foundation bed can be obtained with the provision of geocells. This improvement increased with the increase in the area of the reinforcement. They observed no heaving but instead the fill surface was found to settle. This indicates that the reinforced layer behaves as a slab which deflects under the loading area. The strain at the centre of the geocell layer (i.e. just below the footing) was found to be maximum and their magnitude decreased with the increase in the distance from the centre of the footing. The pressure distribution patterns on the sand subgrade showed that the geocell mattress redistributed the footing pressure over a wider area thus reducing its intensity over the subgrade layer, leading to an improvement of the overall performance.

Dash et al. (2004) compared the performance of different geosynthetics material by conducting model tests on sand beds under strip loading condition. The reinforcement was provided in the form of planar, geocell and randomly distributed mesh elements. The pressure-settlement response showed a failure in case of planar and randomly distributed mesh elements whereas there was no clear cut failure in case of geocell even at a settlement of 45% of the footing width. The planar layer was observed to deflect downwards when the soil underwent shear failure initiating a catastrophic failure whereas the geocell layer supported the load even after shear failure of the infill soil had occurred. They observed that in case of the randomly oriented reinforced bed, much of the strength of the reinforcement remains immobilised thereby giving low improvement. They also observed the geocell supported foundation bed to show less heave and the footing rotation was negligible as compared to the other forms of reinforcement which only suggest that it is the superior form of reinforcement among the three.

Dash et al. (2008) through a series of model tests studied the influence of various parameters such as geometry and position of geocell layer on the subgrade modulus aspect of the geocell-reinforced sand foundation beds. An eight fold increase in subgrade modulus was observed with the provision of the geocell reinforcement in the sand beds. The optimum height and width of the geocell layer beyond which the performance improvement was marginal was found to be 2 and 4 times the footing width respectively. The improvement in subgrade modulus was found to be maximum when the geocell mattress was placed at a distance of 0.1 times the foundation width from the base of the footing. A multiple regression analysis was performed on the test data to obtain a relationship between the effect of reinforcement in terms of subgrade modulus improvement factor and the parameters influencing the reinforcement benefit. The developed equation will be of use in effective utilization of the geocell reinforcement for performance improvement of sand foundations.

2.3.2.2 Geocells reinforced sand bed underlain by clay bed

Rea and Mitchell (1978) conducted laboratory static and repeated plate loading tests using paper grid cells as the reinforcing material. The cells were filled with sand and placed over springs which simulated the soft clay subgrade. The parameters investigated in the study are cell width, ratio of cell width to cell height and the subgrade stiffness. Based on the observations, different failure modes were identified i.e. cell penetration, cell bursting, cell wall buckling, bearing capacity failure, bending failure, durability failure and failure by excessive rutting. Under static load, maximum bearing capacity was obtained for a cell height to cell width ratio of 2.25. They concluded that in order to derive significant reinforcing actions of the geocell reinforcement system, the loading area must cover atleast one complete geocell. They found that the ultimate bearing capacity increases with

increase in the subgrade stiffness. The reinforced structure was observed to offer better resistance to repeated loading.

Bathurst and Jarrett (1988) undertook large scale model tests to study the load-deformation behaviour of cellular polymeric reinforcements placed over peat subgrade. They studied two types of reinforcement viz. geoweb which is the nonperforated plastic strips welded ultrasonically and geocell which is fabricated from geogrid and held together by metal bodkins. The infill material used was crushed limestone aggregate with a maximum particle size of 20 mm. The cellular confinement mechanism was more evident when single layer of reinforcement was used. Results of their studies showed that the geoweb-mattress is equivalent to about twice the thickness of the unreinforced section. They found stiffer geoweb composite to perform better than the less stiff geocell. The improvement in the bearing pressure occurred at a depth of 10 to 22 mm for both geoweb and geocells. However, the performance of geocells with a geogrid layer at the base was same as the one with a single layer of geogrid alone.

Mandal and Gupta (1994) carried out experiments to study the influence of cell opening size and cell height on the bearing capacity of marine clay overlain by geocell reinforced sand layer. The geocells were made from strips of geotextiles pasted together to form the cellular structure of required dimension. The infill sand had a relative density of 60%. They observed that the geocell exhibits a beam like action up to a settlement of 5 - 10% of footing width. Beyond 20% settlement, membrane action of the reinforcement was dominant. They found the BCR to decrease with the decrease in the cell opening size. For a geocell with larger cell opening size, the structure settles more on the application of a particular load. The membrane action of the geocells gets mobilized at larger settlements, leading to an increase in bearing capacity. However in the case of smaller geocell opening

size, failure occurs at relatively lower settlements i.e. before the membrane action of the reinforcement is mobilsed. Thus in order to get maximum benefit from the reinforcement, they recommended the use of geocells with larger opening size for structures where the permissible settlement is high and geocells with smaller opening size for low-settlement structures. The bearing pressure was found to increase with the increase in the height of the geocells.

Mhaiskar and Mandal (1996) studied the efficacy of geotextile cells in reinforcing the sand layer overlying soft clay subgrade. Parameters like the width and height of the geocells, strength of the geocell membrane and relative density of the fill were investigated. The geocell induced improvement in the bearing capacity of the weak soil was studied both experimentally as well as numerically. Numerical study was carried out using ANSYS, which is a general purpose finite element program. They found the optimum value of cell height to loading width ratio to be 0.625 at which the bearing capacity of the reinforced soil is 1.31 times that of the unreinforced case. A loading area having width equal to about 3.5 times the geocell width gives maximum performance improvement. They observed that the increase in the relative density of the backfill and decrease in the aspect ratio (width to height) of the cells lead to an increase in the overall performance. Based on the test data, they recommended that geocells can be used as an alternative to high modulus geotextile.

Lau et al. (2001) conducted laboratory model tests to determine how the inclusion of geocell reinforcement affects the resilient and rutting behaviour of the subbase, placed over soft subgrade. The geocell reinforcing technique was also compared to the conventional cut and fill method where the weak soil was replaced with a relatively stronger ‘beaker run’ material. They observed that with the inclusion of the geocell

reinforcement, the plastic deformation in the reinforced subgrade was limited to 30-50% of the unreinforced section. A 30% increase in the resilient modulus was obtained with the provision of geocell reinforcement in the subbase layer. An analysis using the KENLAYER software showed that the incorporation of geocells increases the service life of the pavement by 10%.

Dash et al. (2003b) studied the bearing capacity of the circular footing supported by geocell reinforced sand underlain by soft soil. The dimensions of the geocell were varied and their influence on the overall performance was observed. They observed that the load carrying capacity improved and the surface heaving of the foundation bed reduced due to the provision of geocell reinforcement. The bearing capacity continued to increase with increase in width of the geocell mattress till 5 times the footing diameter and height of the geocell mattress about twice the footing diameter, beyond which further improvement was only marginal. A satisfactory improvement in load carrying capacity of the foundation bed was observed even when the width of the geocell mattress was just equal to the diameter of the footing. An additional layer of planar geogrid at the base of the mattress further enhanced the load carrying capacity of the footing. However, they found this improvement to decrease with the increase in height of the geocell mattress and became marginal for height of geocell mattress greater than 1.68 times the diameter of footing.

Zhou and Wen (2008) investigated the improvement in bearing capacity of a soft soil by using different types of geosynthetics reinforced sand cushion. Tests were conducted on four different setups – sand cushion overlying soft soil, one layer of geogrid, two layers of geogrids and one layer of geocells placed within the sand cushion. The reinforcement (i.e. single layer geogrid, double layer geogrid and single layer geocell) in the sand

cushion was found to increase the subgrade reaction coefficient by 1600%, 2600% and 3000% respectively. They attributed the improvement of the geogrid reinforced soil to the induced apparent cohesion in the sand. In case of the geocell reinforced sand cushion, the improvement was attributed to the increase in the apparent cohesion as well as the angle of internal friction of the soil. Apart from the increase in the load carrying capacity, a reduction in settlement was also noted, with geocell reinforcement reducing the settlement by about 44%. Compared to the geogrid reinforcement, the geocells produced more even settlement.

Emersleben and Meyer (2008) carried out large scale model tests and in situ field tests to evaluate the influence of geocell reinforcement on the load-deformation behaviour of the soil bed. Static load tests were carried out in a test box in the laboratory on both unreinforced and reinforced test beds with varying height and diameter of the geocells. They found the improvement in load carrying capacity due to addition of a geocell layer to be more than three times that of the unreinforced case. Both increase in height and decrease in diameter of the cells gave higher performance improvement. The geocell reinforcement reduced the vertical stress on the subgrade by as much as 30%. Moreover, in case of unreinforced soil the stresses were found to be concentrated in the area of the load plate while the stresses in case of geocell reinforced soil were distributed over a larger area. This indicates that the geocell acts as a stiff layer distributing loads over a larger area. Falling Weight Deflectometer tests were done on the in situ pavements constructed with and without geocells. The performance of 400 mm thick base course with 200 mm high geocells was found to be comparable to a 700 mm thick unreinforced base layer with similar boundary conditions. The increase in modulus and decrease in the deflection due to the geocell reinforcement in the field tests were in agreement with the results obtained from the laboratory model tests.

Sireesh et al. (2009) evaluated the potential benefits obtained by providing a geocell sand mattress over clay subgrade having a circular void. The different parameters varied were the thickness of the unreinforced sand layer, width, height of the geocell layer and relative density of sand. Their test results showed that with the geocell mattress, a 40 fold increase in bearing capacity and substantial reduction in settlement of the void-clay subgrade can be obtained. They concluded that in order to have beneficial effect, the geocell mattress must be spread beyond the void by a distance atleast equal to the diameter of the void. The optimum width and height of the geocell mattress where maximum improvement was observed was found to be 4.9 and 1.8 times the footing diameter respectively. They also concluded that it is profitable to compact the soil in the geocells to higher density, as the overall bearing capacity is further improved in case of dense soil. Provision of a layer of geogrid below the geocell mattress further enhances the performance of the foundation bed.

2.3.2.3 Clay bed reinforced with geocells

Sitharam et al. (2007) carried out laboratory model tests to explore if locally available soft clay can be used as infill material in the geocells. Series of load tests were done by varying the width, height and depth of placement of the geocell mattress. The influence of additional geogrid layer placed at the base of the mattress was also evaluated and an improvement in bearing capacity of 2.7 was observed even with the width of geocell almost equal to the diameter of the footing. They observed the performance improvement to increase with the increase in width and height of the geocell mattress. The optimum width and height of the geocell mattress giving maximum performance improvement are found to be 4.9 and 2.4 times the diameter of the footing respectively. Further improvement was also observed with the provision of additional planar layer at the base of geocell mattress and maximum improvement was observed when the geocell mattress

was placed immediately below the surface of the footing. The authors observed a 92% reduction in settlement and 485% increase in bearing capacity when geocell mattress was provided on the soft soil bed indicating that in the absence of good quality material such as sand and gravel, locally available soft soil infill in geocells can still give visible performance improvement.

2.3.3 Triaxial Compression tests on Geocells

Bathurst and Karpurapu (1993) carried out triaxial compression tests on cohesionless soil encased in single geocell. The sample size was of 200 mm in diameter with an aspect ratio (height to diameter) of unity. The confinement provided by the reinforcement contributed to the increase in shear strength of the encapsulated soil by about 42% to 62%. The frictional angle however, was found to be the same as that of the unreinforced case. The authors used an elastic membrane model suggested by Henkel and Gilbert (1952) to estimate the magnitude of the additional confining pressure. This additional confining pressure creates an apparent cohesion which is responsible for the increase in the strength and stiffness of the soil. The model proposed by the authors gave a reasonably accurate estimate of the apparent cohesion of the soil-geocell composite sample.

Rajagopal et al. (1999) studied the influence of confinement provided by the multicell geocell system on the strength and stiffness behaviour of granular materials through triaxial compression tests. The geocells were fabricated from geotextiles of different strength and stiffness. They observed failure in most cases to be by bursting of the seams as the seam strength was much less than the geosynthetic materials. Their results showed the trend of failure to be as similar as reported by Bathurst and Karpurapu (1993) where the confinement induced apparent cohesive strength in the geocell encapsulated soils

whereas the frictional strength remained equal to that of an unreinforced soil. They found the increase in the stiffness as well as the strength of the soil to be a function of cell diameter, strength and stiffness of geocell material. The triaxial test results also show that the three interconnected cells in the triaxial test can adequately simulate the multiple geocell system in the field.

Mengelt et al. (2006) evaluated the effect of geocell confinement on the resilient modulus and the plastic deformation of the infill soil. Fine grained as well as coarse grained soil, confined in single geocell, were tested through triaxial compression tests. The triaxial samples were prepared with a relatively smaller aspect ratio of 0.8 and the conventional aspect ratio of 2. The results obtained from samples prepared at these two different aspect ratios were comparable. They found the improvement in resilient modulus to depend on the type of infill material with the coarser material giving an improvement of 1.4 - 3.2% as against the 16.5 - 17.9% improvement in case of the finer infill. Large deformation was observed in case of finer grained material suggesting that this would have likely mobilised greater reinforcing effect of the geocells.

Latha and Murthy (2007) investigated the effects of different reinforcement forms viz. discrete, planar and cellular, on the behaviour of granular soil. Triaxial tests were conducted on samples of 38 mm diameter and 76 mm height. The geocells in the study were made from geotextiles and polyester film. They observed that the failure in case of planar and discrete reinforcement was by bulging but for geocell encased samples, the failure was by bursting of the seam. Even with seam having much lower tensile strength which dictates the response of the geocells, the performance improvement is comparable to that of planar reinforcement having high tensile strength. This suggests that with better welded seam, the geocells would give a much improved performance. They found

polyester geocells to be more efficient than the geotextile geocells. They observed that by using the model proposed by Bathurst and Karpurapu (1993), experimental results are in agreement with the predicted values.

Wesseloo et al. (2009) performed large scale uniaxial compression tests on single and multiple cell geocell-soil composite system to develop a better understanding of the behaviour of geocell structure. The multiple cell structure considered in the study was a square grid of 2×2 cell, 3×3 cell and 7×7 cell. They observed that the deformation behaviour of the geocell-soil composite structures is dependent on the boundary conditions imposed on the structures. For the direct comparison of axial stress in multi cell structure, the axial stress is normalized with respect to the original cell diameter. They found from normalized axial stress-strain behaviour of the structure, both the stiffness and strength decrease with the increase in the number of cell in the structure. They observed peak axial stress of the structure to decrease with the increase in the number of the cells. This decrease in peak strength was quantified by 'efficiency factor' which is defined as the ratio of the axial stress in a single cell structure at a specified diameter and the axial strain rate to the axial stress in a multi-cell structure consisting of the cells with the same cell diameter tested at the same axial strain rate. For a 7×7 cell structure peak axial stress was found to be 55% lower than that of a single cell of same diameter at same strain rate. An equation which relates the efficiency factor with the periphery factor was formulated in order to compare results that were obtained from the different geometries. The periphery factor is based on the fact that the strength of composite is dominated by the hoop stress in the outer membrane. This relation shows that there is a logarithmic decrease in the efficiency with the increase in the number of cell in the structure. They concluded that the relation can be an important tool to

investigate the results obtained from the laboratory which has less number of geocell as compared to the number of geocell used in the field.

2.4 CONCLUDING REMARKS AND SCOPE OF THE PRESENT STUDY

Review of literature highlights the beneficial effect of using planar reinforcements to increase the load carrying capacity of the weak subgrade. The performance improvement in this case is primarily derived through membrane action of the reinforcing layer and development of frictional resistance between the planar reinforcement and the soil. A more effective form of reinforcement is through the use of interconnected three dimensional cells that confine the soil within the pockets thereby forming a much stiffer mattress with high flexural strength. The available literature on geocell reinforcement indicates that substantial improvement in performance can be obtained with the provision of geocell reinforced sand mattress over soft clay subgrade. However, the influence of various key parameters on the overall performance and behaviour of geocell-sand mattress reinforced clay subgrade system are not well understood. Understanding of various mechanisms through study of these parameters will help in developing design guidelines and construction of such structures over soft clay subgrade. In view of this, under the present investigation it is proposed to carry out a detailed parametric study through a series of experiments from which the behaviour of geocell-sand mattress laid over soft clay subgrade, under circular loading can be understood.

CHAPTER 3

EXPERIMENTAL INVESTIGATIONS

3.1 INTRODUCTION

The objective of the present study is to investigate the behaviour of geocell-sand mattress overlying soft clay subgrade, under circular footing. The details of the materials used in this study, the determination of their physical and engineering properties, the experimental setup and testing procedure are described in this chapter.

3.2 MATERIALS USED IN THE STUDY

3.2.1 Clay

For the present study, locally available natural soil is used as a material for the preparation of the subgrade soil. The soil was brought from the site, air-dried and pulverized before it was used. Wet sieve analysis was done [ASTM D 6913-04] and the percentage of soil passing 75-µm sieve was found to be 70%. Further, for the finer portions, hydrometer analysis as per ASTM D 4221-99 was done. The Particle size distribution of the material is shown in Fig. 3.1. The specific gravity [ASTM D 0854-06] of clay was found to be 2.63. Atterberg limit tests were conducted as per ASTM D 4318-05 and the values of liquid limit, plastic limit and plasticity index are reported in Table 3.1. The soil can thus be classified as CL (clay with low plasticity) according to Unified Soil Classification System (USCS) [ASTM D 2487-06].

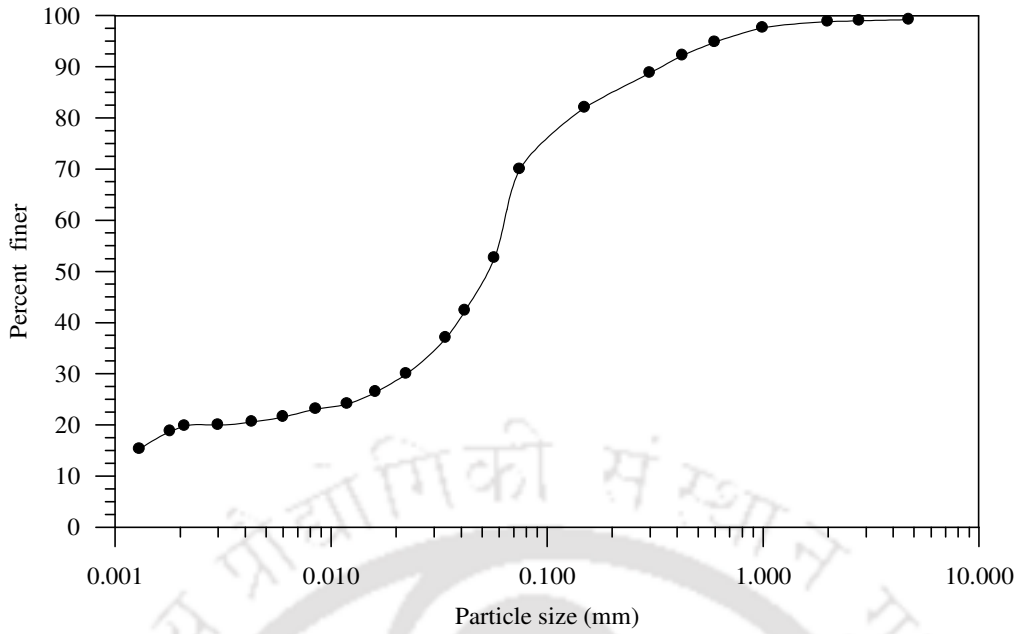

Fig. 3.1 Grain size distribution of soil used in the study

Table 3.1 Properties of soil used in the study.

Property	Values
Specific Gravity	2.63
% fines	70
Liquid limit (%)	40
Plastic limit (%)	21
Plasticity Index (%)	19
Classification (USCS)	CL

3.2.2 Sand

The sand used in the study is a locally available river sand whose particle size distribution [ASTM D 6913-04] is shown in Fig. 3.2. The coefficient of uniformity (C_u) and coefficient of curvature (C_c) were found to be 2.52 and 1.05 respectively. The soil can thus be classified as poorly graded sand, SP, as per Unified Soil Classification System (USCS) [ASTM D 2487-06]. The physical properties of sand such as specific gravity [ASTM D 0854-06], maximum dry density [ASTM D 4253-00] and minimum dry density [ASTM D 4254-00] are reported in Table 3.2.

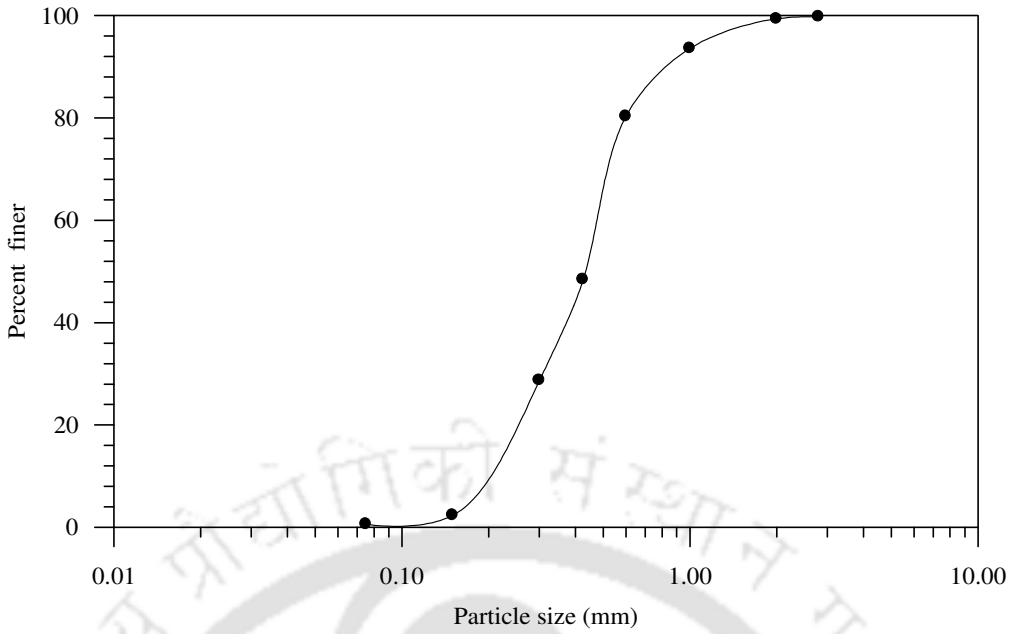

Fig. 3.2 Grain size distribution of sand used in the study

Table 3.2 Properties of sand used in the study.

Property	**Values**
Specific Gravity, G	2.68
D_{10} (mm)	0.19
D_{30} (mm)	0.31
D_{50} (mm)	0.44
D_{60} (mm)	0.48
Coefficient of uniformity, C_u	2.52
Coefficient of curvature, C_c	1.05
Classification (USCS)	SP
Maximum dry density, γ_{dmax} (kN/m^3)	16.51
Minimum dry density, γ_{dmin} (kN/m^3)	13.94
Friction angle (ϕ) from direct shear test	
ID 35%	36°
ID 50%	43°
ID 80%	46°
Dilation angle (ψ) from direct shear test	
ID 35%	2°
ID 50%	12°
ID 80%	20°
Friction angle (ϕ) from triaxial compression test	
ID 35%	35°
ID 50%	40°
ID 80%	44°

Direct shear tests as per ASTM D 6528-07 were performed on samples prepared at relative densities (ID) of 35%, 50% and 80% and the corresponding shear stress-shear strain behaviour are shown in Figs. 3.3, 3.4 and.3.5. The variation of normal stress with peak shear stress is presented in Fig. 3.6 while the friction angles thus obtained are summarized in Table 3.2

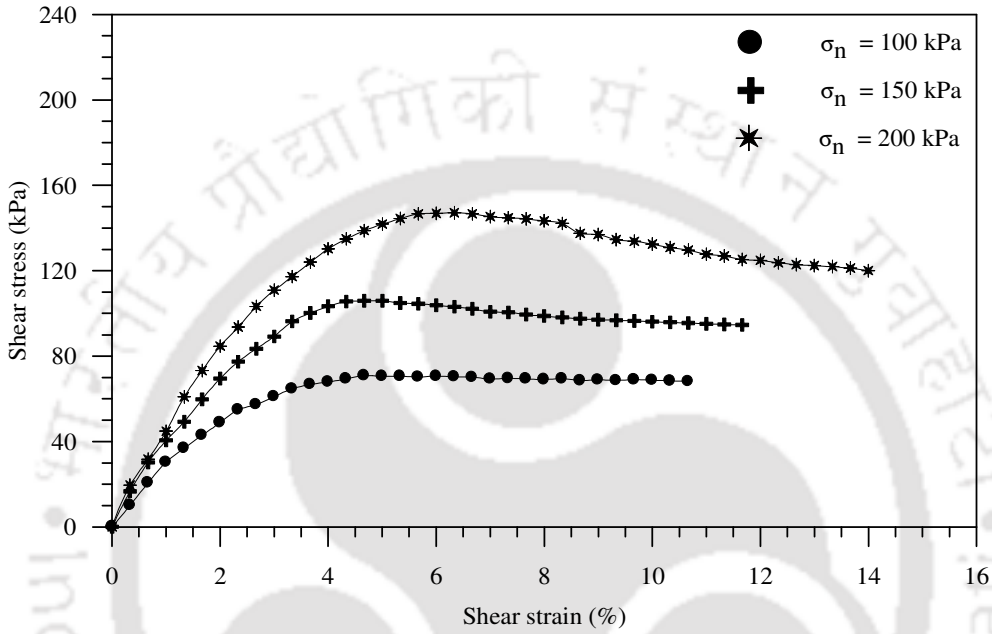

Fig. 3.3 Shear stress-shear strain curves for sand under direct shear test (ID = 35%)

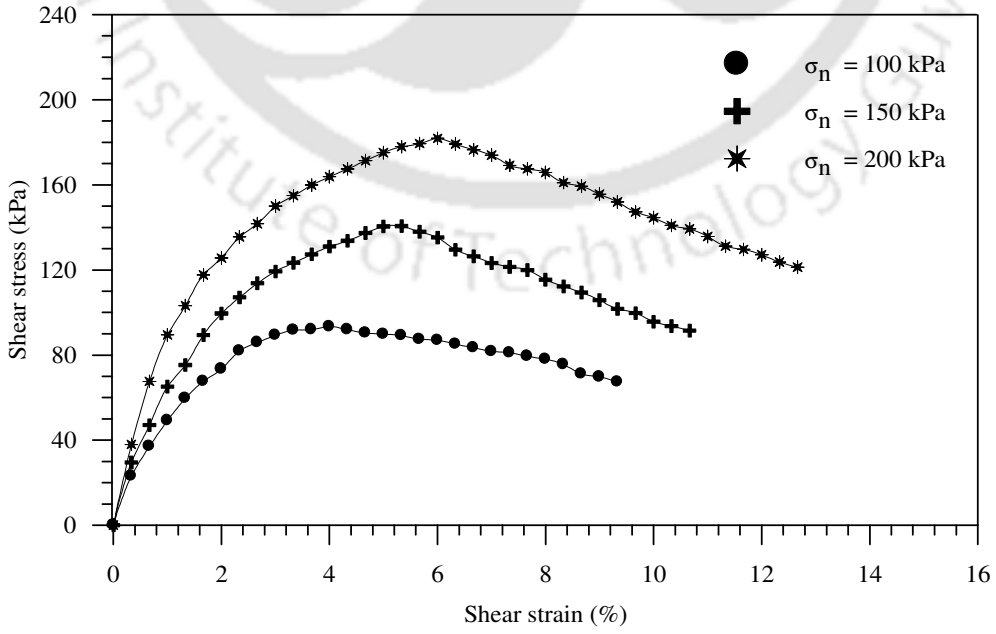

Fig. 3.4 Shear stress-shear strain curves for sand under direct shear test (ID = 50%)

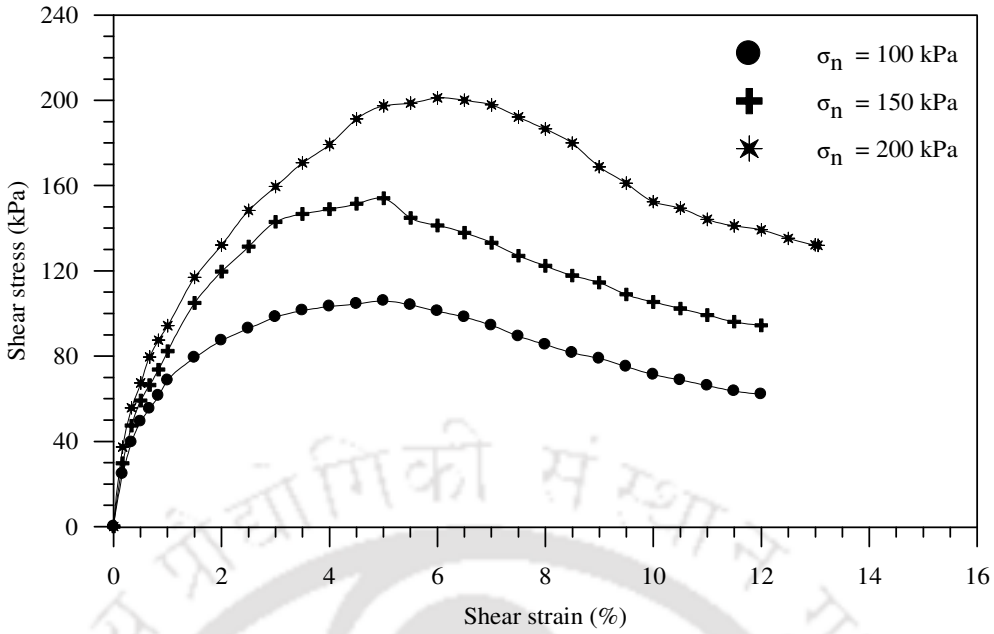

Fig. 3.5 Shear stress-shear strain curves for sand under direct shear test (ID = 80%)

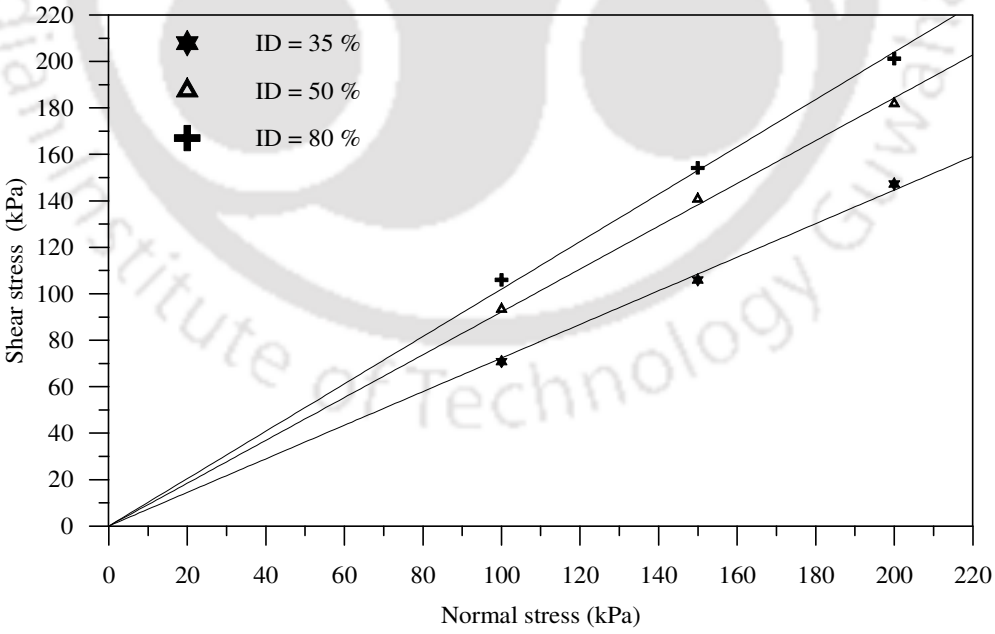

Fig. 3.6 Normal stress-peak shear stress response of sand at different relative densities obtained from direct shear test

The increase in thickness of soil sample versus shearing displacement responses for soils at different relative densities, obtained from direct shear tests, conducted at different normal pressures, are shown in Figs. 3.7 to 3.9. Since dilation decreases with the increase in normal stress (Panda, 2000), to have a clear observation of the dilation, tests were carried out at relatively lower normal stresses of 40 kPa, 50 kPa and 70 kPa. As per Gibson (1953), the dilation angle is defined as the peak slope of increase in thickness of the sample i.e. vertical deformation versus shearing displacement i.e. horizontal deformation. The maximum dilation angle observed for relative densities of 35%, 50% and 80% are reported in Table 3.2.

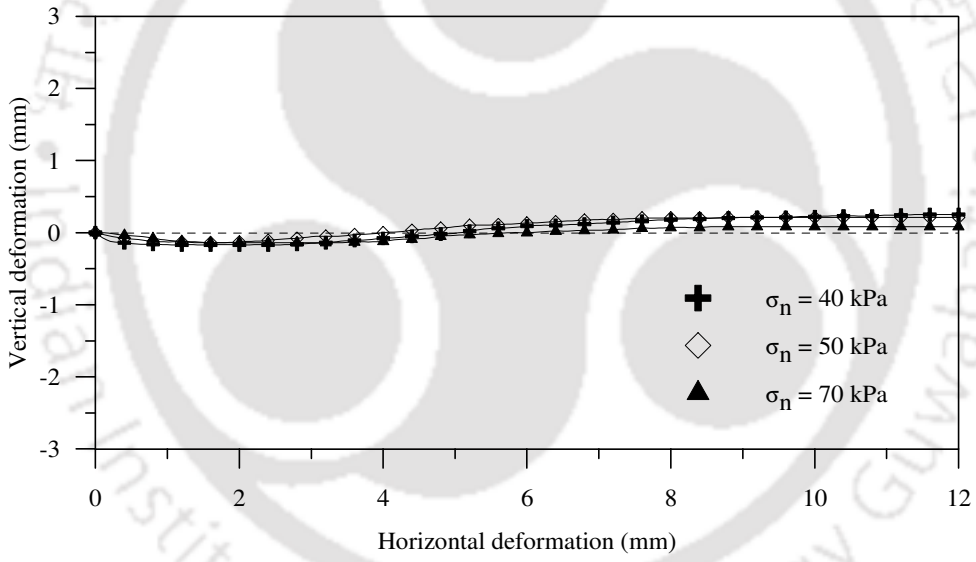

Fig. 3.7 Horizontal-vertical deformation plot for sand obtained from direct shear test (ID = 35%)

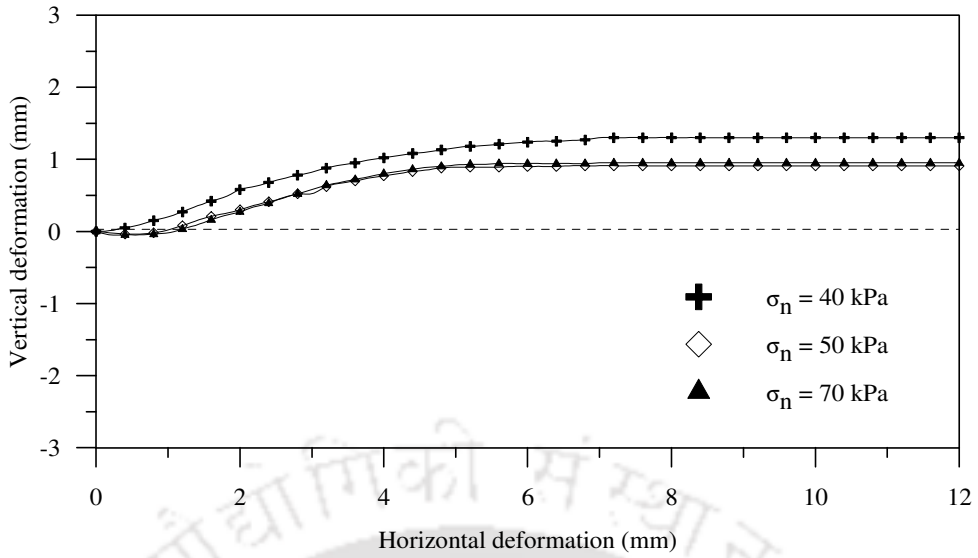

Fig. 3.8 Horizontal-vertical deformation plot for sand obtained from direct shear test (ID = 50%)

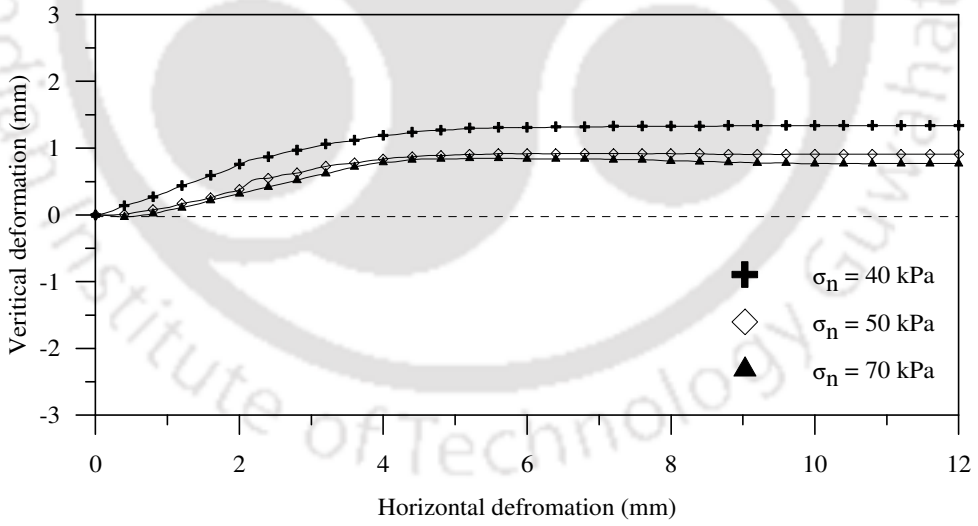

Fig. 3.9 Horizontal-vertical deformation plot for sand obtained from direct shear test (ID = 80%)

Triaxial compression tests were performed on the dry sand samples prepared at relative densities of 35%, 50% and 80% as per ASTM D 2850-03. The samples were prepared by dry vibratory method as per ASTM D 5311-92(04). The amount of sand required to obtain a specimen of desired density was weighed and divided into six equal parts. The sand in each lift was spooned into the membrane line split mould and compacted by vibration to the desired dry density taking care that the bottom layer was slightly under compacted. After the last layer was partially compacted, the top cap was placed in its position and the vibration continued till the desired density was obtained. The stress-strain responses and the corresponding mean normal stress versus shear stress (i.e. p-q) plots are shown in Figs. 3.10 to 3.13. The friction angles obtained at different relative densities are reported in Table 3.2.

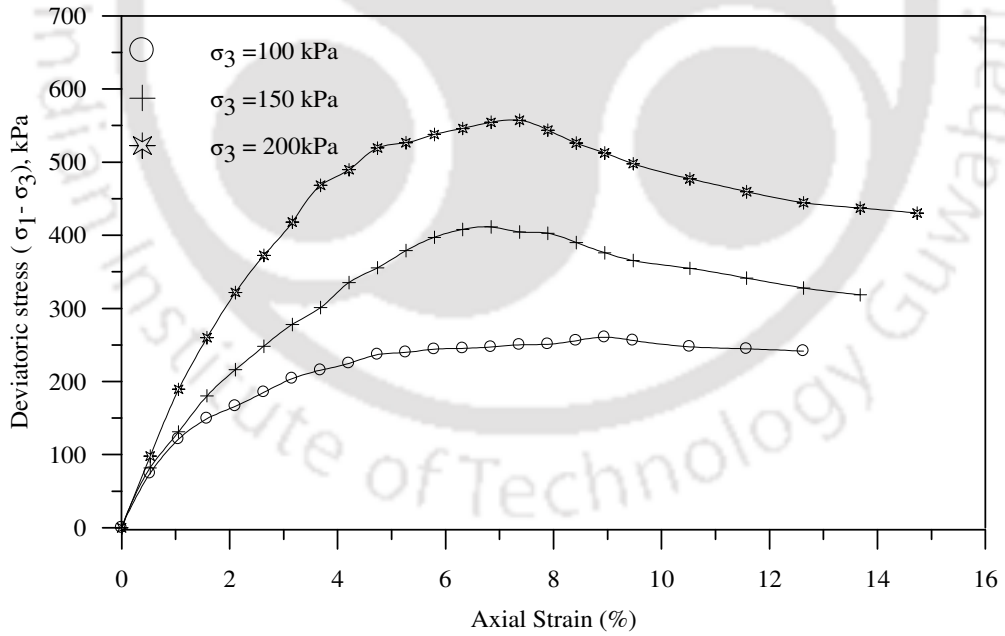

Fig. 3.10 Stress-strain behaviour of sand under triaxial compression test (ID = 35%)

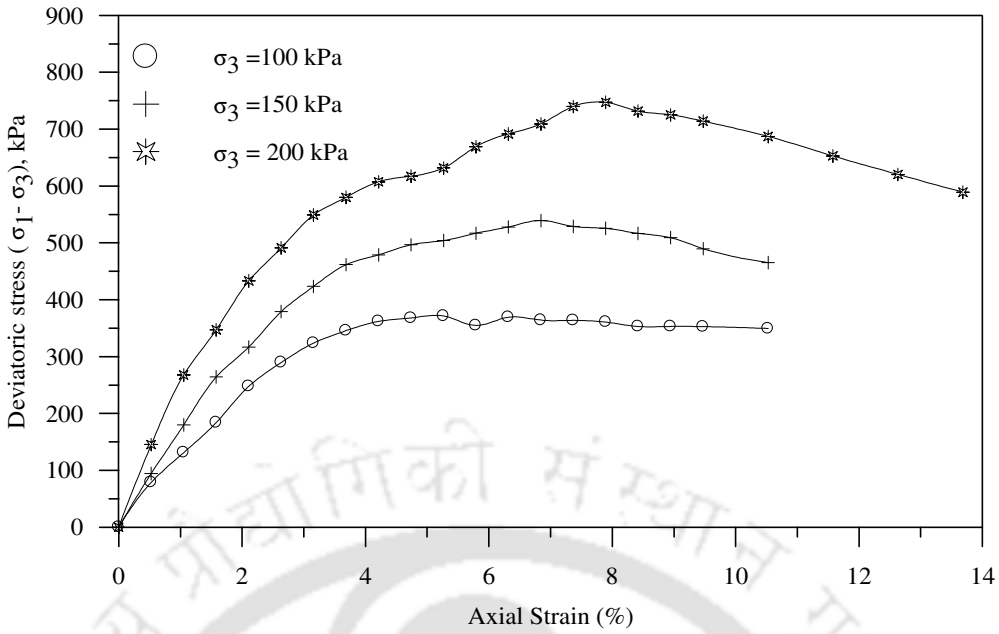

Fig. 3.11 Stress-strain behaviour of sand under triaxial compression test (ID = 50%)

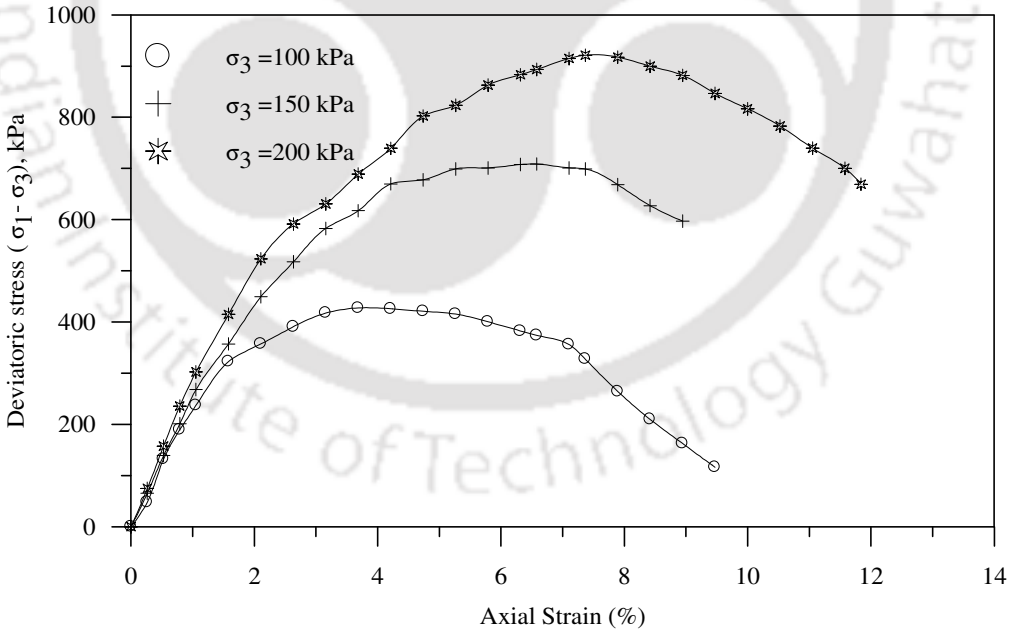

Fig. 3.12 Stress-strain behaviour of sand under triaxial compression test (ID = 80%)

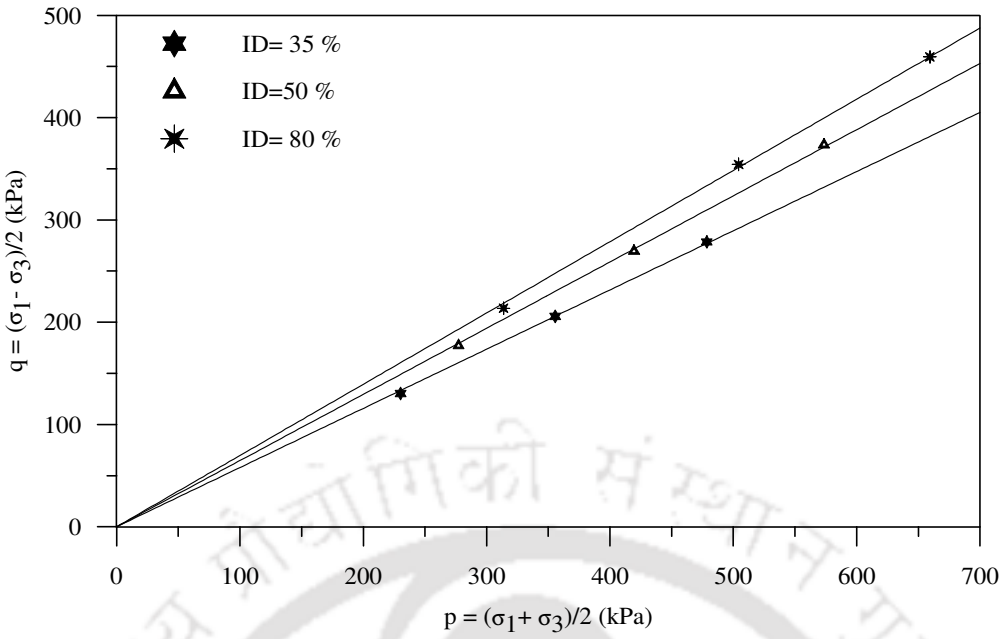

Fig. 3.13 p-q plot for different relative densities of sand under triaxial compression test

3.2.3 Geocells

The geocells used in the study were assembled from commercially available biaxial geogrid made from polypropylene. The photograph of the biaxial geogrid and its dimensions are shown in Photo 3.1(a) and Photo 3.1(b) respectively.

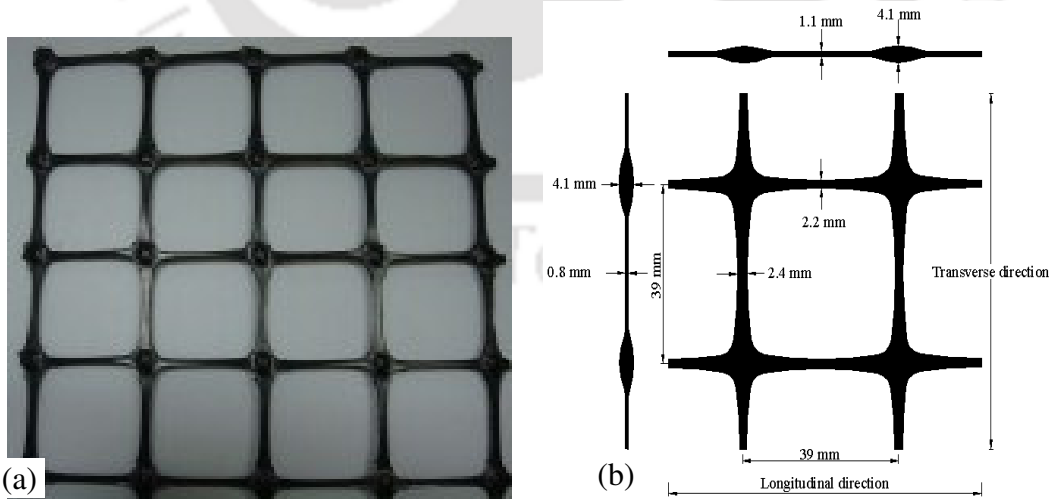

Photo 3.1 (a) Biaxial geogrid (b) Geometry of the geogrid

The properties of the geogrids were determined from standard multi-rib tension test as per ASTM D 6637-01 and are listed in Table 3.3. The load-strain behaviour of geogrid is presented in Fig. 3.14. The joints for the geocells were formed from 6 mm wide, 3 mm thick plastic strips cut from Perspex sheets made of low density polypropylene. The tensile strength of the joints was determined as per ASTM D 4884-09 and was found to be 4.75 kN/m. As the joint is a plastic strip of low strength, the strain could not be obtained. Hence, the load-deformation behaviour is presented in terms of axial deformation in Fig. 3.15.

Table 3.3 Properties of the geogrid used in the study.

Property	Values
Ultimate tensile strength (kN/m)	19.3
Failure strain (%)	28
Secant modulus at 5% strain (kN/m)	135
Aperture Size (mm)	35×35
Shape of aperture opening	square

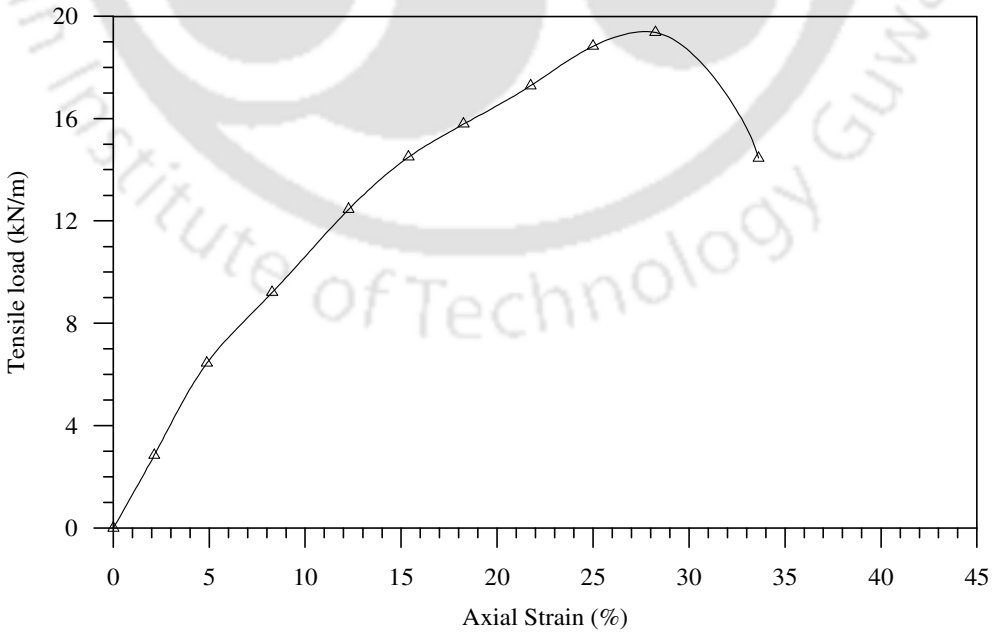

Fig. 3.14 Load-strain behaviour of biaxial geogrid used in the study

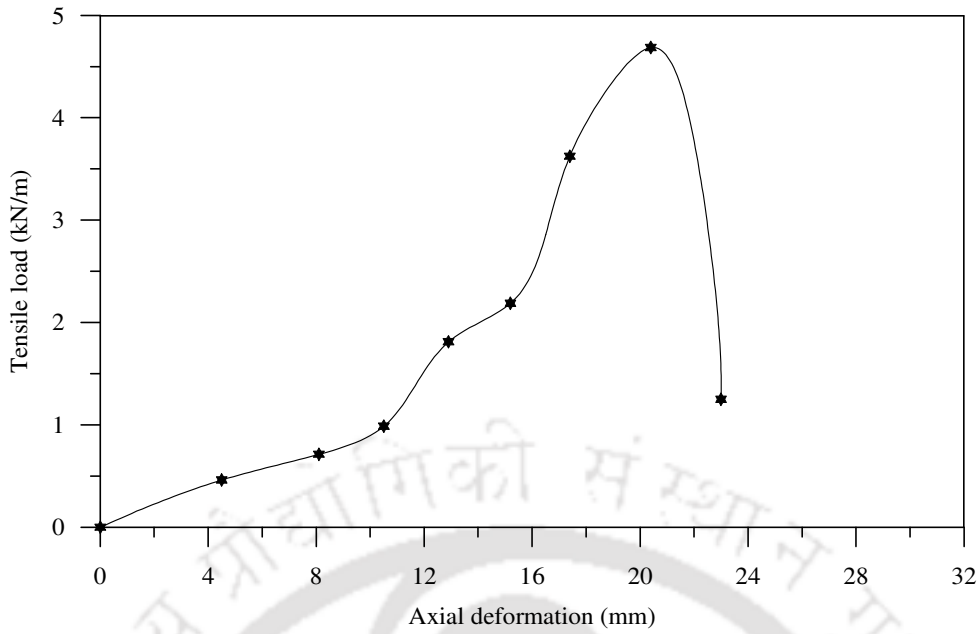

Fig. 3.15 Load-deformation behaviour of the bodkin joint used in the study

The interfacial frictional properties of the geogrid-sand interface for different relative densities i.e. 35%, 50% and 80% of sand were determined through pullout tests as per ASTM D 6706-01. The shear stress versus horizontal displacement responses obtained from the tests are shown in Figs. 3.16, 3.17 and 3.18 respectively. The normal stress-peak interfacial shear stress plots at relative densities of 35%, 50% and 80% are shown in Fig. 3.19. The interfacial friction angles (δ_s) obtained at the aforementioned densities of sand are 24°, 27° and 30° respectively.

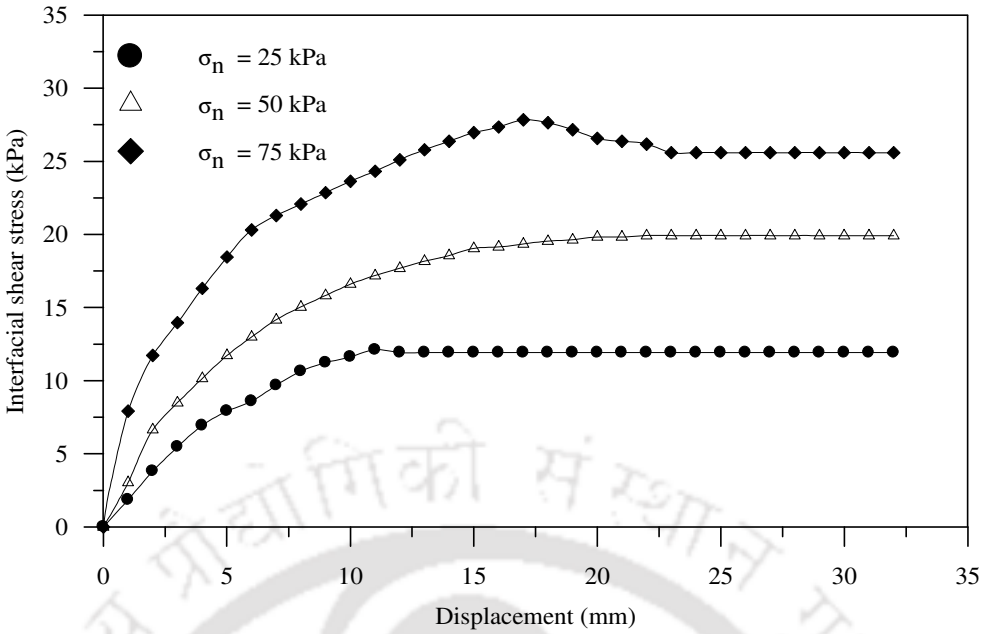

Fig. 3.16 Interfacial shear stress-horizontal displacement responses of geogrid-sand in pullout test (ID = 35%)

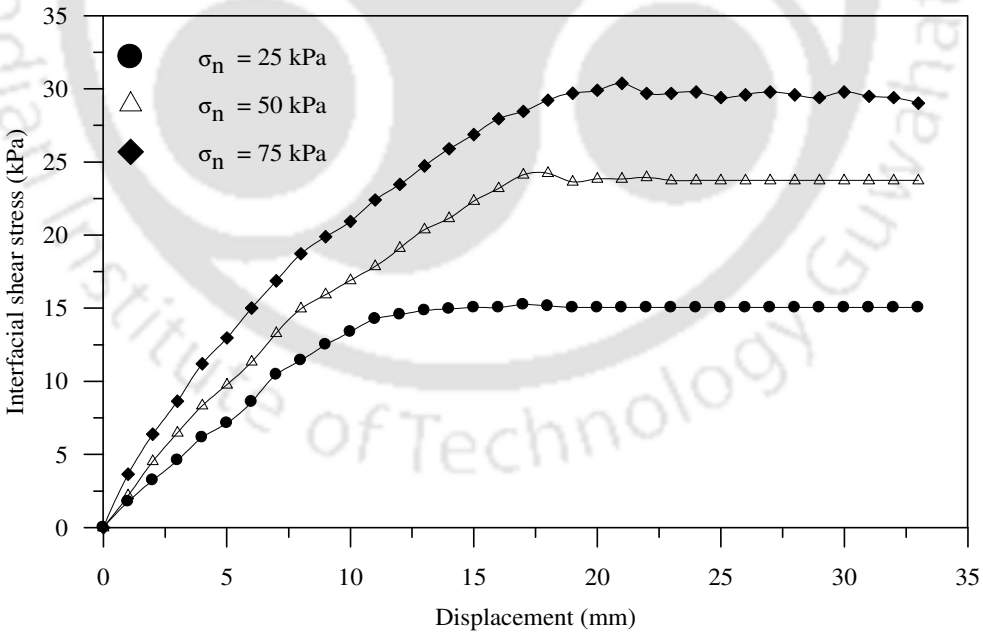

Fig. 3.17 Interfacial shear stress-horizontal displacement responses of geogrid-sand in pullout test (ID = 50%)

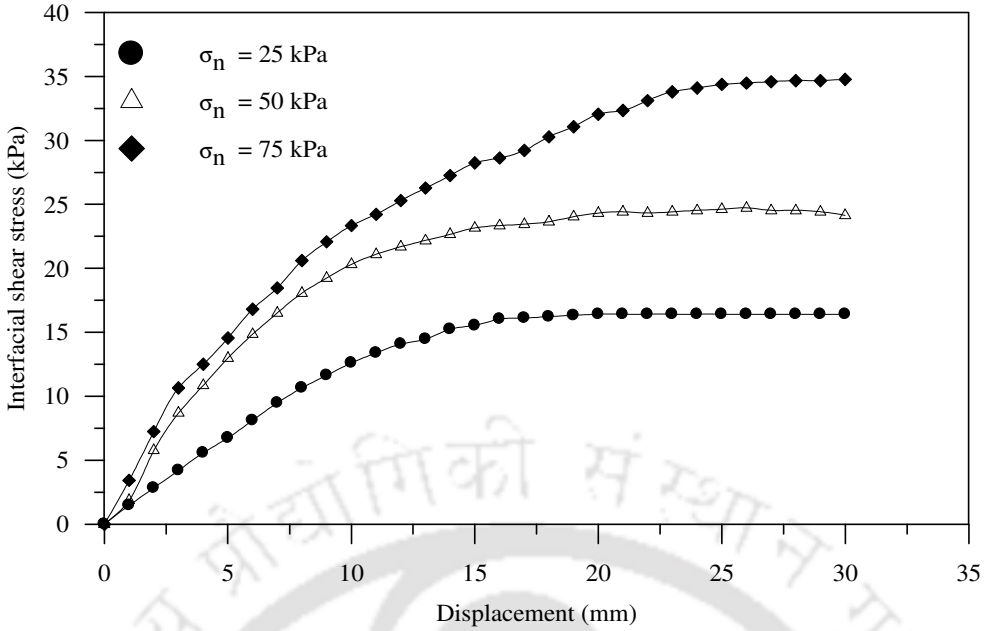

Fig. 3.18 Interfacial shear stress-horizontal displacement responses of geogrid-sand in pullout test (ID = 80%)

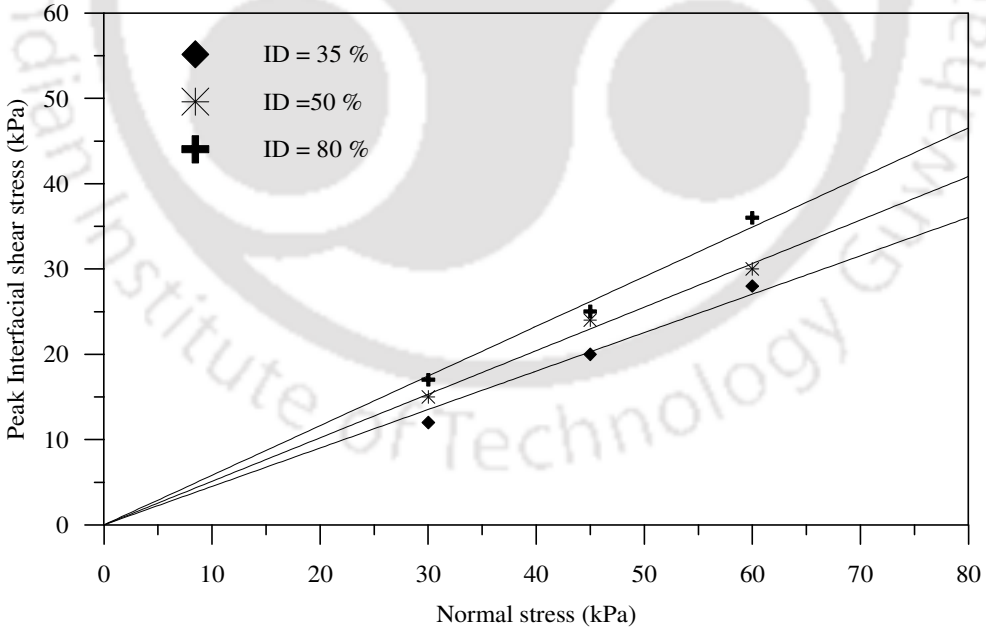

Fig. 3.19 Normal stress-peak interfacial shear stress responses obtained from pullout test

3.3 PLANNING OF EXPERIMENTS

The experiments in this study were planned in a systematic manner to bring out the benefit of using geocells as reinforcement on soft soils. The various parameters varied in the experimental programme are pocket size of geocell (d), depth of placement of the geocell mattress from base of the footing (u), pattern of formation of geocell, relative density of infill sand (ID), height of geocell mattress (h) and the provision of an additional planar geogrid layer at the base of the geocell mattress. The geometry of the reinforced foundation bed and the different parameters are illustrated in Fig. 3.20, Fig. 3.21 and Photo 3.2. The pocket size of the geocell is taken as the diameter of the equivalent circular area of the geocell pocket opening. A typical geocell pocket is shown through the hatched area in Fig. 3.21.

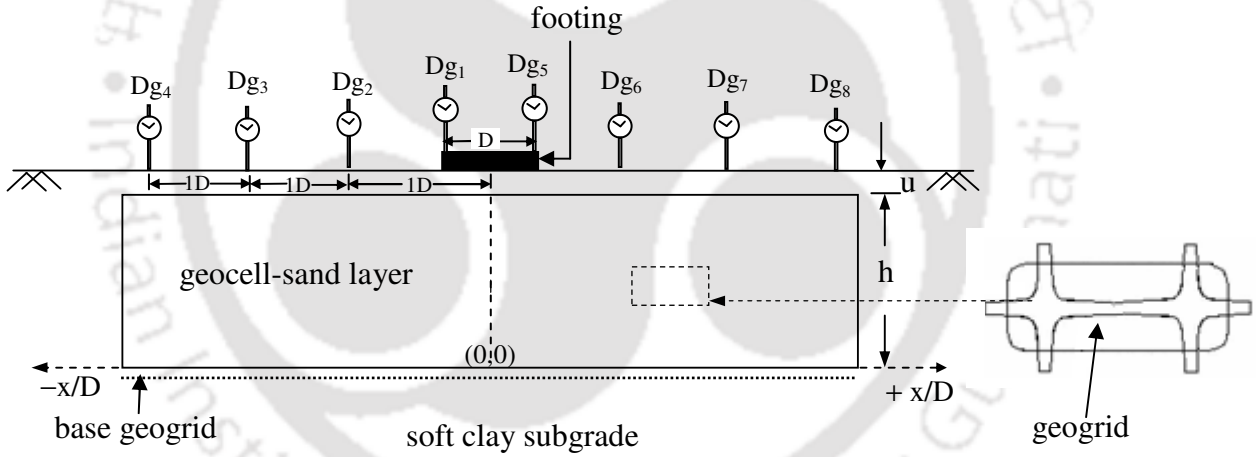

Fig. 3.20 Geometry of the reinforced foundation bed

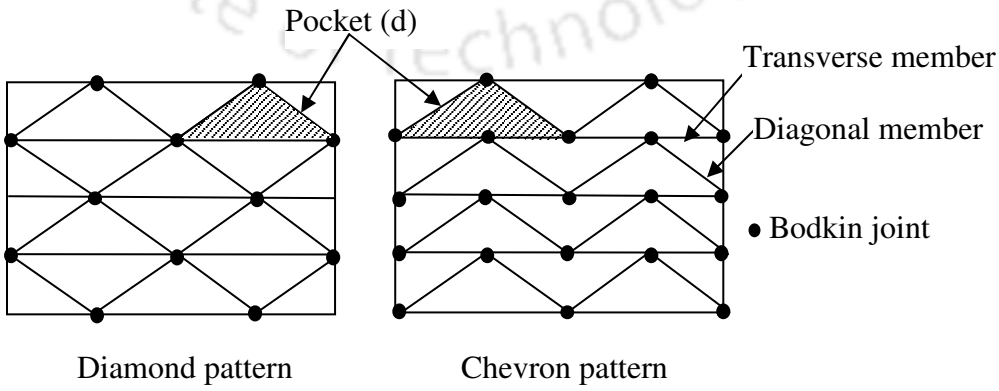

Fig. 3.21 Patterns of formation of geocell mattress

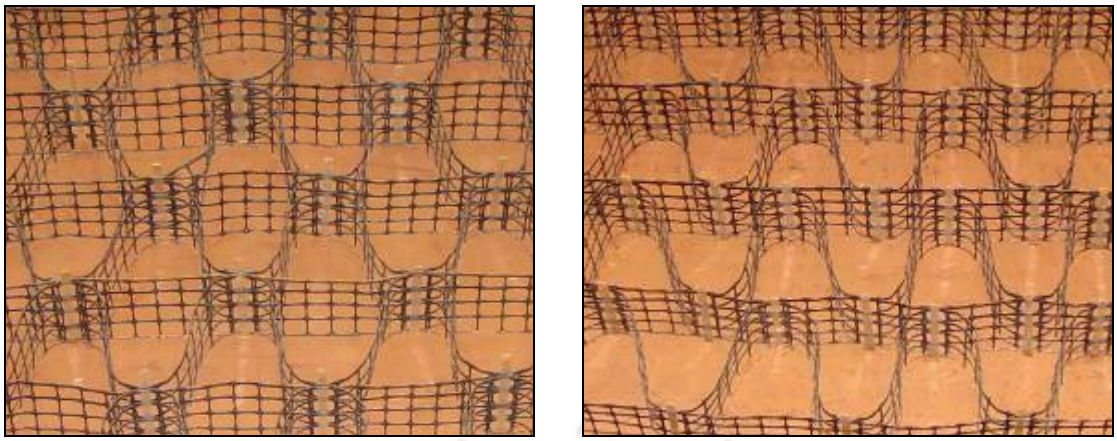

Diamond pattern Chevron pattern

Photo 3.2 Photographs showing different patterns of formation of geocell mattress placed on clay subgrade

In total 129 number of tests spreading over 42 series were carried out in order to evaluate the contribution of each parameter to the enhancement of the performance of the reinforced foundation bed. The complete description of the test series is summarized in Table 3.4. All the parameters are expressed in a non-dimensional form with respect to the footing diameter (D). The critical dimension obtained from a given series of tests was adopted in the next series of tests.

Test Series A1 was conducted on the unreinforced clay subgrade prepared at an undrained shear strength, c_u, of 6 kPa. This represents the in-situ condition of the untreated ground. Under tests series A2, A3, A4, A5 and A6, the response of the model footing supported on the unreinforced sand layer placed over the soft clay subgrade was investigated. The influence of relative density and height of the sand layers were studied under these series.

Table 3.4 Details of series of model tests.

Series	Reinforcement	Details of test parameters	
		Constant	Variable
A1	Unreinforced	c_u = 6kPa	H/D = 0
A2	Unreinforced	c_u = 6kPa, ID = 80%	H/D = 0.27,0.37,052, 0.77, 0.8,0.9, 1.05,1.3
A3	Unreinforced	c_u = 6kPa, H/D = 0.37	ID = 35%, 50%, 80%
A4	Unreinforced	c_u = 6kPa, H/D = 0.63	ID = 35%, 50%, 80%
A5	Unreinforced	c_u = 6kPa, H/D = 0.90	ID = 35%, 50%, 80%
A6	Unreinforced	c_u = 6kPa, H/D = 1.17	ID = 35%, 50%, 80%
B1	Geocell	c_u = 6kPa, chevron, ID = 80%, h/D = 0.27, u/D = 0	d/D = 0.4,0.8,1.2,1.6
B2	Geocell	c_u = 6kPa, chevron, ID = 80%, h/D = 0.27, u/D=0.1	d/D = 0.4,0.8,1.2,1.6
B3	Geocell	c_u = 6kPa, chevron, ID = 80%, h/D = 0.27, u/D = 0.25	d/D = 0.4,0.8,1.2,1.6
B4	Geocell	c_u = 6kPa, chevron, ID = 80%, h/D = 0.27, u/D = 0.50	d/D = 0.4,0.8,1.2,1.6
B5	Geocell	c_u = 6kPa, chevron, ID = 80%, h/D = 0.8, d/D = 0.8	u/D = 0,0.1,0.25,0.50
C1	Geocell	c_u = 6kPa, diamond, ID = 80%, h/D = 0.27, u/D = 0	d/D = 0.4,0.8,1.2,1.6
C2	Geocell	c_u= 6kPa, diamond, ID = 80%, h/D = 0.27, u/D = 0.1	d/D = 0.4,0.8,1.2,1.6
C3	Geocell	c_u = 6kPa, diamond, ID = 80%, h/D = 0.27, u/D= 0.25	d/D = 0.4,0.8,1.2,1.6
C4	Geocell	c_u = 6kPa, diamond, ID = 80%, h/D = 0.27, u/D = 0.50	d/D = 0.4,0.8,1.2,1.6
C5	Geocell	c_u = 6kPa, diamond, ID = 80%, u/D = 0.1, d/D = 0.8	h/D = 0.27,0.53,0.8, 1.07
C6	Geocell	c_u = 6kPa, diamond, ID = 80%, u/D = 0.1, h/D = 0.53	d/D = 0.4,0.8,1.2
C7	Geocell	c_u = 6kPa,diamond, u/D = 0.1, h/D = 0.53, d/D = 0.8	ID = 35%, 50%, 80%
D1	Geocell	c_u = 6kPa, chevron, u/D = 0.1 h/D = 0.27, ID = 35%	d/D = 0.4,0.8,1.2
D2	Geocell	c_u = 6kPa, chevron, u/D = 0.1 h/D = 0.27, ID = 50%	d/D = 0.4,0.8,1.2
D3	Geocell	c_u = 6kPa, chevron, u/D = 0.1 h/D = 0.27, ID = 80%	d/D = 0.4,0.8,1.2
E1	Geocell	c_u = 6kPa, chevron, u/D = 0.1 h/D = 0.53, ID = 35%	d/D = 0.4,0.8,1.2
E2	Geocell	c_u = 6kPa, chevron, u/D = 0.1 h/D = 0.53, ID = 50%	d/D = 0.4,0.8,1.2

Table 3.4 Details of series of model tests (continued)

Series	Reinforcement	Details of test parameters	
		Constant	Variable
E3	Geocell	c_u = 6kPa, chevron, u/D = 0.1 h/D = 0.53, ID = 80%	d/D = 0.4,0.8,1.2
F1	Geocell	c_u =6kPa, chevron, u/D=0.1 h/D = 0.80, ID = 35%	d/D = 0.4,0.8,1.2
F2	Geocell	c_u = 6kPa, chevron, u/D = 0.1 h/D = 0.80, ID = 50%	d/D = 0.4,0.8,1.2
F3	Geocell	c_u = 6kPa, chevron, u/D = 0.1 h/D = 0.80, ID = 80%	d/D = 0.4,0.8,1.2
G1	Geocell	c_u = 6kPa, chevron, u/D = 0.1 h/D = 1.07, ID = 35%	d/D = 0.4,0.8,1.2
G2	Geocell	c_u = 6kPa,chevron, u/D = 0.1 h/D = 1.07, ID = 50%	d/D = 0.4,0.8,1.2
G3	Geocell	c_u = 6kPa, chevron, u/D = 0.1 h/D = 1.07, ID = 80%	d/D = 0.4,0.8,1.2
H1	Geocell + basal geogrid	c_u = 6kPa, chevron, u/D = 0.1 h/D = 0.27, ID = 35%	d/D = 0.4,0.8,1.2
H2	Geocell + basal geogrid	c_u = 6kPa, chevron, u/D = 0.1 h/D = 0.27, ID = 50%	d/D = 0.4,0.8,1.2
H3	Geocell + basal geogrid	c_u = 6kPa, chevron, u/D = 0.1 h/D = 0.27, ID = 80%	d/D = 0.4,0.8,1.2
I1	Geocell + basal geogrid	c_u =6kPa, chevron, u/D=0.1 h/D = 0.53, ID = 35%	d/D = 0.4,0.8,1.2
I2	Geocell + basal geogrid	c_u = 6kPa,chevron, u/D = 0.1 h/D = 0.53, ID = 50%	d/D = 0.4,0.8,1.2
I3	Geocell + basal geogrid	c_u = 6kPa, chevron, u/D = 0.1 h/D = 0.53, ID = 80%	d/D = 0.4,0.8,1.2
J1	Geocell + basal geogrid	c_u =6kPa, chevron, u/D=0.1 h/D = 0.80, ID = 35%	d/D = 0.4,0.8,1.2
J2	Geocell + basal geogrid	c_u = 6kPa, chevron, u/D = 0.1 h/D = 0.80, ID = 50%	d/D = 0.4,0.8,1.2
J3	Geocell + basal geogrid	c_u = 6kPa, chevron, u/D = 0.1 h/D = 0.80, ID = 80%	d/D = 0.4,0.8,1.2
K1	Geocell + basal geogrid	c_u = 6kPa, chevron, u/D = 0.1 h/D = 1.07, ID = 35%	d/D = 0.4,0.8,1.2
K2	Geocell + basal geogrid	c_u = 6kPa, chevron, u/D = 0.1 h/D = 1.07, ID = 50%	d/D = 0.4,0.8,1.2
K3	Geocell + basal geogrid	c_u = 6kPa, chevron, u/D = 0.1 h/D = 1.07, ID = 80%	d/D = 0.4,0.8,1.2

Under series A2, the density of sand was kept constant (i.e. ID = 80%) while the height of the sand layer (H) was varied from 0.27D to 1.3D. The height of the sand layer was kept equal to that of the geocell-sand mattress, tested in the present study. This is to facilitate comparison between the reinforced and unreinforced test beds. Under series A3, the height of the sand layer was kept constant at H/D ratio of 0.37 while the relative density was varied from 35% to 80%. Similarly, the variation of relative density was investigated for higher heights of the sand layer under series A4, A5 and A6.

The tests under series B and series C were conducted using geocell reinforcement in the sand layer overlying the soft clay subgrade. The parameters varied in these series are the depth of placement of the mattress from the base of the footing (u), pattern of formation and pocket size (d) of the geocells. Within each series, only one parameter was varied, so as to study its influence on the overall behaviour of the system, while the others were kept constant. For all tests in series B, the geocell mattress was formed in chevron pattern. Under Test Series B1, the geocell mattress was placed immediately below the footing (i.e. u = 0) while the pocket sizes of geocells were varied. Similarly, the influence of pocket size was further examined under series B2 to B4 wherein tests were conducted at different pocket sizes (d) for varying depths of placement (u) of the geocell mattress. Under each series, one depth of placement was kept constant at a time, while the pocket size was varied. The pocket size giving the maximum benefit and the critical depth of placement of the geocell mattress were obtained on the basis of the test results. All the tests under these series were conducted for a geocell mattress of a constant height i.e. for h/D ratio of 0.27. To find the influence of height (h) of the geocell mattress on the critical depth of placement of geocell mattress, tests were done under series B5 at an increased height of geocell mattress (i.e. h = 0.8D).

The tests under series C were conducted using the geocell mattress prepared in diamond pattern. The parameters investigated include, the pocket size and the depth of placement of geocell mattress. All test program under series C1 to series C4 were kept similar to that of series B1 to B4, so that, in addition to the behaviour of the geocell mattress prepared using the diamond pattern, a direct comparison between the performance of the geocell reinforcement formed in diamond and chevron pattern could be obtained. The pocket size and the critical depth of placement giving maximum performance improvement with geocells formed in diamond pattern were thus obtained. Also, a comparison between the two patterns of formation was studied and the more efficient pattern of formation giving better performance improvement was arrived at on the basis of the test results.

The tests under series B1 to B4 and C1 to C4 were carried out with geocell mattress of height, h = 0.27D and the infill soil compacted to a dense state (i.e. ID = 80%). The comparisons between the two patterns were further carried out for different configurations of geocell mattress. The height and pocket size of geocells; relative density of the infill sand for a geocell mattress prepared using the diamond pattern were varied under test series C5, C6 and C7 respectively. Similar tests with geocell mattress prepared using the chevron pattern of formation were carried out in the later sections (Test series D3, E1, E2, E3, F3 and G3). Thus the influence of height and pocket size of geocells; relative density of the infill sand on the more efficient pattern of formation was obtained

Under series D to series G, tests were performed on geocell-sand mattress overlying soft clay subgrade. The parameters varied in these series are the relative density (ID) of infill sand, the pocket size (d) and the height (h) of the geocell mattress. In each series, a combination of two parameters was kept constant while the third parameter was varied to find its influence on the overall performance of the reinforced structure. The critical depth

of placement and more efficient pattern of formation of the geocell mattress, obtained from earlier tests, were used in these series. Under series D1, tests were conducted with varying pocket size while the relative density of sand and the height of geocell mattress were kept constant. Keeping the height constant, the variation of pocket size was investigated at different relative densities under series D2 and D3. Thus the influence of relative density and pocket size for a particular height was obtained. Subsequently, the variation of relative density and pocket size were investigated for higher heights of geocell mattress under series E, F and G. Under each series, a combination of height and relative density was kept constant while the pocket size was varied. From the tests conducted under these series, the critical dimensions of the geocell mattress and the relative density of the infill sand, giving maximum performance improvement were arrived at.

The added benefit due to the provision of a planar geogrid layer along with the geocell mattress was investigated in series H, I, J and K. As per the findings of Dash et al. (2001b), the planar geogrid layer was placed below the geocell mattress to get maximum performance improvement. The parameters investigated are the relative density of the infill soil, pocket size and height of geocell reinforcement. Tests under series H1, H2 and H3 were carried out at different relative densities of the infill sand and pocket sizes of the geocells varying one parameter at a time. These series of tests were carried out at a constant height of geocell mattress. The variation of pocket size and relative density was investigated for different heights of the geocell mattress under series I to series K. The critical parameters of the composite structure giving maximum performance improvement were obtained on the basis of the test results.

3.4 TEST DESCRIPTION

3.4. 1 Test Set-up

The Test Set up required for the study was constructed inside the laboratory. The test pit was 2000 mm long, 2000 mm wide and 1500 mm deep. The schematic diagram view and the photograph of the test setup are shown in Fig. 3.22 and Photo 3.3 respectively.

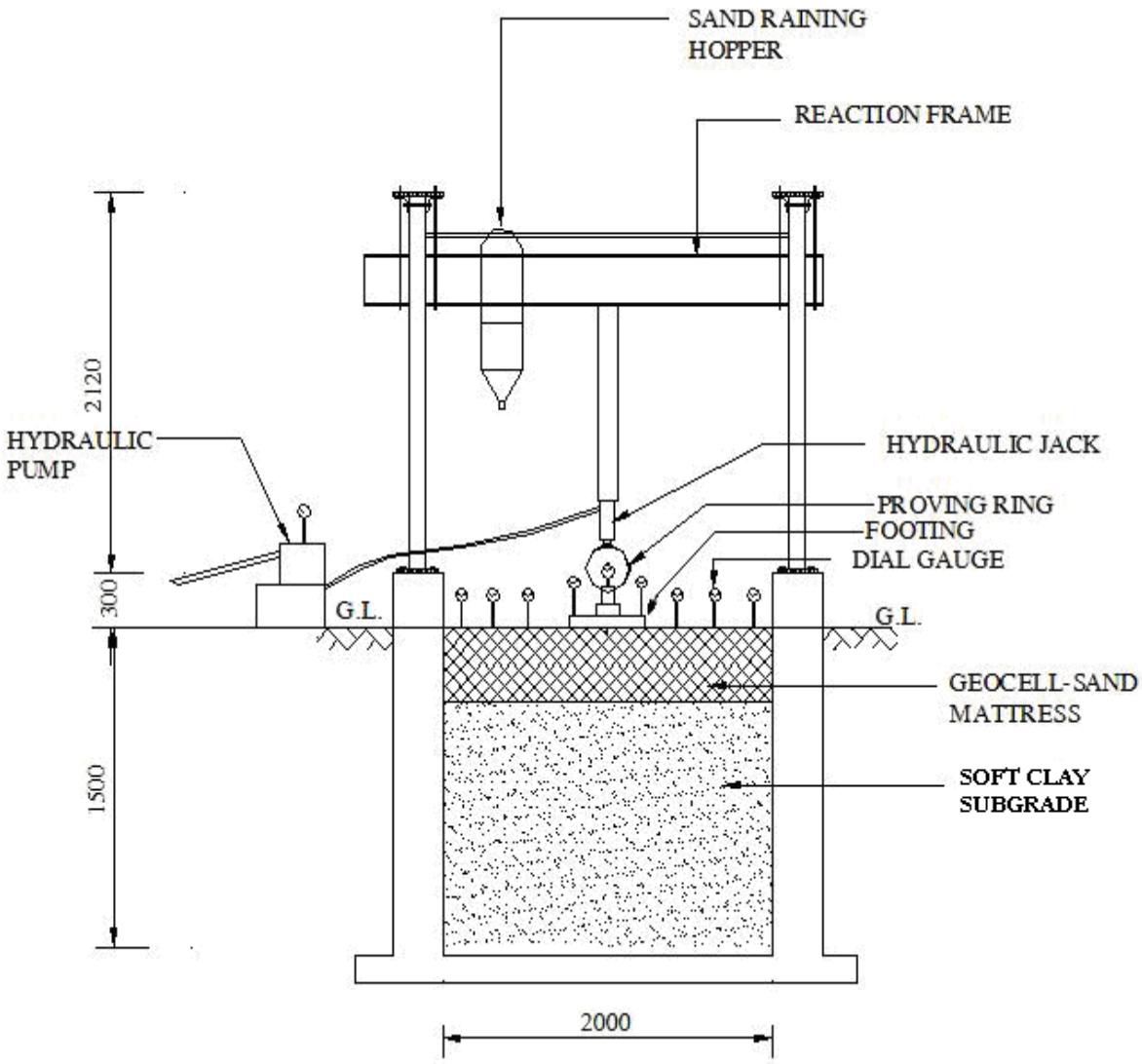

Fig. 3.22 Schematic diagram of the test setup(Not to scale, all dimensions are in mm)

Photo 3.3 Complete test setup

The loading frame comprises of a reaction frame of I-section with suitable foundations anchored to the ground, to which is clamped a manually operated hydraulic jack of 1000 kN capacity. The load from the hydraulic jack was transferred to the subgrade soil through the circular model footing having a diameter of 300 mm. A pre-calibrated proving ring placed between loading jack and the footing was used to measure the magnitudes of applied load. A ball bearing was positioned between the proving ring and the footing to ensure that the load applied to the footing was vertical. Dial gauges having a least count of 0.01 mm were used to measure the settlement of the footing and the surface deformations. Two dial gauges were placed on top of the footing diagonally to measure the average settlement of the footing. Three dial gauges were placed on either sides of the footing at a distance of one, two and three times the diameter of the footing, from the centre of the footing to record the surface deformations (settlement/heave) due to applied load. The dial gauges were fixed to a reference beam through nut and bolt

arrangement. The spindle of the dial gauges for measuring deformation on fill surface rested on small plates made from Perspex sheets placed over the subgrade soil. The failure wedge in dense sand bed under strip loading (of width B) is found to be extended around 3B on either side of the footing center line and at a depth of about 1.1B from the footing base (Chummar, 1972). In case of loose sand and soft clay, failure of the foundation is generally by punching mode and the side wise extent of failure wedge is smaller than 3B. For the present study, the depth and width of the foundation was 5D and 6.6D respectively, where 'D' is the diameter of the footing. With geocell reinforcement the fill surface is found to undergo settlement, which is discussed in Chapter 5. This indicates that the geocell mattress sinks down, under footing penetration, and hence is pulled away from the wall of the tank and that the wall does not have any effect on the performance of the reinforcement. From these observations, it could be concluded that the tank used in the current investigation is considerably large enough and is not likely to interfere with the zone of deformation of soil and geocell and hence the experimental results.

3.4.2 Test Bed Preparation

The model test beds were constructed within the test pit. The method of preparation of different layers of the test bed is described below.

3.4.2.1 Preparation of the clay subgrade

The soil was pulverized, mixed with pre-determined amount of water and stored in airtight containers for about a week before it can be used. This curing was done in order to achieve moisture equilibrium condition in the soil. The soil was placed in the tank, leveled out and compacted in a layer of 50 mm each till the desired depth in the tank was reached. The compaction was done by allowing the rammer to fall from a certain height

onto the plywood board placed on the soil surface. To achieve uniform compaction of each layer, equal number of blows was applied at all heights. The number of blows required to compact the soil to a required density was determined a priori by conducting some trial tests. Thus by controlling the water content and the compaction effort, a fairly uniform test condition was maintained. A photographic view of the compacted clay bed is shown in Photo 3.4. Undisturbed samples were collected from different locations of the clay bed, using the core cutter, to determine the in situ water content and density of the soil. Vane shear tests were carried out to determine the undrained shear strength of the test bed**.** For these tests, cylindrical mould was gently inserted with its open end pressing against the soft clay bed. The closed end of the mould had a hole of 1 mm diameter to prevent air locking. The filled mould was then mounted on the motorised vane shear apparatus and the tests were carried out. Table 3.5 shows that the average shear strength of the subgrade soil to be 6 kPa, thus representing the poor condition of the soil. The range of variation of the parameters, in the test bed, and their average values are also reported in Table 3.5. The coefficient of variability of test data (i.e. moisture content, bulk density and shear strength) pertaining to the soil samples, collected from different locations of the test bed was found to be within 1%. The degree of saturation (S_r) of the soil was back calculated from the measured value of moisture content and bulk density and was found to be 98%.

Table 3.5 Properties of clay subgrade.

Parameter	Range	Average Values
Moisture Content	33.56 - 34.59%	34 %
Unit Weight	18.06 - 18.12 kN/m^3	18.1 kN/m^3
Vane Shear Strength	5.43 - 6.33 kPa	6 kPa

Photo 3.4 View of the prepared clay subgrade

3.4.2.2 Preparation of overlying sand bed

Unreinforced sand bed

For the unreinforced sand bed, sand was placed directly on top of the subgrade soil using raining technique (Photo 3.5). The schematic diagram of the sand raining device is shown in Fig. 3.23. The sand was stored in a hopper which has a holding capacity of 25 kg. During the raining process, the plastic stopper at the end of the hopper was opened and sand was allowed to fall through a 690 mm long hollow pipe which had an internal diameter of 31 mm. A 60° inverted cone was connected to this pipe at its base for the uniform dispersion of sand. The height of fall was taken as the distance from the base of the cone to the level of the subgrade soil unto which the sand was to be poured. A given height of fall during raining was maintained through a small adjustable rod attached to the side of the pipe. By varying the heights of fall, a range of placement densities of sand

were obtained. To achieve lower range of relative densities, the bottom cone was removed and sand was allowed to fall freely. A calibration chart showing the relationship between the relative density and the corresponding height of fall for different cases is presented Fig. 3.24. In order to verify the accuracy and consistency of the density of sand, small aluminum cans of known volume were placed at different locations of the test tank. After the cans were filled with sand under raining during test bed preparation, they were taken out and their weights were measured. The coefficient of variability of the obtained values at different locations in the tank was found to be within 1.5%.

Photo 3.5 Sand raining in progress

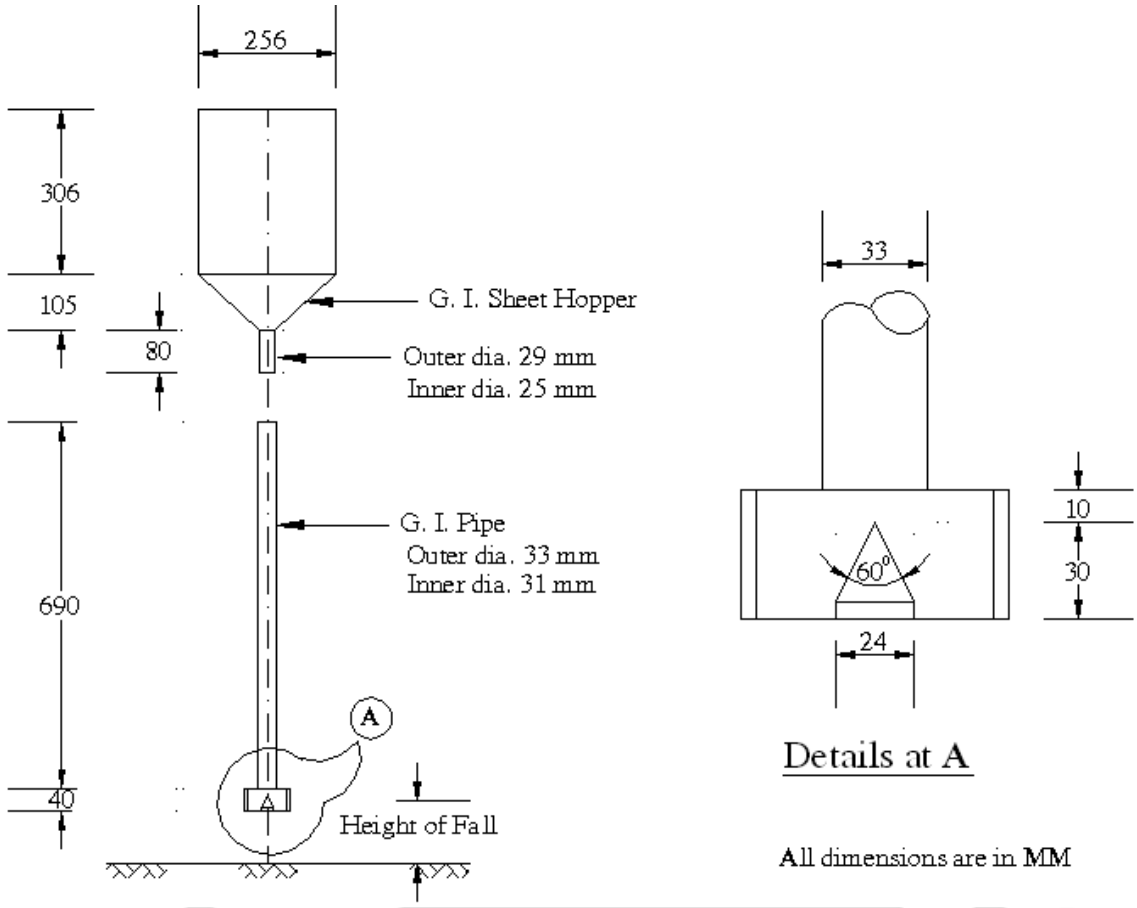

Fig. 3.23 Schematic diagram of sand raining device used in the study

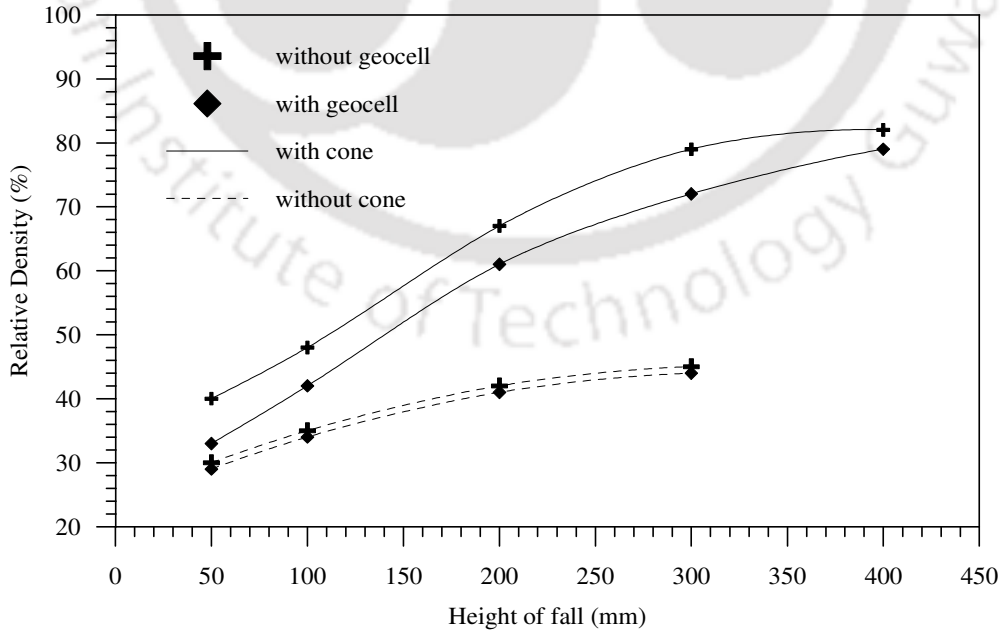

Fig. 3.24 Calibration chart showing relationship between relative density and height of fall of sand

Geocell reinforced sand bed

The geocell mattress was assembled by cutting long rolls of geogrids to get strips of required length and width and placing them in transverse and diagonal direction alternately. They were then connected by bodkin joints at the required interval so as to form honeycombed pockets. The prepared geocell mattress was placed on top of the clay subgrade and their pockets were filled with sand by raining technique as shown in Photo 3.6. The sand was rained from a pre-determined height to obtain a desired density (Fig. 3.24). It was observed that the presence of the geocell mattress caused some interference to the dispersion of the sand and the relative density thus obtained was relatively less. In order to compensate for this loss in relative density, the height of fall of sand was increased accordingly, as per the calibration. However, for the case when there was no cone at the bottom of the pipe, there was marginal difference (Fig. 3.24) between the reinforced and unreinforced cases. This is because the sand in this case is allowed to fall freely in a vertical direction without being dispersed, thus the interference due to the geocell walls is practically negligible. The pockets were filled in steps of about 50 mm each till the full height of the geocell mattress was reached. The density of the sand was checked by placing small aluminum containers within the geocell pockets at different locations. The coefficient of variability of the obtained values was found to be within 1.5%. The photograph showing a half filled geocell mattress is presented in Photo 3.7.

Photo 3.6 Sand raining in progress

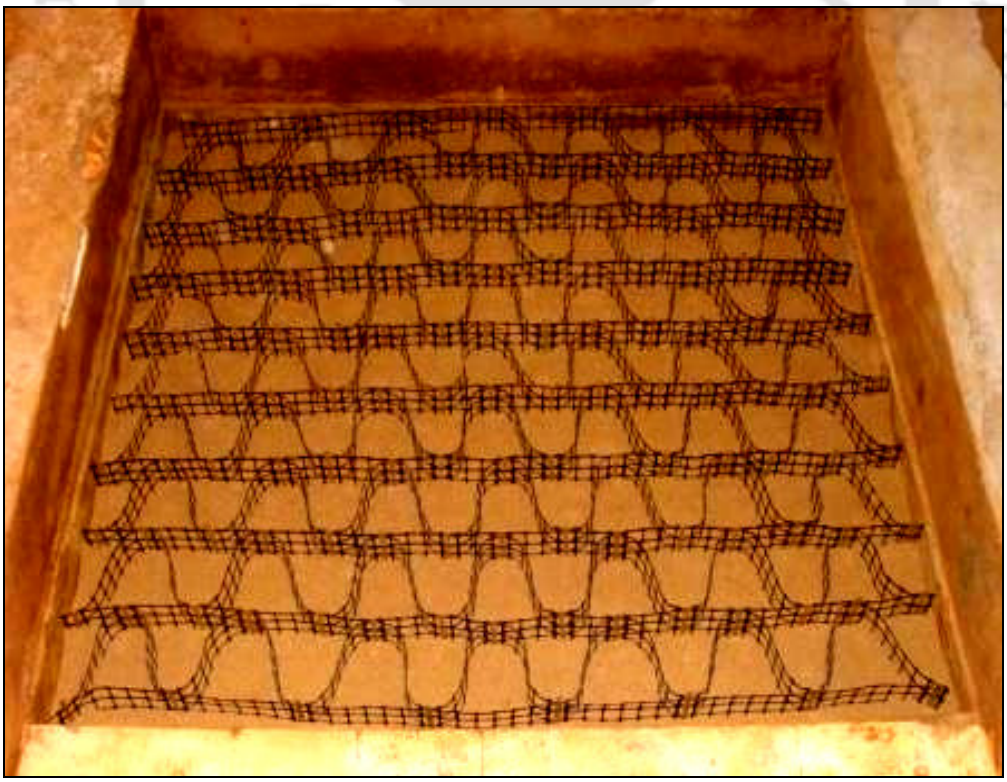

Photo 3.7 Half-filled geocell mattress

3.4.3. Test Procedure

Upon filling the test tank to the desired height, the fill surface was leveled and the footing was placed over it. The footing was placed at the centre of the tank, in such a way that in all of the model tests, its centre coincides with the centre of the central geocell pocket. The footing was loaded through a hydraulic jack and was pushed into the soil at a rate of nearly 0.002 m per minute. This relatively fast rate of loading would produce undrained response in the saturated clay bed, which is one of the worst field conditions expected as in this case the angle of friction of the saturated clay soil is zero. Such phenomenon is common in case of railways and highways, where the loading is transient in nature. The load transferred to the footing was measured by the pre-calibrated proving ring placed between the ball bearing and the loading jack. Footing settlements were measured through two dial gauges (Dg_1 and Dg_5; Fig. 3.20) placed on either side of the centre line of the footing. The footing settlement reported here is the average value of the readings taken at the two points. The deformations on fill surface were recorded by the dial gauges (Dg_2, Dg_3, Dg_4, Dg_6, Dg_7, Dg_8; Fig. 3.20). The resulting footing settlement and surface deformations were recorded at regular intervals. The loading was continued till a settlement of about 20% of the footing diameter was reached.

The test bed for each test was prepared afresh. The results obtained from the experiments, are presented and discussed in Chapters 4, 5 and 6.

भारतीय प्रौद्योगिकी संस्थान गुवाहाटी
Indian Institute of Technology Guwahati

CHAPTER 4

RESULTS AND DISCUSSIONS ON EXPERIMENTAL DATA

BEHAVIOUR OF UNREINFORCED SAND LAYER OVERLYING SOFT CLAY SUBGRADE

4.1 INTRODUCTION

In this chapter, the results of the tests that were carried out on soft clay subgrade only (Test Series A1) and on sand layer overlying soft clay subgrade (Test Series A3 to A6) are presented and discussed. The details of the test series are available in the preceding chapter (Table 3.4). The shear strength of the clay bed was kept constant at 6 kPa throughout. The parameters varied under series A3 to A6 are relative density (ID) and thickness (H) of the sand layer. The results obtained from this section are used further in the following chapters to compare and quantify the benefit of using geocell reinforcement.

4.2 SOFT CLAY SUBGRADE

Test Series A1 was carried out on clay subgrade alone, prepared at an undrained shear strength of 6 kPa. The tests were repeated in order to verify the repeatability of the test data. The results obtained are discussed in details in the following section. The variation of bearing pressure with footing settlement for clay subgrade is depicted in Fig. 4.1. The figure shows a close match between the results from the repeated tests (Test 1 and Test 2) which indicate the uniformity achieved in the test conditions. It could be observed that at a pressure of about 25 kPa, the footing continues to settle and the pressure-settlement plot is almost vertical. Hence the ultimate bearing capacity of the clay subgrade is 25 kPa.

Fig. 4.2 shows the surface deformation profile at different footing settlements. The footing settlement ‘s’ and surface deformation ‘δ’ (settlement/heave) are expressed in

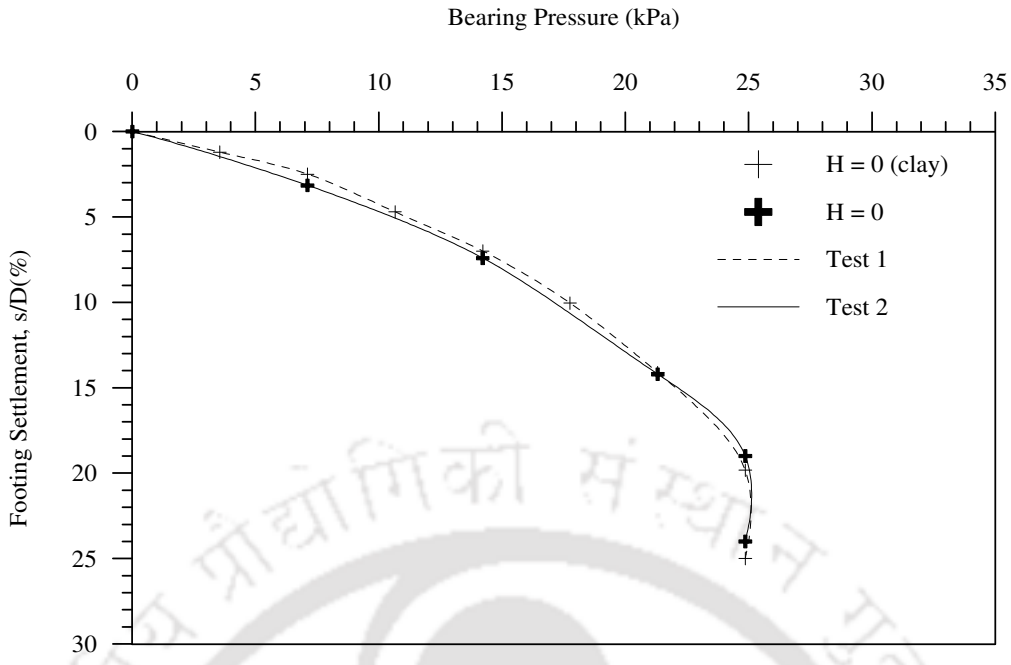

Fig. 4.1 Variation of bearing pressure with footing settlement for an unreinforced soft clay subgrade – Test Series A1

non-dimensional form in terms of footing diameter (D) as s/D (%) and δ/D (%) respectively. In all the graphs, settlements are reported with a positive sign (+) and heave with a negative sign (−). As the readings were noted at incremental loads, it is not possible to present these results at regular intervals of settlement. At higher levels of settlement (s/D = 14%) the footing has settled more on its right side than on the left side indicating that it has undergone rightward rotation. The corresponding variations of average (i.e. average of left and right side readings) deformation on fill surface (δ) at a distance of x = D, 2D, and 3D from the centre of footing; with footing settlement are presented in Fig. 4.3. The footing has undergone substantial heaving at x = D. This heaving reduces with an increase of distance (x) and becomes marginal at x = 3D. The clay subgrade being saturated and tests being run at a faster rate, leads to an undrained condition. Hence, practically there is no volume change that takes place leading to heaving on the fill surface.

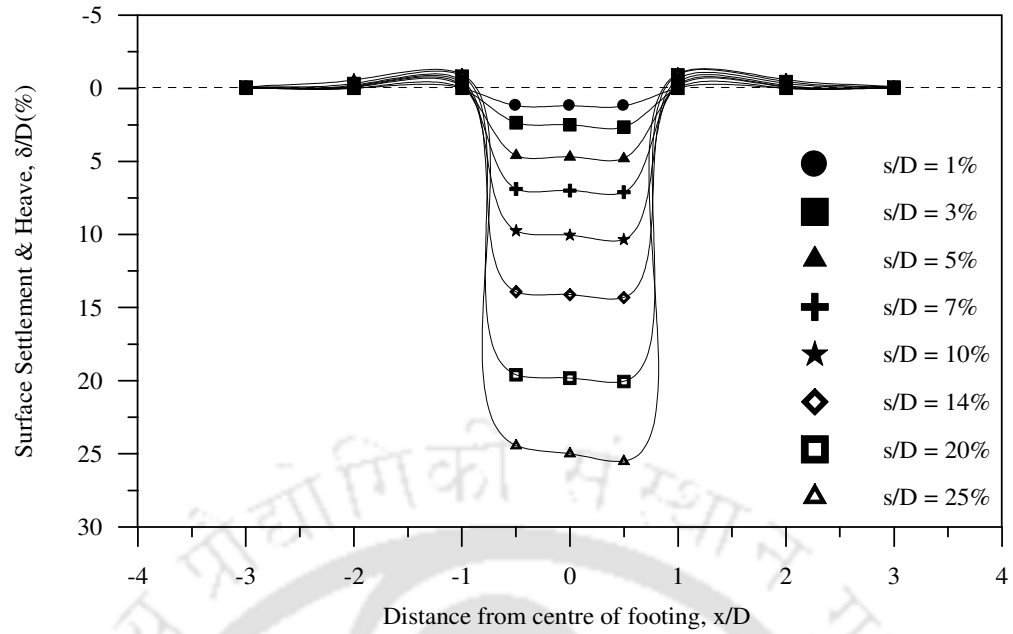

Fig. 4.2 Surface deformation profiles for an unreinforced soft clay subgrade (Test 1) – Test Series A1

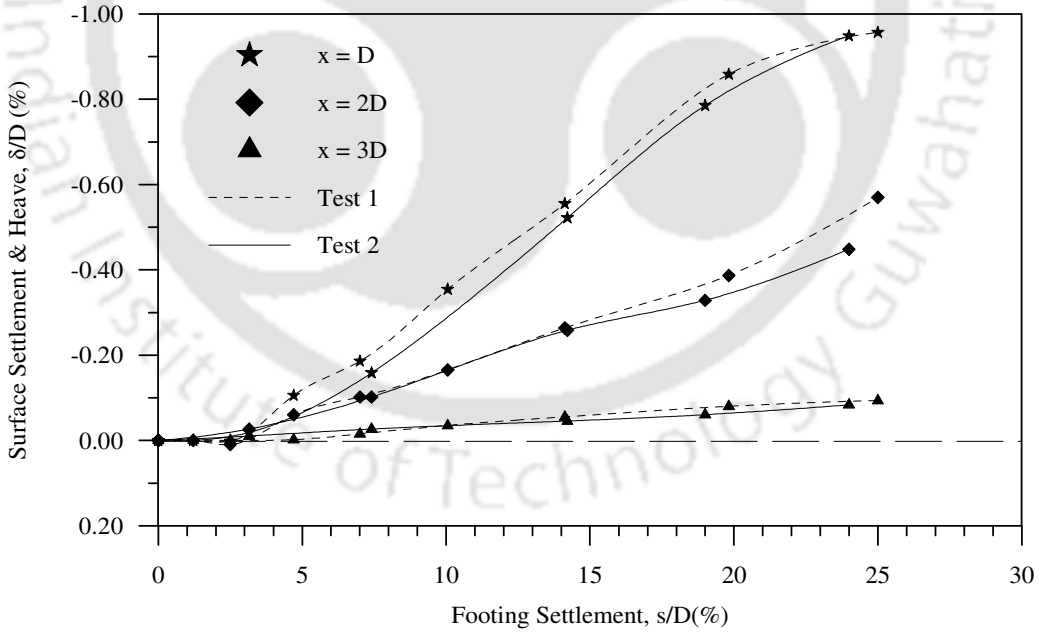

Fig. 4.3 Variation of average surface deformation with footing settlement at a distance x = D, 2D and 3D from the centre of the footing, for an unreinforced soft clay subgrade – Test Series A1

4.3 SAND LAYER OVERLYING SOFT CLAY SUBGRADE

Tests under series A3 to A6 were carried out with sand layer overlying the soft clay subgrade. In these tests the thickness of the sand layers (H) was varied from 0.37D to 1.17D and the relative density of sand (ID) was varied from 35% to 80%.

4.3.1 Influence of relative density (ID) of sand

Variation of bearing pressure with footing settlement for different relative densities of sand with H/D = 0.37 are shown in Fig. 4.4. The bearing capacity improvement due to the sand layer is quantified using a non dimensional factor, IF_s. This factor is defined as the ratio of footing pressure (q_s) with sand layer overlying clay subgrade at a given settlement to the corresponding footing pressure (q_o) with soft clay subgrade alone. Fig. 4.5 depicts the variation of IF_s with footing settlement as obtained from Fig. 4.4. It could be observed that the increase in the bearing capacity (IF_s) is more initially but continues to decrease with increase in settlement upto about 15% of the footing diameter beyond which it remains almost constant. With the increase in footing penetration (s), the sand layer continues to deform and tends towards failure thereby leading to a reduction in the performance improvement factor (IF_s).

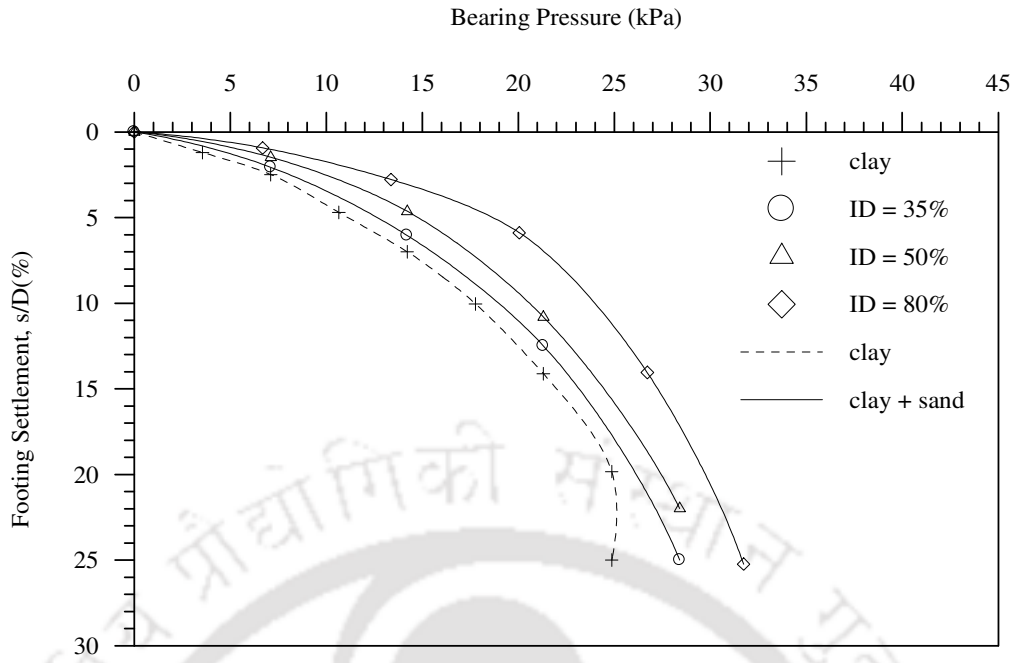

Fig. 4.4 Variation of bearing pressure with footing settlement for different relative densities (ID) of overlying sand – Test Series A3, H = 0.37D

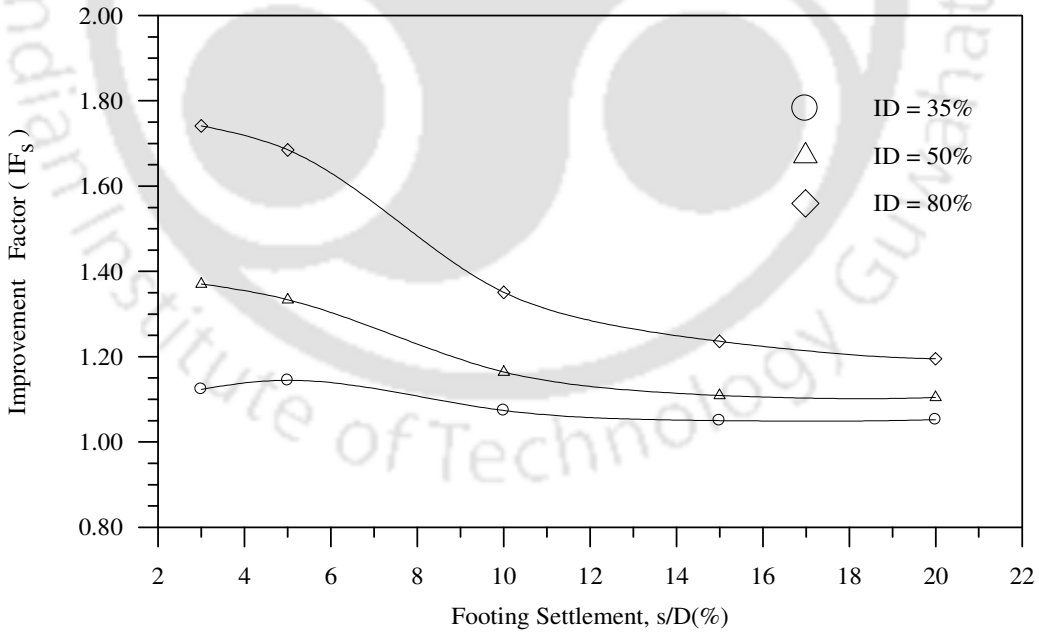

Fig. 4.5 Variation of improvement factor with footing settlement for different relative densities (ID) of overlying sand – Test Series A3, H = 0.37D

The surface deformation profiles for relative density of 35%, 50% and 80% are shown in Figs. 4.6, 4.7 and 4.8 respectively. It could be seen that in all of the cases, the footing has undergone rotation at settlement close to failure indicating that the sand layer has broken down. Variation of average surface deformation (δ) with respect to footing settlement at a distance (x) of D, 2D and 3D from centre of the footing, are depicted in Figs. 4.9, 4.10 and 4.11 respectively. At distance x = D, the fill surface has undergone mostly settlement. This is due to the dispersion of footing pressure over a relatively larger area. Little heave is observed in case of ID = 80% at settlement (s/D) beyond 15%. This is attributed to dilation of the dense sand. At distance x = 2D and 3D the fill surface has undergone only heaving, which is the cumulative effect of heaving of soft clay subgrade and the sand layer.

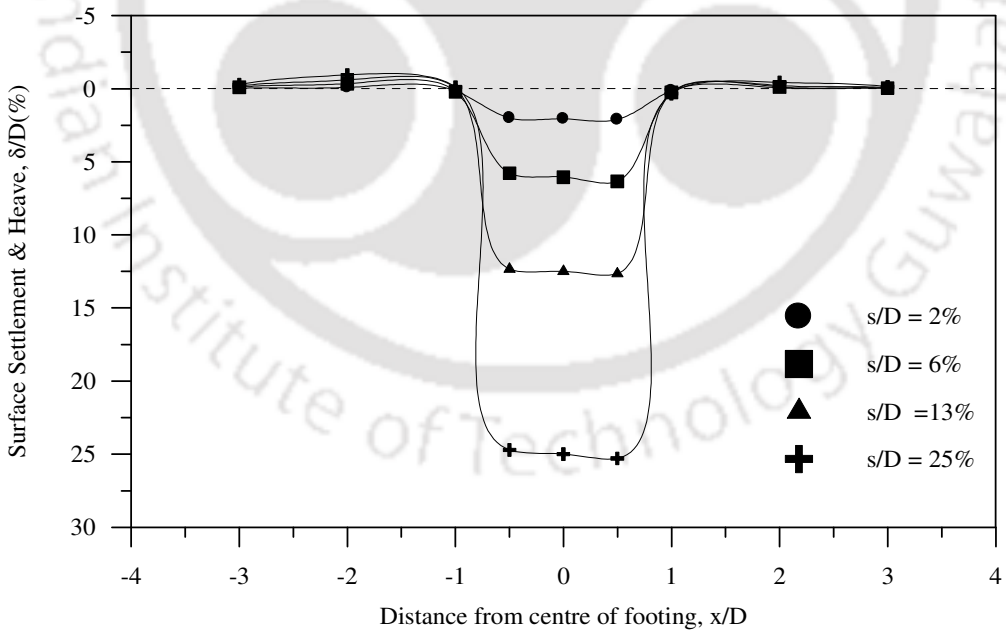

Fig. 4.6 Surface deformation profiles for an unreinforced sand bed prepared at a relative density of 35% – Test Series A3, H = 0.37D

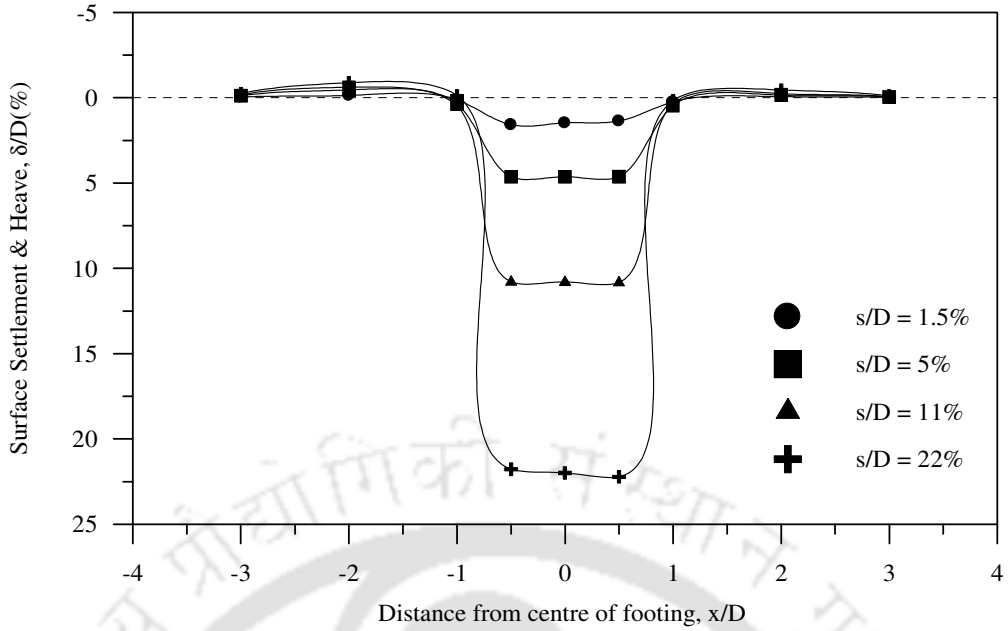

Fig. 4.7 Surface deformation profiles for an unreinforced sand bed prepared at a relative density of 50% – Test Series A3, H = 0.37D

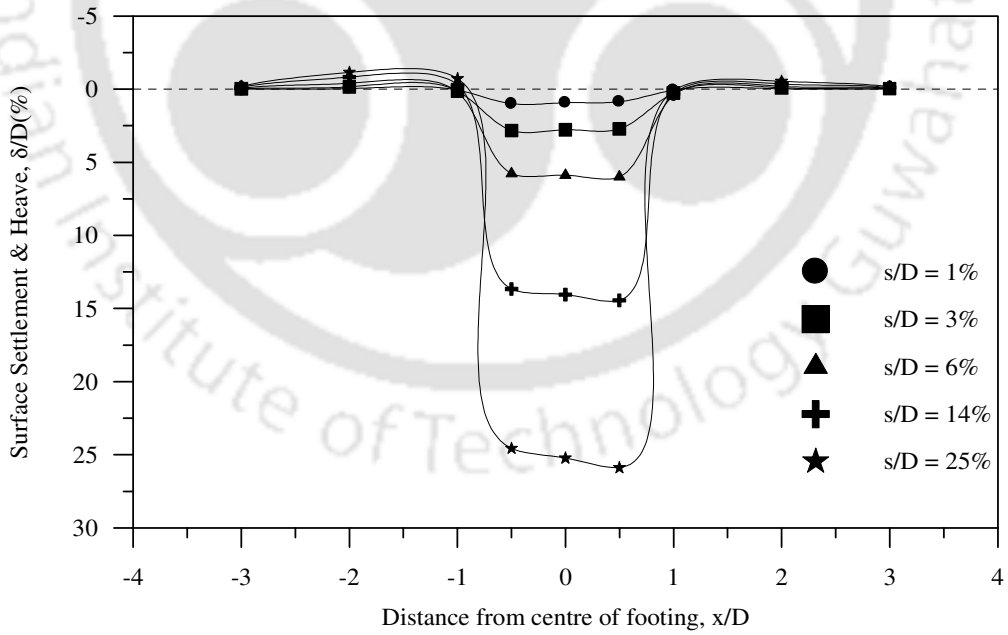

Fig. 4.8 Surface deformation profiles for an unreinforced sand bed prepared at a relative density of 80% – Test Series A3, H = 0.37D

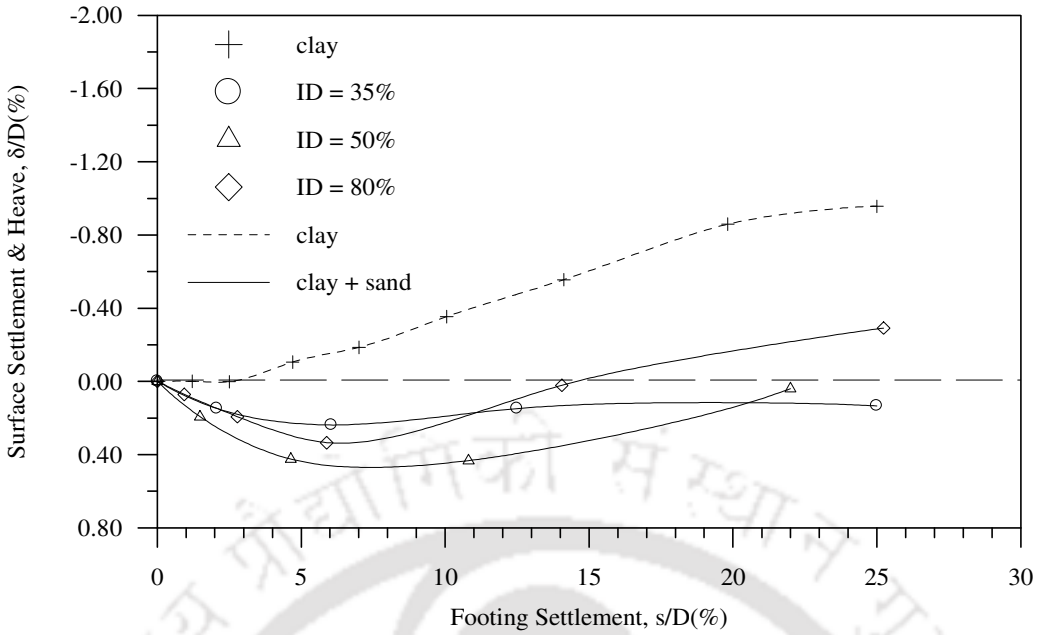

Fig. 4.9 Variation of average surface deformation with footing settlement at a distance x = D from the centre of the footing, for different relative densities (ID) of overlying sand – Test Series A3, H = 0.37D

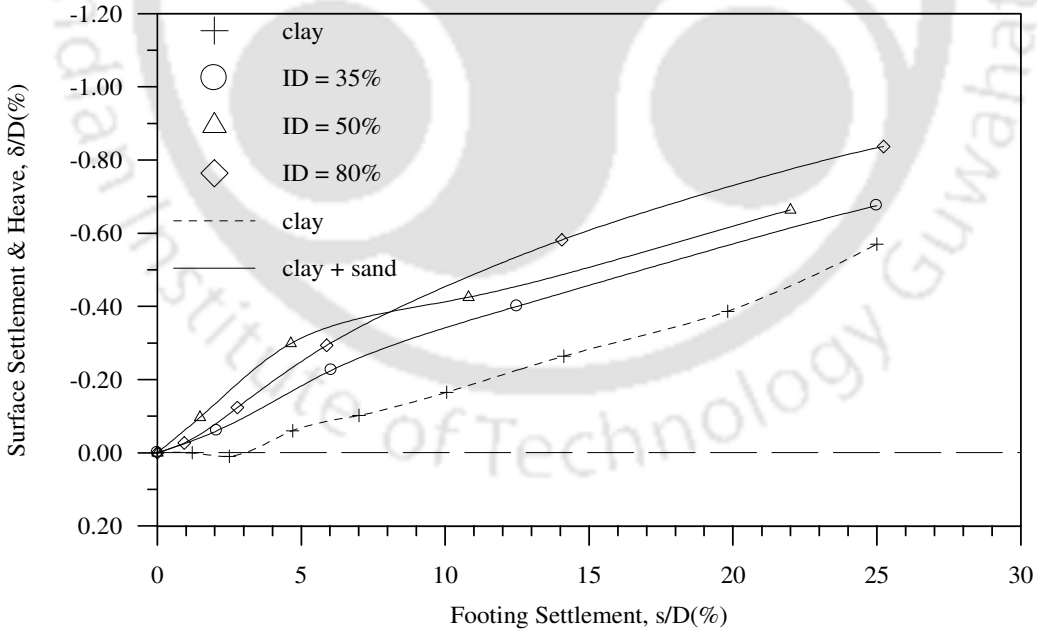

Fig. 4.10 Variation of average surface deformation with footing settlement at a distance x = 2D from the centre of the footing, for different relative densities (ID) of overlying sand – Test Series A3, H = 0.37D

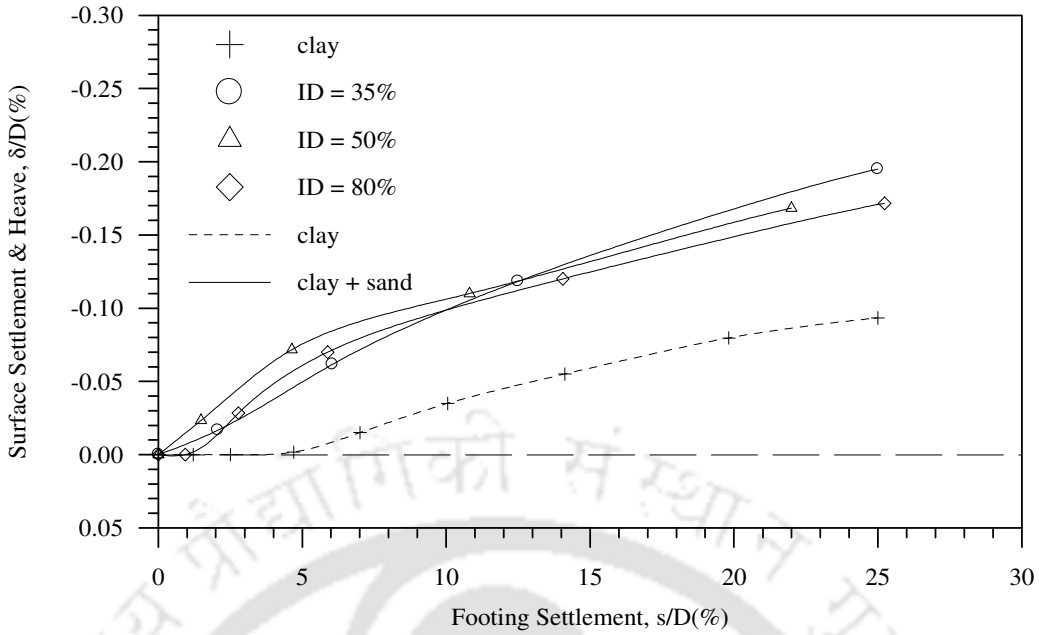

Fig. 4.11 Variation of average surface deformation with footing settlement at a distance x = 3D from the centre of the footing, for different relative densities (ID) of overlying sand – Test Series A3, H = 0.37D

Figs. 4.12, 4.20 and 4.28 present the pressure-settlement responses of the footing for different densities (ID) of overlying sand with H = 0.63D, 0.9D and 1.17D respectively. The corresponding variations of bearing capacity improvement factor (IF_s) are depicted in Figs. 4.13, 4.21 and 4.29 respectively. The trends of variation are similar to that with H = 0.37D. The performance improvement increases with increase in density of sand because of increased dilation and redistribution of footing pressure over relatively larger area. The corresponding surface deformations profiles are depicted in Figs. 4.14 to 4.16, 4.22 to 4.24, 4.30 to 4.32 and the variation of average surface deformation (δ) at x = D, 2D and 3D are depicted in Figs. 4.17 to 4.19, 4.25 to 4.27 and 4.33 to 4.35. The numerical values of the improvement factor (IF_s) for different cases are presented in Table 4.1. In general, the IF_s value for ID = 80% is proportionately higher compared to that with ID = 35% and 50%. The surface deformation plots show higher heaving with ID = 80% indicating that general shear tendency is more prominent in this case while in case with ID = 35% and 50%, punching mechanism is dominant.

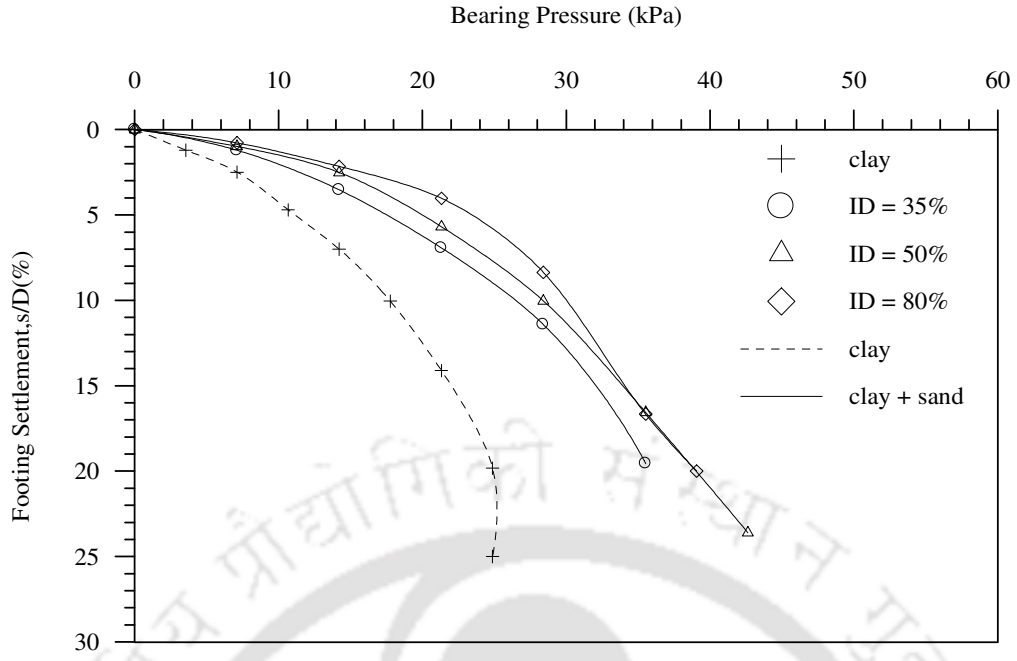

Fig. 4.12 Variation of bearing pressure with footing settlement for different relative densities (ID) of overlying sand – Test Series A4, H = 0.63D

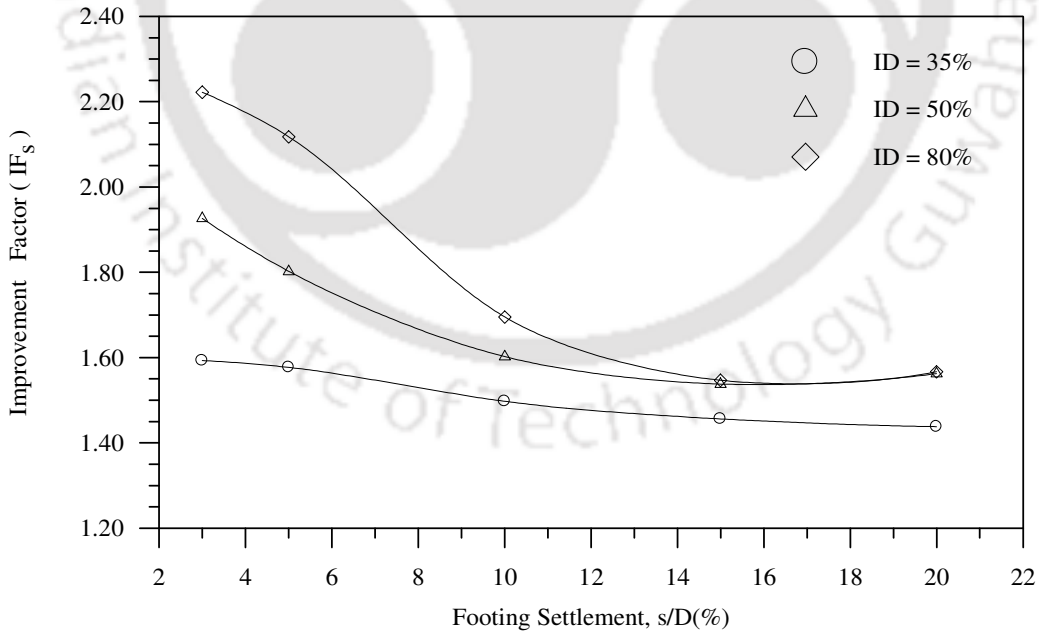

Fig. 4.13 Variation of improvement factor with footing settlement for different relative densities (ID) of overlying sand – Test Series A4, H = 0.63D

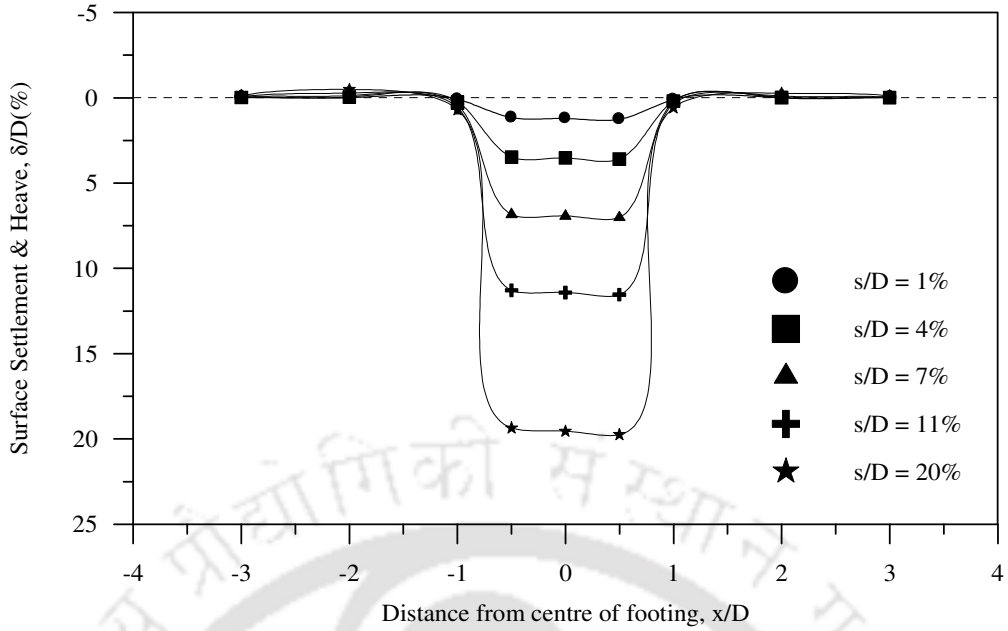

Fig. 4.14 Surface deformation profiles for an unreinforced sand bed prepared at a relative density of 35% – Test Series A4, H = 0.63D

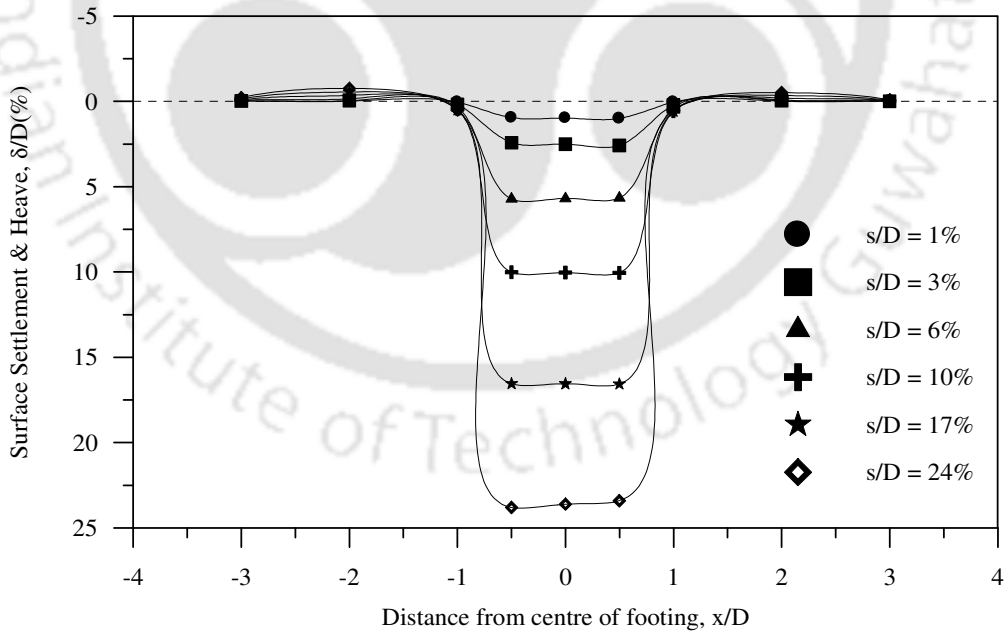

Fig. 4.15 Surface deformation profiles for an unreinforced sand bed prepared at a relative density of 50% – Test Series A4, H = 0.63D

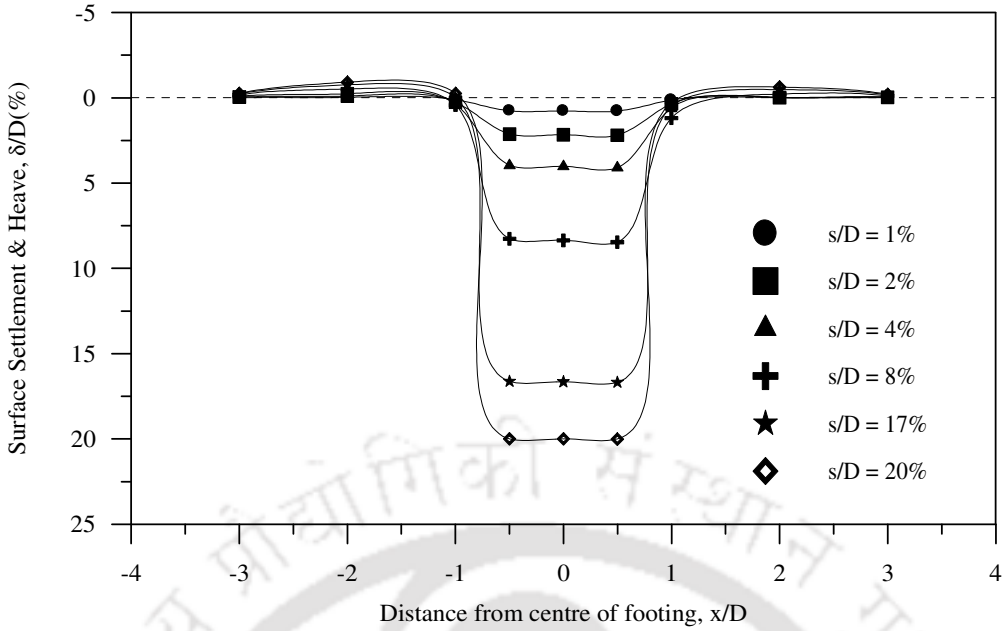

Fig. 4.16 Surface deformation profiles for an unreinforced sand bed prepared at a relative density of 80% – Test Series A4, H = 0.63D

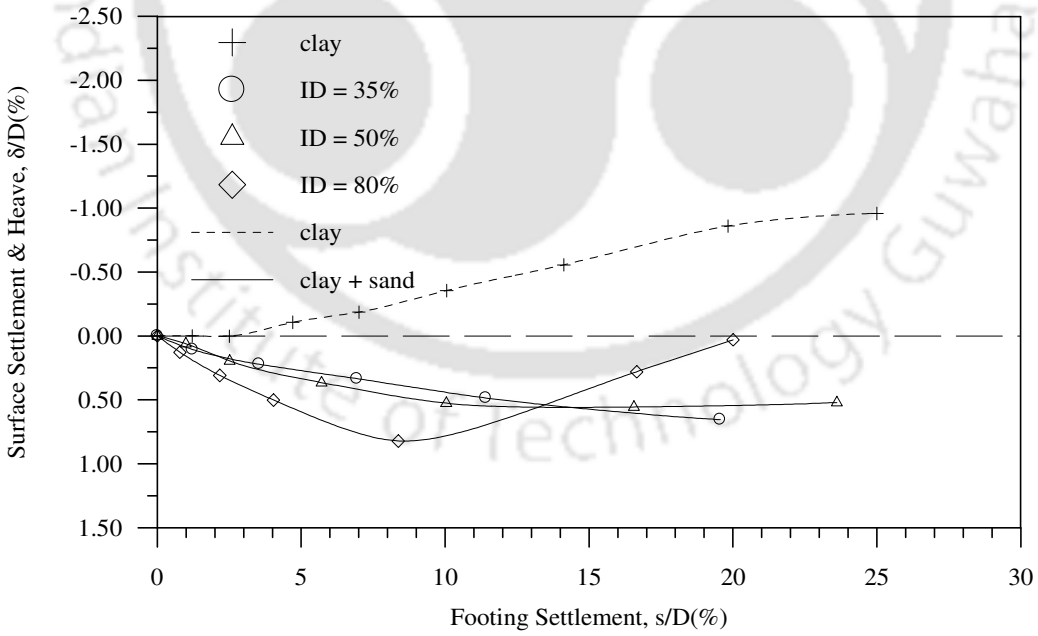

Fig. 4.17 Variation of average surface deformation with footing settlement at a distance x = D from the centre of the footing, for different relative densities (ID) of overlying sand – Test Series A4, H = 0.63D

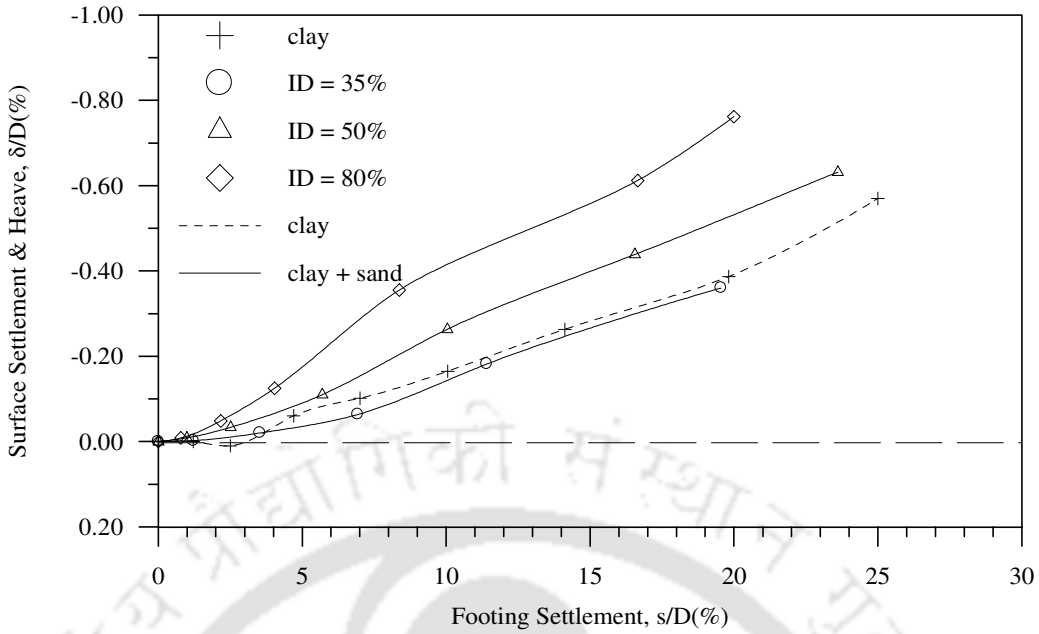

Fig. 4.18 Variation of average surface deformation with footing settlement at a distance x = 2D from the centre of the footing, for different relative densities (ID) of overlying sand – Test Series A4, H = 0.63D

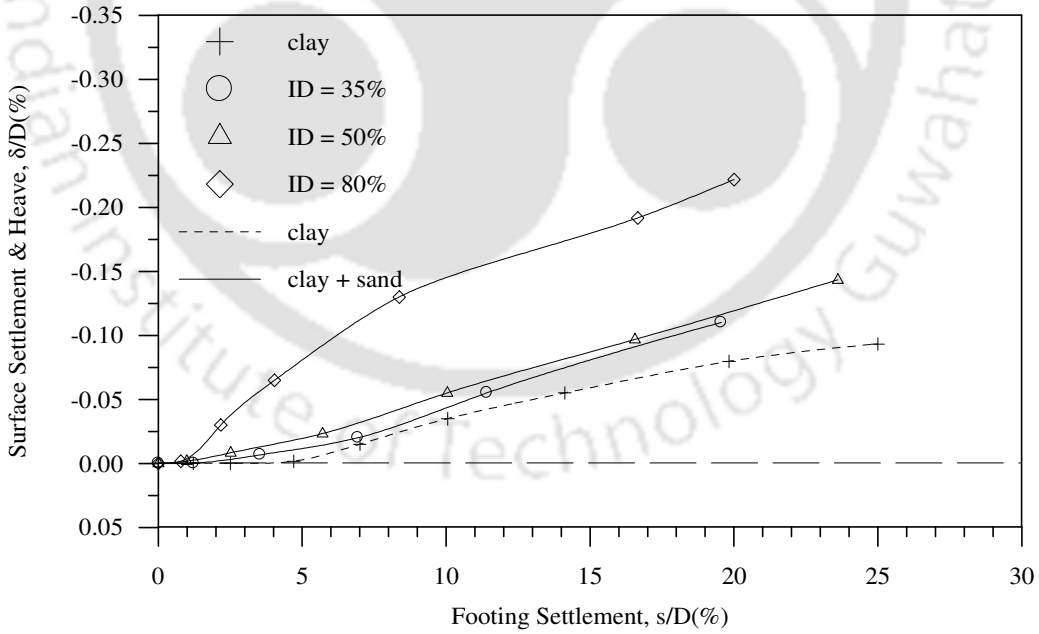

Fig. 4.19 Variation of average surface deformation with footing settlement at a distance x = 3D from the centre of the footing, for different relative densities (ID) of overlying sand – Test Series A4, H = 0.63D

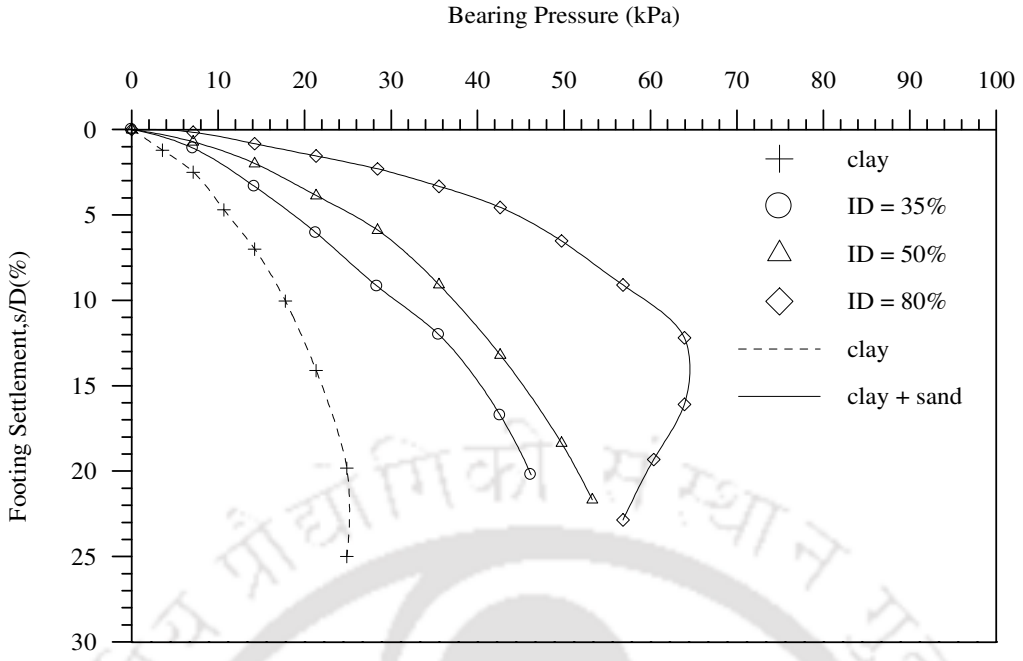

Fig. 4.20 Variation of bearing pressure with footing settlement for different relative densities (ID) of overlying sand – Test Series A5, H = 0.90D

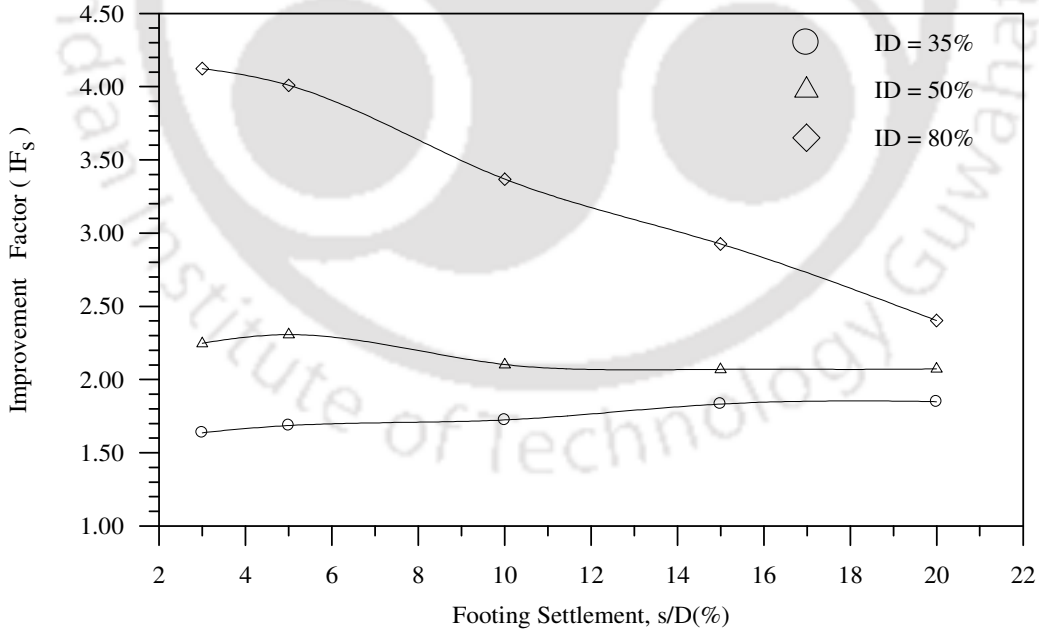

Fig. 4.21 Variation of improvement factor with footing settlement for different relative densities (ID) of overlying sand – Test Series A5, H = 0.90D

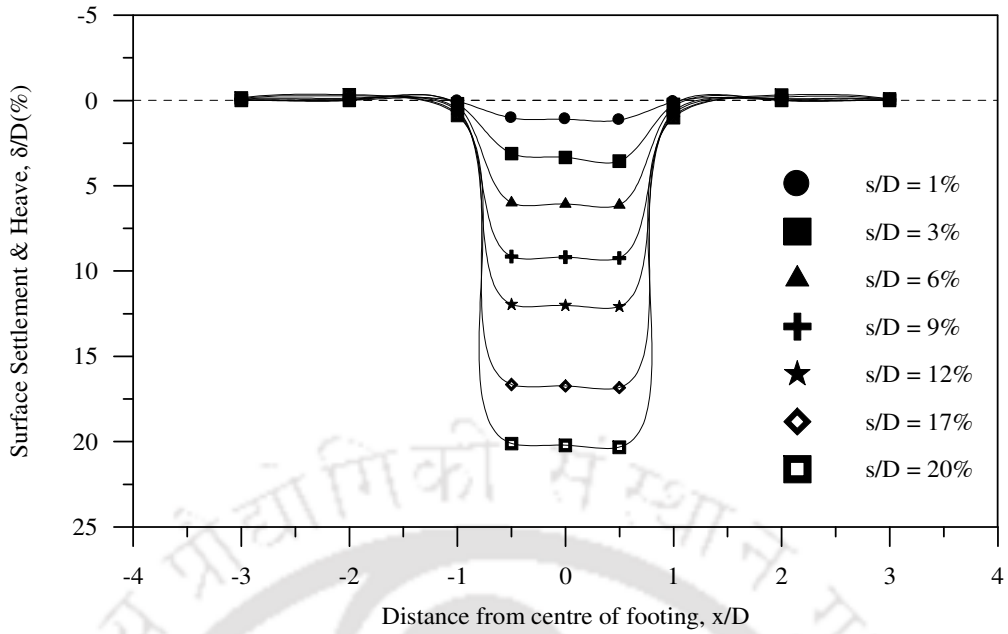

Fig. 4.22 Surface deformation profiles for an unreinforced sand bed prepared at a relative density of 35% – Test Series A5, H = 0.90D

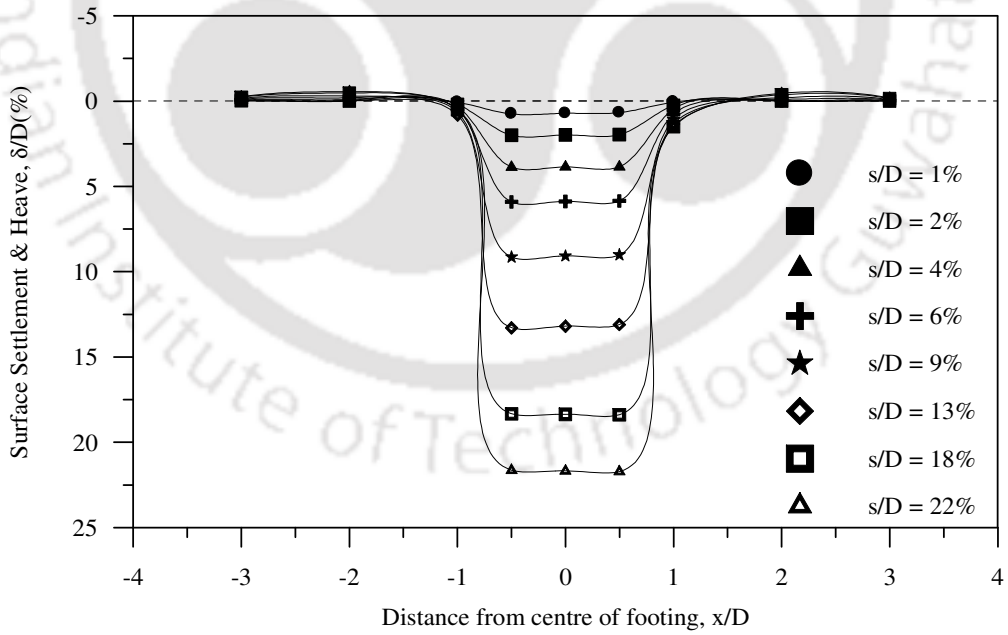

Fig. 4.23 Surface deformation profiles for an unreinforced sand bed prepared at a relative density of 50% – Test Series A5, H = 0.90D

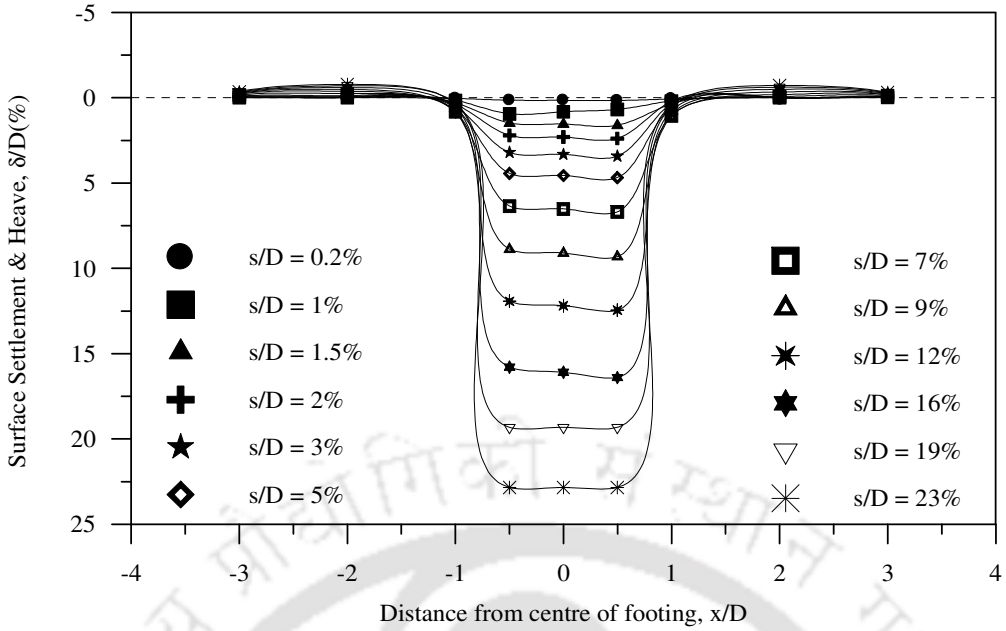

Fig. 4.24 Surface deformation profiles for an unreinforced sand bed prepared at a relative density of 80% – Test Series A5, H = 0.90D

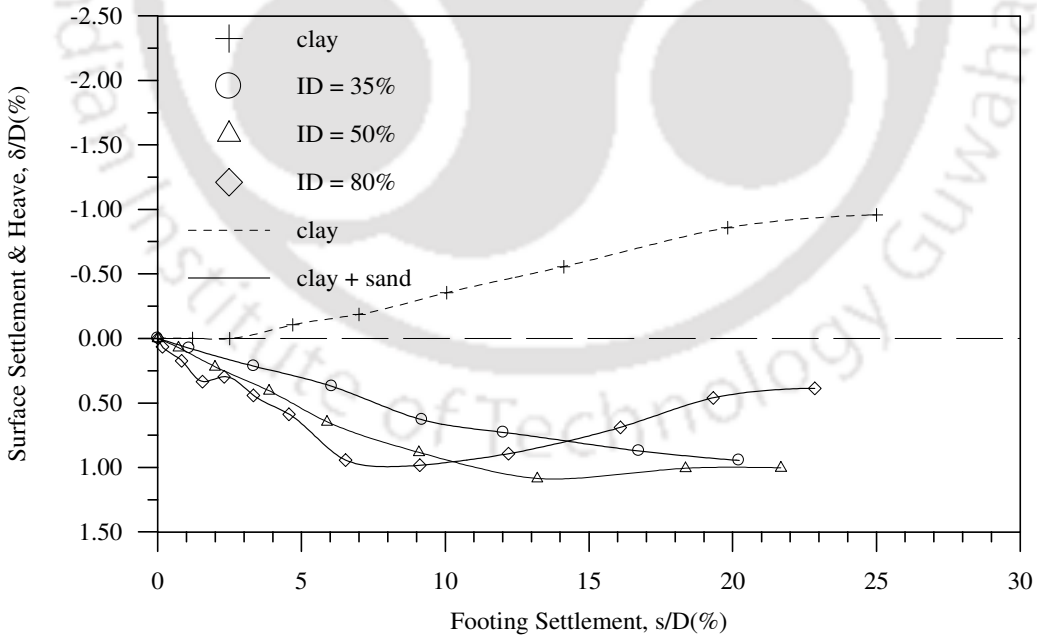

Fig. 4.25 Variation of average surface deformation with footing settlement at a distance x = D from the centre of the footing, for different relative densities (ID) of overlying sand – Test Series A5, H = 0.90D

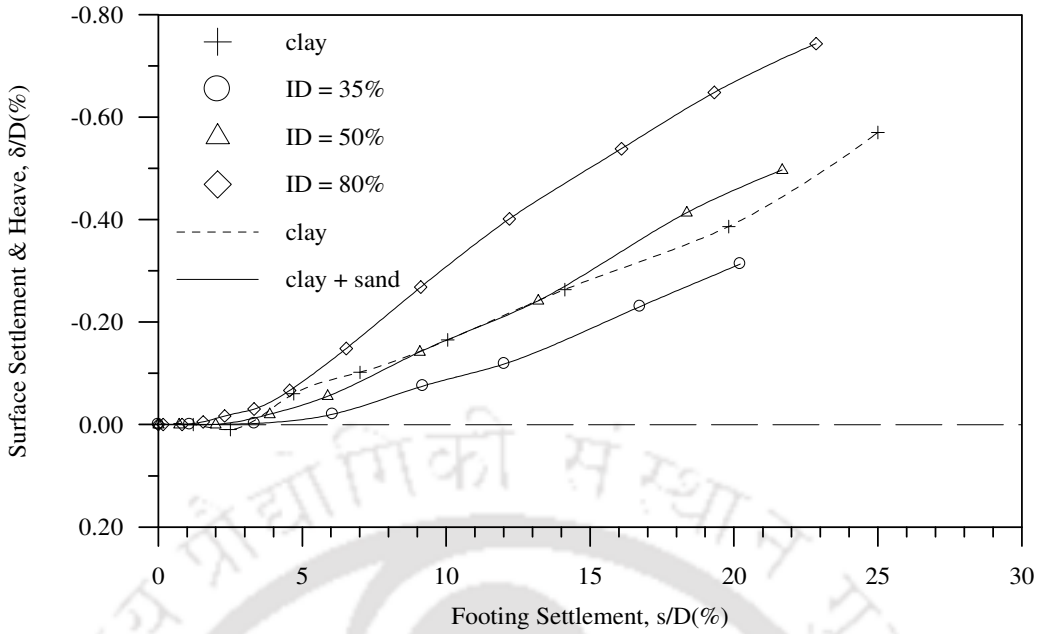

Fig. 4.26 Variation of average surface deformation with footing settlement at a distance x = 2D from the centre of the footing, for different relative densities (ID) of overlying sand – Test Series A5, H = 0.90D

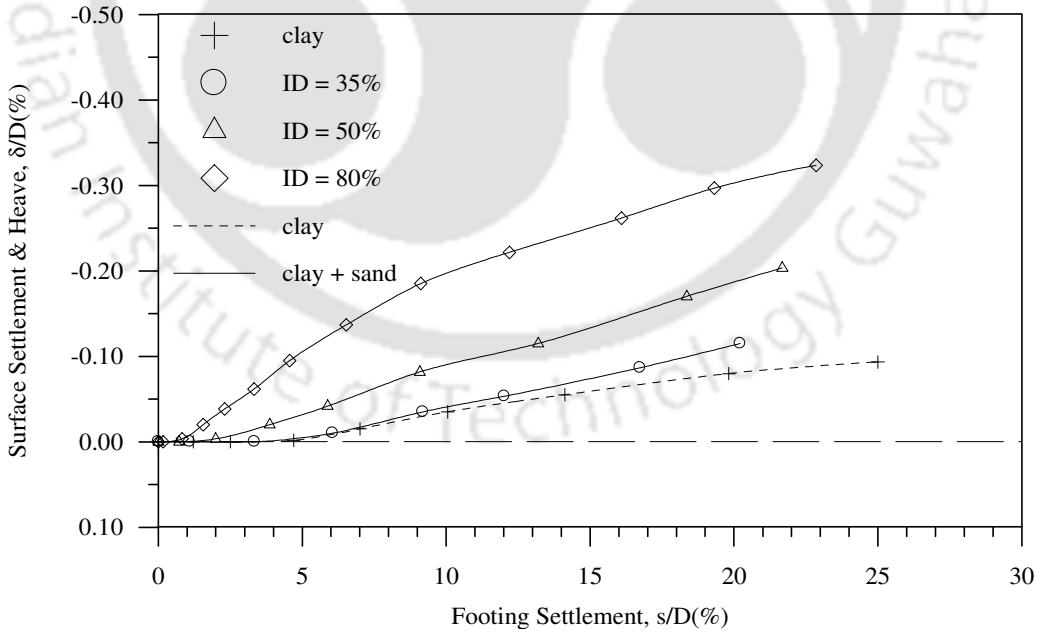

Fig. 4.27 Variation of average surface deformation with footing settlement at a distance x = 3D from the centre of the footing, for different relative densities (ID) of overlying sand – Test Series A5, H = 0.90D

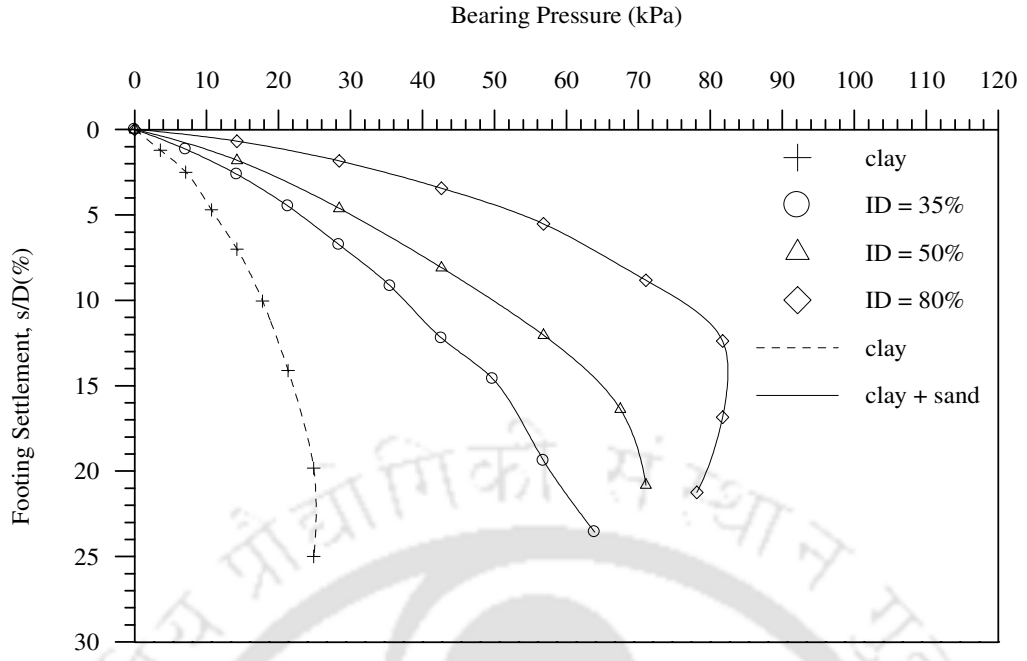

Fig. 4.28 Variation of bearing pressure with footing settlement for different relative densities (ID) of overlying sand – Test Series A6, H = 1.17D

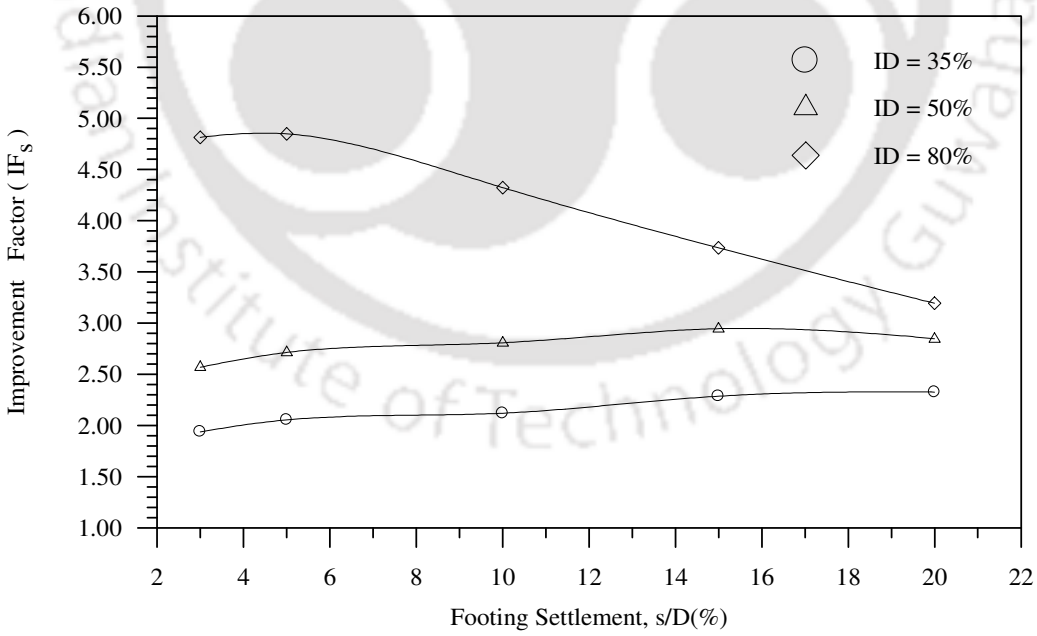

Fig. 4.29 Variation of improvement factor with footing settlement for different relative densities (ID) of overlying sand – Test Series A6, H = 1.17D

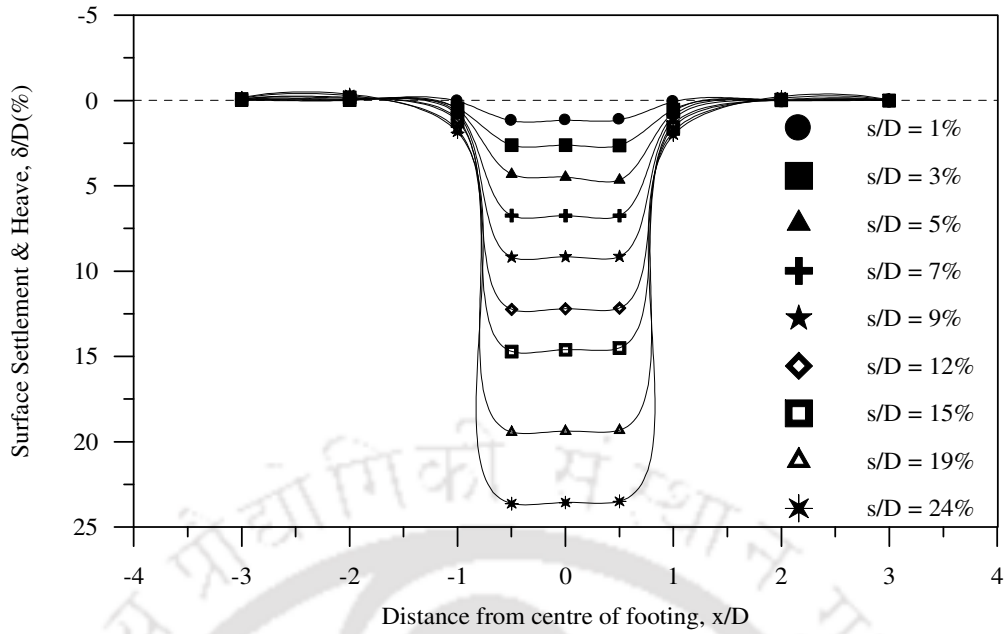

Fig. 4.30 Surface deformation profiles for an unreinforced sand bed prepared at a relative density of 35% – Test Series A6, H = 1.17D

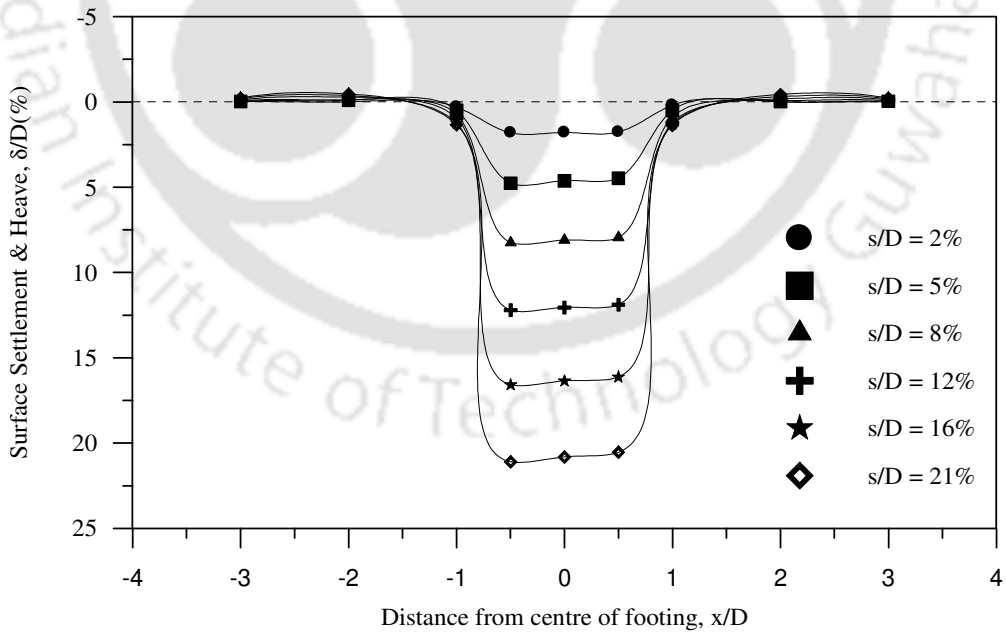

Fig. 4.31 Surface deformation profiles for an unreinforced sand bed prepared at a relative density of 50% – Test Series A6, H = 1.17D

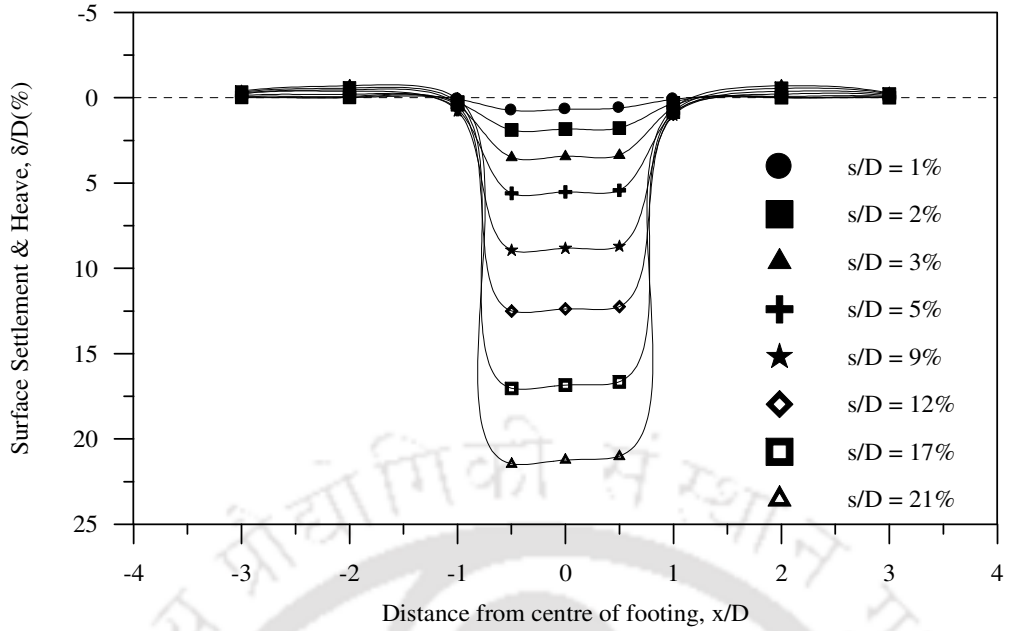

Fig. 4.32 Surface deformation profiles for an unreinforced sand bed prepared at a relative density of 80% – Test Series A6, H = 1.17D

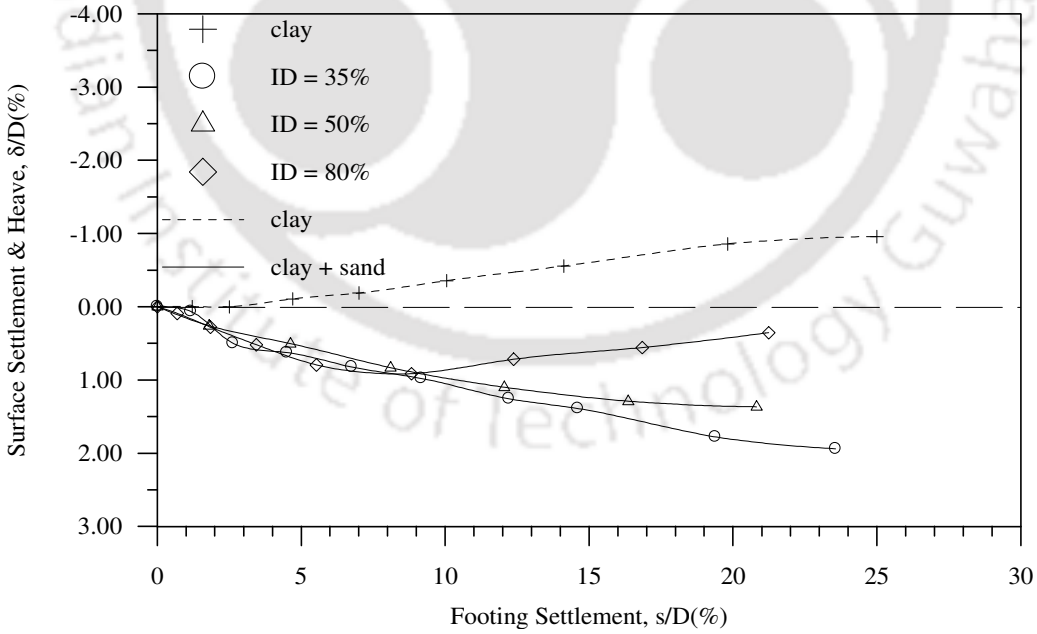

Fig. 4.33 Variation of average surface deformation with footing settlement at a distance x = D from the centre of the footing, for different relative densities (ID) of overlying sand – Test Series A6, H = 1.17D

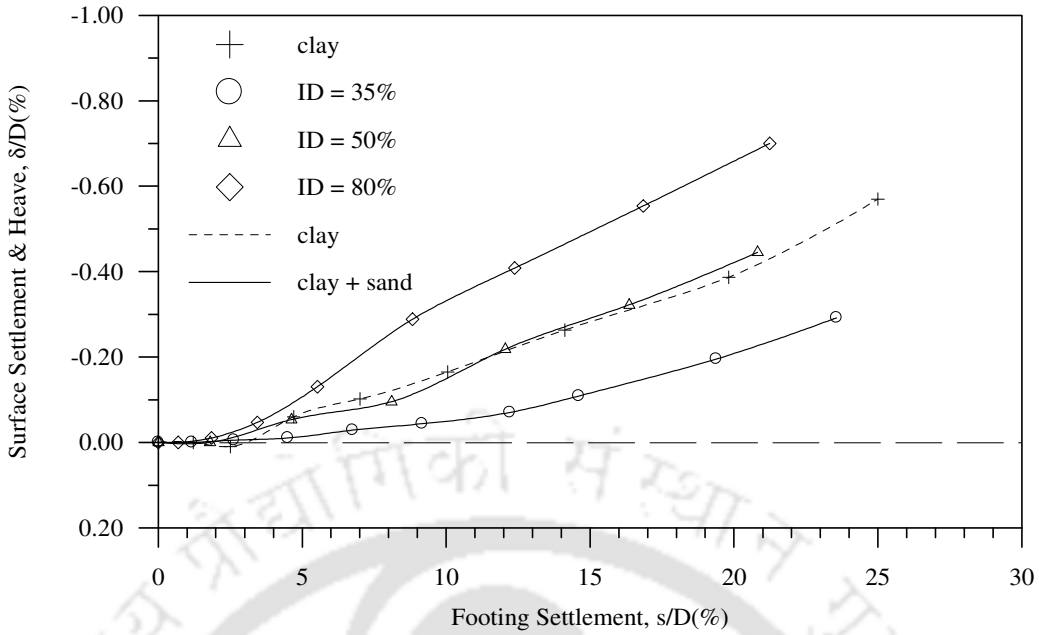

Fig. 4.34 Variation of average surface deformation with footing settlement at a distance x = 2D from the centre of the footing, for different relative densities (ID) of overlying sand – Test Series A6, H = 1.17D

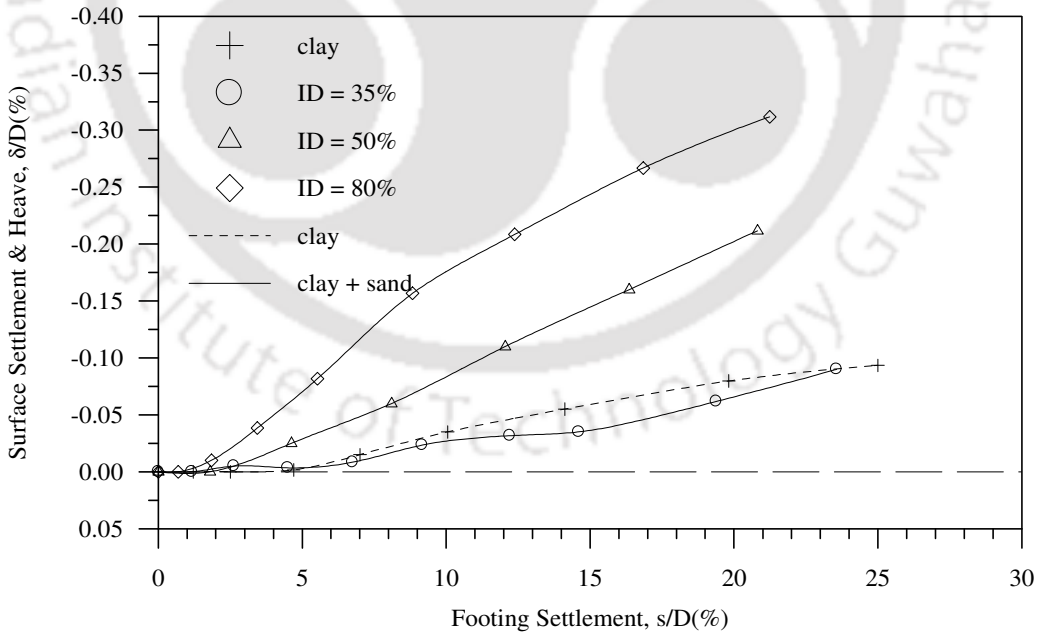

Fig. 4.35 Variation of average surface deformation with footing settlement at a distance x = 3D from the centre of the footing, for different relative densities (ID) of overlying sand – Test Series A6, H = 1.17D

Table 4.1 Summary of results in terms of bearing capacity improvement factor (IF_s) showing the influence of relative density (ID) of overlying sand.

Test Series	Variable Parameter		Bearing capacity improvement factor (IF_s)				
			(s/D) 3%	(s/D) 5%	(s/D) 10%	(s/D) 15%	(s/D) 20%
	H/D	ID(%)					
A3	0.37	35	1.12	1.14	1.07	1.05	1.05
		50	1.37	1.33	1.16	1.11	1.10
		80	1.74	1.69	1.35	1.24	1.20
A4	0.63	35	1.59	1.58	1.50	1.46	1.44
		50	1.93	1.80	1.60	1.54	1.56
		80	2.22	2.12	1.70	1.55	1.57
A5	0.90	35	1.64	1.69	1.72	1.83	1.85
		50	2.25	2.31	2.10	2.07	2.07
		80	4.12	4.01	3.37	2.93	2.40
A6	1.17	35	1.94	2.05	2.12	2.29	2.33
		50	2.57	2.71	2.81	2.94	2.85
		80	4.82	4.85	4.32	3.74	3.19

4.3.2 Influence of height (H) of sand

Bearing pressure versus settlement responses of soil bed with different thickness of overlying sand layers for relatively densities of 35%, 50% and 80% are depicted in Figs. 4.36, 4.41 and 4.46 respectively. The pressure-settlement responses for higher relative density (ID) and higher thickness (H) of sand layer have shown strain softening behaviour. The dense sand owing to its compact nature tends to shear away under footing penetration. When thickness of sand layer is adequate enough to stand against breakage, it facilitates formation of general shear mode of slip plane within the sand layer leading to strain softening response of the footing. In cases of sand layer of lower relative density and lower thickness the pressure-settlement response shows a gradual increase in bearing pressure with footing settlement which is typical of punching shear behaviour. From Figs. 4.37, 4.42 and 4.47 it can be observed that for overlying sand layer with higher thickness

and higher relative density where strain softening behaviour is observed, the improvement factor visibly reduces with the increase in settlement. This is attributed to the sidewise shearing of sand layer leading to reduced support to the footing and hence lowers value of IF_s while for cases with lower thickness the improvement factor mostly remains unchanged. This is because the sand layer being less in thickness undergoes breakage and hence is unable to harness higher performance improvement. Little increase in IF_s value with settlement, for sand layer with large thickness and lower relative density is attributed to an increased extent of downward punching slip plane. The surface deformation plots are depicted in Figs. 4.38 to 4.40, 4.43 to 4.45 and 4.48 to 4.50. With ID = 35% and 50% and H = 0.37D, heaving is maximum. The clay layer being at shallow depth undergoes heaving under footing penetration which is reflected on the surface (δ). Whereas for higher relative density (ID 80%, Fig. 4.50), heaving with H = 0.37D is the least. This is because the general shear induced heave in the sand layer is large enough to reduce the influence of heaving in the clay layer for H = 0.37D.

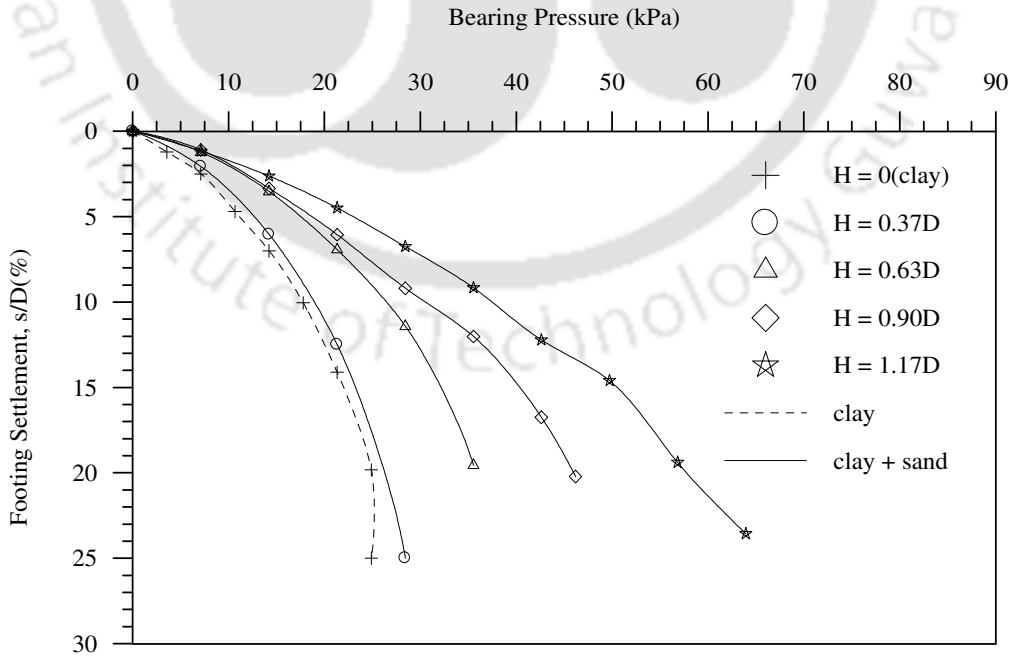

Fig. 4.36 Variation of bearing pressure with footing settlement for different heights (H) of overlying sand – Test Series A3, A4, A5, A6, ID = 35%

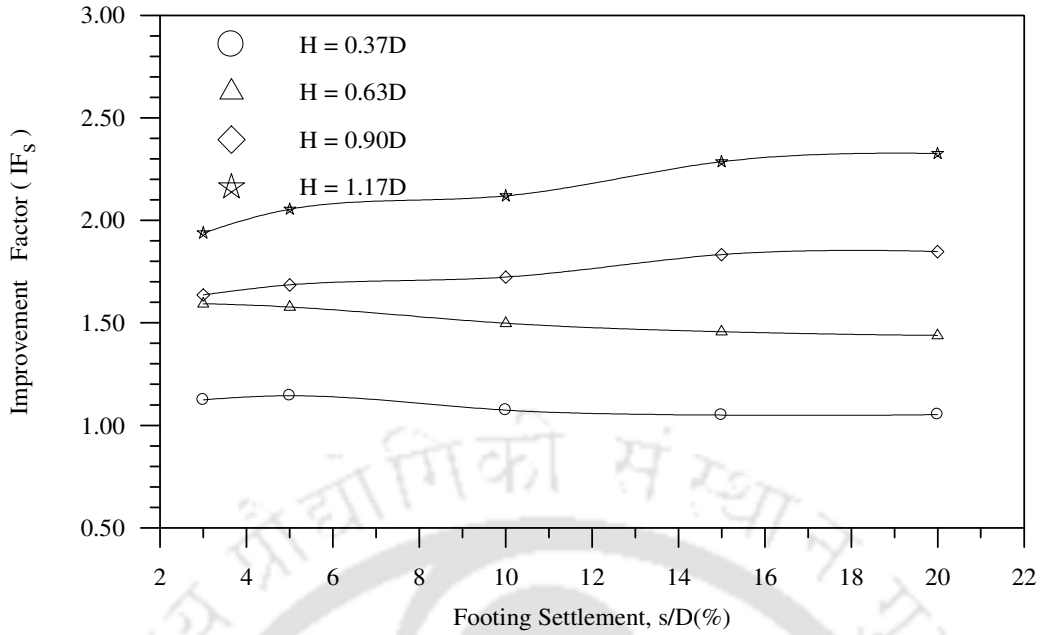

Fig. 4.37 Variation of improvement factor with footing settlement for different heights (H) of overlying sand – Test Series A3, A4, A5,A6, ID = 35%

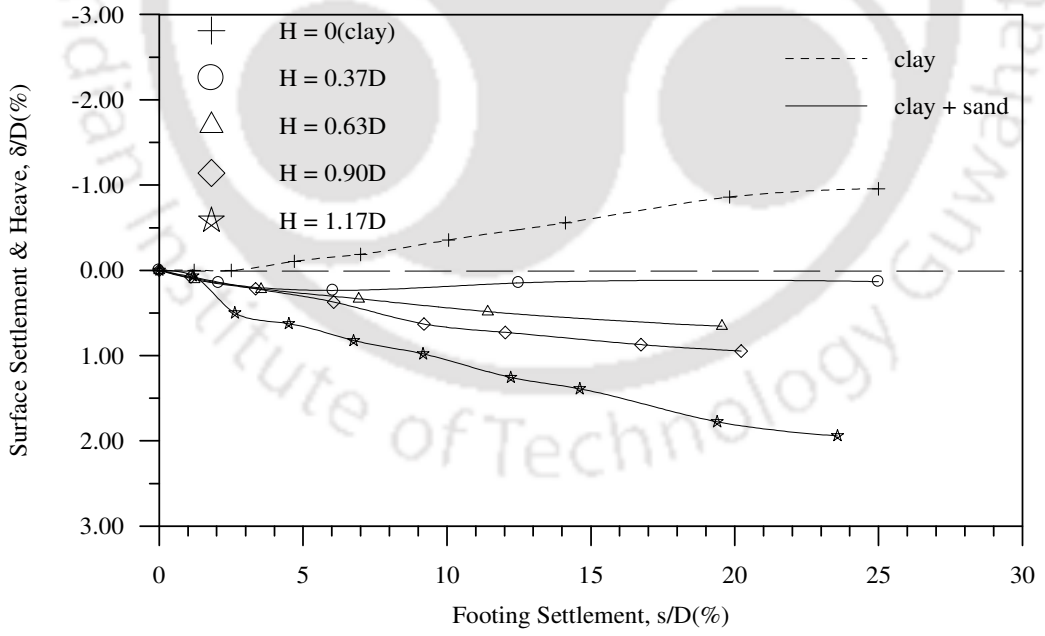

Fig. 4.38 Variation of average surface deformation with footing settlement at a distance x = D from the centre of the footing, for different heights (H) of overlying sand. Test Series A3, A4, A5, A6 – ID = 35%

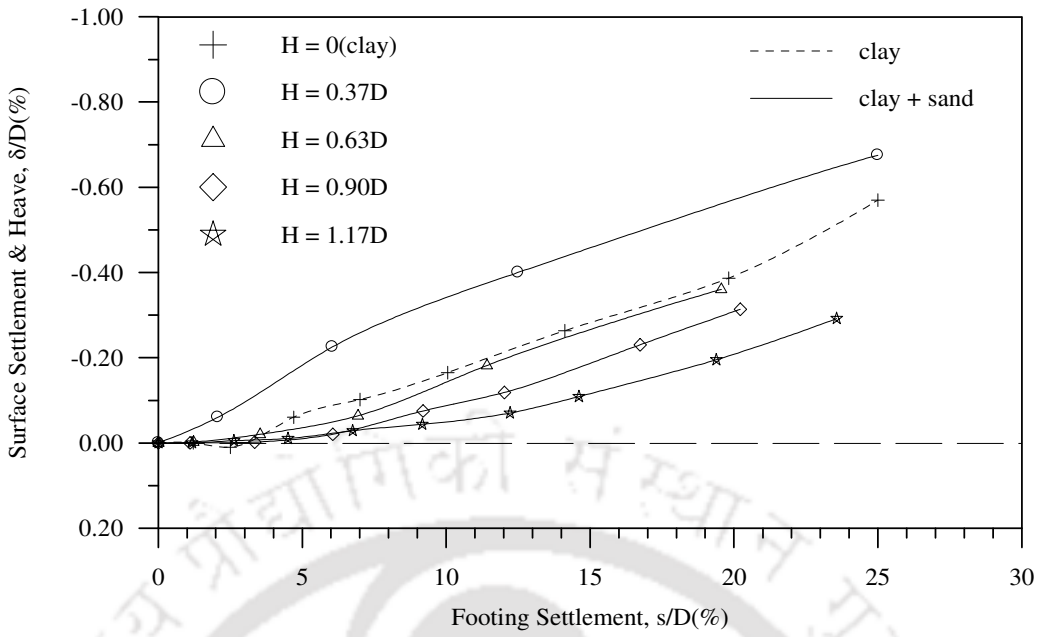

Fig. 4.39 Variation of average surface deformation with footing settlement at a distance x = 2D from the centre of the footing, for different heights (H) of overlying sand.Test Series A3, A4, A5, A6 – ID = 35%

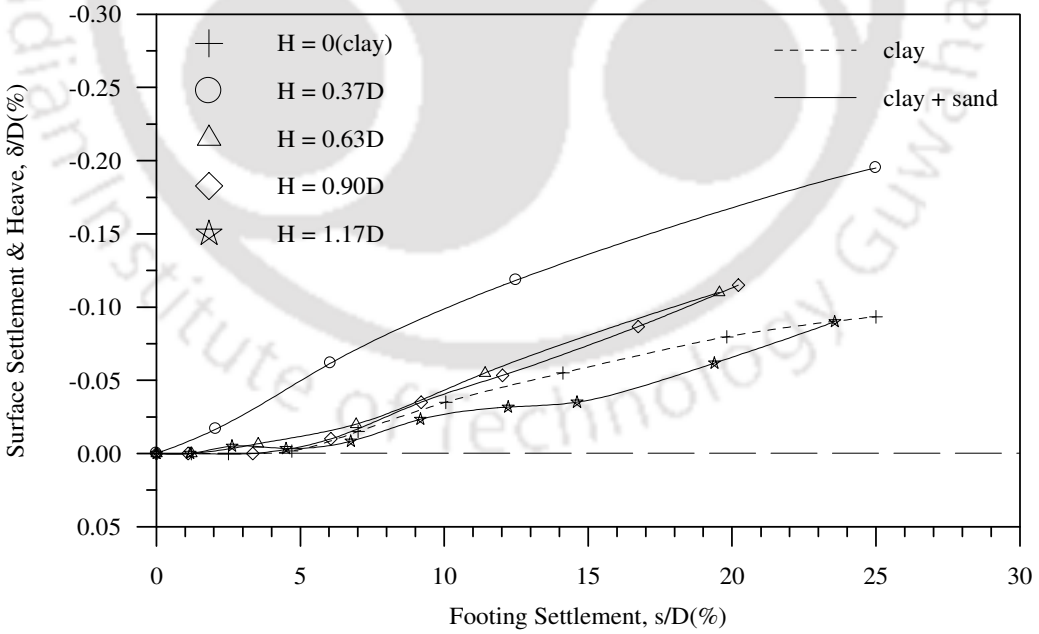

Fig. 4.40 Variation of average surface deformation with footing settlement at a distance x = 3D from the centre of the footing, for different heights (H) of overlying sand. Test Series A3, A4, A5, A6 – ID = 35%

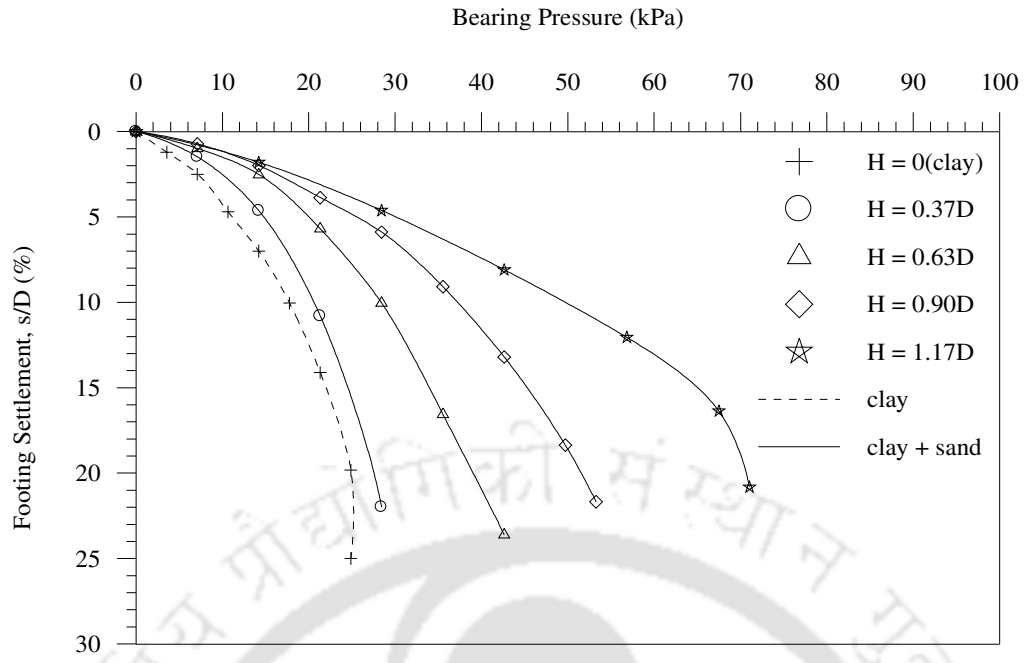

Fig. 4.41 Variation of bearing pressure with footing settlement for different heights (H) of overlying sand – Test Series A3, A4, A5,A6, ID = 50%

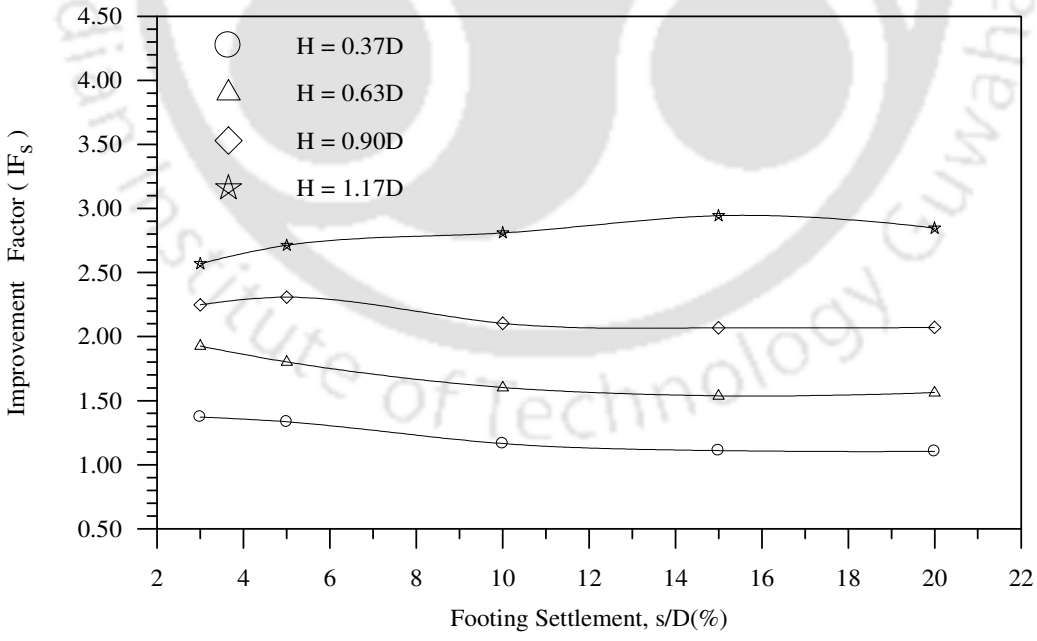

Fig. 4.42 Variation of improvement factor with footing settlement for different heights (H) of overlying sand – Test Series A3, A4, A5, A6, ID = 50%

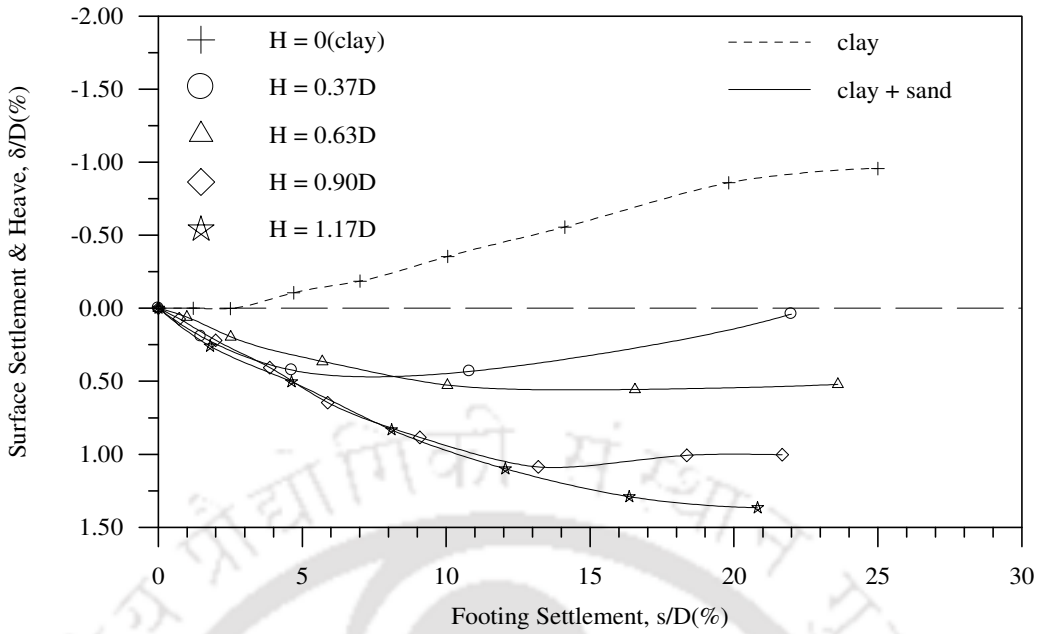

Fig. 4.43 Variation of average surface deformation with footing settlement at a distance x = D from the centre of the footing, for different heights (H) of overlying sand. Test Series A3, A4, A5, A6 – ID = 50%

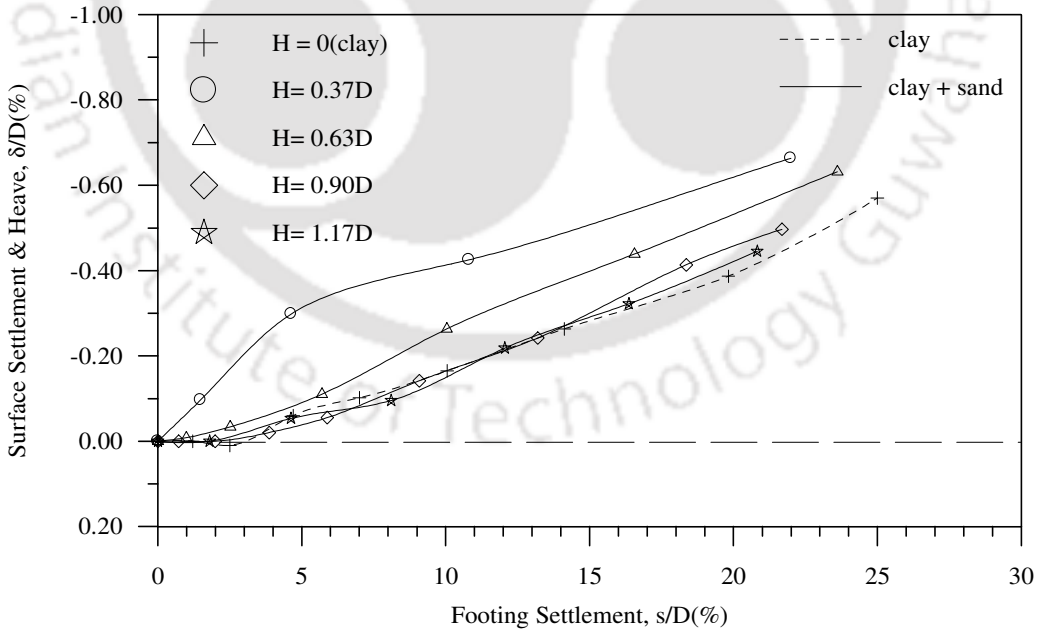

Fig. 4.44 Variation of average surface deformation with footing settlement at a distance x = 2D from the centre of the footing, for different heights (H) of overlying sand. Test Series A3, A4, A5, A6 – ID = 50%

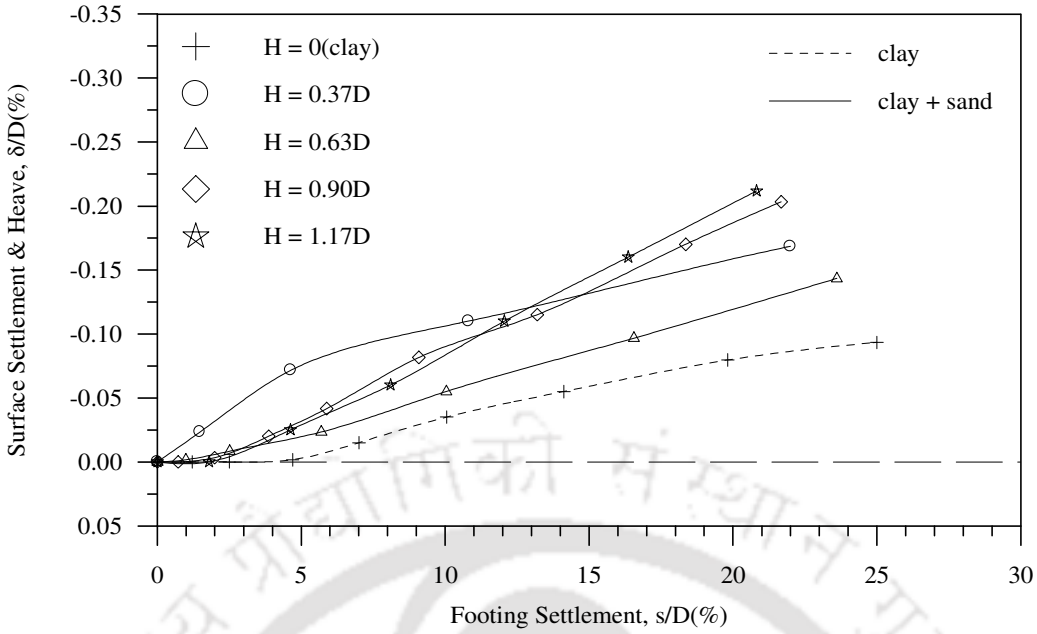

Fig. 4.45 Variation of average surface deformation with footing settlement at a distance x = 3D from the centre of the footing, for different heights (H) of overlying sand. Test Series A3, A4, A5, A6 – ID = 50%

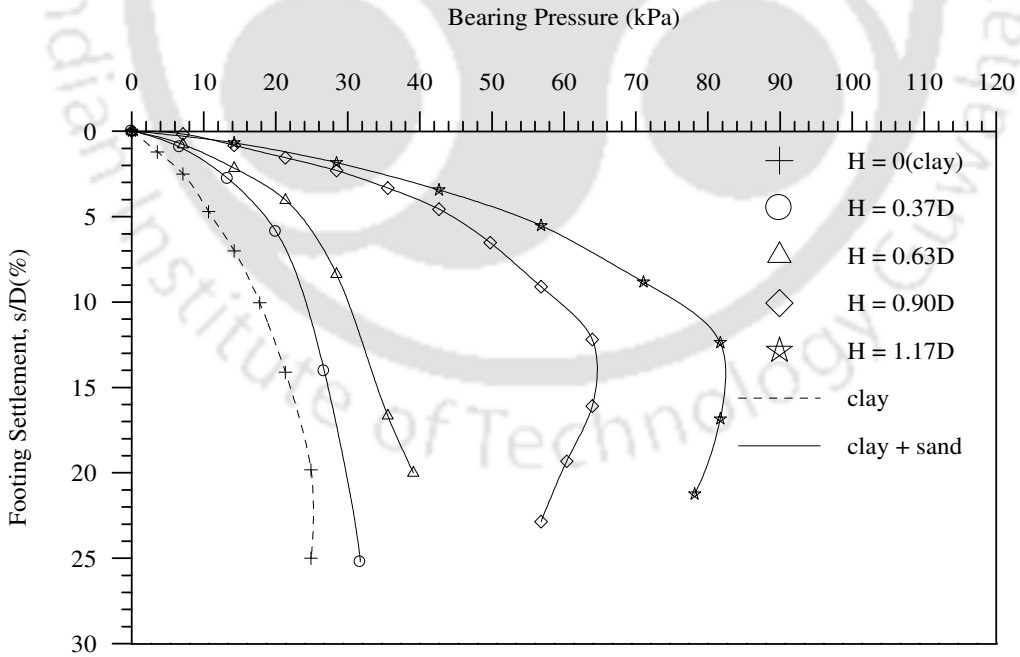

Fig. 4.46 Variation of bearing pressure with footing settlement for different heights (H) of overlying sand - Test Series A3, A4, A5, A6, ID = 80%

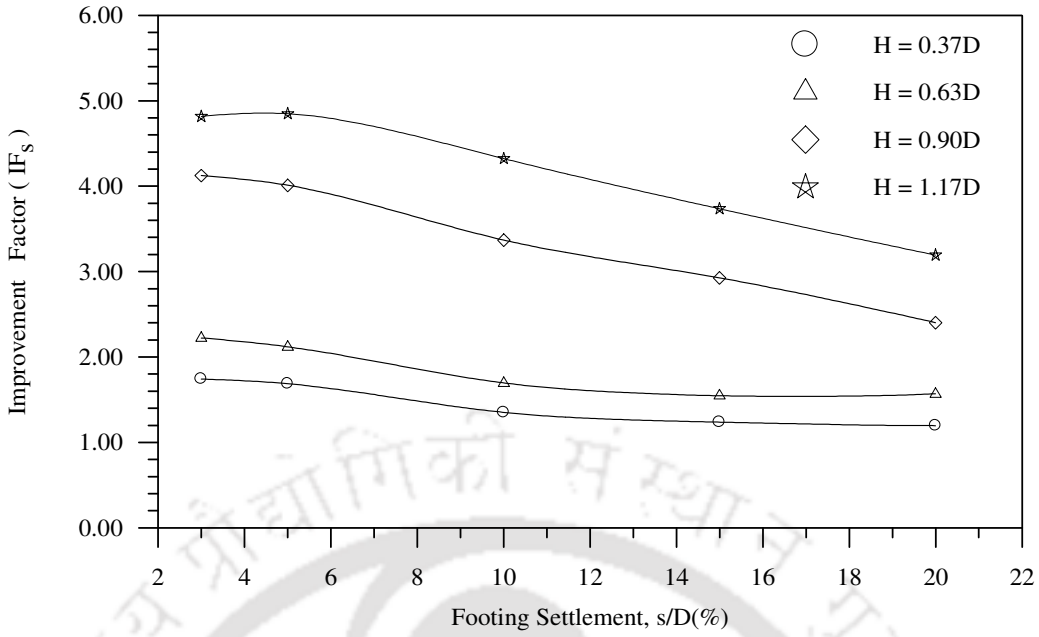

Fig. 4.47 Variation of improvement factor with footing settlement for different heights (H) of overlying sand – Test Series A3, A4, A5, A6, ID = 80%

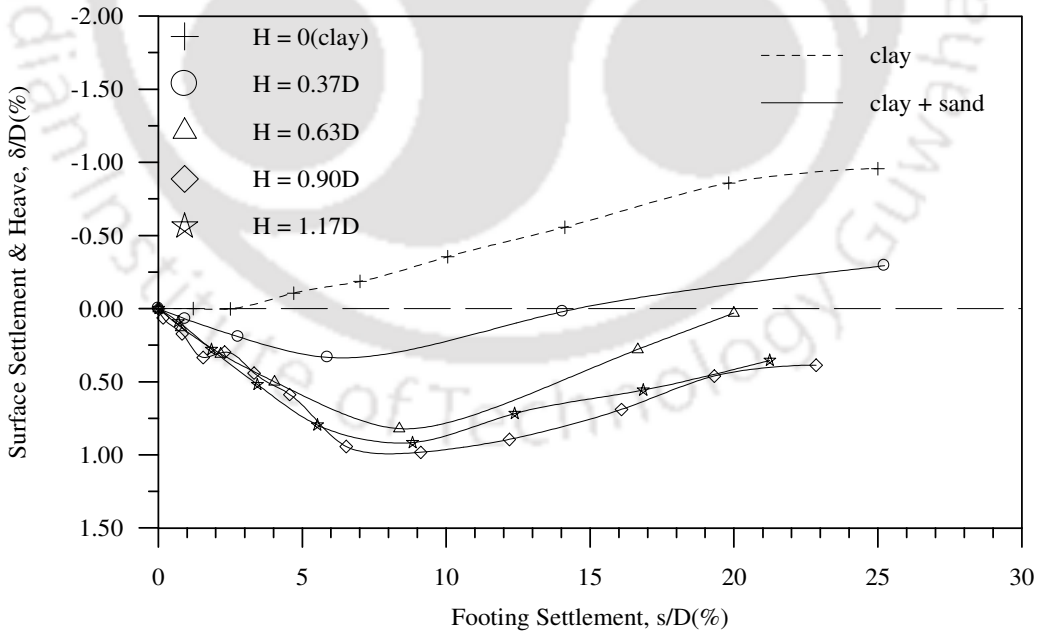

Fig. 4.48 Variation of average surface deformation with footing settlement at a distance x = D from the centre of the footing, for different heights (H) of overlying sand. Test Series A3, A4, A5, A6 – ID = 80%

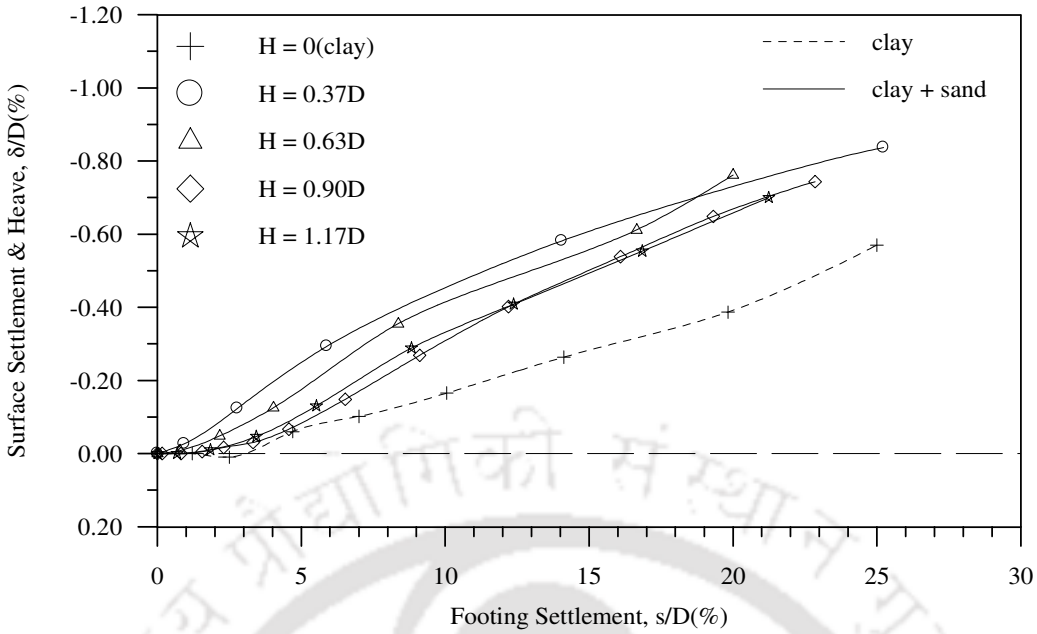

Fig. 4.49 Variation of average surface deformation with footing settlement at a distance x = 2D from the centre of the footing, for different heights (H) of overlying sand. Test Series A3, A4, A5, A6 – ID = 80%

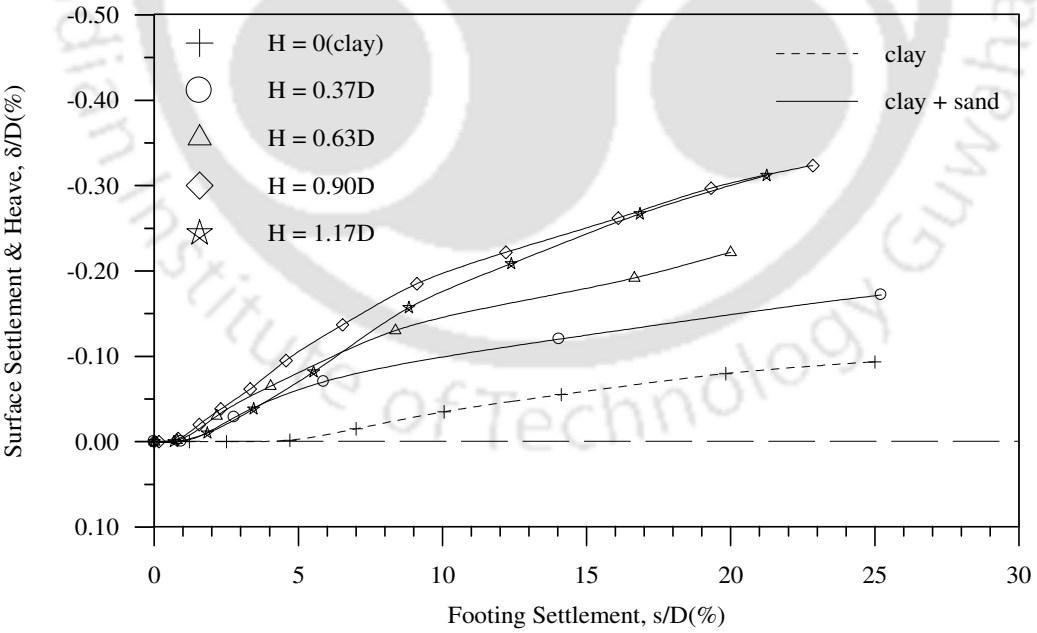

Fig. 4.50 Variation of average surface deformation with footing settlement at a distance x = 3D from the centre of the footing, for different heights (H) of overlying sand. Test Series A3, A4, A5, A6 – ID = 80%

CHAPTER 5

GEOCELL REINFORCED SAND LAYER OVERLYING CLAY SUBGRADE

5.1 INTRODUCTION

In this chapter, results of model load tests on geocell reinforced sand beds supported by soft clay subgrade are presented and discussed. Twenty-four different series of tests (Test Series B1 to G3) were carried out to study the behaviour of geocell reinforced sand mattress overlying clay subgrade, under circular loading. The details of the test series are presented in Table 3.4. The parameters varied in these tests include, depth of placement of geocell mattress, pattern of formation, pocket size of geocells, height of geocell mattress and relative density of the infill sand in the geocells.

Fig. 5.1 shows typical pressure-settlement responses for: soft clay subgrade, sand overlying clay subgrade and geocell-sand mattress overlying clay subgrade. It could be observed that in case of the clay subgrade, though there is no pronounced peak pressure, yet the pressure-settlement plot is almost vertical beyond a settlement of about 20% of footing diameter indicating that the soil has undergone punching failure. With the sand layer over the clay subgrade, there is an increase in both the stiffness and load carrying capacity of the foundation bed. However, for settlement beyond 12% of footing diameter, the pressure-settlement response has undergone strain softening, indicating that the system has failed in general shear mode. In comparison to the unreinforced cases, no clear cut failure was observed in the response with geocell reinforcement and the bearing pressure continued to increase with increase in footing settlement. It is also evident from the figure that the geocell reinforced bed exhibits a much stronger and stiffer response compared to the unreinforced cases. This is because the three dimensional geocells

restrict the movement of soil when acted upon by the external loading leading to an increase in the overall rigidity of foundation bed, thereby redistributing the applied load to a wider area. This in turn reduces the pressure on the underlying soft subgrade, giving rise to increased performance improvement.

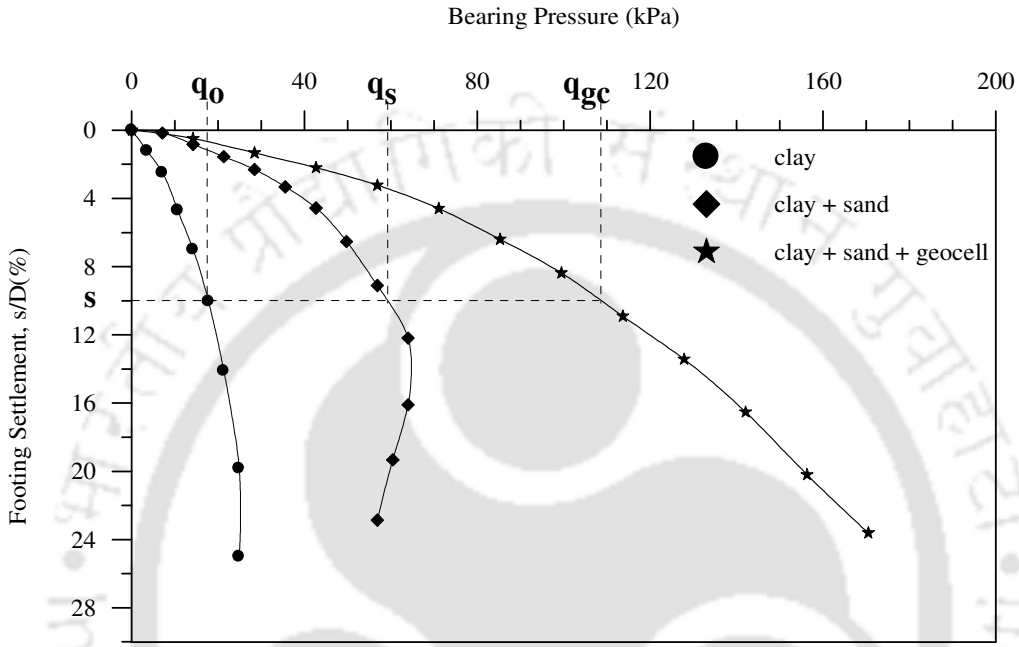

Fig. 5.1 Variation of bearing pressure with footing settlement for different foundation conditions – Test Series A1, A5, F3

The performance improvement due to geocell reinforcement is quantified using a non-dimensional improvement factor, IF_{gc}, which is defined as the ratio of bearing pressure (q_{gc}) with geocell reinforced soil to bearing pressure on unreinforced soil (q_s), both taken at equal settlement(s) of the footing (Fig. 5.1). The bearing pressure improvement due to the sand layer, IF_s, has already been defined in the previous chapter. It could be observed that while for the clay subgrade, at a settlement of about 10% of the footing diameter, the bearing pressure is 18 kPa, for the clay subgrade overlain by sand it is about 60 kPa. The bearing pressure increases to about 110 kPa with the inclusion of the geocell-sand mattress over the clay subgrade. Thus about a three fold ($IF_s \approx 3$) increase in bearing pressure can be obtained due to the sand layer. With the provision of geocell

reinforcement in the sand layer the bearing pressure further increases by a factor of 2 (i.e. $IF_{gc} \approx 2$). Hence, with the provision of geocell-sand mattress, the load carrying capacity of the clay subgrade can be increased by as much as six times ($IF_{gc} \times IF_s = 6$).

The footing settlement 's' and surface deformation 'δ' (settlement/heave) are expressed in non-dimensional form in terms of footing diameter (D) as s/D (%) and δ/D (%) respectively. In all the graphs, settlements are reported with a positive sign (+) and heave with a negative sign (−). Typical surface deformation profile for geocell reinforced bed is shown in Fig. 5.2. It could be observed that in the region near to the footing (x = D), the fill surface has undergone settlement. In contrast, the surface deformation profile for the clay subgrade (Fig. 4.2) shows substantial heaving on the fill surface close to the footing area. The saturated soft subgrade when subjected to a relatively faster rate of loading, being unable to offer adequate resistance to the applied load has undergone punching under the footing thus inducing heave at the adjacent fill surface. However, with the provision of the geocell mattress, the geocell-soil structure behaves as a composite unit and deflects like a centrally loaded slab under the footing, thereby transmitting the pressure over a wider area giving rise to a much wider settlement zone.

Influences of individual parameters on the pressure-settlement and surface deformation behaviour of the foundation system are presented and discussed in the following sections. Based on the analysis of the test data, the critical value of the different geocell, soil parameters giving maximum performance improvement are brought out.

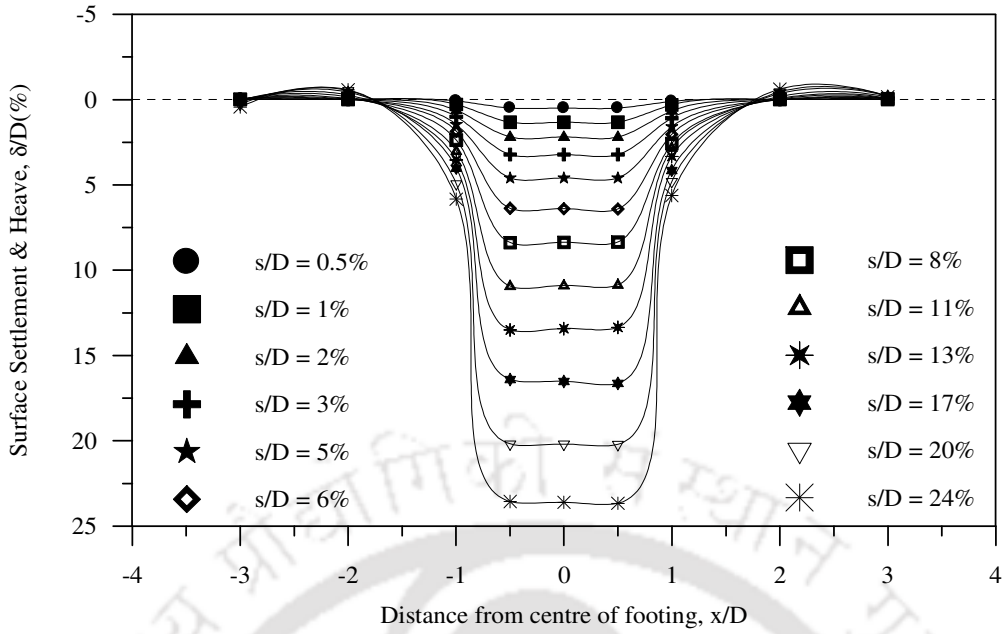

Fig. 5.2 Surface deformation profile with geocell reinforcement

5.2 DEPTH OF PLACEMENT

Tests under series B1 to B4 were conducted with varied depth of placement (u) of geocell mattress (i.e. u = 0, 0.1D, 0.25D and 0.5D) for different pocket sizes of geocells (i.e. d = 1.6D, 1.2D, 0.8D and 0.4D) while the pattern of formation, height (h) of geocell mattress and relative density (ID) of infill sand were kept constant (i.e. chevron pattern, 0.27D and 80% respectively). The corresponding tests with diamond pattern were carried out under series C1 to C4. In series B5, tests were carried out with varied 'u' for an increased height (i.e. h = 0.8D) of geocell mattress, while other parameters were kept constant. Tests in these nine series were conducted primarily to evaluate the critical depth of placement (u_{cr}) giving maximum performance improvement for varied conditions of geocell mattress (i.e. pattern of formation, pocket size and height). The following subsections bring out the influence of the parameters on the critical depth of placement of the geocell mattress (u_{cr}).

5.2.1 Influence of pattern of formation

5.2.1.1 Chevron Pattern

For chevron pattern of formation with geocells of h = 0.27D and ID = 80%, bearing pressure versus settlement responses due to varied depths of placement and for pocket sizes (d) of 1.6D, 1.2D, 0.8D and 0.4D, are depicted in Figs. 5.3, 5.4, 5.5 and 5.6 respectively. The responses for the corresponding unreinforced case (Test Series A2) wherein the thickness of the sand (H) is same as that of the geocell mattress (h + u), are included for comparisons. It could be observed that for d = 1.6D (Fig. 5.3), responses for the unreinforced and reinforced cases are nearly similar till settlement of about 5 - 10% of footing diameter indicating that over this settlement range the influence of reinforcement is marginal. It is only at higher settlement that the improvement due to the geocell reinforcement is manifested. However, with the reduced pocket sizes of geocells (d = 1.2D, 0.8D and 0.4D), the influence of the reinforcement is observed at much lower settlement (Figs. 5.4 to 5.6). These observations indicate that for geocells of very large pocket size (d = 1.6D), the deformed sand under the footing, passes down almost unhindered through the large openings of the geocell pockets which indicate that the geocell reinforcement plays only a marginal role. It is only at very large deformation that the reinforcing effect is manifested possibly through some indirect actions such as mobilization of anchorage and passive resistance from soil in the region outside the loading area. While with reduced pocket size, the relatively closer geocell structure effectively restrains the downward moving soil mass, under footing penetration, leading to manifestation of reinforcing action at much earlier stages of settlement.

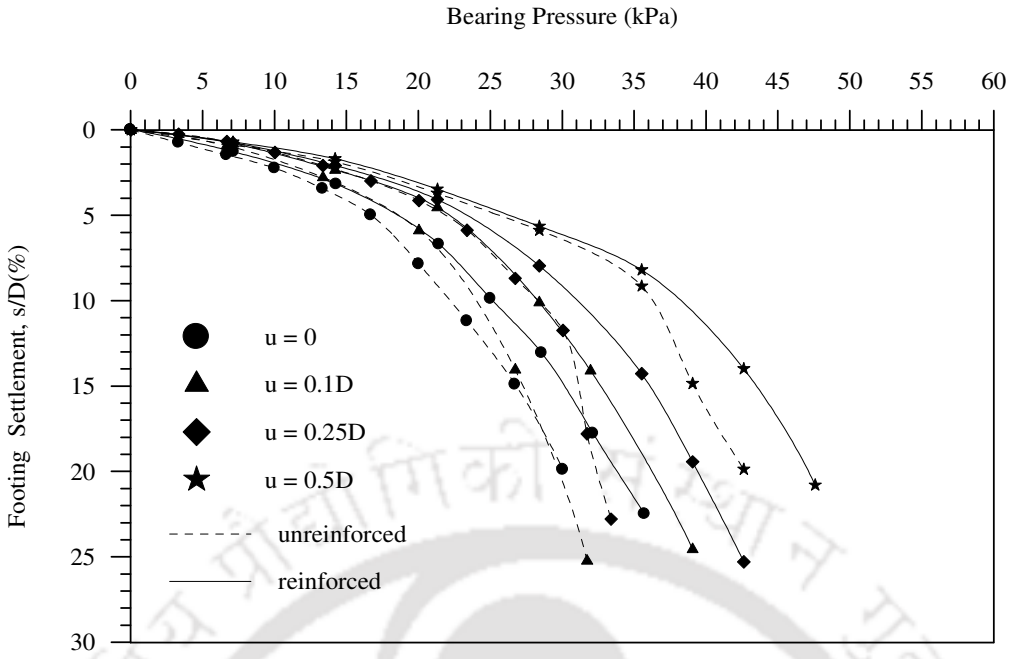

Fig. 5.3 Variation of bearing pressure with footing settlement for different depths of placement (u) of geocell mattress – Test Series A2, B1 to B4, h = 0.27D, chevron, d = 1.6D

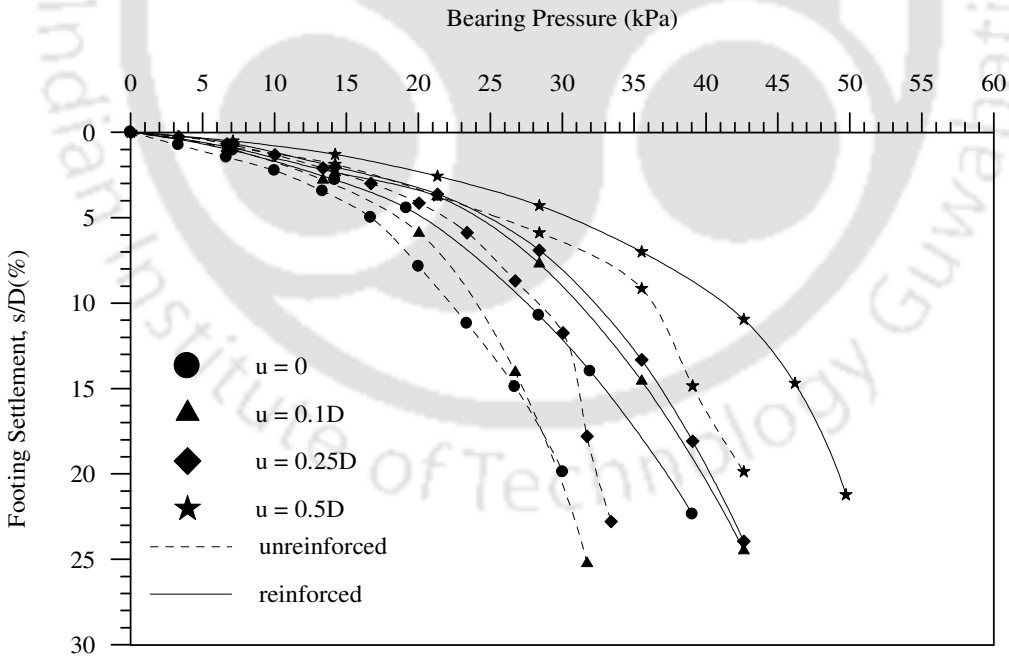

Fig. 5.4 Variation of bearing pressure with footing settlement for different depths of placement (u) of geocell mattress – Test Series A2, B1 to B4, h = 0.27D, chevron, d = 1.2D

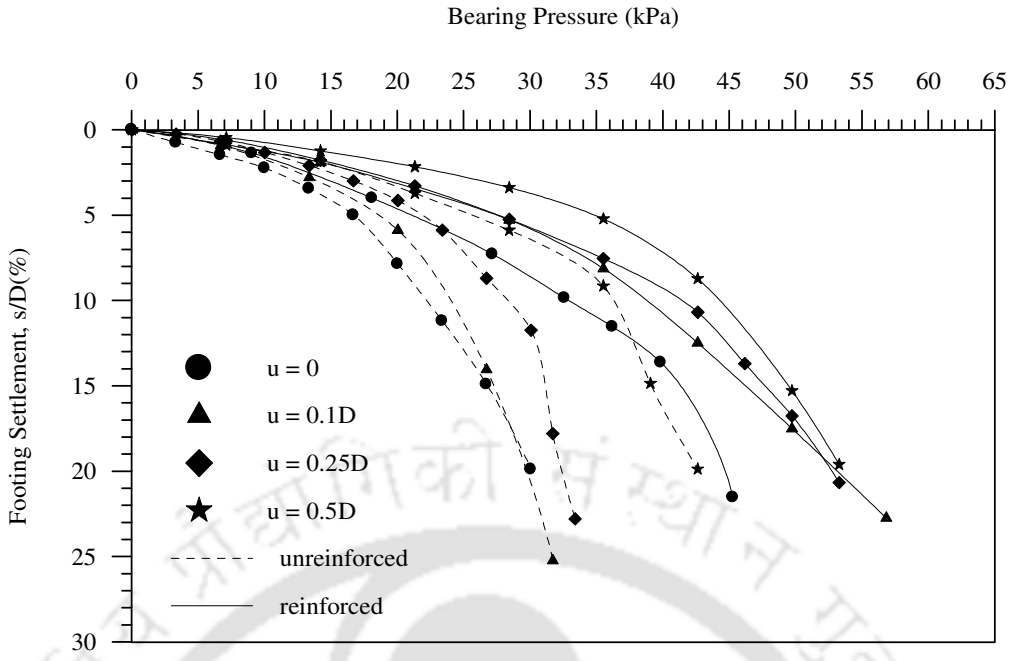

Fig. 5.5 Variation of bearing pressure with footing settlement for different depths of placement (u) of geocell mattress – Test Series A2, B1 to B4, h = 0.27D, chevron, d = 0.8D

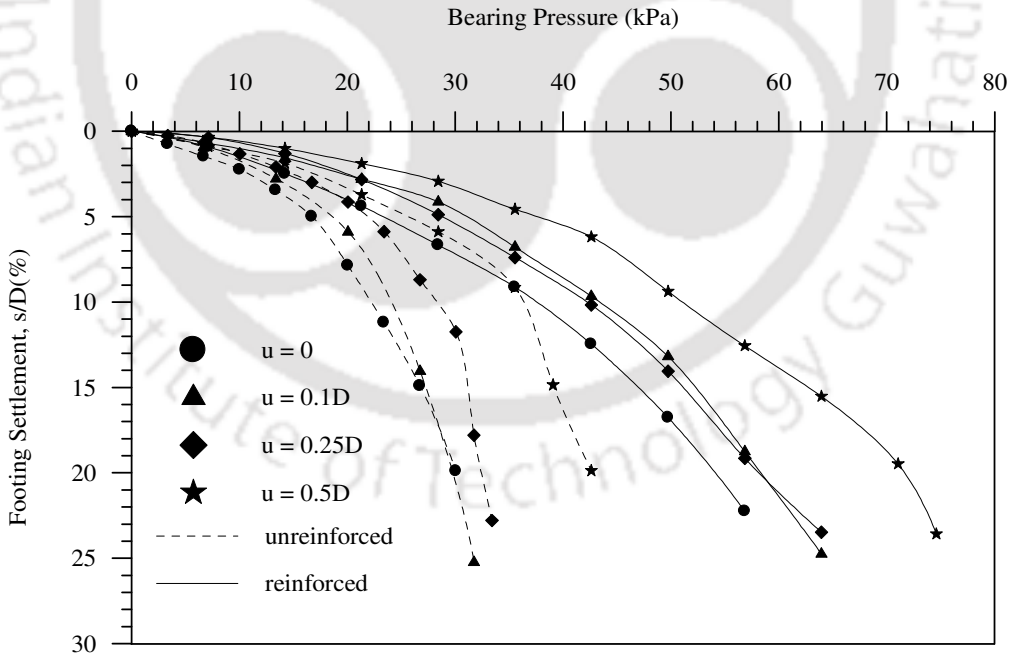

Fig. 5.6 Variation of bearing pressure with footing settlement for different depths of placement (u) of geocell mattress – Test Series A2, B1 to B4, h = 0.27D, chevron, d = 0.4D

The bearing capacity improvement due to geocell reinforcement (IF_{gc}) at different levels of footing settlement (s/D), as obtained from Figs. 5.3 to 5.6, are presented in Table 5.1. It is observed that, in general, there is an increase in the improvement factor with the increase in the footing settlement. This is due to the increased mobilization of the strength of reinforcement due to increased straining that is attributed to increased deflection of geocell mattress. It is of interest to note that for higher depth of placement (u = 0.5D), the improvement factor, IF_{gc}, initially decreases after which it increases with increase in footing settlement. This is because, in the beginning, the load is carried by the relatively thick sand cushion above the geocell mattress. With the increase in the applied load, the sand layer above the geocell mattress starts shearing off and the resistance to downward penetration of the footing is reduced. This leads to increased settlement thereby reducing the overall performance improvement. However at higher settlements, as the overlying sand cushion shears away, the footing moves closer to the geocell reinforcement therefore the reinforcement benefit is mobilized, thereby leading to an increase in the performance improvement.

From Table 5.1, it could further be observed that the improvement factor (IF_{gc}) increases with the increase in the depth of placement (u) from 0 to 0.1D, after which it continues to decrease. The trend remains the same irrespective of the settlement of the footing and the pocket size of the geocells. When the geocell mattress is placed immediately below the footing (u = 0), the geocell walls buckle locally, due to stress concentration under the applied load, reducing the beneficial effect of the reinforcement. This is confirmed through the post test examination which shows deformation of the portion of the geocell walls lying below the footing (Photo 5.1). When the depth of placement is increased to 0.1D, the load is distributed through the sand cushion onto the geocells that avoids the stress concentration. This prevents the buckling of the reinforcement giving rise to higher

performance improvement. When the depth of placement of geocell mattress is further increased, an increased portion of the sand cushion remains outside the zone of influence of the reinforcement that it tends to move laterally away, on the application of load. This leads to increase in the vertical settlement keeping much of the reinforcement strength immobilised and hence a reduction in improvement factor is observed.

Table 5.1 Summary of results in terms of bearing capacity improvement factor (IF_{gc}) showing the influence of depths of placement (u) of the geocell mattress. Test Series B1 to B4

Variable Parameter		Bearing capacity improvement factor (IF_{gc})				
		(s/D) 3%	(s/D) 5%	(s/D) 10%	(s/D) 15%	(s/D) 20%
(d/D)	(u/D)					
1.6	0	1.11	1.11	1.13	1.13	1.12
	0.1	**1.18**	**1.18**	**1.19**	**1.19**	**1.22**
	0.25	1.07	1.07	1.10	1.16	1.22
	0.50	1.04	1.03	1.05	1.11	1.12
1.2	0	1.22	1.22	1.23	1.23	1.24
	0.1	**1.29**	**1.29**	**1.31**	**1.32**	**1.34**
	0.25	1.13	1.14	1.14	1.18	1.25
	0.50	1.24	1.19	1.13	1.19	1.16
0.8	0	1.22	1.26	1.48	1.55	1.50
	0.1	**1.37**	**1.47**	**1.62**	**1.70**	**1.79**
	0.25	1.20	1.26	1.47	1.53	1.63
	0.50	1.40	1.35	1.22	1.26	1.26
0.4	0	1.32	1.40	1.69	1.75	1.80
	0.1	**1.59**	**1.66**	**1.82**	**1.92**	**1.96**
	0.25	1.31	1.32	1.49	1.64	1.80
	0.50	1.53	1.46	1.40	1.60	1.68

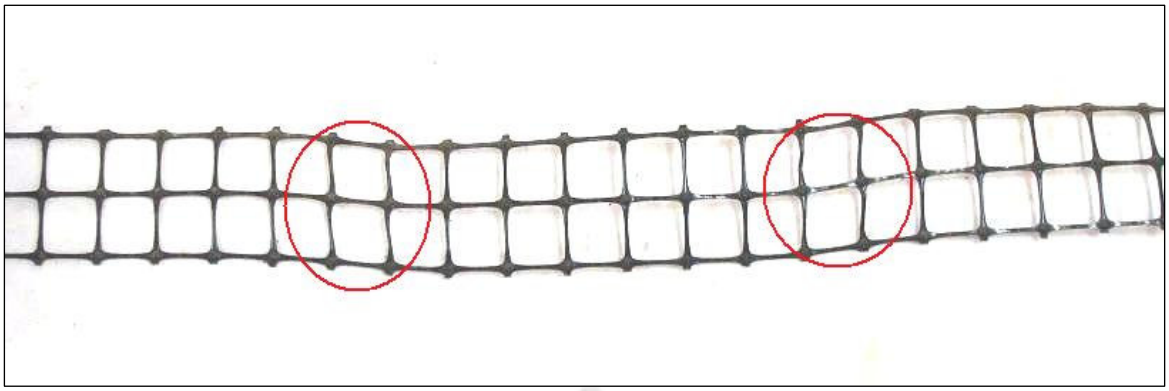

Photo 5.1 Deformation in the vertical ribs of the exhumed geocell reinforcement

The test data can further be analysed through surface deformation (δ) responses. Typical surface deformation profiles for geocell mattress having a pocket size of d = 0.8D and placed at different depths (u = 0, 0.1D, 0.25D and 0.5D) are shown in Figs. 5.7 to 5.10 respectively. Nearly similar surface deformation profiles are obtained for other pocket sizes (i.e. d = 1.6D, 1.2D and 0.4D) which are reported in Appendix 1 (Figs. A1.1 to A1.12).

Fig. 5.7 that depicts the surface deformation profile for the footing which rest directly on the geocells (i.e. u = 0) shows substantial heaving on fill surface. This is attributed to two different reasons: First, the footing directly being on the geocell mattress, the geocell mattress behaves as a centrally loaded soft subgrade supported slab, under footing loading and through mobilization of anchorage from the encapsulated soil in the region outside loading, the mattress tends to stand against the footing penetration. The settlement in the central portion (i.e. under the footing) and anchorage at the end makes the relatively flexible geocell mattress to undergo a sagging deformation at middle and hogging deformation at both the ends. This hogging deformation has produced the heaving in the fill surface. Second the saturated clay layer, being subjected to a relatively faster rate of loading, when settles under the footing produces heaving in the adjacent region which

contributes to heaving on the fill surface. With increase in the placement depth (u) of the geocell mattress below the base of the footing, both the geocell mattress and the clay move away to a relatively greater distance from the loading region (i.e. footing). Therefore, both heaving of the clay and bending of the geocell mattress reduce leading to reduced heave on the fill surface (Figs. 5.8, 5.9 and 5.10). The heaving in these cases is mostly due to squeezing away of the sand cushion over the geocell mattress, under footing penetration. Besides, with increase in depth of placement (u), the total thickness of the geocell-sand mattress increases and in turn offers more resistance against footing penetration. This reduces the punching of clay below, leading to reduced heaving.

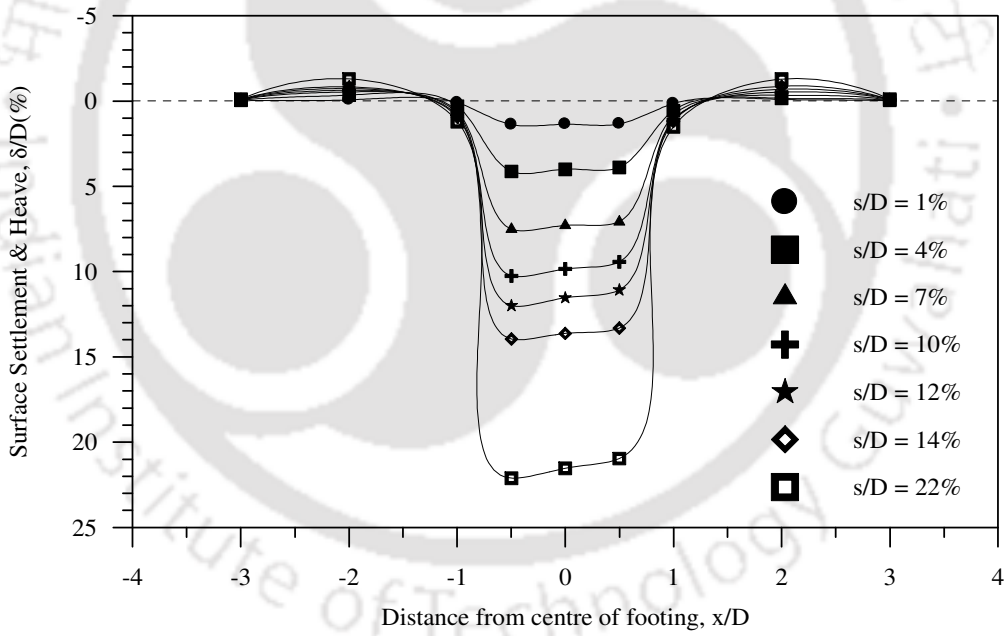

Fig. 5.7 Surface deformation profiles with geocell reinforcement – Test Series B1, chevron, u/D = 0, d = 0.8D

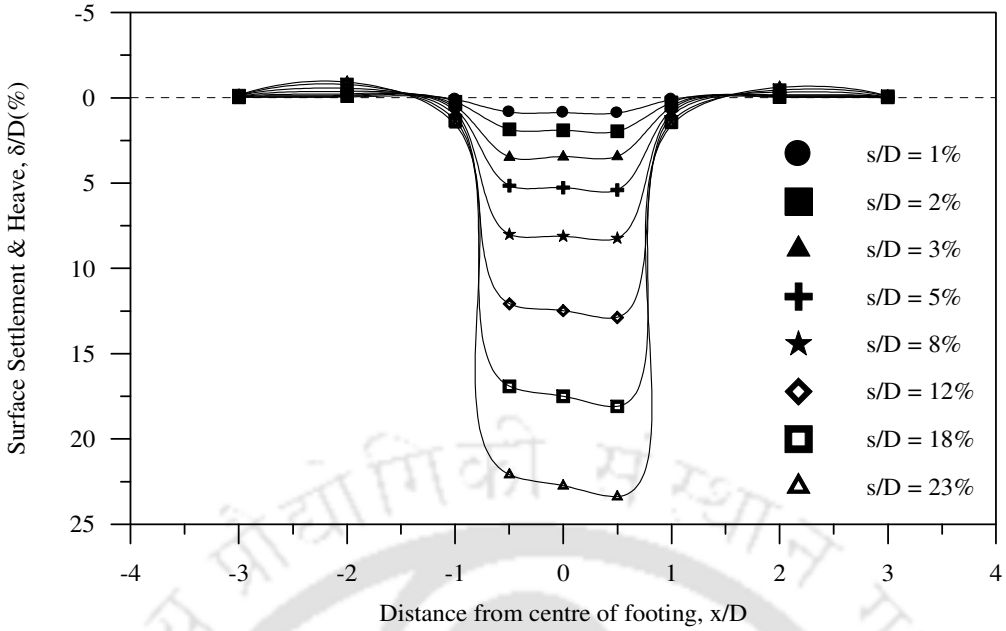

Fig. 5.8 Surface deformation profiles with geocell reinforcement – Test Series B2, chevron, u/D = 0.1, d = 0.8D

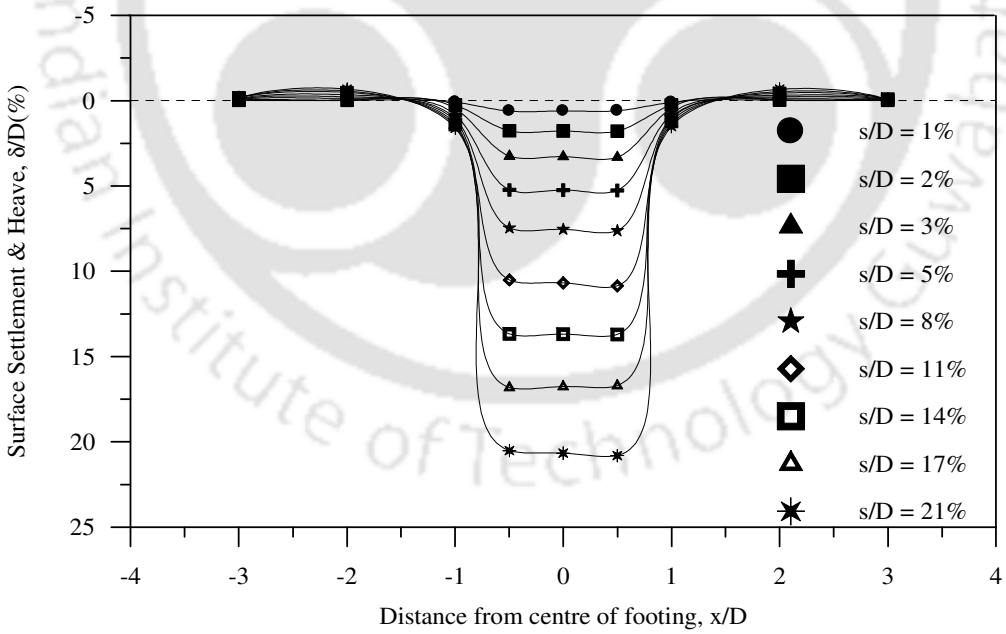

Fig. 5.9 Surface deformation profiles with geocell reinforcement – Test Series B3, chevron, u/D = 0.25, d = 0.8D

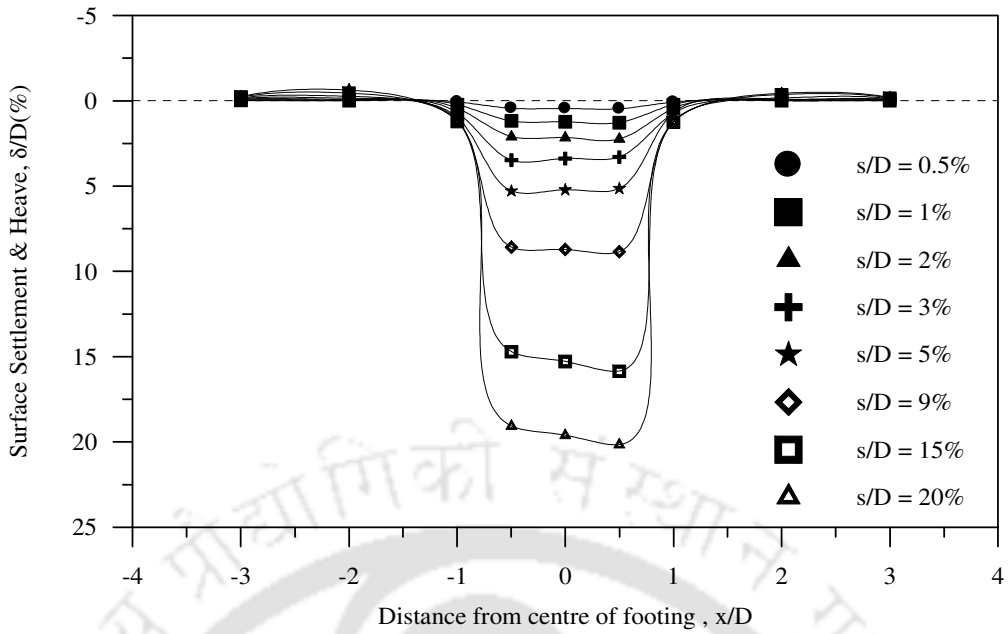

Fig. 5.10 Surface deformation profiles with geocell reinforcement – Test Series B4, chevron, u/D = 0.5, d = 0.8D

The variation of average surface deformation (settlement/heave) 'δ' with footing settlement (s) for varied depths of placement (u), at a distance of x = D from the centre of footing, with pocket sizes of d = 1.6D, 1.2D, 0.8D and 0.4D are presented in Figs. 5.11, 5.12, 5.13 and 5.14 respectively. In these plots, the corresponding unreinforced responses (Test Series A2) are also included, for comparison purpose. It could be observed that invariably for all cases (i.e. reinforced and unreinforced), the fill surface near the footing (i.e. x = D) settles at initial stages of loading (i.e. s/D < 10%). This is due to dispersion of footing pressure over a wider area. With increased footing settlement, the soil fails and heaving takes place. Even with geocell mattress which is relatively flexible and yields under footing penetration, heaving is expected. Truely, Figs. 5.11 and 5.12 show that for larger pocket sizes (i.e. d = 1.6D and 1.2D), the surface deformation responses for both the reinforced and unreinforced cases follow a similar pattern. It is also observed that for relatively shallow depths of placement (i.e. u = 0, 0.1D and 0.25D), the settlement on the fill surface with geocell reinforcement is less compared to the corresponding unreinforced

soil bed. However, when depth of placement of geocell mattress is increased to 0.5D, settlement for both the unreinforced and reinforced foundation bed is almost same indicating that at larger depth of placement, the influence of geocell reinforcement is marginal. Fig. 5.13 shows that with the decrease in the pocket size, the fill surface, without showing any heave continues to settle with increase in the footing penetration. This is because with smaller pocket sizes the soil is effectively confined and the geocell-sand bed behaves as a coherent composite mattress and therefore settles as a centrally loaded slab till large footing loading giving rise to a wider settlement zone around the footing. This phenomenon is more evident when the pocket size is decreased further (d = 0.4D, Fig. 5.14).

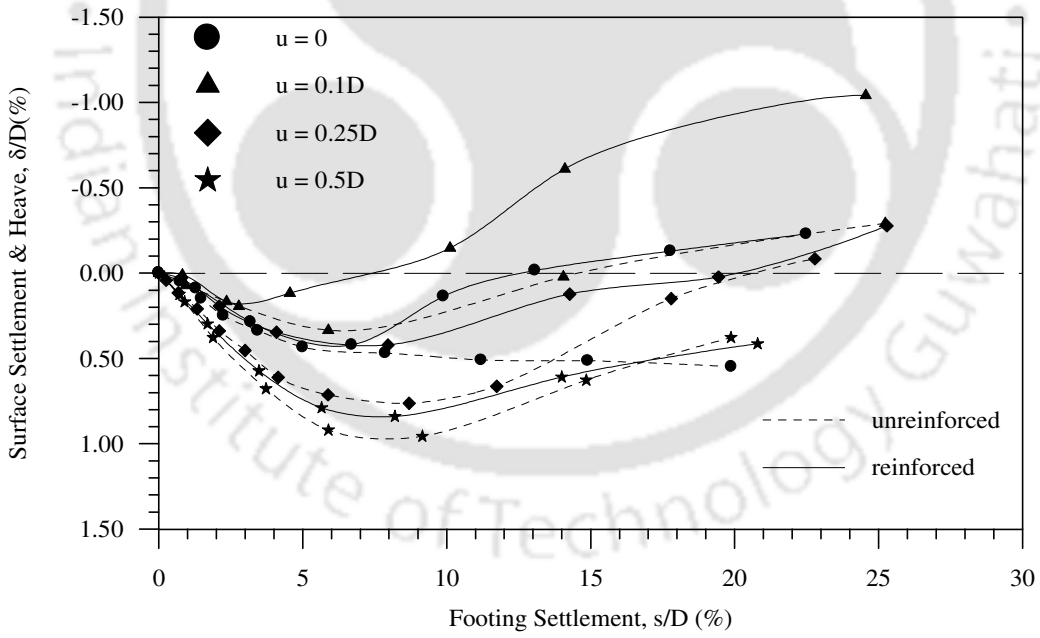

Fig. 5.11 Variation of average surface deformation with footing settlement at a distance x = D from the centre of footing, for different depths of placement (u) of geocell mattress. Test Series A2, B1 to B4, h = 0.27D, chevron, d = 1.6D

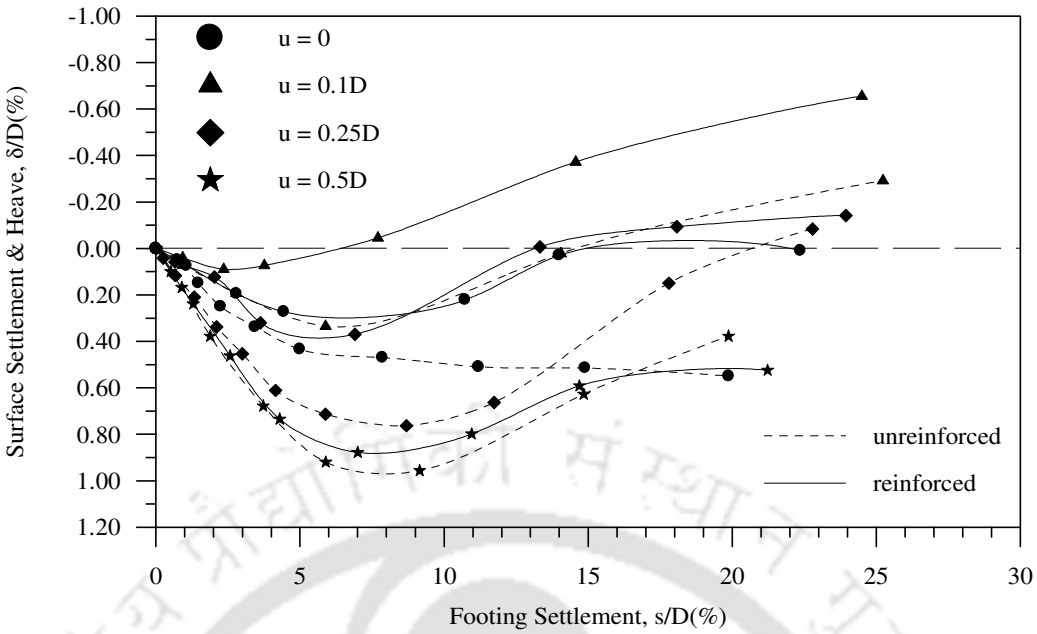

Fig. 5.12 Variation of average surface deformation with footing settlement at a distance x = D from the centre of footing, for different depths of placement (u) of geocell mattress. Test Series A2, B1 to B4, h = 0.27D, chevron, d = 1.2D

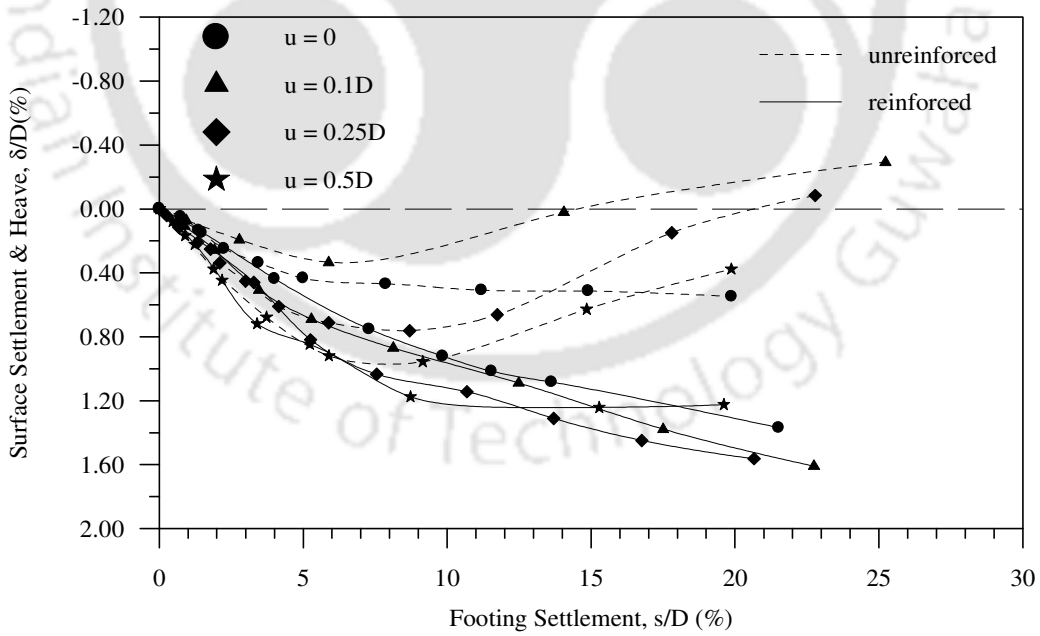

Fig. 5.13 Variation of average surface deformation with footing settlement at a distance x = D from the centre of footing, for different depths of placement (u) of geocell mattress. Test Series A2, B1 to B4, h = 0.27D, chevron, d = 0.8D

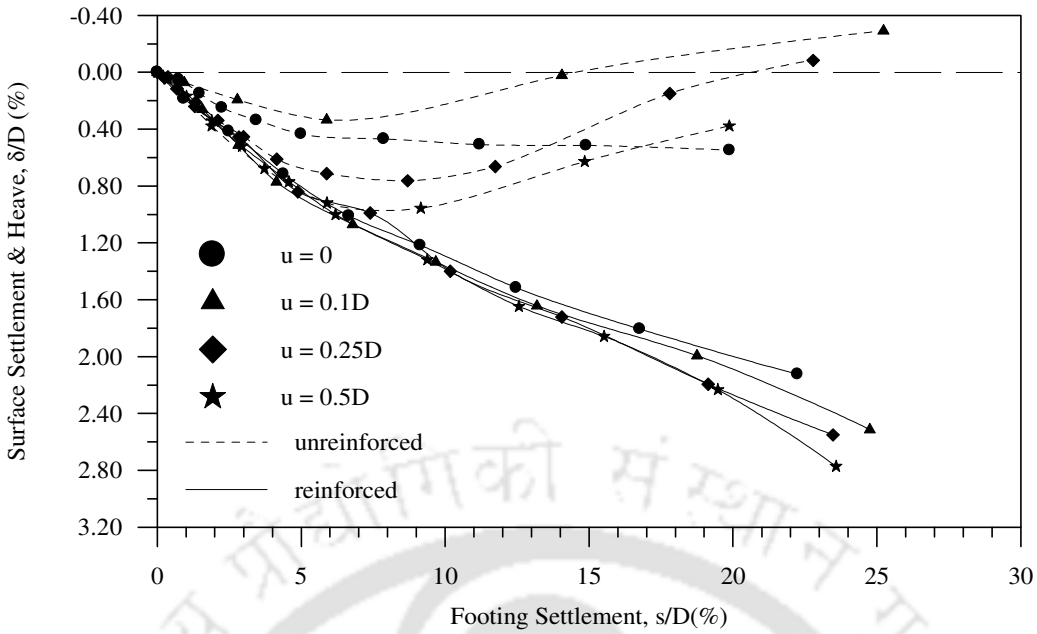

Fig. 5.14 Variation of average surface deformation with footing settlement at a distance x = D from the centre of footing, for different depth of placement (u) of geocell mattress. Test Series A2, B1 to B4, h = 0.27D, chevron, d = 0.4D

The surface deformation versus footing settlement plots, for different depths of placement (u) of geocell mattress, at a distance of x = 2D from the centre of footing, for pocket sizes of d = 1.6D, 1.2D, 0.8D and 0.4D are presented in Figs. 5.15, 5.16, 5.17 and 5.18 respectively. The corresponding surface deformation plots at a distance of x = 3D are presented in Figs. 5.19, 5.20, 5.21 and 5.22 respectively.

It can be seen from Figs. 5.15 and 5.16 that for larger pocket sizes, the surface has undergone almost the same amount of heave for both the unreinforced and the geocell reinforced soil beds. However for smaller pocket sizes (Figs. 5.17 and 5.18) a prominent heaving of the surface is observed when the geocell mattress is placed immediately below the base of the footing. The reason for this may be that the size of the pockets now being smaller, there is more probability of a dial gauge resting directly on the geocell wall. Upon loading, local lifting of the geocell wall takes place, thereby the dial gauge spindle

gets lifted up recording an apparently higher heave. However, in general, heaving is found to decrease with the provision of geocell mattress.

Heaving of the surface at x = 3D (Figs. 5.19 to 5.22) is found to be lesser in magnitude as compared to that at x = 2D. This is because the geocell almost ends at x = 3D, therefore the geocell mattress bending (hogging) induced heave is least at this place. The heave at this place is mostly due to heaving of underlying clay and squeezing out of the sand in the cushion above the geocell layer. Indeed maximum heaving in the unreinforced soil bed is observed when the thickness of the sand layer above the clay subgrade is more. However, with the provision of the geocell reinforcement, a reduction in surface heaving is observed.

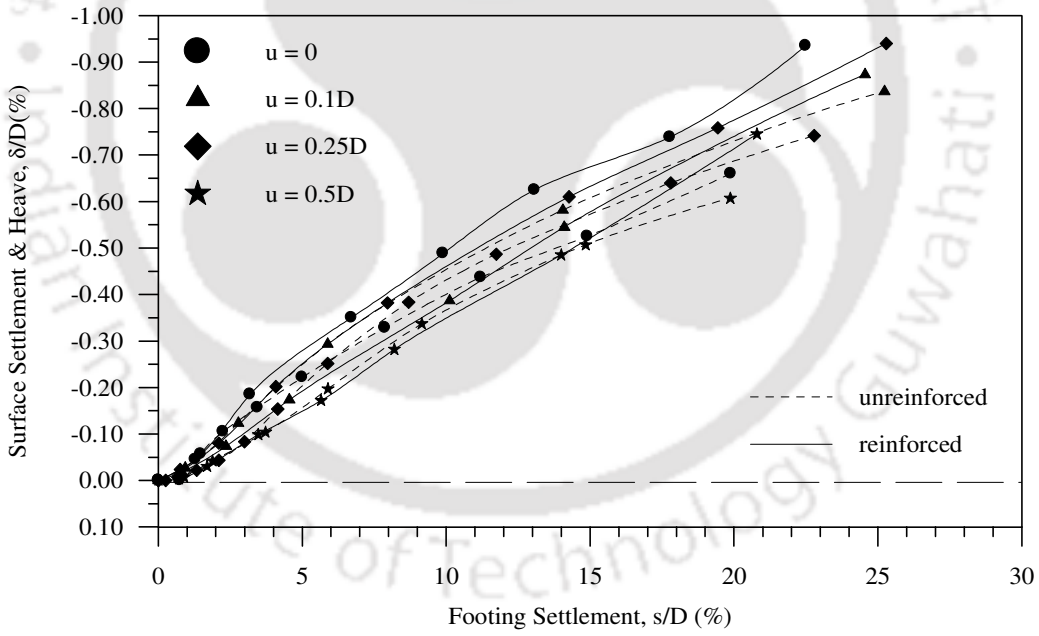

Fig. 5.15 Variation of average surface deformation with footing settlement at a distance x = 2D from the centre of footing, for different depths of placement (u) of geocell mattress. Test Series A2, B1 to B4, h = 0.27D, chevron, d = 1.6D

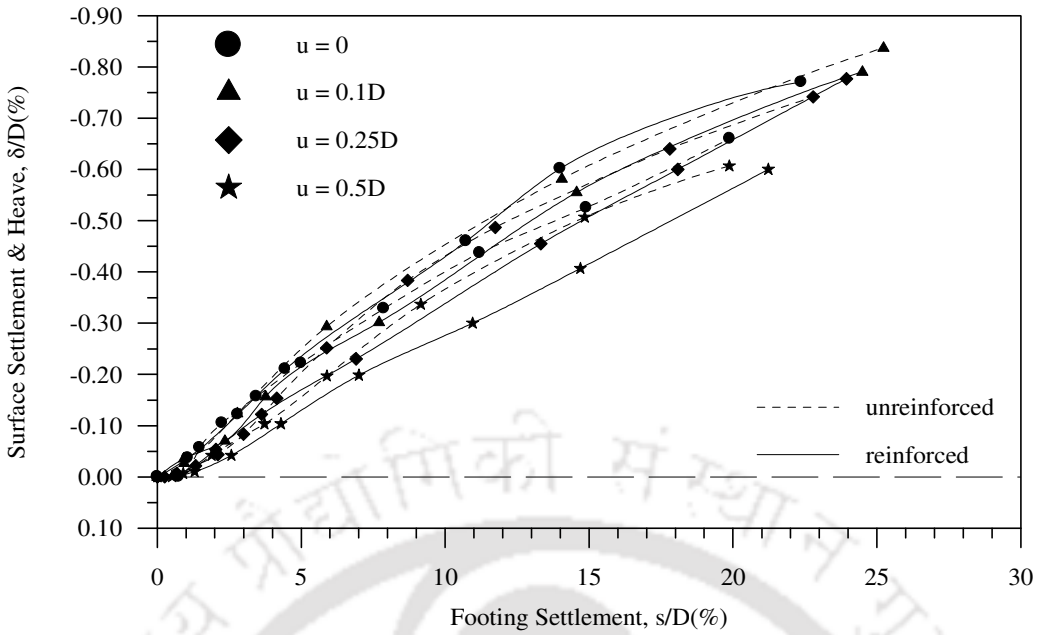

Fig. 5.16 Variation of average surface deformation with footing settlement at a distance x = 2D from the centre of footing, for different depths of placement (u) of geocell mattress. Test Series A2, B1 to B4, h = 0.27D, chevron, d = 1.2D

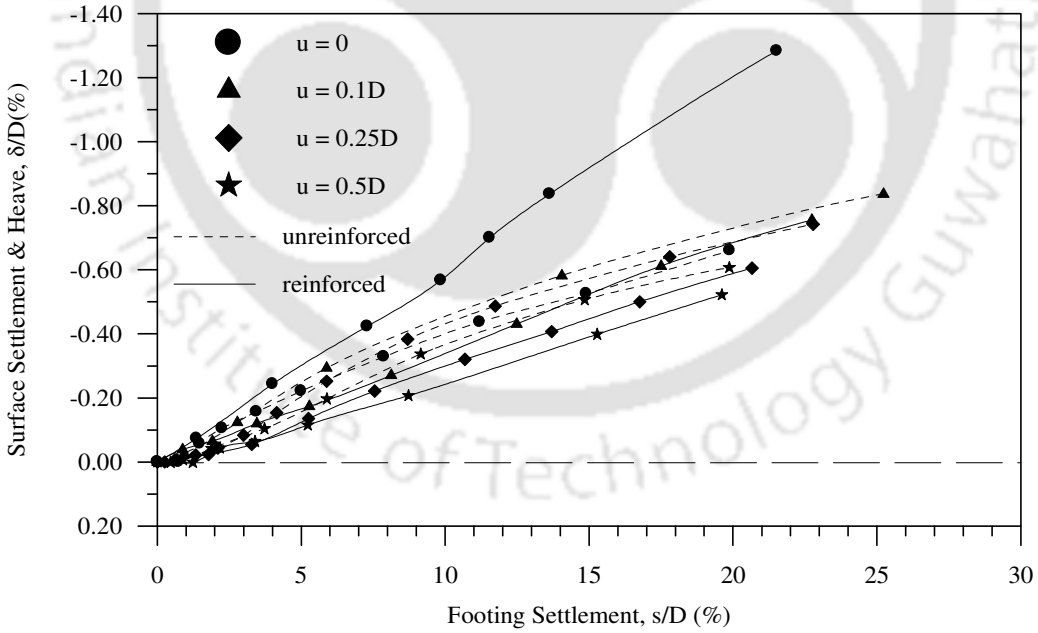

Fig. 5.17 Variation of average surface deformation with footing settlement at a distance x = 2D from the centre of footing, for different depths of placement (u) of geocell mattress. Test Series A2, B1 to B4, h = 0.27D, chevron, d = 0.8D

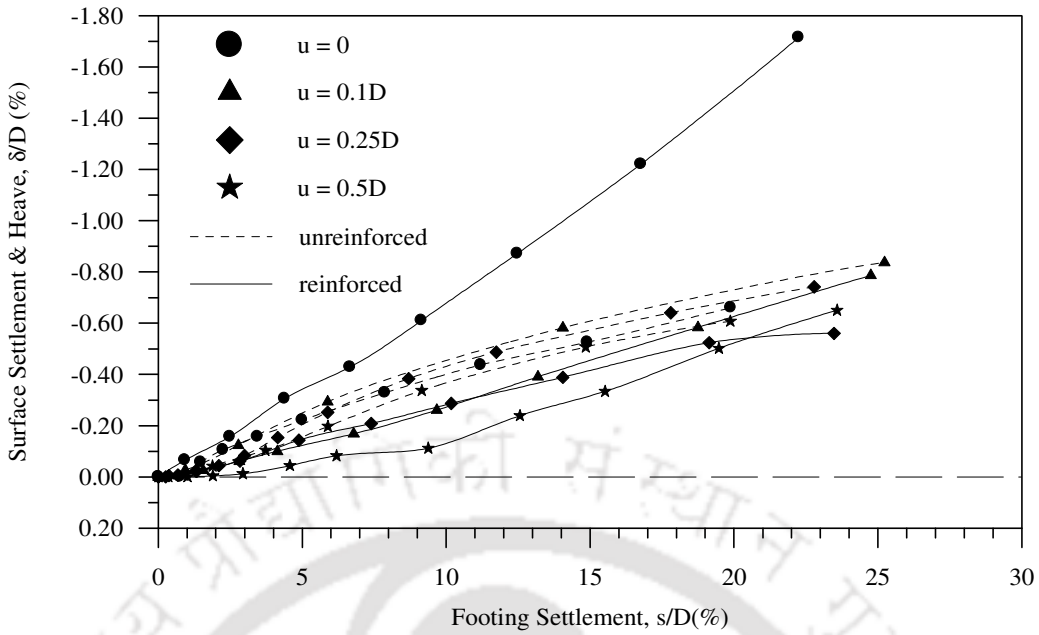

Fig. 5.18 Variation of average surface deformation with footing settlement at a distance x = 2D from the centre of footing, for different depths of placement (u) of geocell mattress. Test Series A2, B1 to B4, h = 0.27D, chevron, d = 0.4D

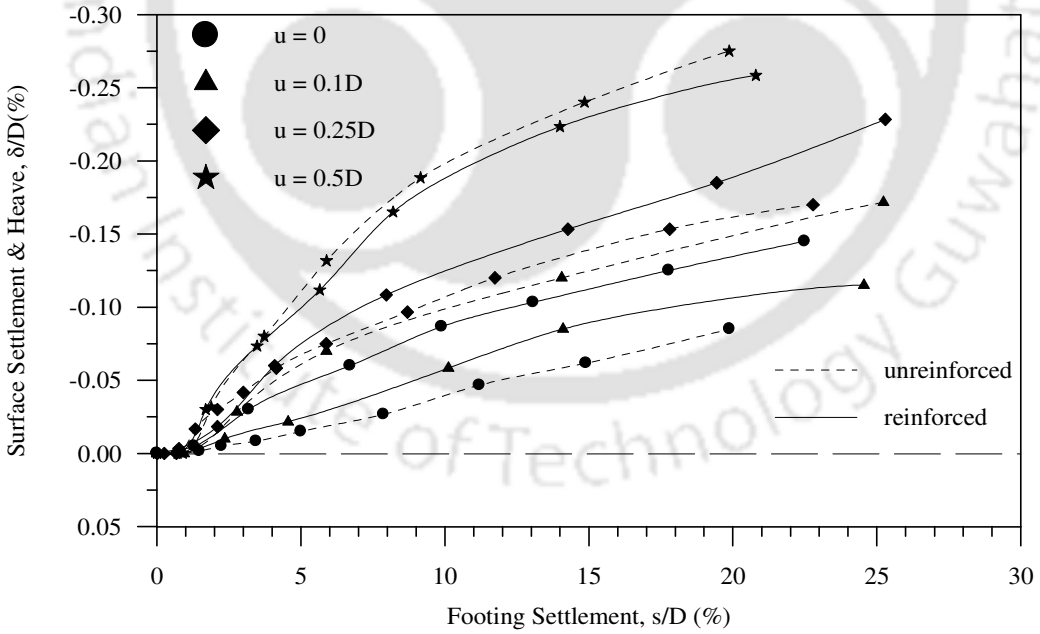

Fig. 5.19 Variation of average surface deformation with footing settlement at a distance x = 3D from the centre of footing, for different depths of placement (u) of geocell mattress. Test Series A2, B1 to B4, h = 0.27D, chevron, d = 1.6D

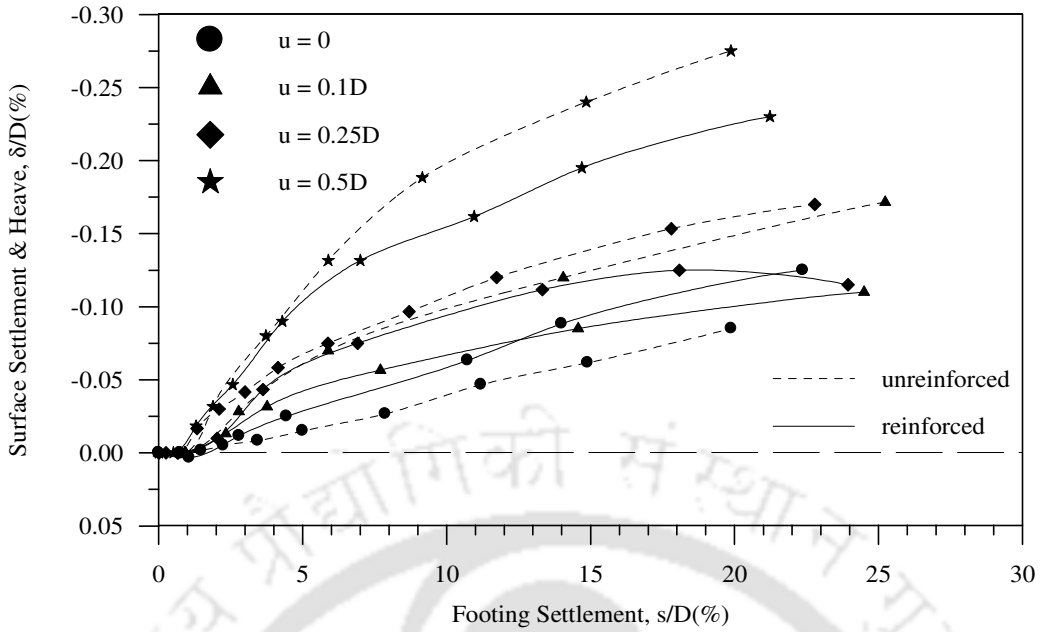

Fig. 5.20 Variation of average surface deformation with footing settlement at a distance x = 3D from the centre of footing, for different depths of placement (u) of geocell mattress. Test Series A2, B1 to B4, h = 0.27D, chevron, d = 1.2D

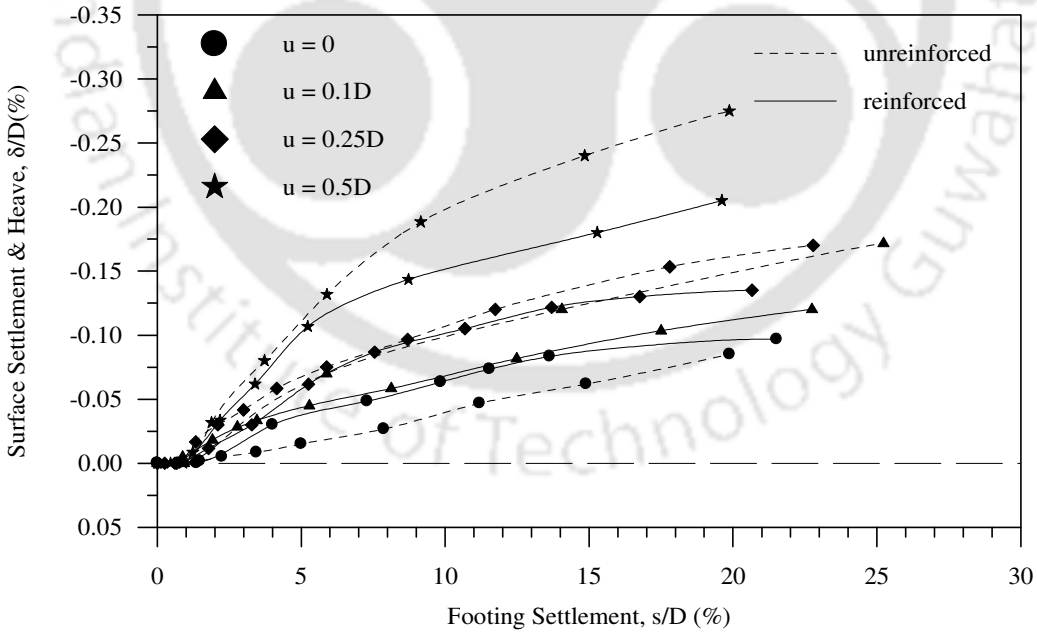

Fig. 5.21 Variation of average surface deformation with footing settlement at a distance x = 3D from the centre of footing, for different depths of placement (u) of geocell mattress. Test Series A2, B1 to B4, h = 0.27D, chevron, d = 0.8D

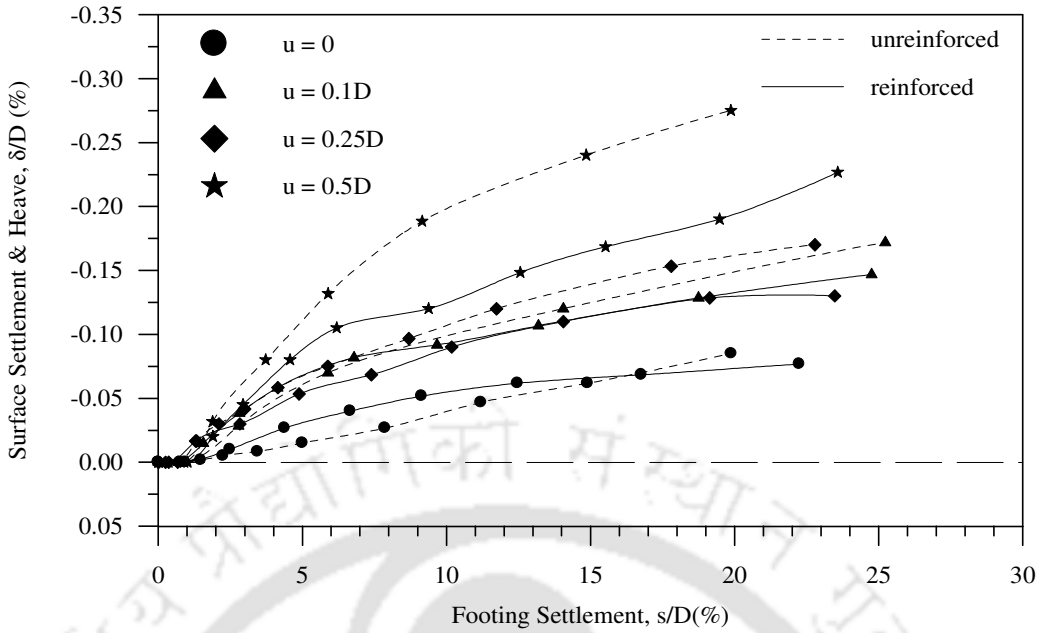

Fig. 5.22 Variation of average surface deformation with footing settlement at a distance x = 3D from the centre of footing, for different depths of placement (u) of geocell mattress. Test Series A2, B1 to B4, h = 0.27D, chevron, d = 0.4D

5.2.1.2 Diamond pattern

The bearing pressure-settlement responses for varying depths of placement of geocell mattress (i.e. u = 0, 0.1D, 0.25D and 0.5D) from the base of the footing prepared using the diamond pattern with height h = 0.27D and pocket sizes, d = 1.6D, 1.2D, 0.8D and 0.4D, are depicted in Figs. 5.23 to 5.26 respectively. These pressure-settlement responses with diamond pattern are nearly similar to those obtained using the chevron pattern of formation. The earlier observation (i.e. chevron pattern) that with geocells having smaller pockets sizes, the beneficial effect of reinforcement is mobilized at much lower settlement than for the larger pocket sizes holds good for the diamond pattern too. The performance improvement, IF_{gc}, obtained from the plots (Figs. 5.23 to 5.26), are tabulated in Table 5.2. Table 5.2 shows that for a given pocket size (d) and depth of placement (u) of geocell mattress, the IF_{gc} generally increases with increase in footing settlement except

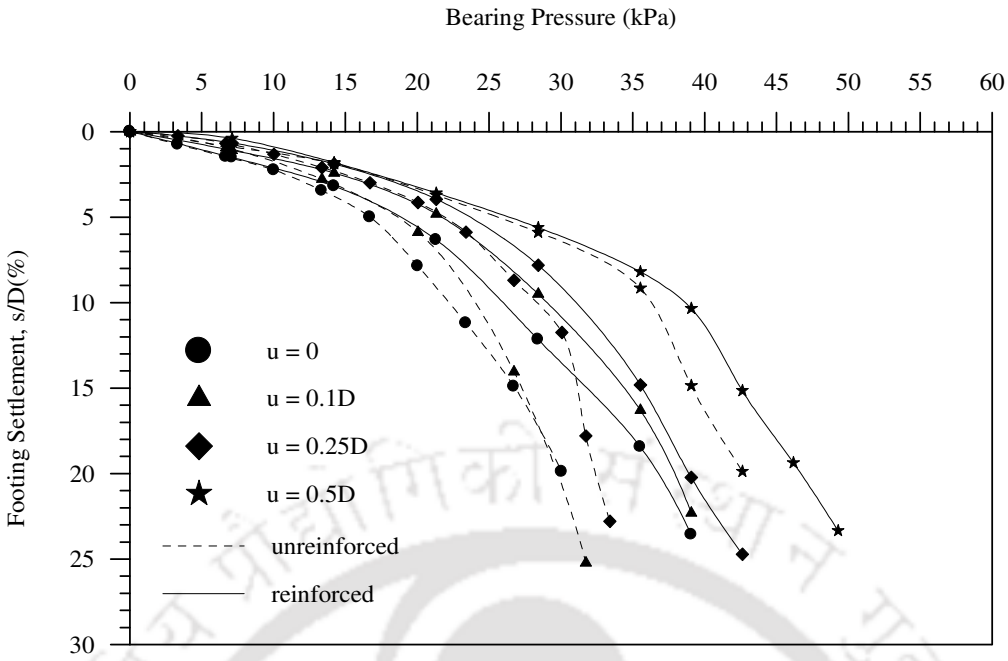

Fig. 5.23 Variation of bearing pressure with footing settlement for different depths of placement (u) of geocell mattress – Test Series A2, C1 to C4, h = 0.27D, diamond, d = 1.6D

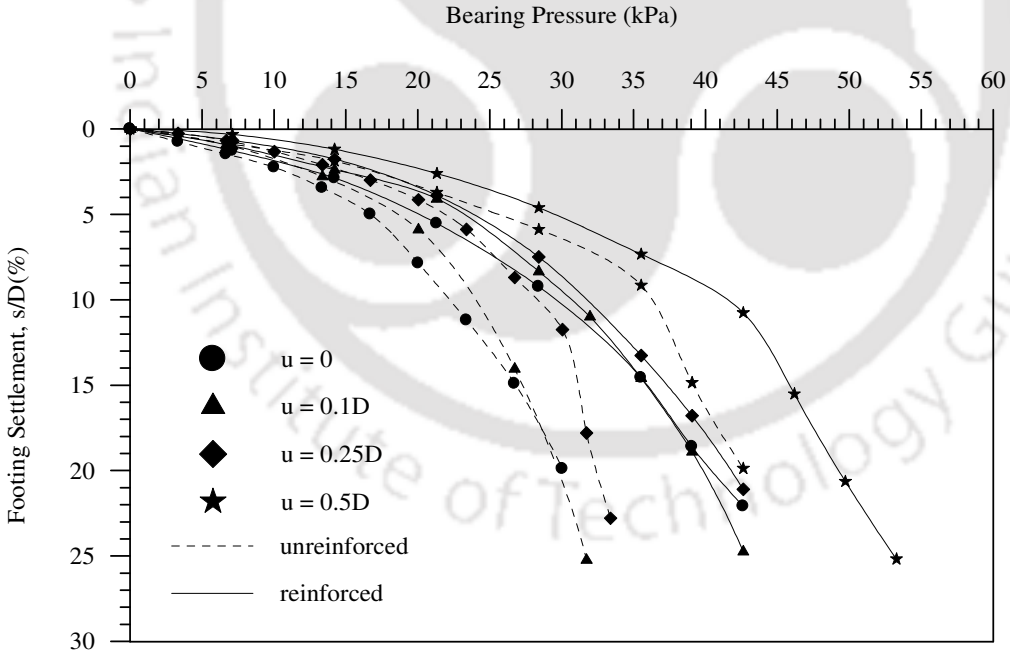

Fig. 5.24 Variation of bearing pressure with footing settlement for different depths of placement (u) of geocell mattress – Test Series A2, C1 to C4, h = 0.27D, diamond, d = 1.2D

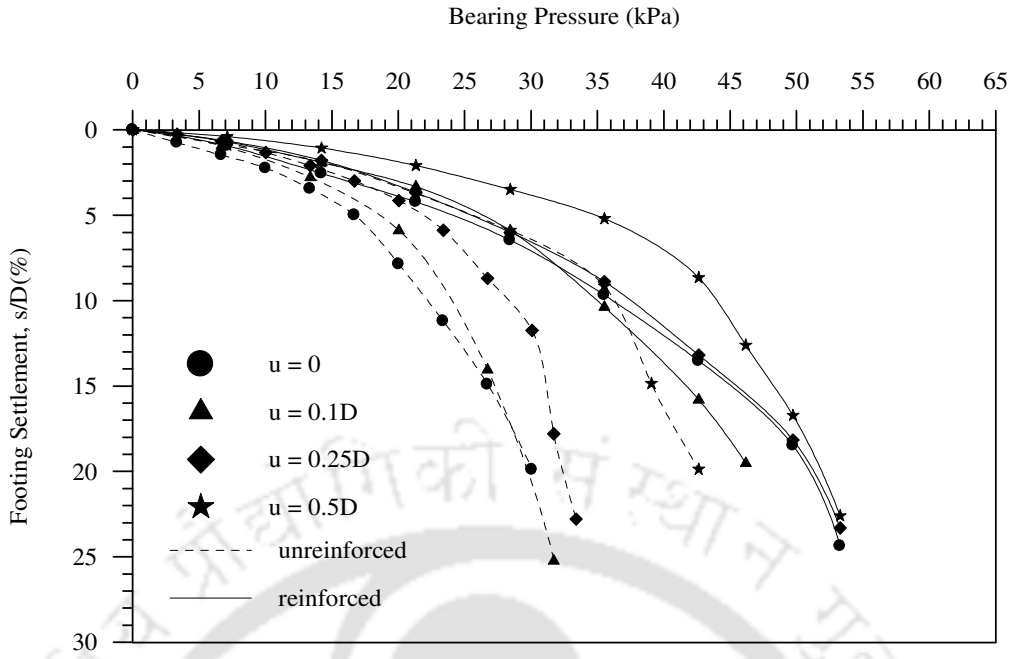

Fig. 5.25 Variation of bearing pressure with footing settlement for different depths of placement (u) of geocell mattress – Test Series A2, C1 to C4, h = 0.27D, diamond, d = 0.8D

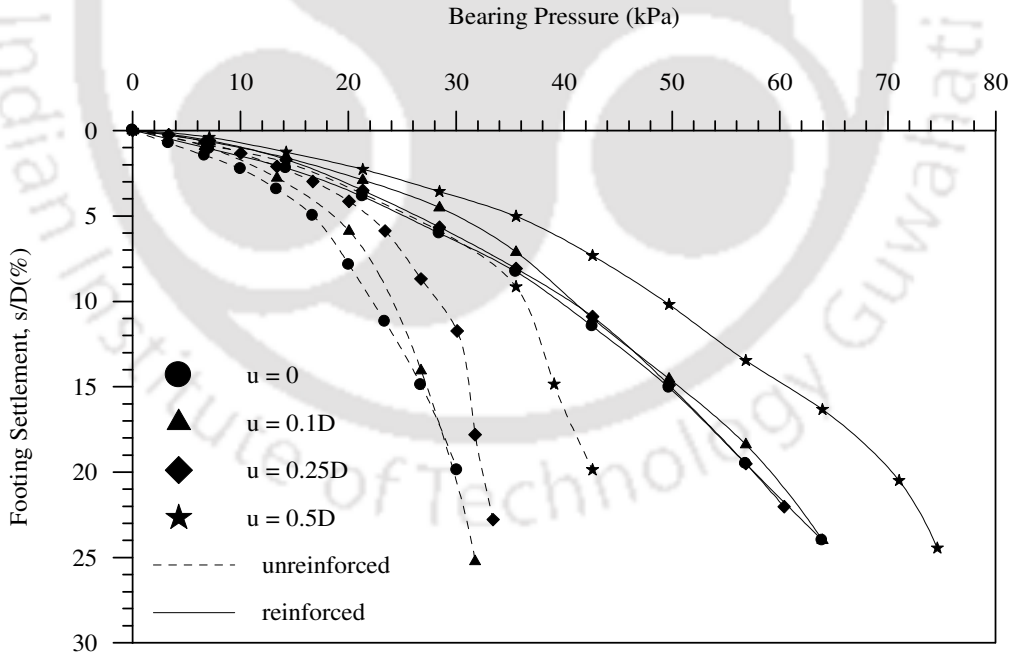

Fig. 5.26 Variation of bearing pressure with footing settlement for different depths of placement (u) of geocell mattress – Test Series A2, C1 to C4, h = 0.27D, diamond, d = 0.4D

for the case when u = 0.5D where the IF_{gc} initially decreases, after which it continues to increase. The critical depth of placement of geocell mattress, $u_{cr,}$ is found to be 0.1D. These results are in agreement with the previous findings using the chevron pattern of formation (Table 5.1). A closer look at Table 5.2 shows that u_{cr} for a pocket size of d = 0.8D is 0 instead of 0.1D. This variation in the result can be attributed to some local effects. Therefore, it could be said that irrespective of the pocket size, geocells both in chevron and diamond pattern, when placed at a depth of 0.1D from the base of the footing, provide maximum performance improvement.

Table 5.2 Summary of results in terms of bearing capacity improvement factor (IF_{gc}) showing the influence of depths of placement (u) of the geocell mattress. Test Series – C1 to C4

Variable Parameter		Bearing capacity improvement factor (IF_{gc})				
		(s/D) 3%	(s/D) 5%	(s/D) 10%	(s/D) 15%	(s/D) 20%
(d/D)	(u/D)					
1.6	0	1.11	1.14	1.17	1.19	1.22
	0.1	**1.16**	**1.17**	**1.22**	**1.26**	**1.28**
	0.25	1.11	1.08	1.10	1.14	1.20
	0.50	1.03	1.02	1.06	1.09	1.10
1.2	0	1.19	1.20	1.31	1.33	1.34
	0.1	**1.24**	**1.24**	**1.31**	**1.33**	**1.34**
	0.25	1.13	1.09	1.12	1.20	1.29
	0.50	1.22	1.15	1.14	1.17	1.16
0.8	**0**	1.32	**1.44**	**1.63**	**1.68**	**1.70**
	0.1	**1.41**	1.41	1.46	1.53	1.56
	0.25	1.14	1.16	1.33	1.46	1.59
	0.50	1.38	1.36	1.21	1.23	1.22
0.4	0	1.47	1.50	**1.78**	1.85	1.91
	0.1	**1.55**	**1.60**	1.71	**1.86**	**1.99**
	0.25	1.17	1.20	1.43	1.60	1.78
	0.50	1.35	1.38	1.35	1.55	1.65

A typical surface deformation profile of a geocell mattress with diamond pattern of formation, having a pocket size of d = 0.8D and placed immediately below the footing (i.e. u = 0) is presented in Fig. 5.27. The surface deformation profiles for other cases (i.e. d = 1.6D, 1.2D, 0.8D, 0.4D; u = 0 to 0.5D) are reported in Appendix 1 (Figs. A1.13 to A1.27). The heaving patterns observed on the fill surface closely resemble that of the chevron pattern.

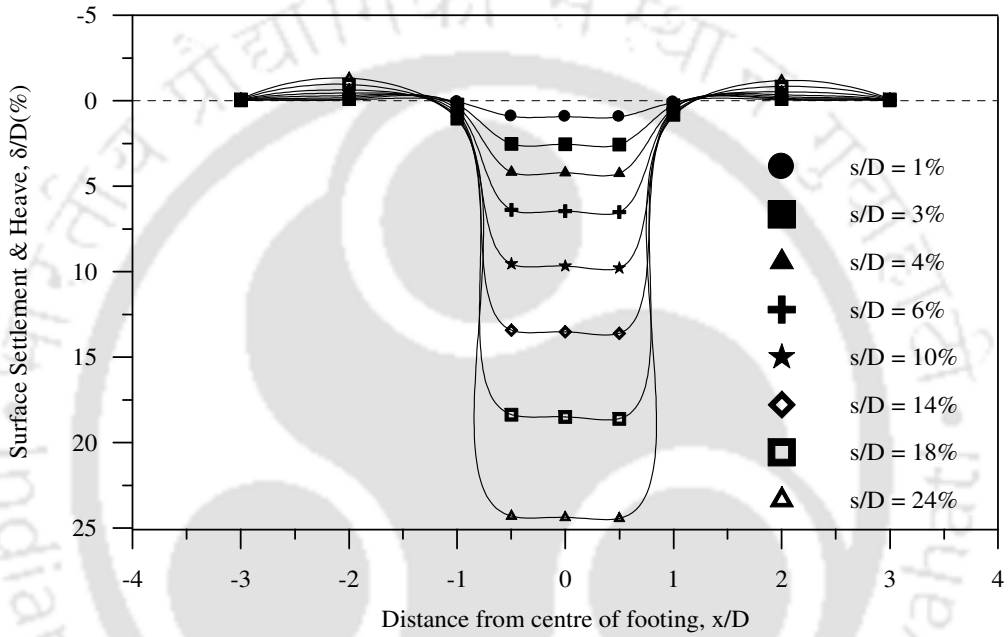

Fig. 5.27 Surface deformation profiles with geocell reinforcement to Test Series C1, diamond, u/D = 0, d = 0.8D

Typical variations of surface deformation with footing settlement for geocell mattress of pocket size d = 1.6D and 0.4D, at a distance of x = D from the centre of footing are presented in Figs. 5.28 and 5.29 respectively. The surface deformation response at x = 3D is shown in Fig. 5.30. The remaining surface deformation responses for various pocket sizes, depths of placement and at different distances from the centre are presented in Appendix 1 (Figs. A1.28 to A1.36). It could be observed that the typical trend i.e. at x = D, the fill surface settles initially and then heaves in case of geocell mattress with larger pocket size whereas it continues to settle with footing settlement for smaller pocket sized

geocells, is in general agreement to that with chevron pattern as seen earlier (Figs. 5.11 to 5.14). Fig. 5.30 shows that the deformation on the fill surface (x = 3D) is found to have similar response to that earlier observed with chevron pattern (Fig. 5.22). The surface generally heaves in this zone and heaving reduces with the provision of geocell mattress, invariably for both shallow and deeper depth of placement of geocell mattress.

This nearly similar response for both the patterns of formation is attributed to equal size and number of geocell pockets in both the cases (Fig. 3.21), giving rise to nearly equal confinement to the encapsulated soil.

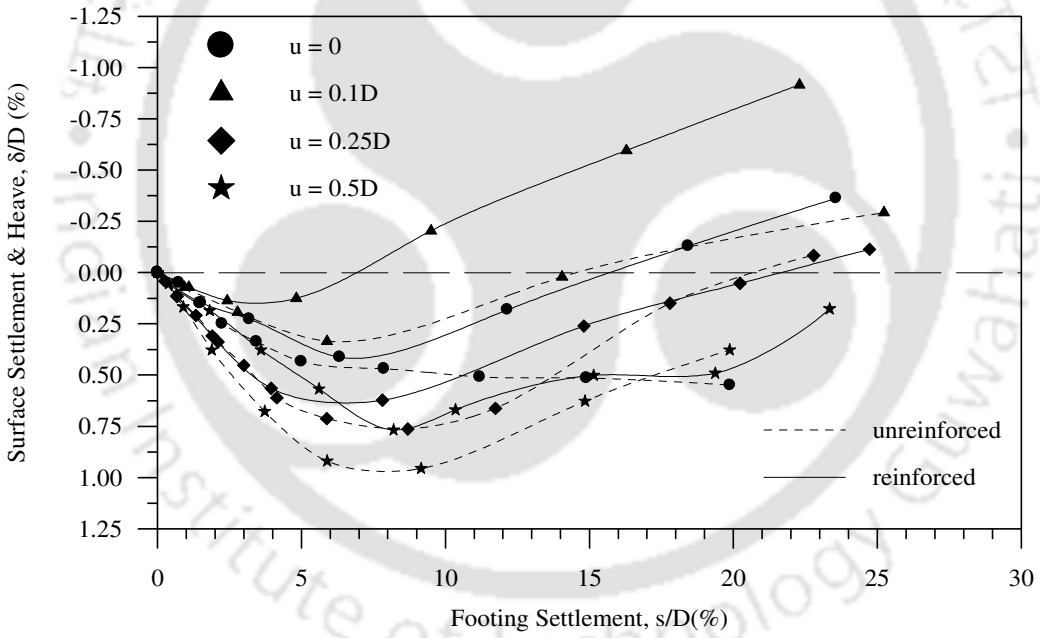

Fig. 5.28 Variation of average surface deformation with footing settlement at a distance x = D from the centre of footing, for different depths of placement (u) of geocell mattress. Test Series A2, C1 to C4, h = 0.27D, diamond, d = 1.6D

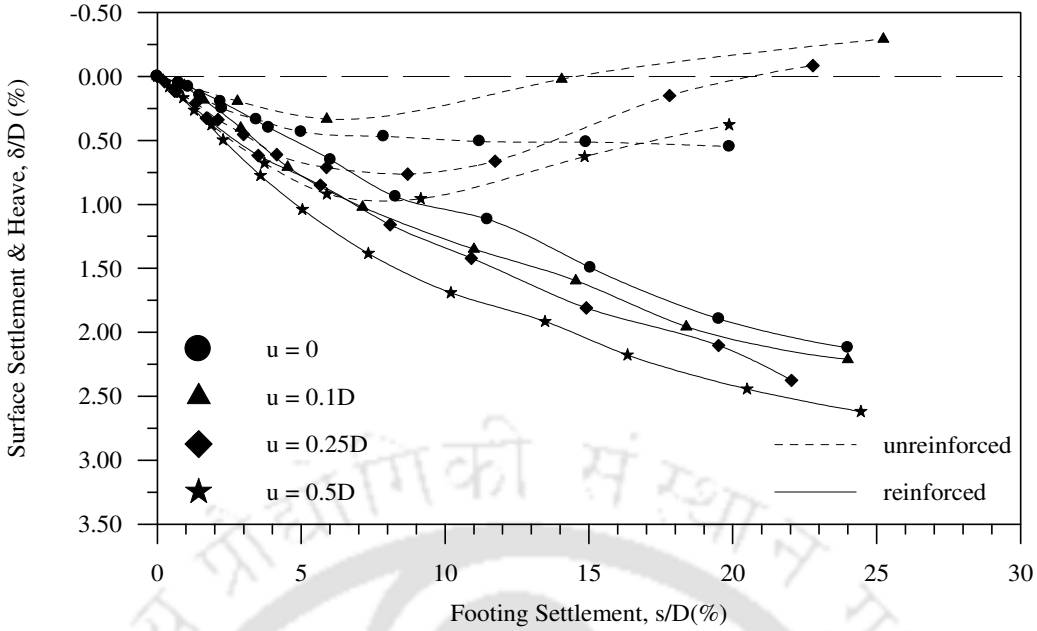

Fig. 5.29 Variation of average surface deformation with footing settlement at a distance x = D from the centre of footing, for different depths of placement (u) of geocell mattress. Test Series A2, C1 to C4, h = 0.27D, diamond, d = 0.4D

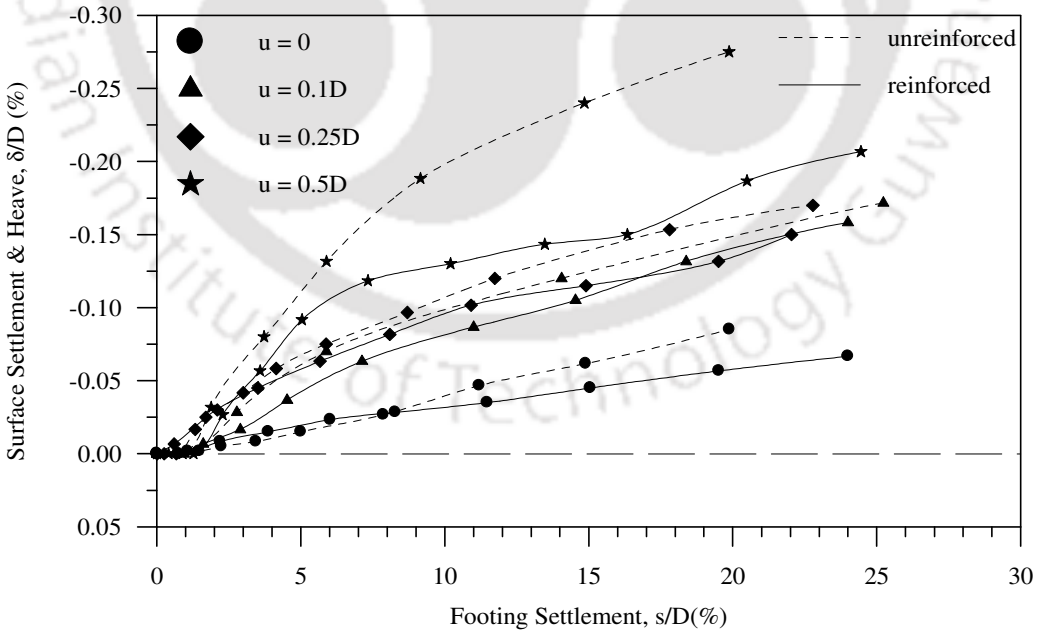

Fig. 5.30 Variation of average surface deformation with footing settlement at a distance x = 3D from the centre of footing, for different depths of placement (u) of geocell mattress. Test Series A2, C1 to C4, h = 0.27D, diamond, d = 0.4D

5.2.2 Influence of height of geocell mattress

The previous series of tests (B1 to B4, C1 to C4) were performed primarily to evaluate the influence of pattern of formation of geocells on the critical depth of placement of geocell mattress (u_{cr}). All the tests in the above series were done using geocell mattress of shallow height (i.e. h = 0.27D). A series of tests (Test Series B5) were further carried out with an increased height of geocell mattress (i.e. h = 0.8D) to study the influence of height on the critical value of 'u'. In these tests, the pattern of formation and the pocket size of the geocells were kept constant as chevron and 0.8D, respectively. The variation of bearing pressure with footing settlement for different depths of placement (i.e. u = 0 to 0.5D) of geocell layer with height, h = 0.8D is shown in Fig. 5.31. As opposed to the case with h = 0.27D (Fig. 5.5), wherein a considerable improvement in load carrying capacity is observed even at a larger depth of placement of geocell mattress (i.e. u = 0.5D), it is seen from Fig. 5.31 that for geocell mattress of higher height (h = 0.8D), the influence of geocell reinforcement is marginal at u = 0.5D. This can be explained by the fact that with the increase in the height of the geocell mattress, the thickness of the corresponding unreinforced sand layer also increases. The unreinforced sand layer, due to induced arching effect, by itself is capable of sustaining certain percentage of footing load. The arching induced soil resistance increases exponentially with increase in the thickness of sand layer (Terzaghi, 1943). As sand layer of very large thickness such as the present one (H = h + u = 0.8D + 0.5D = 1.3D) can sustain substantial amount of footing loading, very less percentage of load is transferred to the reinforcement. Therefore, the contribution of the geocell reinforcement is only marginal in this case.

It is of interest to note that while with h = 0.27D, the pressure-settlement responses have shown an increasing trend with increase in 'u' (Fig. 5.5) but with h = 0.8D the pressure-settlement response with u = 0.5D has shown a reduced trend compared to that with u =

0.25D (Fig. 5.31). A geocell mattress of shallow height (h = 0.27D) being flexible deforms under footing loading that the intermediate sand cushion (u) moves along with it as an integral part. But a geocell mattress of higher height (h = 0.8D) owing to its increased rigidity stands against the footing penetration as a result of which the intermediate sand cushion, particularly of relatively larger thickness (u = 0.5D), overcomes the friction between the geocell pockets and footing base thereby tends to get squeezed away, leading to reduced load carrying capacity.

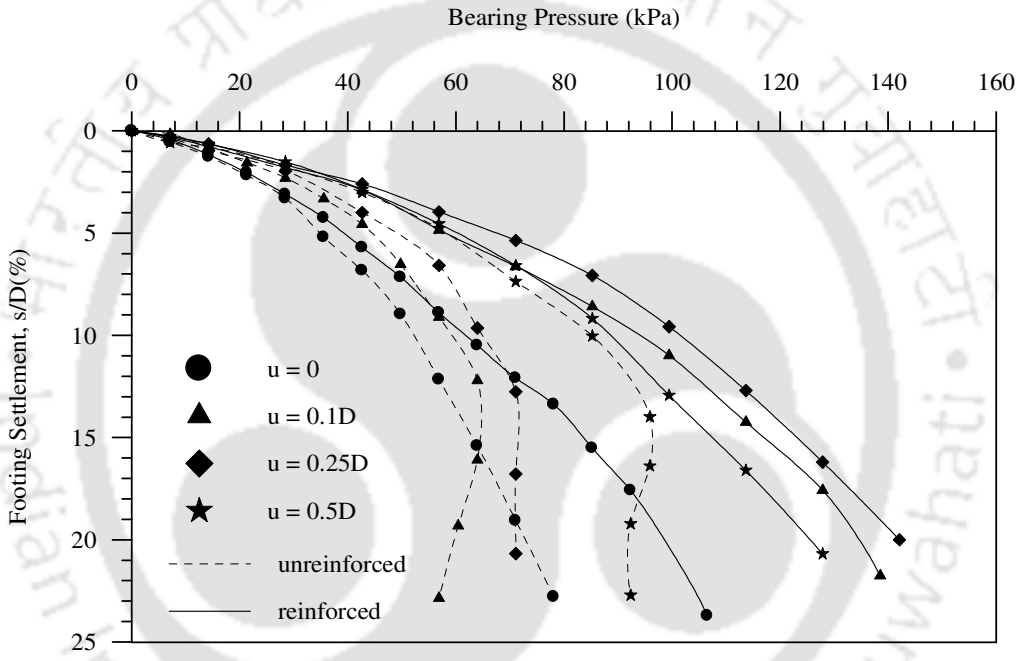

Fig. 5.31 Variation of bearing pressure with footing settlement for different depths of placement (u) of geocell mattress – Test Series B5, h = 0.8D, chevron, d = 0.8D

The comparsion of the improvement factor (IF_{gc}) obtained with geocell mattress of two different heights (i.e. h = 0.27D and 0.8D) is shown in Table 5.3. From the table, it could be seen that for both smaller and higher height geocell mattress, the value of improvement factor (IF_{gc}) increases significantly from u = 0 to 0.1D, after which it continues to decrease with further increase in depth of placement. The consistency in the results obtained from tests conducted at two different heights of the geocell mattress

proves that the height of the geocell mattress has little influence on the critical depth of placement (u_{cr}) of the geocell mattress. Comparing the improvement factors obtained at critical depth of placement, u_{cr} = 0.1D, it can be seen from the table (Table 5.3), that at lower settlement range (s/D < 15%), the value of IF_{gc} is higher for geocell mattress of smaller height (i.e. h = 0.27D) while beyond a settlement of 15% of footing diameter, geocell mattress of higher height (i.e. h = 0.8D) gives better performance improvement. This is because for smaller height of geocell mattress, the thin layer of sand above the clay subgrade being unable to sustain the footing load transfers a higher percentage of load to the geocell reinforcement. As the benefit from reinforcement is mobilized at an early stage, a higher improvement factor is obtained at low settlement levels. However for the case of higher height of geocell mattress, the footing load is initially taken up by the sand layer. It is only at higher settlement when the soil begins to fail that the reinforcing action of the geocells becomes dominant thereby bringing about an increase in the improvement factor.

Table 5.3 Summary of results in terms of bearing capacity improvement factor (IF_{gc}) showing the influence of height on the critical depth of placement (u_{cr}) of the geocell mattress. Test Series B1 to B5

Variable Parameter		Bearing capacity improvement factor (IF_{gc})				
		(s/D) 3%	(s/D) 5%	(s/D) 10%	(s/D) 15%	(s/D) 20%
(h/D)	(u/D)					
0.27	0	1.22	1.26	1.48	1.55	1.50
	0.1	**1.37**	**1.47**	**1.62**	**1.70**	**1.79**
	0.25	1.20	1.26	1.47	1.53	1.63
	0.50	1.40	1.35	1.22	1.26	1.26
0.8	0	1.03	1.13	1.18	1.33	1.35
	0.1	**1.31**	1.31	**1.58**	**1.81**	**2.25**
	0.25	1.31	**1.36**	1.57	1.72	2.00
	0.50	1.03	1.03	1.04	1.11	1.37

The surface deformation profiles for various depths of placement of geocell mattress with height, h = 0.8D are similar to those obtained earlier using geocell mattress of h = 0.27D, therefore are presented in Appendix 1 (Figs. A1.37 to A1.40). The surface deformation versus footing settlement responses at distances of x = D, 2D and 3D from the centre of the footing are shown in Figs. 5.32 to 5.34. Figs. 5.13 and 5.32 that depict the deformation on the surface at x = D, for geocell mattress of height, h = 0.27D and 0.8D respectively, show that the settlement on the fill surface is more with geocell mattress of h = 0.8D. It can be seen that with geocell mattress of smaller height, at a settlement of 20% of footing diameter (s/D = 20%), the maximum settlement on the fill surface (δ) is about 1.6% of the footing diameter while it becomes almost double (δ/D = 3.2%) with the provision of a higher height geocell mattress. This indicates that the settlement zone has increased which is attributed to the increased ability of the relatively rigid foundation bed to distribute the footing pressure over a much wider area beyond the footing. The prominent heaving on the fill surface which was observed earlier in case of h = 0.27D, at x = 2D (δ/D = -1.3%; Fig. 5.17), is absent in the present case of higher height geocell layer (Fig. 5.33). This is because as explained earlier the geocell mattress of shallow height being flexible undergoes a sagging type deformation under the loading and correspondingly hogging type deformation in the region outside thereby giving rise to an induced higher heaving at x = 2D. Whereas, the geocell mattress of higher height behaves as a relatively rigid pad that it settles in a much uniform manner leading to reduced heave on fill surface. Also, the magnitude of surface heave, at all depths of placement (u), is found to be less in case of geocell mattress of higher height. At x = 3D, the heaving, in general, is found to reduce with the provision of geocell reinforcement for both smaller and higher height geocell mattress as seen in Figs. 5.21 and 5.34 respectively. However the percentage reduction in heave, due to reinforcement, is greater for geocell mattress of

higher height than for the corresponding geocell mattress of smaller height. Thus, irrespective of depth of placement, the effect of geocell reinforcement increases with increase in height, h/D. This is because, besides increasing the rigidity of the structure, the increased height of geocell reinforcement also offers better confinement of the infill material thus leading to lesser heave.

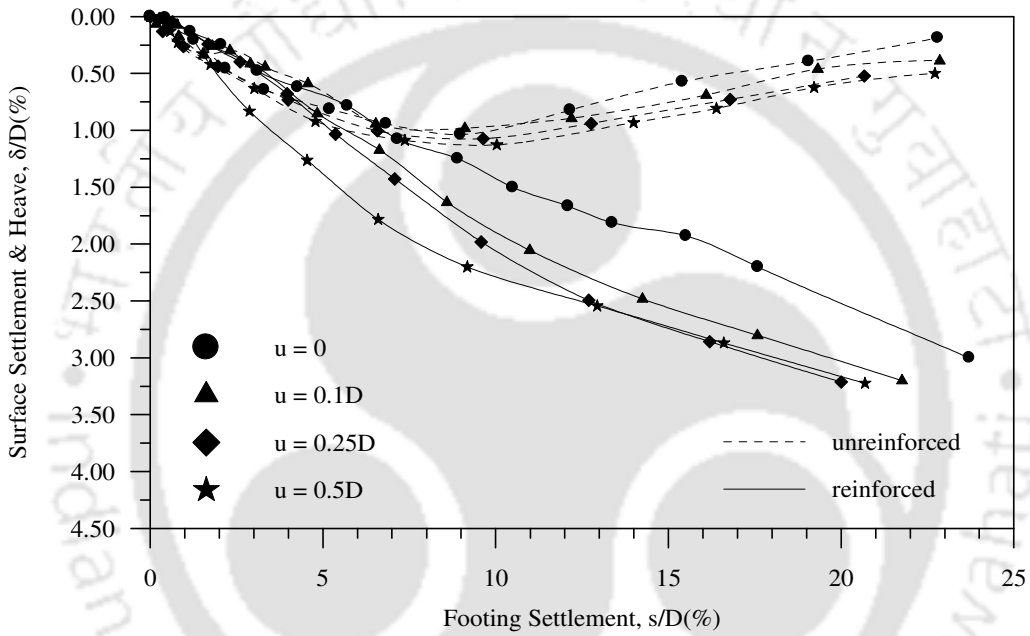

Fig. 5.32 Variation of average surface deformation with footing settlement at a distance x = D from the centre of footing, for different depths of placement (u) of geocell mattress. Test Series B5, h = 0.80D, chevron, d = 0.8D

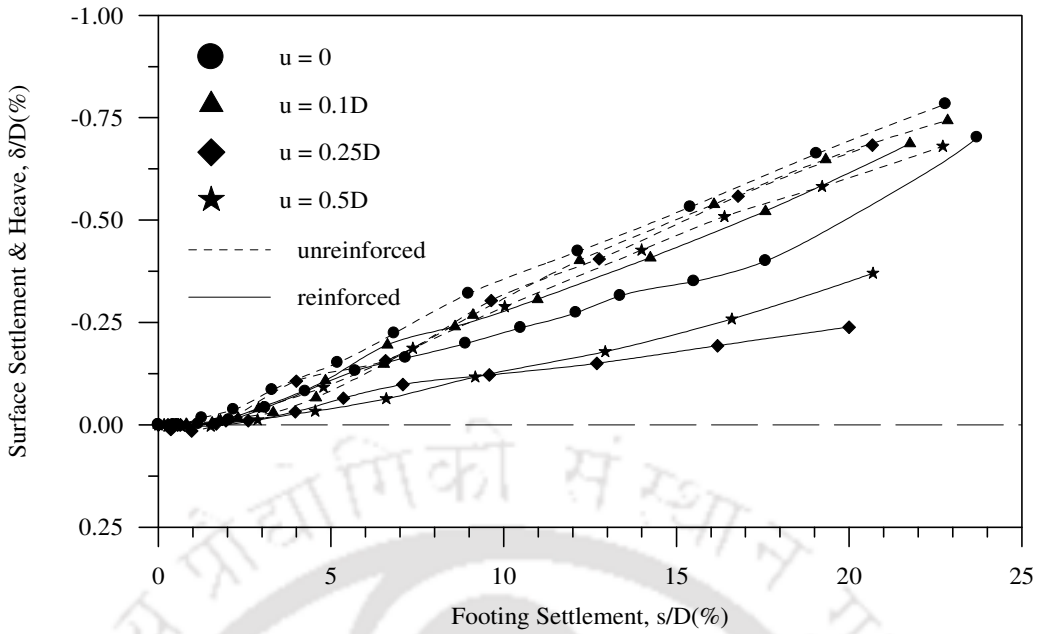

Fig. 5.33 Variation of average surface deformation with footing settlement at a distance x = 2D from the centre of footing, for different depths of placement (u) of geocell mattress. Test Series B5, h = 0.80D, chevron, d = 0.8D

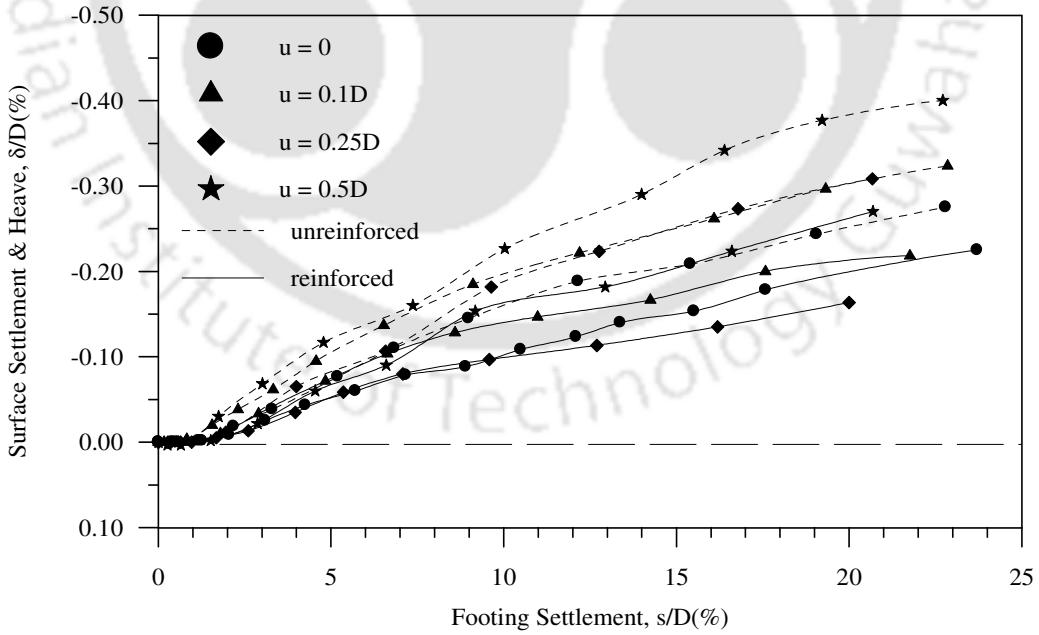

Fig. 5.34 Variation of average surface deformation with footing settlement at a distance x = 3D from the centre of footing, for different depths of placement (u) of geocell mattress. Test Series B5, h = 0.80D, chevron, d = 0.8D

5.2.3 Influence of pocket size of geocells

The influence of pocket size on the value of critical depth of placement of geocell mattress was investigated under series B1 to B4 and series C1 to C4 for the chevron and diamond pattern of formation respectively. Table 5.1 summarizes the results obtained for chevron pattern of formation of geocells with pocket sizes, (d) of 1.6D, 1.2D, 0.8D and 0.4D and depth of placement (u) varying from 0 to 0.5D. It is seen that irrespective of the pocket size of the geocells, the value of critical depth of placement (u_{cr}) of the geocell mattress remains constant (i.e. $u_{cr} = 0.1D$). Similar conclusions can be drawn from Table 5.2 for geocell mattress with the diamond pattern of formation.

Based on the above discussions it can be said that the critical depth of placement (u_{cr}) of the geocell mattress giving maximum performance improvement is about 0.1D from the base of the footing. The pattern of formation, pocket size and height of the geocell mattress has little influence on the critical depth of placement of the geocell mattress.

5.3 PATTERN OF FORMATION

The geocell reinforcements in this study were formed using two different patterns (i.e. chevron and diamond; Fig. 3.21). A number of tests were done to compare the performance of the geocells formed using these two patterns and to arrive at the more efficient pattern giving better performance improvement. For all tests, the placement depth of the geocell mattress was kept equal to the critical depth obtained earlier (i.e. $u = u_{cr} = 0.1D$). The comparisons between the two patterns are carried out for different configurations of geocell mattress i.e. for pocket size varying from 1.6D to 0.4D, height varying from 0.27D to1.07D and relative density of infill soil varying from 35% to 80%. The details of these tests are presented in Table 3.4 (Test series B2, C2, C5, C6, C7, D3,

E1, E2, E3, F3 and G3). The influences of these parameters on the formation type giving better performance improvement are discussed in details in the following subsections.

5.3.1 Influence of pocket size of geocells

The pressure-settlement responses for the two patterns of formation of geocells, at height (h) of 0.27D with pocket sizes, d = 1.6D, 1.2D, 0.8D and 0.4D (Test series B2, C2) and at height (h) of 0.53D with pocket sizes, d = 1.2D, 0.8D and 0.4D (Test series C6, E3) are presented in Figs. 5.35 and 5.36 respectively. The improvements in performance (IF_{gc}), due to geocell reinforcements, for the two different patterns, are presented in Table 5.4. It could be seen that, in general, the chevron pattern of formation gives higher improvement in terms of bearing capacity and this is irrespective of the pocket size of the geocells. This can be explained through Fig. 3.21 which shows that for the same plan area, 20 numbers of joints are involved with chevron pattern for formation of geocells as against 12 numbers of joints with diamond pattern. Owing to the higher number of joints, the geocells formed in chevron pattern are relatively more rigid than the diamond pattern and consequently give rise to higher improvement factor. Another advantage of having higher number of joints in the mattress is that in the event of failure of an individual joint during its service life, it will pose less problems to the stability of the structure.

It could also be observed from Table 5.4 that the difference in the performance between the two patterns becomes more apparent with the decrease in pocket size of the geocells. This is because with the reduction in pocket size, the number of cells that can be accommodated within a given area is more. As the difference between the number of joints in chevron and diamond pattern are higher in case of smaller pocket sized geocells, the difference in the performance between the two formation types becomes more evident with the reduction in pocket size.

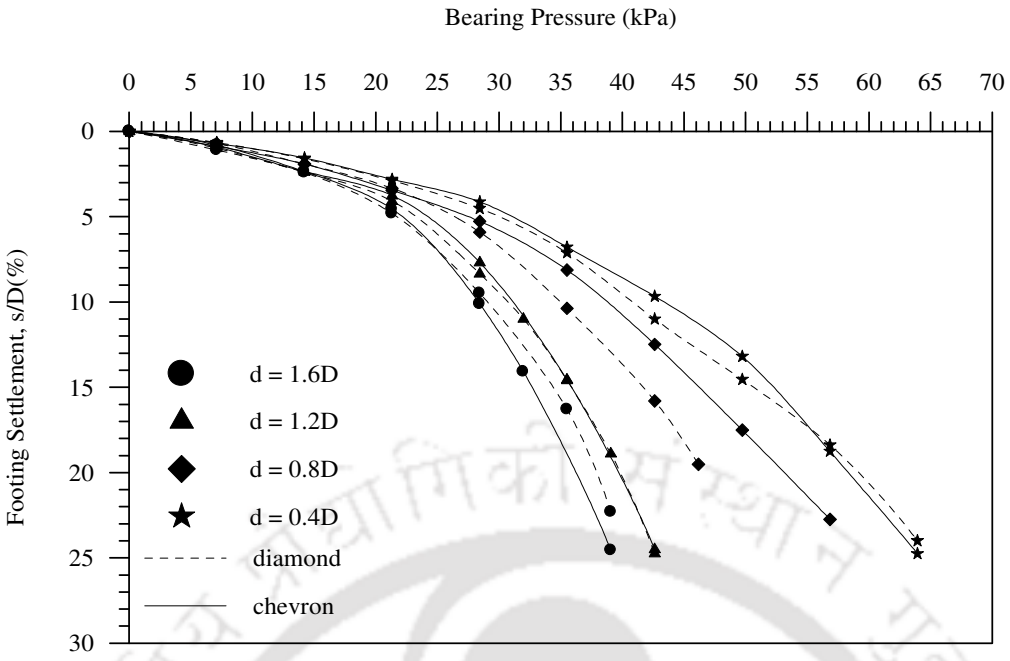

Fig. 5.35 Variation of bearing pressure with footing settlement for different patterns of formation of geocell mattress – Test Series B2, C2, u/D = 0.1, ID = 80%, h = 0.27D

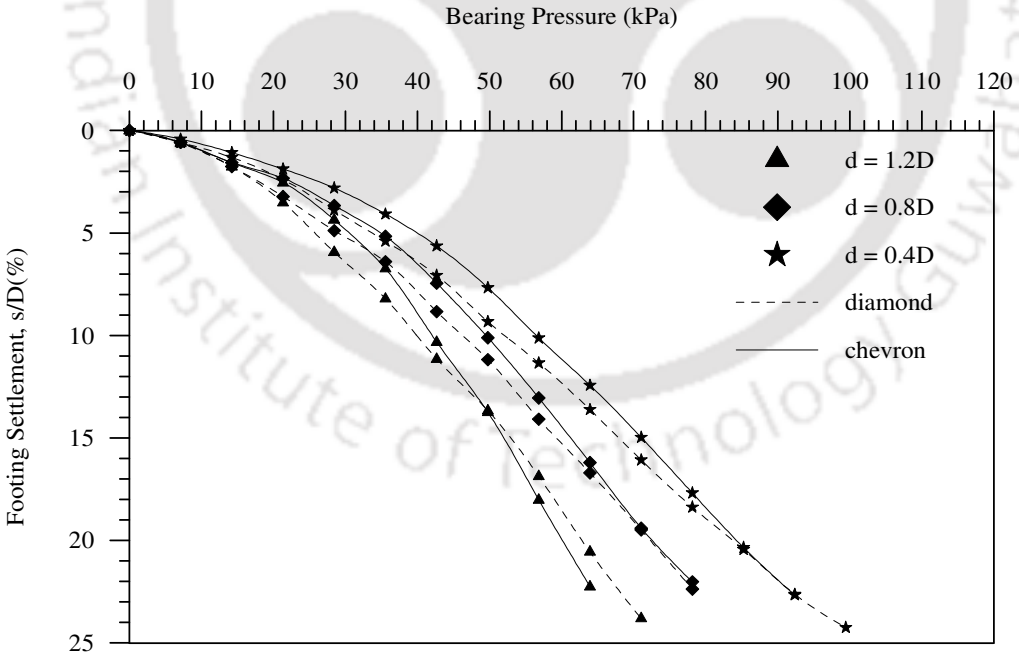

Fig. 5.36 Variation of bearing pressure with footing settlement for different patterns of formation of geocell mattress – Test Series C6, E3, u/D = 0.1, ID = 80%, h = 0.53D

Table 5.4 Summary of results in terms of bearing capacity improvement factor (IF_{gc}) showing the influence of pocket size (d) and height (h) on the more efficient pattern of geocell formation.

Variable parameter			Bearing capacity improvement factor (IF_{gc})				
			(s/D) 3%	(s/D) 5%	(s/D) 10%	(s/D) 15%	(s/D) 20%
(h/D)	(d/D)						
0.27	1.6	chevron	**1.18**	**1.18**	1.19	1.19	1.22
		diamond	1.16	1.17	**1.22**	**1.26**	**1.28**
	1.2	**chevron**	**1.29**	**1.29**	**1.31**	1.32	**1.34**
		diamond	1.24	1.24	**1.31**	**1.33**	**1.34**
	0.8	**chevron**	1.37	**1.47**	**1.62**	**1.70**	**1.79**
		diamond	1.41	1.41	1.46	1.53	1.56
	0.4	**chevron**	**1.59**	**1.66**	**1.82**	**1.92**	**1.96**
		diamond	1.55	1.60	1.71	1.86	1.99
0.53	1.2	**chevron**	**1.29**	**1.30**	**1.40**	1.52	1.54
		diamond	1.08	1.09	1.33	**1.55**	**1.61**
	0.8	**chevron**	**1.37**	**1.49**	**1.65**	**1.80**	**1.86**
		diamond	1.12	1.23	1.54	1.74	1.85
	0.4	**chevron**	**1.64**	**1.70**	**1.88**	**2.09**	**2.16**
		diamond	1.35	1.43	1.73	1.99	2.15
0.8	0.8	**chevron**	**1.31**	**1.31**	**1.58**	**1.81**	**2.25**
		diamond	1.06	1.09	1.29	1.55	2.07
1.07	0.8	**chevron**	**1.19**	**1.31**	**1.51**	**1.71**	**2.08**
		diamond	1.08	1.08	1.34	1.56	1.95

Figs. 5.37 and 5.38 depict the surface deformation versus footing settlement responses at a distance of x = D and x = 2D from the centre of footing, for both the patterns of formation of geocell mattress with height, h = 0.27D and pocket sizes varying from 1.6D to 0.4D, respectively. It could be observed that for most cases, the surface deformation responses for the chevron and diamond pattern are almost same. This is because the number of cells and the effective pocket size for both patterns are same which gives nearly equal confinement to the soil mass.

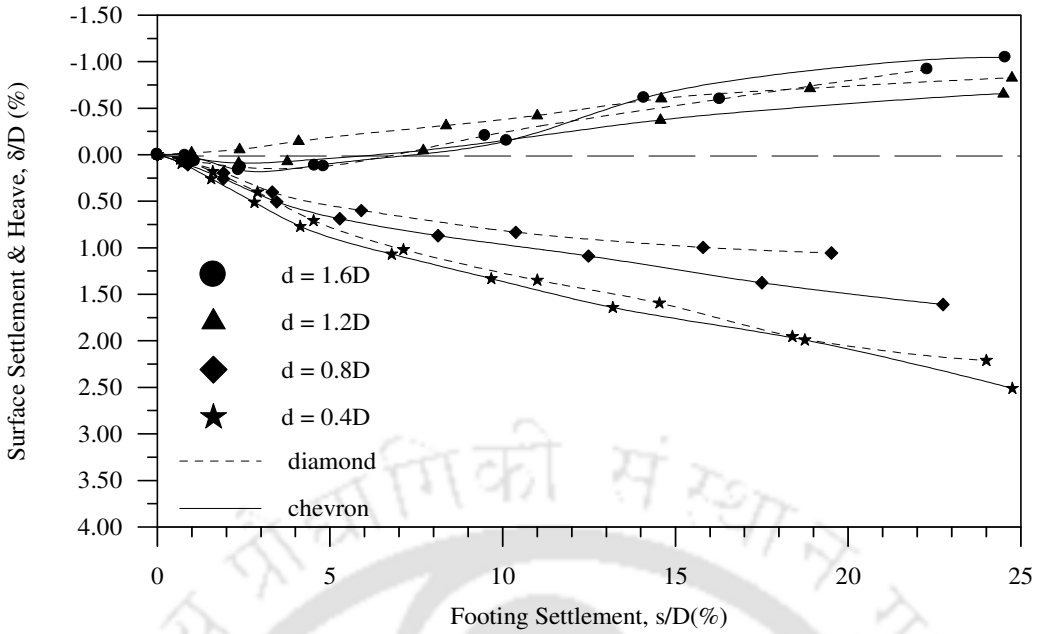

Fig. 5.37 Variation of average surface deformation with footing settlement at a distance x = D from the centre of the footing for different patterns of formation of geocell mattress – Test Series B2, C2, u/D = 0.1, ID = 80%, h = 0.27D

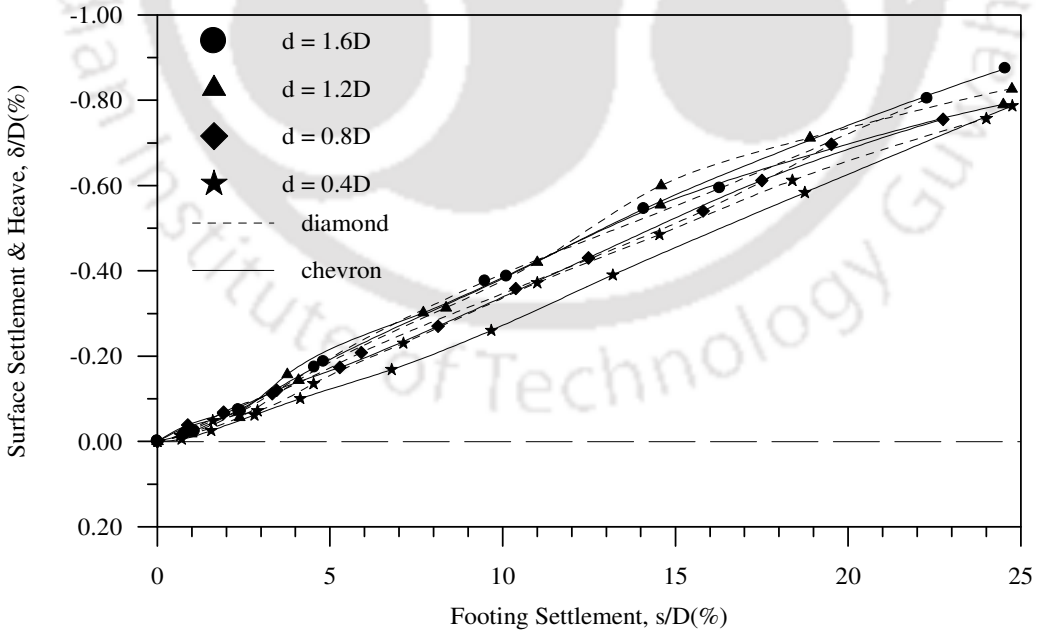

Fig. 5.38 Variation of average surface deformation with footing settlement at a distance x = 2D from the centre of the footing for different patterns of formation of geocell mattress – Test Series B2, C2, u/D = 0.1, ID = 80%, h = 0.27D

5.3.2 Influence of height of geocell mattress

A comparison between the two patterns of formation (chevron and diamond) were carried out with different heights of geocell mattress (h = 0.27D, 0.53D, 0.8D and 1.07D) under various series (Test series C5, D3, E3, F3, G3). The pocket size (d) of the geocells and the relative density (ID) of the infill sand were kept constant at 0.8D and 80% respectively. The variation of bearing pressure with footing settlement due to different patterns of formation, for geocell heights of h = 0.27D to 1.07D, is presented in Fig. 5.39 and the bearing capacity improvement factor subsequently obtained is summarized in Table 5.4. It could be seen that at almost all heights of geocell mattress, the chevron pattern gives better performance improvement than the diamond pattern. However, the trend is clearer for higher height of geocell mattress. This is because with smaller height, the geocell system being flexible gets pulled in under footing penetration. But with increased height, it stands against the footing thereby shares increased percentage of loading through mobilization of its rigidity. As a result of which, the increased rigidity due to increase in joints plays a greater role, thereby giving rise to prominently increased performance improvement with the chevron pattern.

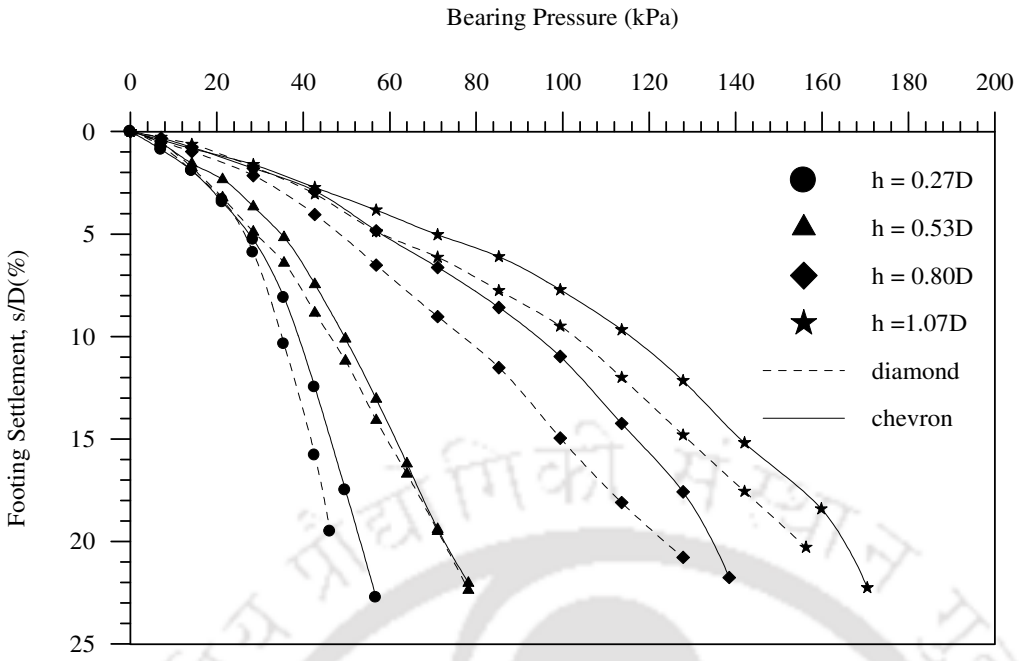

Fig. 5.39 Variation of bearing pressure with footing settlement for different patterns of formation of geocell mattress – Series C5, D3, E3, F3,G3, u/D = 0.1, ID = 80%, d = 0.8D

5.3.3 Influence of relative density of infill sand

The influence of relative density of the infill sand on the performance of the formation type was investigated for geocell mattress of height, h = 0.53D and pocket size, d = 0.8D, under series C7, E1, E2 and E3. The different relative densities considered in these series are 35%, 50% and 80%. The pressure-settlement responses for geocells formed using diamond and chevron patterns with different relative densities of sand are shown in Fig. 5.40 and their improvement factors (IF_{gc}) are tabulated in Table 5.5. It could be seen that the improvement factor (IF_{gc}) at different levels of footing settlement is more in the case of geocell formed in chevron pattern. This is true for all relative densities of the infill sand.

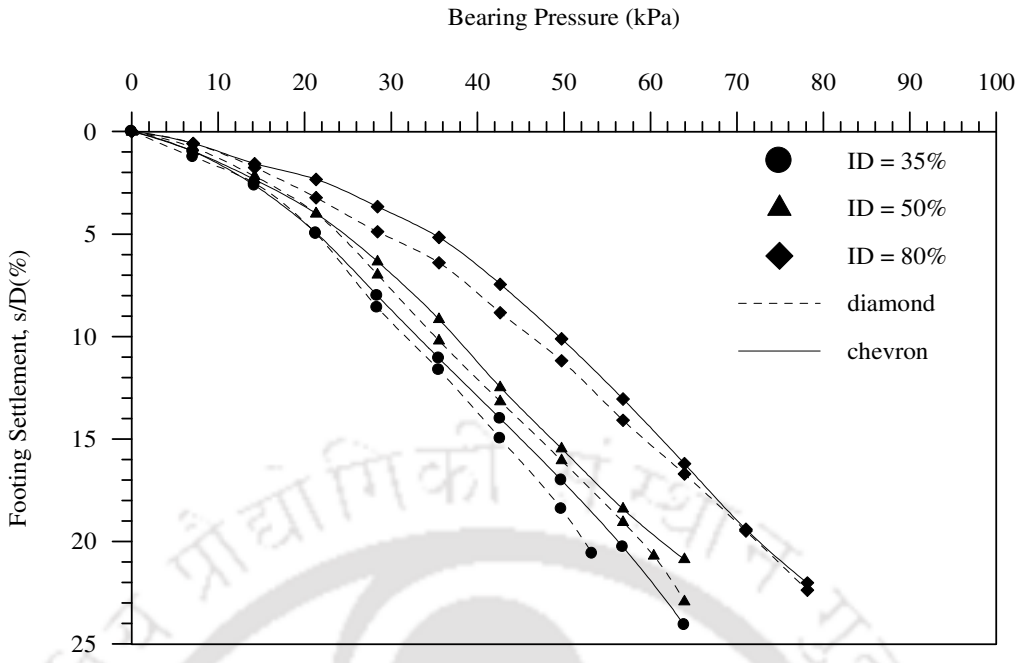

Fig. 5.40 Variation of bearing pressure with footing settlement for different patterns of formation of geocell mattress – Test Series C7, E1, E2, E3, u/D = 0.1, h = 0.53D, d = 0.8D

Table 5.5 Summary of results in terms of bearing capacity improvement factor (IF_{gc}) showing the influence of relative density on the more efficient pattern of geocell formation.

Variable parameter			Bearing capacity improvement factor (IF_{gc})				
			(s/D) 3%	(s/D) 5%	(s/D) 10%	(s/D) 15%	(s/D) 20%
(h/D)	(ID)						
0.53	35%	**chevron**	**1.21**	**1.22**	**1.25**	**1.40**	**1.57**
		diamond	1.21	1.22	1.19	1.33	1.46
	50%	**chevron**	**1.12**	**1.22**	**1.32**	**1.43**	**1.58**
		diamond	1.12	1.20	1.24	1.39	1.51
	80%	**chevron**	**1.37**	**1.49**	**1.65**	**1.80**	**1.86**
		diamond	1.13	1.23	1.54	1.74	1.85

From the above discussions it can be concluded that the chevron pattern of formation gives a higher performance improvement as compared to the diamond pattern. This is true irrespective of the relative density of the infill soil, pocket size and height of the geocell mattress.

5.4 POCKET SIZE OF GEOCELLS

A typical plot showing the variation of improvement factors (IF_{gc}) with footing settlement for different pocket sizes (d = 1.6D, 1.2D, 0.8D and 0.4D) of geocells formed in chevron pattern is shown in Fig. 5.41 (Test series B2). Similar observations for various cases of geocell mattress (i.e. pattern of formation and depth of placement) are presented in Tables 5.1 and 5.2. From Fig. 5.41, it could be observed that the performance improvement increases with the decrease in the pocket size of the geocells. With decrease in the size of the pockets, the number of cells and consequently the joints per unit area increases due to which the overall rigidity of the structure increases. In addition to this, the confinement offered by the cells per unit volume of soil increases. This in turn, again increases the bearing capacity of foundation bed leading to higher performance improvement. Fig. 5.41 also shows that the improvement factor (IF_{gc}) for geocells having larger pocket sizes (d = 1.6D, 1.2D) remains constant at all levels of footing settlement (s/D) whereas it continues to increase with increase in footing settlement for the smaller pocket sizes (d = 0.8D, 0.4D). This is because the geocells with larger pocket sizes being relatively less rigid, yields under footing penetration and punches into the soil. As the benefit of the reinforcement remains immobolised, the improvement factor doesn't increase with increase in footing settlement. On the contrary, the geocells with smaller pocket size offers more resistance to the footing penetration by mobilizing the higher strength of the reinforcement, leading to an increase in the performance improvement. This phenomenon is clearly evident from the surface deformation responses reported earlier (Figs. 5.11 to 5.14) wherein punching induced heave is observed on the surface for geocells with larger pocket sizes (i.e. d = 1.6D, 1.2D; Figs. 5.11, 5.12). Whereas for geocells with smaller pocket sizes (i.e. d = 0.8D, 0.4D; Figs. 5.13, 5.14), the surface is found to settle with increase in footing settlement. This is due to increased coherence of the geocell-soil

system that it settles as a centrally loaded composite mattress which effectively arrests the heaving in the underlying clay bed.

The other factor to be considered is the relative size of footing with respect to the size of the geocell pocket openings. In case of d = 1.6D and 1.2D the pocket size of geocells being larger than the footing diameter, the footing rests only on the soil encapsulated in the geocell pocket. Therefore the improvement in bearing capacity is solely due to the confinement-induced benefit imparted to the soil by the geocells. However for the cases with d = 0.8D and 0.4D the footing size being larger than the geocell pocket opening size, the footing rests over the geocell-soil composite structure, with geocell walls under the footing. This enables the footing to derive substantial resistance from the reinforcement cage leading to a quantum jump in performance improvement from d = 1.2D to d = 0.8D (Fig. 5.41).

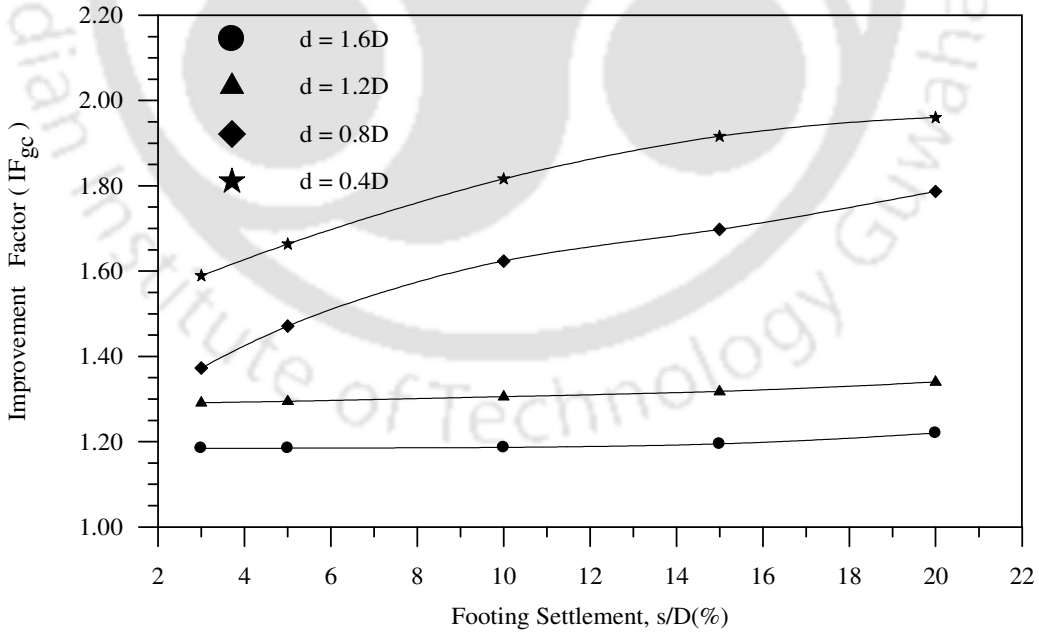

Fig. 5.41 Variation of improvement factor with footing settlement for different pocket sizes (d) of geocell mattress – Test Series B2, chevron, u = 0.1D

It can therefore be concluded that, in general, the performance improvement in bearing pressure increases with reduction in the pocket size (d) of the geocells. However, when the footing size is larger than the geocell pocket size, the performance improvement is substantially high. For all practical applications, the geocell reinforcement and footing should be designed such that the footing completely covers atleast one geocell pocket opening.

5.5 HEIGHT OF GEOCELL MATTRESS

Twelve series of tests (Test series D1 to G3) were conducted, details of which are elaborated in Table 3.4, to evaluate the critical height (h_{cr}) of the geocell mattress giving maximum performance improvement for varied condition of geocell mattress (i.e. relative density of infill sand and pocket size of geocells). For this purpose, the heights (h) of geocell mattress are varied from 0.27D to 1.07D, pocket sizes are varied from 1.2D to 0.4D and the relative densities of infill sand are varied from 35% to 80%. The critical parameters obtained earlier are used in these tests, i.e. the depth of placement (u) and the pattern of formation of geocells are kept constant at 0.1D and chevron, respectively. The influences of the relative density of the infill sand and the pocket size on the critical height (h_{cr}) of the geocell mattress are discussed in the following subsections.

5.5.1 Influence of relative density of infill sand

The pressure-settlement responses for different heights of geocell mattress (i.e. h = 0.27D, 0.53D, 0.8D and 1.07D) with pocket sizes (d) = 1.2D, 0.8D and 0.4D and relative densities of the infill material varying from 35% to 80% are presented in Figs. 5.42 to 5.50. A substantial increase in the initial stiffness as well as the load carrying capacity of the foundation bed could be observed with the increase in the height of the geocell mattress till a height of 0.8D, beyond which the increase in stiffness and load carrying

capacity is marginal. With increase in the height of the geocell mattress, the flexural rigidity of the reinforced bed increases. Moreover, the overall frictional resistance restraining the downward punching of the encapsulated sand also increases due to increase in the surface area of the geocell reinforcement. These two factors lead to redistribution of footing loading over a larger area on clay subgrade giving rise to increased load carrying capacity of the foundation bed. This explanation is also substantiated through the surface deformation profiles (Figs. 5.51 to 5.54) wherein the heave on the surface has changed to settlement with the increase in the height of the geocell reinforcement. Beyond a height (h) of 0.8D, the geocell walls just below the footing buckle locally under higher load, due to which much of the reinforcement remains immobilized. Hence, only a marginal increase in performance improvement is obtained, with further increase in height of the geocell mattress.

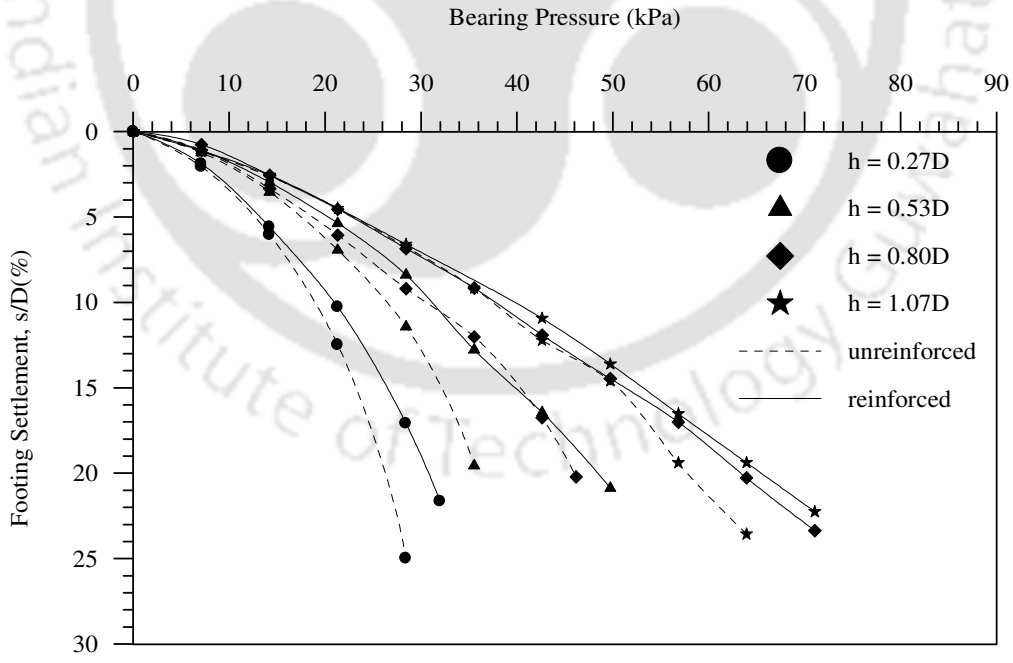

Fig. 5.42 Variation of bearing pressure with footing settlement for different heights (h) of geocell mattress – Test Series A3 to A6, D1, E1, F1, G1, ID = 35%, d = 1.2D

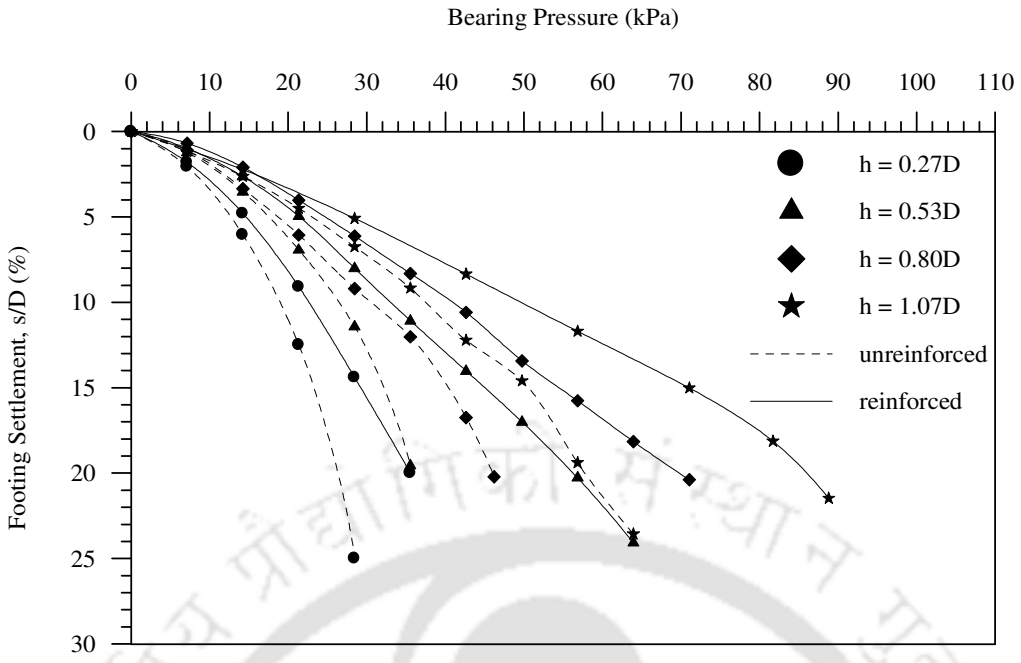

Fig. 5.43 Variation of bearing pressure with footing settlement for different heights (h) of geocell mattress – Test Series A3 to A6, D1, E1, F1, G1, ID = 35%, d = 0.8D

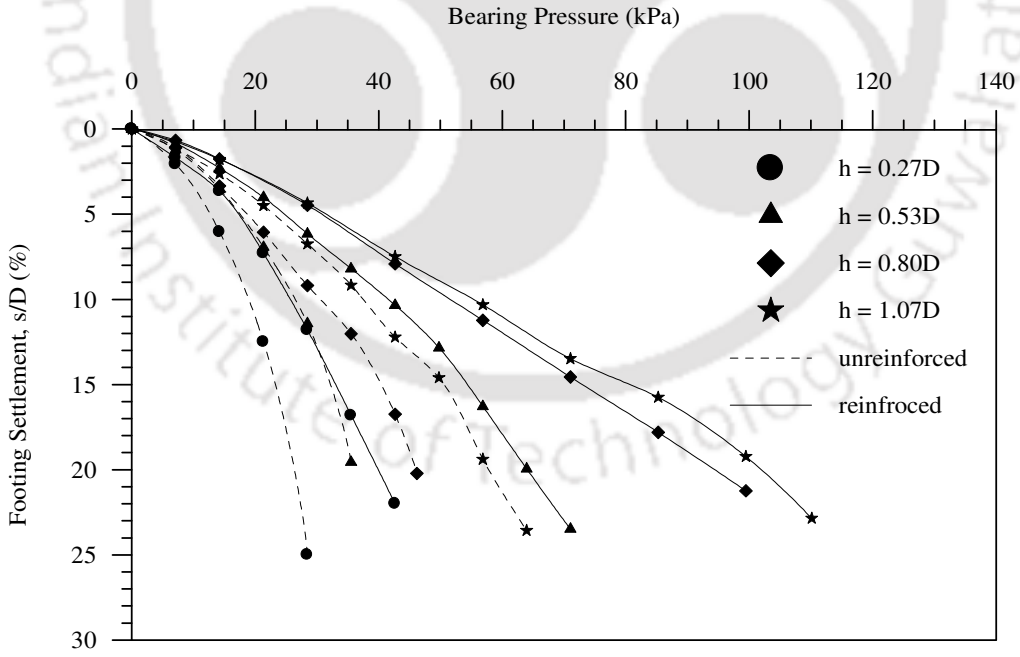

Fig. 5.44 Variation of bearing pressure with footing settlement for different heights (h) of geocell mattress – Test Series A3 to A6, D1, E1, F1, G1, ID = 35%, d = 0.4D

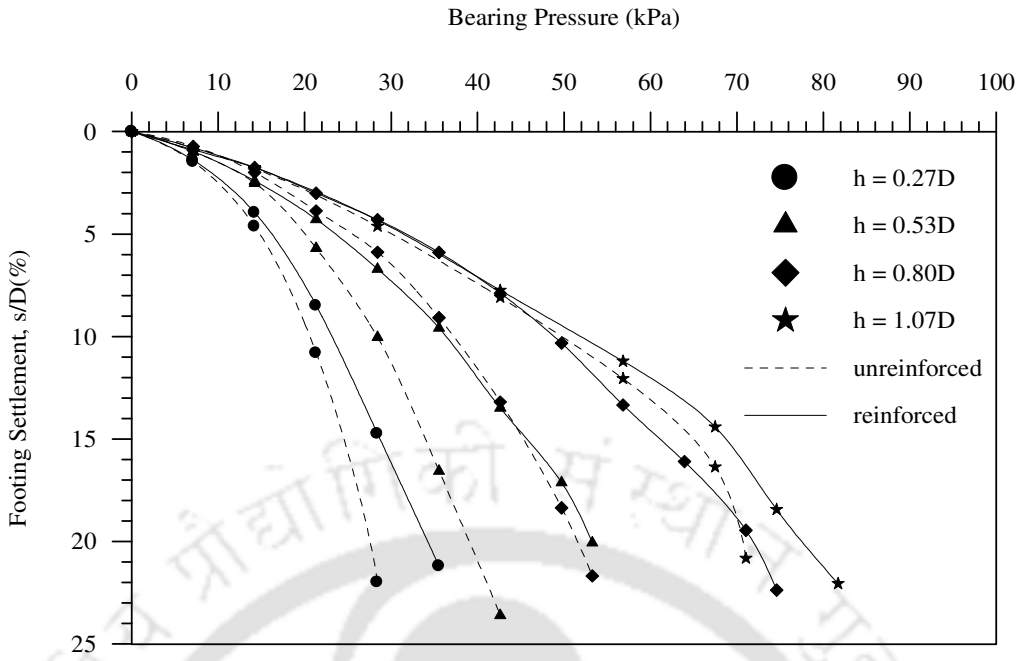

Fig. 5.45 Variation of bearing pressure with footing settlement for different heights (h) of geocell mattress – Test Series A3 to A6, D2, E2, F2, G2, ID = 50%, d = 1.2D

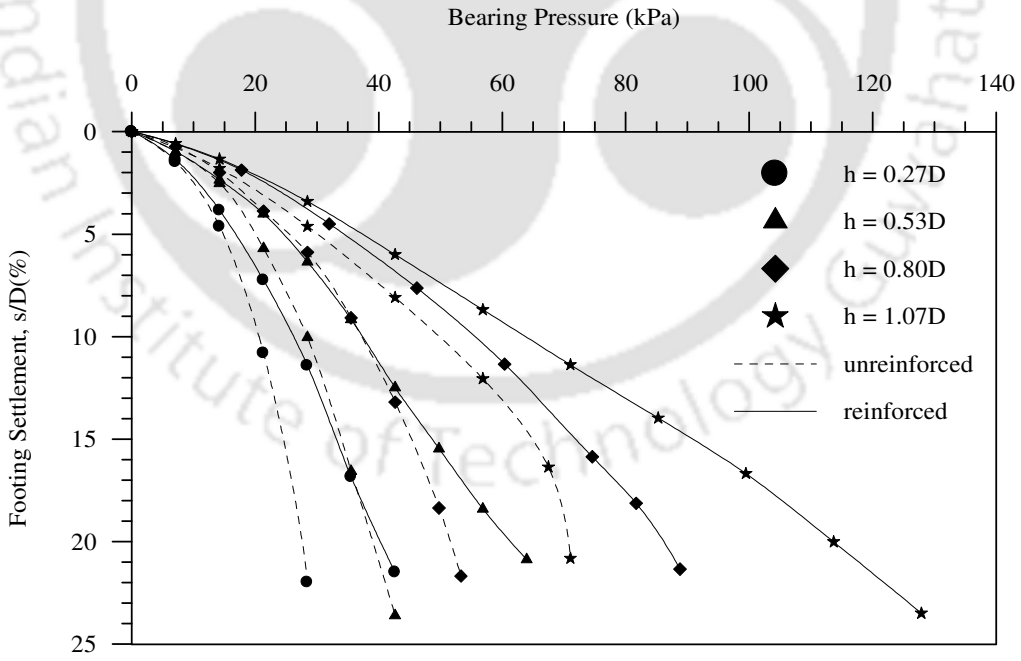

Fig. 5.46 Variation of bearing pressure with footing settlement for different heights (h) of geocell mattress – Test Series A3 to A6, D2, E2, F2, G2, ID = 50%, d = 0.8D

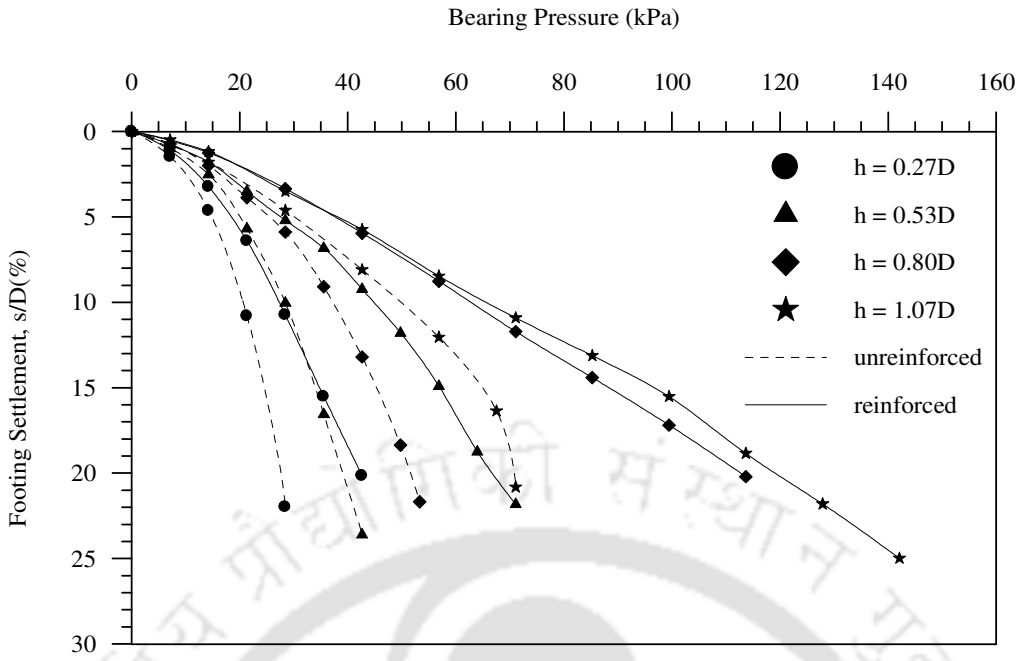

Fig. 5.47 Variation of bearing pressure with footing settlement for different heights (h) of geocell mattress – Test Series A3 to A6, D2, E2, F2, G2, ID = 50%, d = 0.4D

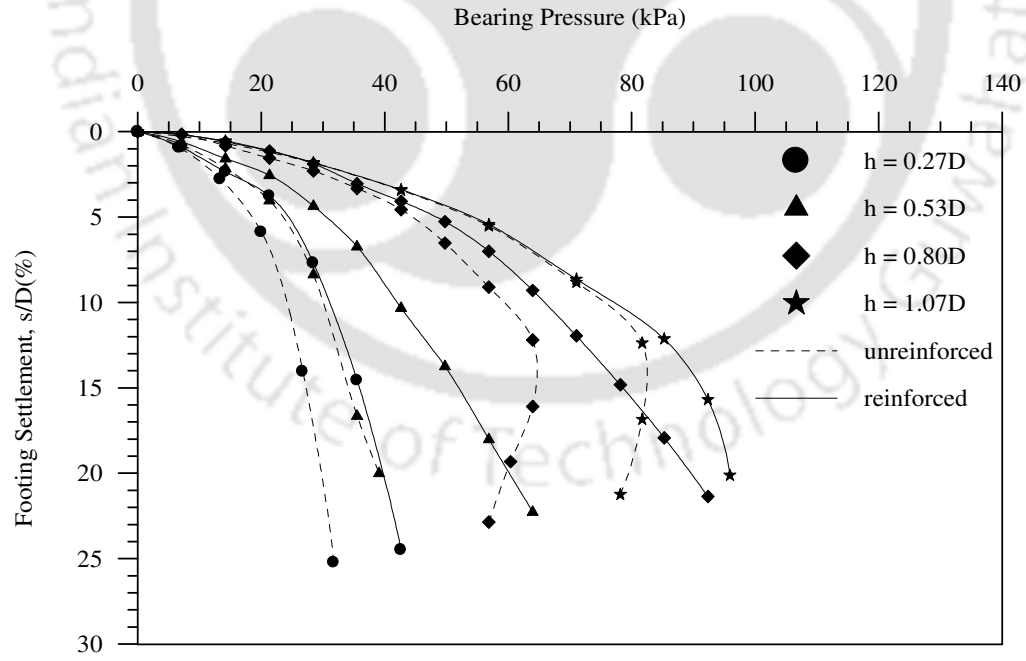

Fig. 5.48 Variation of bearing pressure with footing settlement for different heights (h) of geocell mattress – Test Series A3 to A6, D3, E3, F3, G3, ID = 80%, d = 1.2D

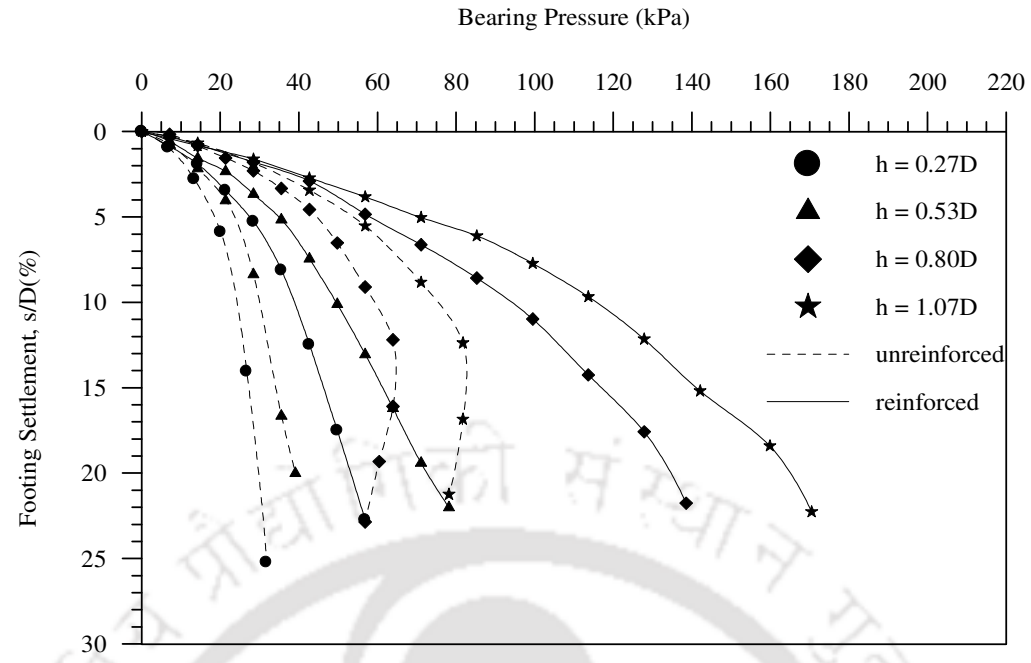

Fig. 5.49 Variation of bearing pressure with footing settlement for different heights (h) of geocell mattress – Test Series A3 to A6, D3, E3, F3, G3, ID = 80%, d = 0.8D

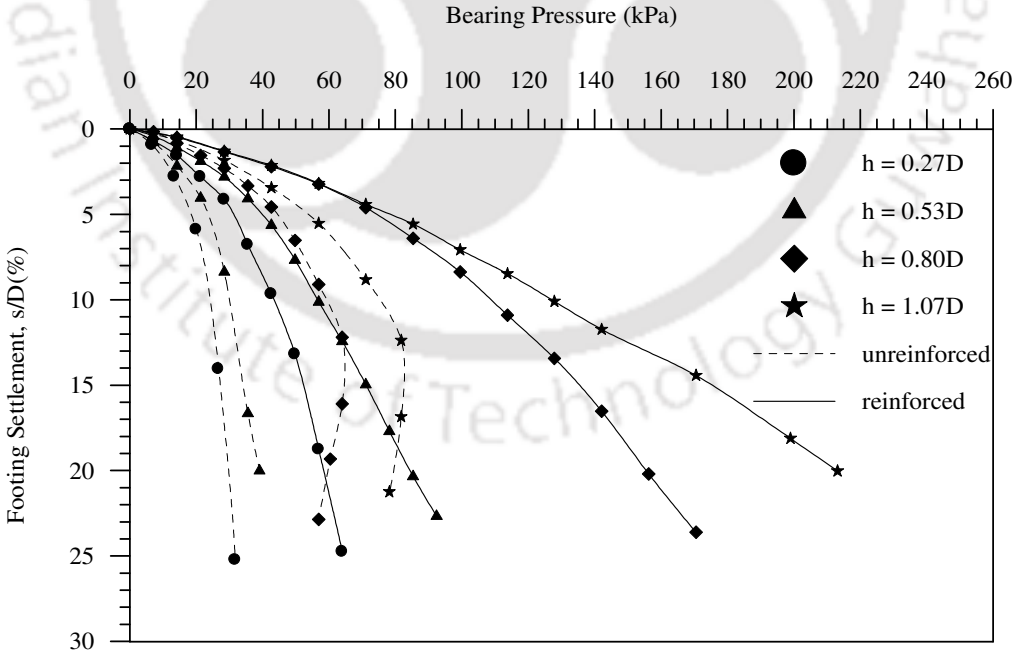

Fig. 5.50 Variation of bearing pressure with footing settlement for different heights (h) of geocell mattress – Test Series A3 to A6, D3, E3, F3, G3, ID = 80%, d = 0.4D

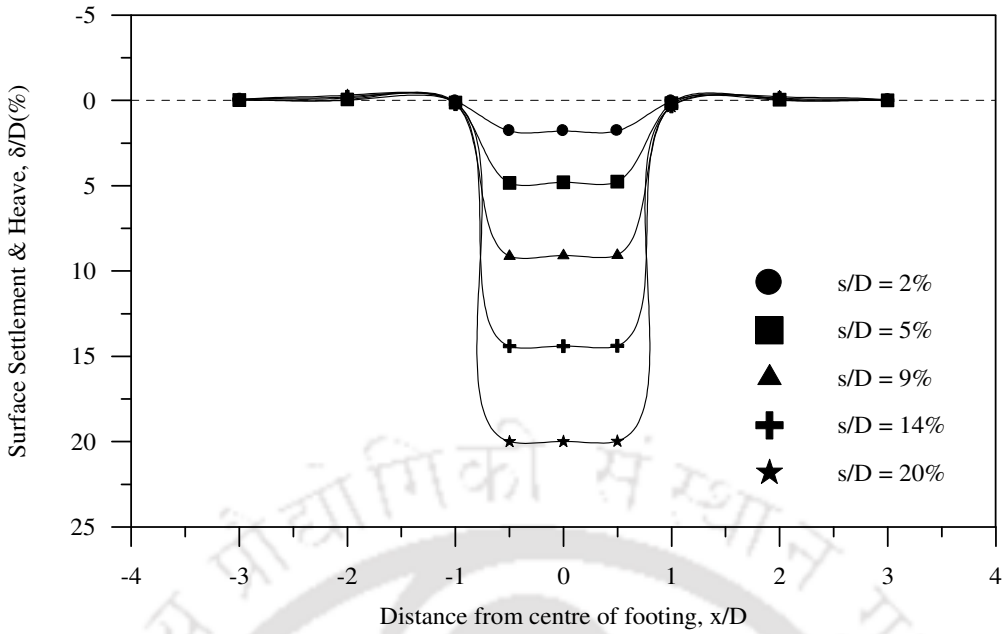

Fig. 5.51 Surface Deformation profiles with geocell reinforcement - Test Series D1, ID = 35%, d = 0.8D, h = 0.27D

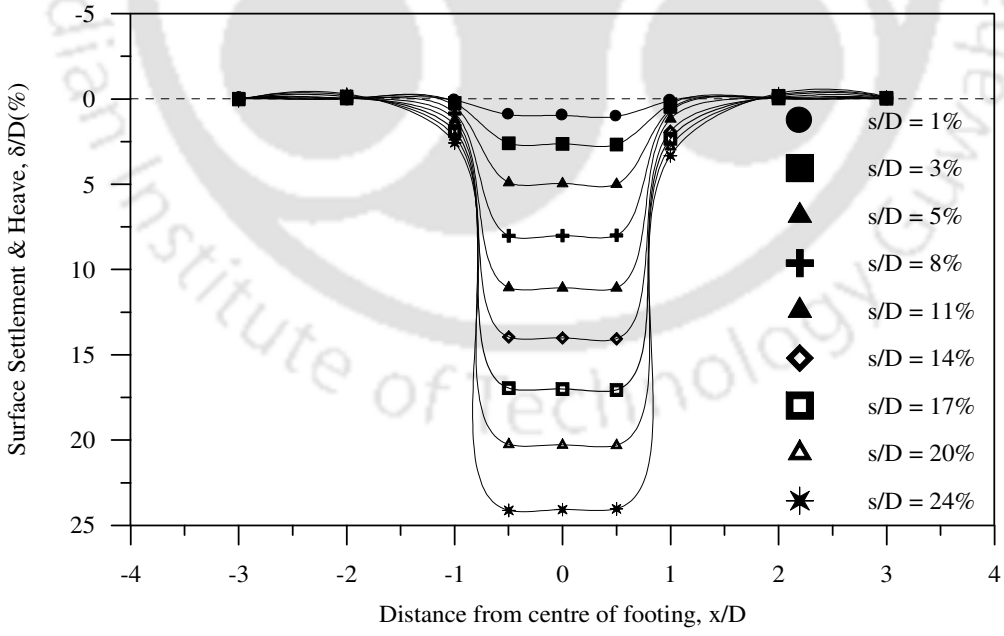

Fig. 5.52 Surface Deformation profiles with geocell reinforcement - Test Series E1, ID = 35%, d = 0.8D, h = 0.53D

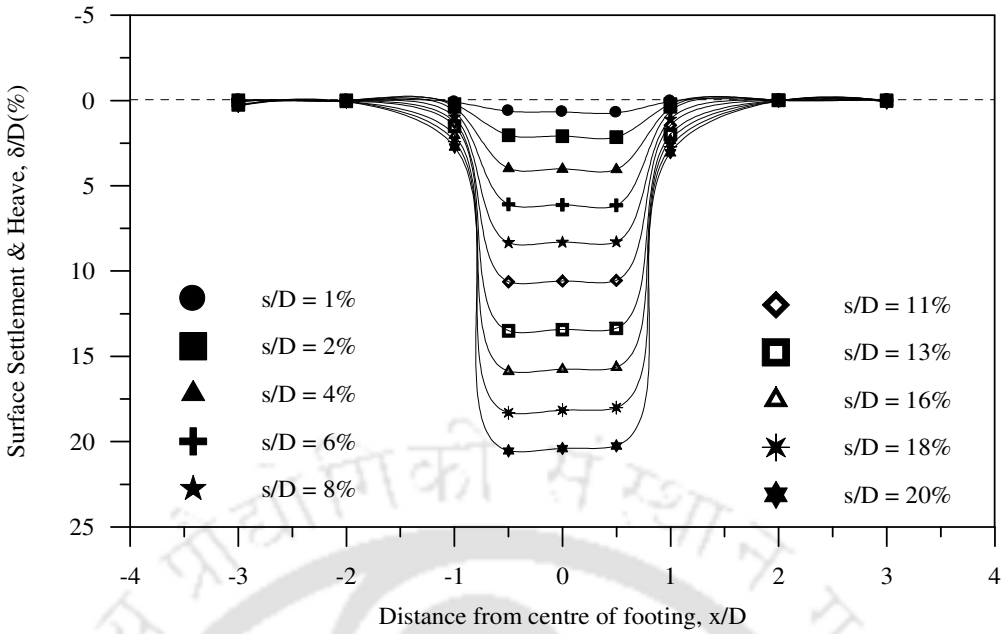

Fig .5.53 Surface Deformation profiles with geocell reinforcement - Test Series F1, ID = 35%, d = 0.8D, h = 0.8D

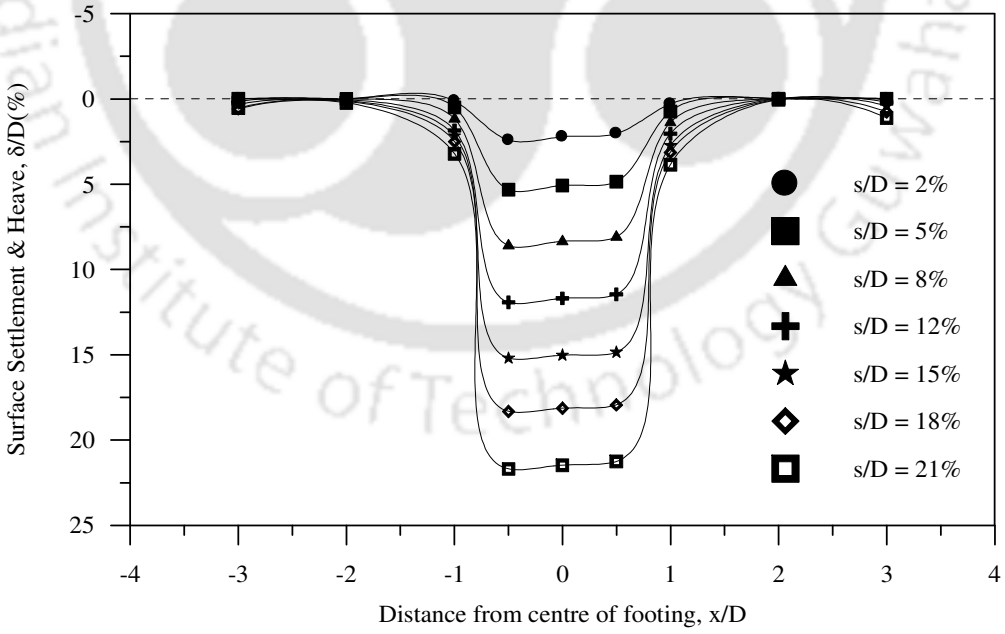

Fig. 5.54 Surface Deformation profiles with geocell reinforcement - Test Series G1, ID = 35%, d = 0.8D, h = 1.07D

The test data are further analysed in terms of bearing pressure improvement factor (IF_{gc}). Tables 5.6, 5.7 and 5.8 summarize the performance improvement in bearing capacity (IF_{gc}) due to geocell reinforcement, with infill sand of relative density (ID) = 35%, 50% and 80% respectively. It could be observed that when the relative density of the infill sand is 35% and 50%, the value of IF_{gc} increases with increase in height of the geocell mattress till a critical height (h_{cr}) of 0.8D, beyond which it decreases. However, in case of higher relative density (i.e. ID = 80%), the critical height (h_{cr}) giving maximum performance improvement is about 0.53D. The decrease in the performance improvement beyond a certain critical height (i.e. h_{cr} of 0.8D for ID = 35%, 50%; h_{cr} of 0.53D for ID = 80%) of geocell mattress is attributed to the arching induced increase in the shearing resistance of the corresponding sand layer which reduces the contribution of the geocell reinforcement. The pressure-settlement responses for lesser thickness of sand layer, irrespective of the density, follow a typical punching shear behaviour as shown in Figs. 5.42 to 5.50. This indicates that at smaller heights of the geocell mattress (h), due to inadequate bearing capacity, the sand layer gets deformed under footing loading and hence the geocell structure plays a dominant role in sustaining the footing load. With increase in height, the geocell reinforcement shares a higher percentage of the footing load, thereby leading to higher performance improvement. However, with further increase in height (h > 0.53D), the pressure-settlement response for higher relative density (ID = 80%) shows a strain softening behaviour (Figs. 5.48 to 5.50). At this height, the thickness of the sand layer is adequate to sustain a substantial amount of footing load and therefore relatively less load is transferred to the reinforcement. In view of this, the contribution of the reinforcement to the increase in footing pressure remains immobilized, thereby leading to an apparent decrease in improvement factor (IF_{gc}). Thus, to obtain maximum benefit from reinforcement with higher relative density of infill sand (ID = 80%), the

height of the geocell mattress should be about 0.53D. In case of lower relative densities (ID = 35%, 50%), due to relatively lower shear strength of the sand, the punching shear behaviour is observed till a much higher height (i.e. h = 0.8D, Figs. 5.42 to 5.47). It is only beyond this height that the sand layer has adequate strength to stand against footing resistance, therefore, the critical height of the geocell reinforcement obtained in this case is higher (i.e. h_{cr} = 0.8D).

Table 5.6 Summary of results in terms of bearing capacity improvement factor (IF_{gc}) showing the influence of height of geocell mattress, ID = 35%, Test Series D1, E1, F1, G1

Variable Parameter		Bearing capacity improvement factor (IF_{gc})				
		(s/D) 3%	(s/D) 5%	(s/D) 10%	(s/D) 15%	(s/D) 20%
(d/D)	(h/D)					
1.2	0.27	1.04	1.04	1.10	1.16	1.17
	0.53	1.11	1.16	1.18	1.24	1.35
	0.8	**1.18**	**1.21**	**1.24**	**1.27**	**1.38**
	1.07	1.03	1.03	1.06	1.06	1.13
0.8	0.27	1.13	1.15	1.19	1.26	1.36
	0.53	1.21	1.22	1.25	1.40	1.57
	0.8	**1.33**	**1.33**	**1.34**	**1.35**	**1.52**
	1.07	1.17	1.23	1.32	1.41	1.49
0.4	0.27	1.34	1.35	1.36	1.43	1.52
	0.53	1.34	1.41	1.57	1.69	1.79
	0.8	**1.62**	**1.64**	**1.69**	**1.81**	**2.05**
	1.07	1.36	1.38	1.48	1.60	1.76

Table 5.7 Summary of results in terms of bearing capacity improvement factor (IF_{gc}) showing the influence of height of geocell mattress, ID = 50%, Test Series D2, E2, F2, G2

Variable Parameter		Bearing capacity improvement factor (IF_{gc})				
		(s/D) 3%	(s/D) 5%	(s/D) 10%	(s/D) 15%	(s/D) 20%
(d/D)	(h/D)					
1.2	0.27	1.08	1.10	1.12	1.18	1.24
	0.53	1.08	1.16	1.28	1.35	1.37
	0.8	**1.18**	**1.23**	**1.31**	**1.35**	**1.39**
	1.07	1.04	1.05	1.05	1.06	1.10
0.8	0.27	1.09	1.14	1.27	1.35	1.46
	0.53	**1.12**	1.22	1.32	1.43	1.58
	0.8	**1.34**	**1.34**	**1.49**	**1.59**	**1.67**
	1.07	1.23	1.24	1.28	1.40	1.60
0.4	0.27	1.23	1.24	1.33	1.42	1.54
	0.53	1.24	1.38	1.58	1.68	1.72
	0.8	**1.45**	**1.47**	**1.69**	**1.94**	**2.19**
	1.07	1.25	1.26	1.32	1.49	1.68

Table 5.8 Summary of results in terms of bearing capacity improvement factor (IF_{gc}) showing the influence of height of geocell mattress, ID = 80%, Test Series D3, E3, F3, G3

Variable Parameter		Bearing capacity improvement factor (IF_{gc})				
		(s/D) 3%	(s/D) 5%	(s/D) 10%	(s/D) 15%	(s/D) 20%
(d/D)	(h/D)					
1.2	0.27	1.29	1.29	1.31	1.32	1.34
	0.53	**1.29**	**1.30**	**1.40**	**1.52**	**1.54**
	0.8	1.08	1.09	1.11	1.22	1.50
	1.07	1.01	1.01	1.01	1.11	1.21
0.8	0.27	1.37	1.47	1.62	1.70	1.79
	0.53	**1.37**	**1.49**	**1.65**	**1.80**	**1.86**
	0.8	1.31	1.31	1.58	1.81	2.25
	1.07	1.19	1.31	1.51	1.71	2.08
0.4	0.27	1.59	1.66	1.82	1.92	1.96
	0.53	**1.64**	**1.70**	**1.88**	**2.09**	**2.16**
	0.8	1.62	1.67	1.82	2.10	2.60
	1.07	1.40	1.46	1.66	2.13	2.68

The variation of surface deformation with footing settlement for different heights of geocell mattress (h), at a distance of x = D, x = 2D and x = 3D from the centre of footing, with lower relative density of infill sand (ID = 35%) and pocket size (d) = 0.8D are shown in Fig. 5.55, 5.57 and 5.59 respectively. The surface deformation responses for the same configuration (d = 0.8D, h = 0.27D to 1.07D) of geocell reinforcement but with higher relative density of infill sand (ID = 80%) are presented in Figs. 5.56, 5.58 and 5.60 respectively. The remaining surface deformation responses for different combinations of pocket sizes (d = 1.2D, 0.8D, 0.4D) and relative densities of sand (ID = 35%, 50%, 80%) are presented in Appendix 1 (Figs. A1.41 to A1.61).

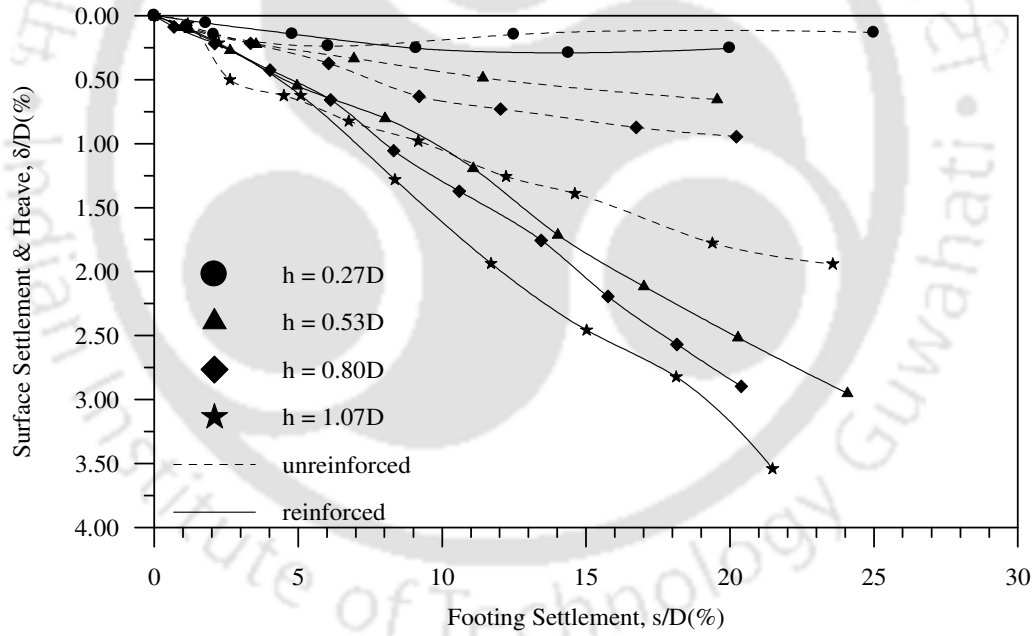

Fig. 5.55 Variation of average surface deformation with footing settlement at a distance x = D from the centre of the footing, for different heights (h) of geocell mattress – Test Series A3 to A6, D1, E1, F1, G1, d = 0.8D, ID = 35%

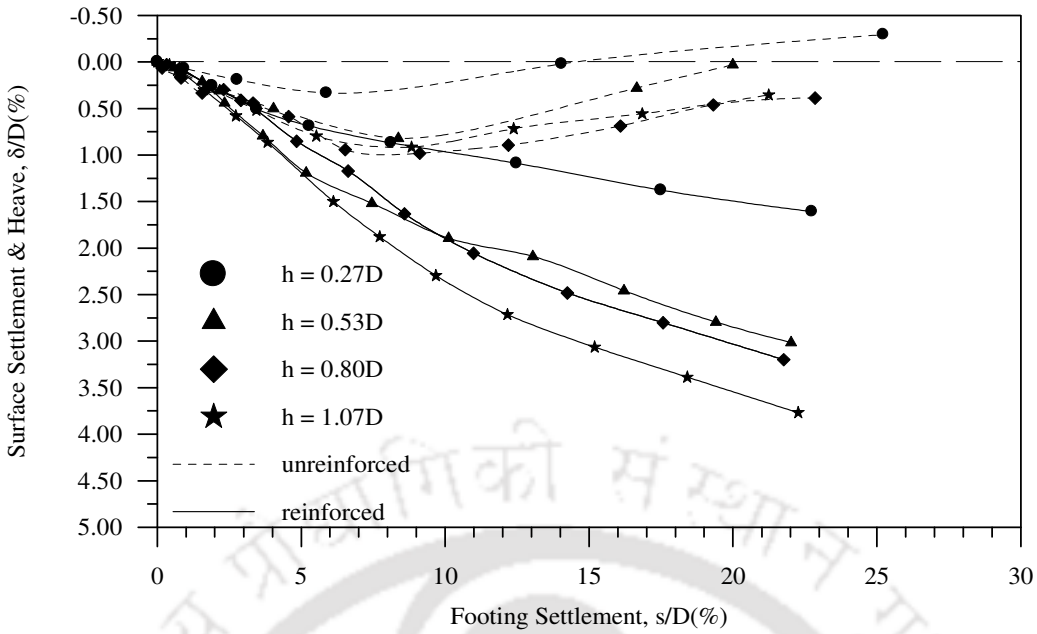

Fig. 5.56 Variation of average surface deformation with footing settlement at a distance x = D from the centre of the footing, for different heights (h) of geocell mattress – Test Series A3 to A6, D3, E3, F3, G3, d = 0.8D, ID = 80%

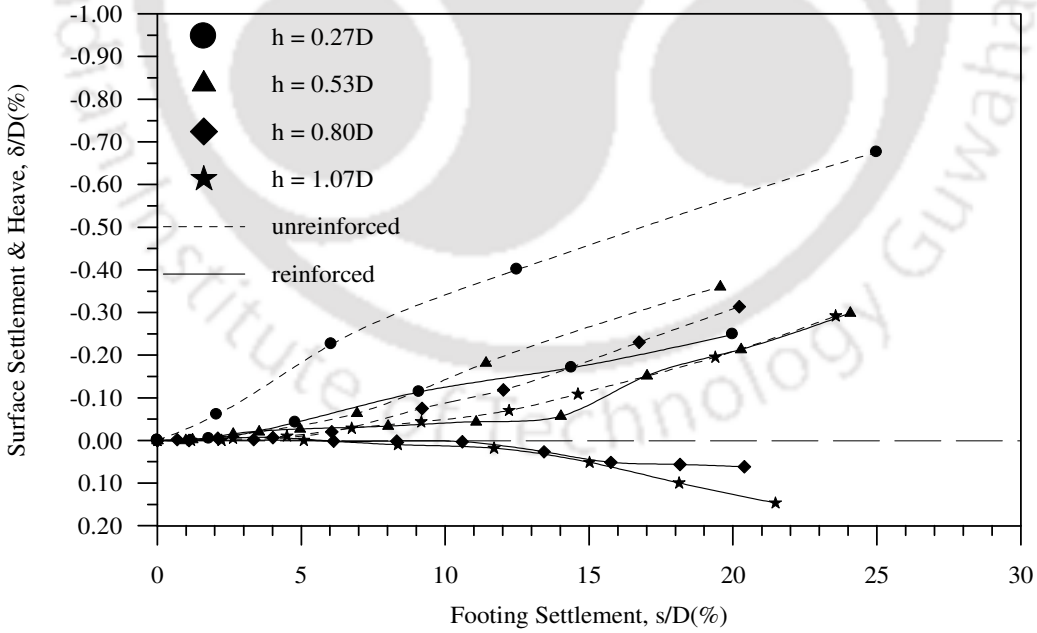

Fig. 5.57 Variation of average surface deformation with footing settlement at a distance x = 2D from the centre of the footing, for different heights (h) of geocell mattress – Test Series A3 to A6, D1, E1, F1, G1, d = 0.8D, ID = 35%

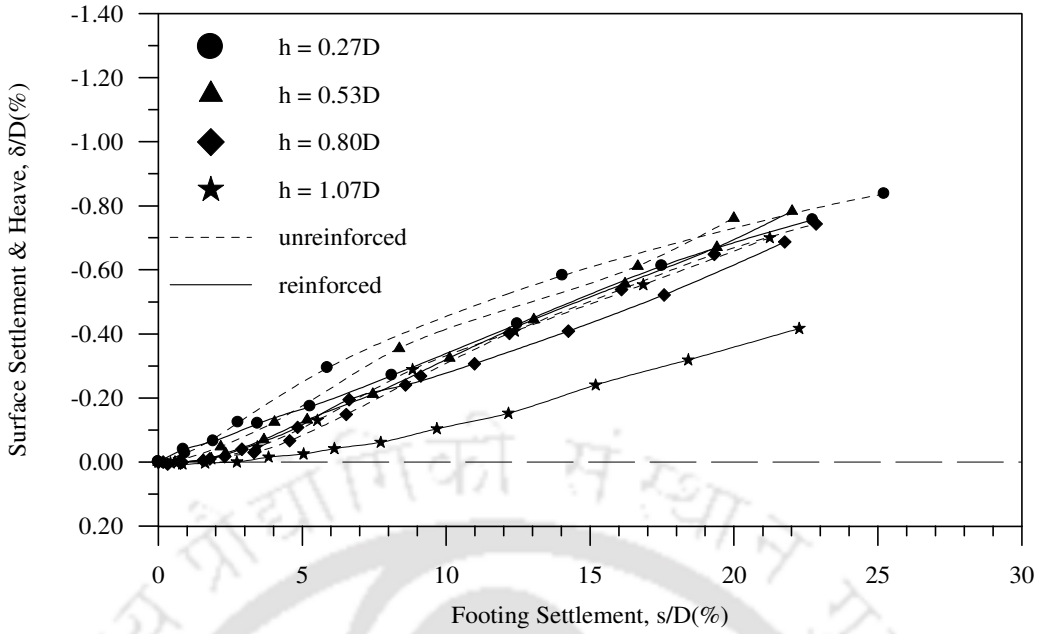

Fig. 5.58 Variation of average surface deformation with footing settlement at a distance x = 2D from the centre of the footing, for different heights (h) of geocell mattress – Test Series A3 to A6, D3, E3, F3, G3, d = 0.8D, ID = 80%

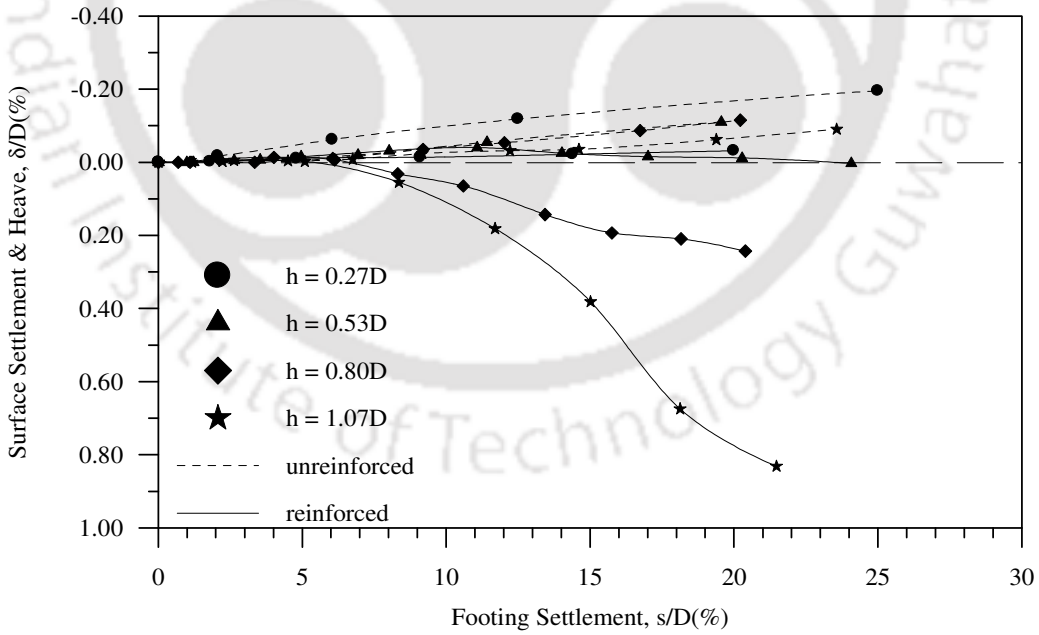

Fig. 5.59 Variation of average surface deformation with footing settlement at a distance x = 3D from the centre of the footing, for different heights (h) of geocell mattress – Test Series A3 to A6, D1, E1, F1, G1, d = 0.8D, ID = 35%

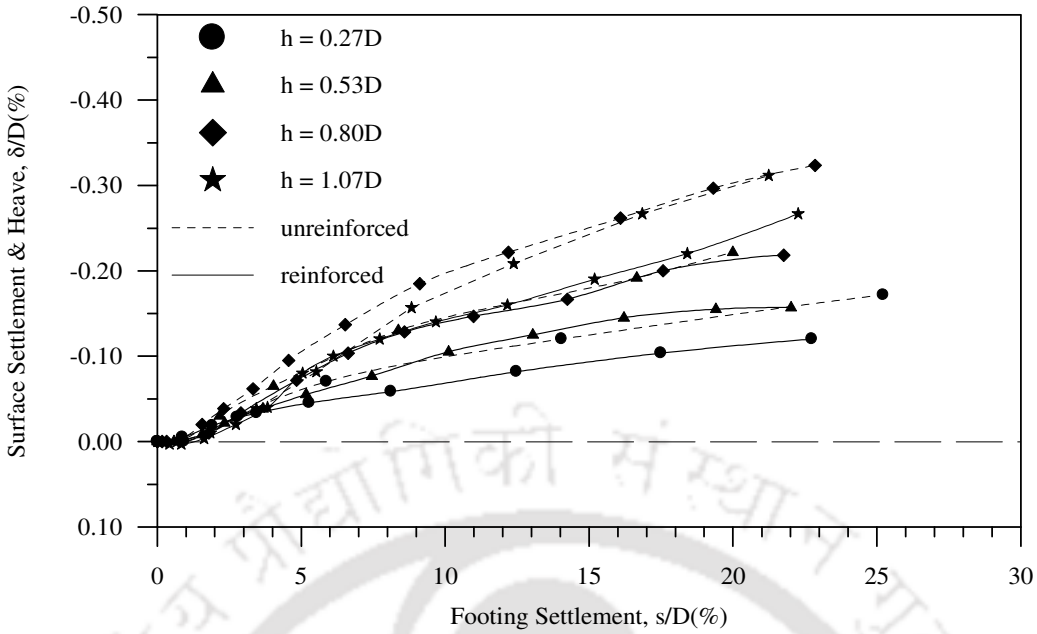

Fig. 5.60 Variation of average surface deformation with footing settlement at a distance x = 3D from the centre of the footing, for different heights (h) of geocell mattress – Test Series A3 to A6, D3, E3, F3, G3, d = 0.8D, ID = 80%

It could be observed that with smaller height of the geocell mattress (h = 0.27D, Fig. 5.55), the surface near the footing (i.e. x = D) initially settles and then heaves whereas it continues to settle with increase in footing settlement for higher heights of geocell mattress (Figs. 5.55 and 5.56). The heaving on the surface is induced due to the yielding of the geocell mattress under footing load as explained earlier. With the increase in height, the relatively more rigid geocell-sand mattress behaves as a coherent composite mattress thereby stands against the footing and distributes the load over a wider area beyond the footing thus resulting in more settlement in the region close to the footing. For the case of lower relative density (ID = 35%) of sand, it could be observed that, at a distance of x = 2D and x = 3D, the heaving on the fill surface reduces with the increase in height of the geocell reinforcement. With further increase in height (i.e. h > 0.53D), the surface is found to settle instead of heave (Figs. 5.57 and 5.59). This is because at smaller heights of the geocell mattress, the sand within the geocell pockets overcomes the

frictional resistance of the walls and pushes down into the soft subgrade leading to surface heave. As the height of the geocell mattress is increased, the movement of the sand is arrested due to higher frictional resistance and the entire mattress deflects as a composite mass thus resulting in settlement on the surface. The surface deformation responses for a relative density of 80%, at x = 2D (Fig. 5.58) also show the same trend as with ID = 35%. However, relatively higher heaving is observed in case of densely packed sand (ID = 80%). This is due to the dilation induced volumetric expansion of sand. Fig. 5.60 shows that at x = 3D, heaving is maximum for geocell mattress of height, h = 1.07D. The same trend is also observed in case of unreinforced sand indicating that the shear and dilation induced heave of sand is more dominant than due to heaving of the clay subgrade in the case of dense sand.

5.5.2 Influence of pocket size of geocells

Tables 5.6, 5.7 and 5.8 present a summary of the performance improvement in bearing pressure (IF_{gc}) obtained using geocell mattress of various heights, pocket sizes and relative densities of infill soil. The details of the test parameters have already been discussed in the previous section. It could be seen from Tables 5.6 and 5.7 that for low (ID = 35%) and medium dense (ID = 50%) infill sand, the critical height of the geocell mattress (h_{cr}) is about 0.8D. The critical height (h_{cr}) at which maximum benefit from reinforcement is obtained, did not change with the variation in the pocket size (d = 1.2D, 0.8D and 0.4D) of the geocells. For a higher relative density of sand (ID = 80%, Table 5.8), the critical height (h_{cr}), is about 0.53D, irrespective of the pocket size of the geocells.

On the basis of the test results, it can be said that the critical height (h_{cr}) of the geocell reinforcement giving maximum performance improvement depends on the relative density

(ID) of the infill sand. It is about 0.8D for low to medium dense sand and 0.53D for dense sand. However, for a given relative density of infill sand, the critical height (h_{cr}) is independent of the pocket size (d) of the geocells.

5.6 RELATIVE DENSITY OF INFILL SAND

The influence of relative density of the infill sand was studied with different heights (h = 0.27D to 1.07D) and pocket sizes (d = 1.2D to 0.4D) of geocell reinforcement under test series D1 to G3. The pressure-settlement responses with different relative densities (ID = 35%, 50% and 80%) of sand for a given height (h) and pocket size (d) of geocells are shown in Figs. 5.61 to 5.72. The corresponding bearing pressure improvement factors (IF_{gc}) obtained at different settlement levels of footing are summarized in Tables 5.9, 5.10, 5.11 and 5.12. The pressure-settlement responses indicate that in general, the bearing capacity of the foundation bed increases with increase in the relative density of sand in the geocells. From the pullout tests conducted with geogrid reinforcement and sand of varying densities, it was observed that the resistance of the soil-reinforcement interfaces increases with the increase in the density of soil (Figs. 3.16 to 3.19). This in turn facilitates the geocell reinforcement to mobilize higher anchorage from the infill soil. Besides, a dense soil matrix, through dilation derives higher confinement from the geocells which enhances the soil stiffness so that it effectively transmits the footing pressure and redistributes it over a wider area onto the soft subgrade below. These two factors are believed to have contributed to the enhanced bearing capacity.

The contribution of the geocell reinforcement quantified through the improvement factor (IF_{gc}) however shows deviations from this trend. It is of interest to note that, in general, better performance improvement is observed with dense sand (ID = 80%) when geocell mattress is of smaller height (h = 0.27D, 0.53D, Tables 5.9, 5.10). However with higher

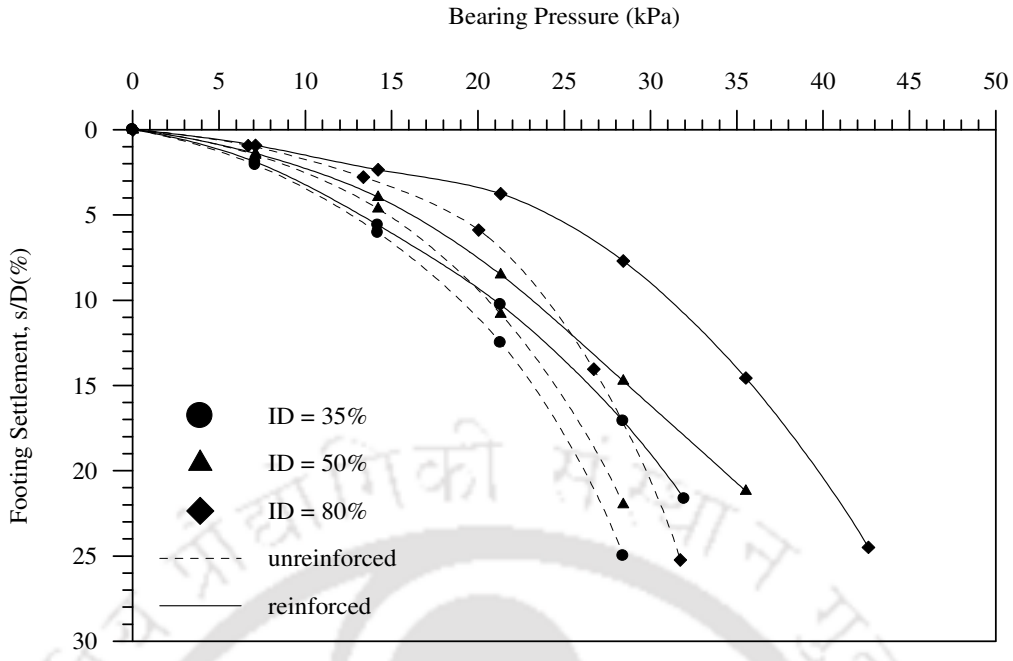

Fig. 5.61 Variation of bearing pressure with footing settlement for different relative densities (ID) of infill sand in geocells – Test Series A3, D1 to D3, h = 0.27D, d = 1.2D

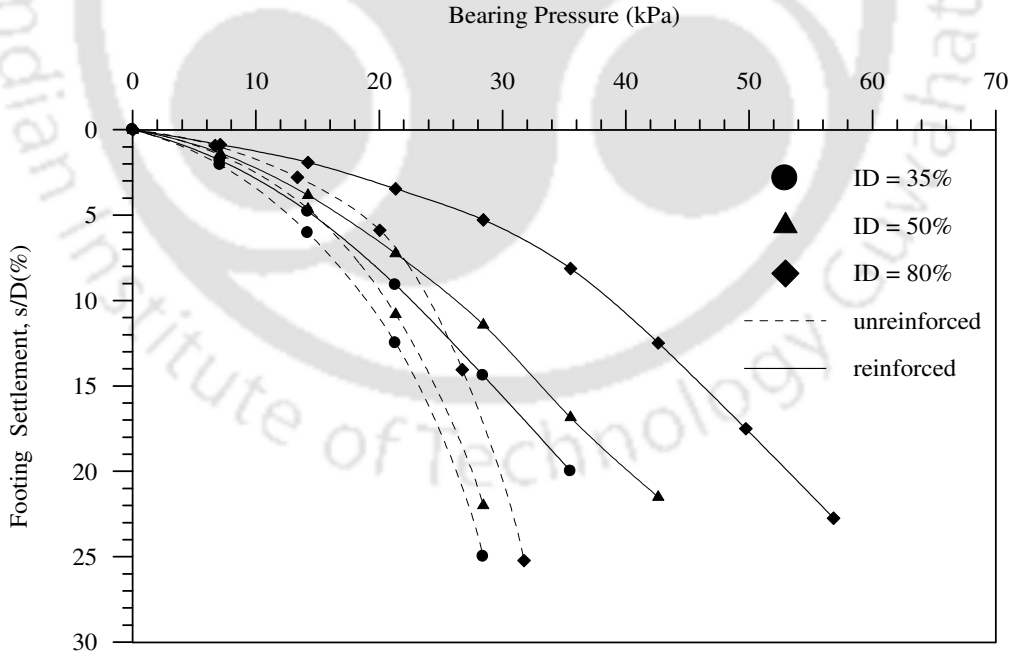

Fig. 5.62 Variation of bearing pressure with footing settlement for different relative densities (ID) of infill sand in geocells – Test Series A3, D1 to D3, h = 0.27D, d = 0.8D

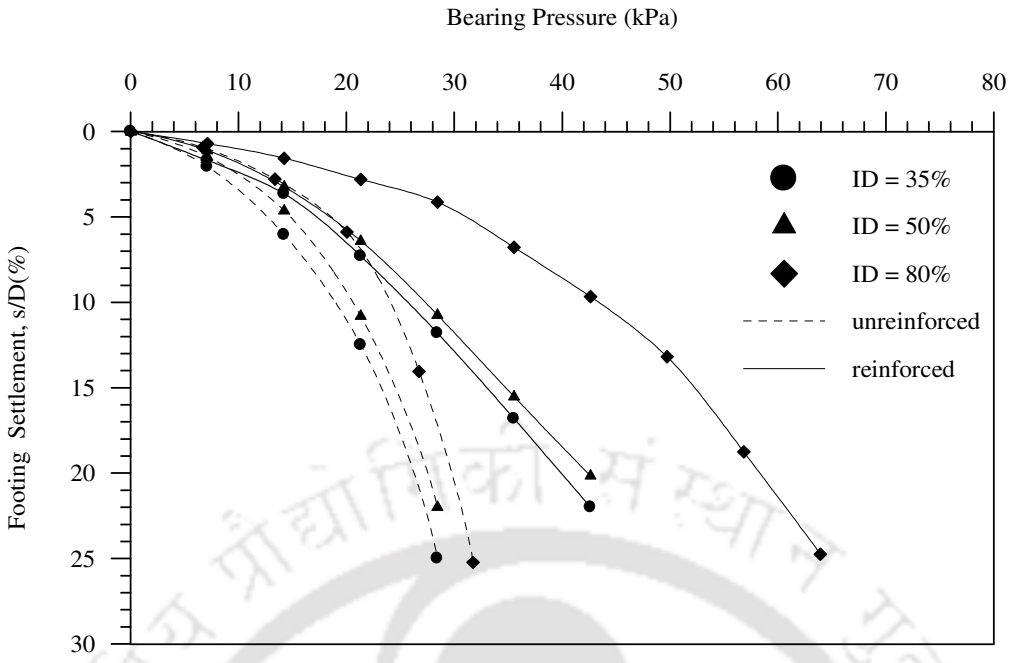

Fig. 5.63 Variation of bearing pressure with footing settlement for different relative densities (ID) of infill sand in geocells – Test Series A3, D1 to D3, h = 0.27D, d = 0.4D

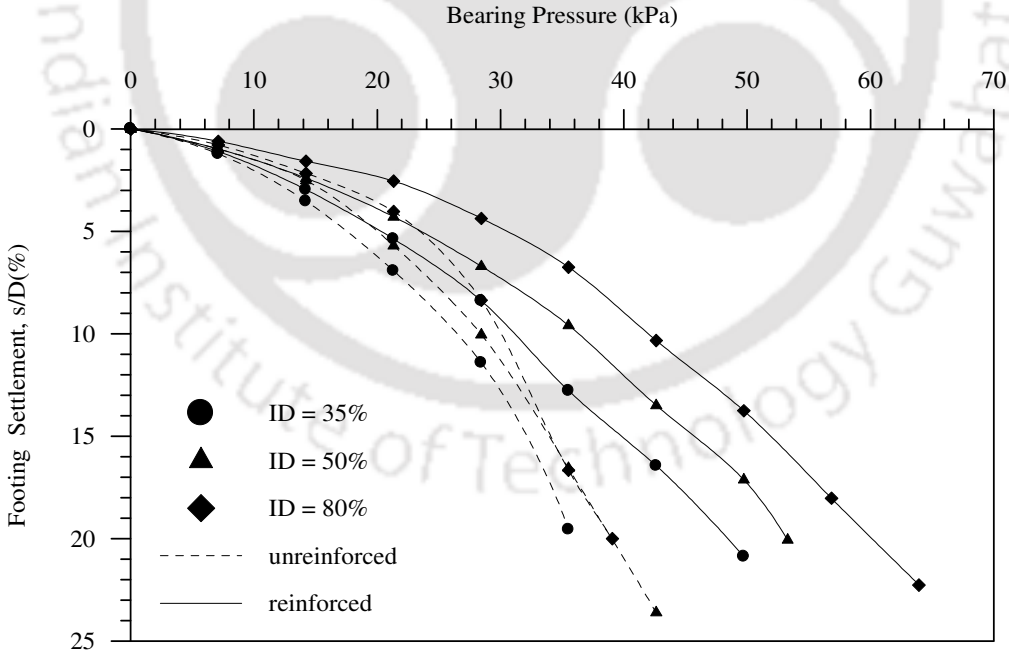

Fig. 5.64 Variation of bearing pressure with footing settlement for different relative densities (ID) of infill sand in geocells – Test Series A4, E1 to E3, h = 0.53D, d = 1.2D

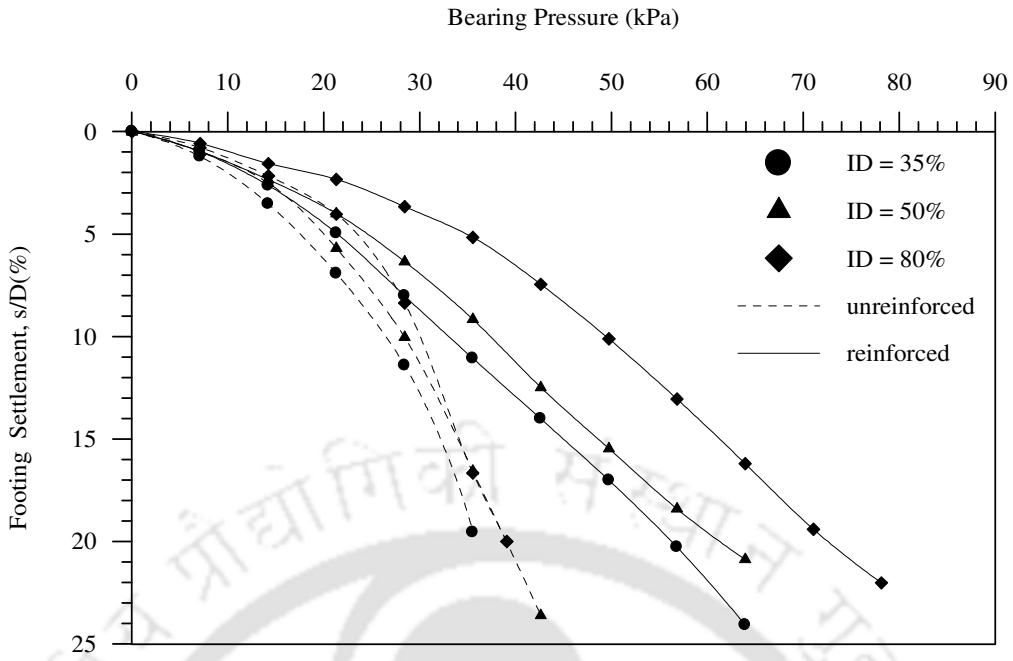

Fig. 5.65 Variation of bearing pressure with footing settlement for different relative densities (ID) of infill sand in geocells – Test Series A4, E1 to E3, h = 0.53D, d = 0.8D

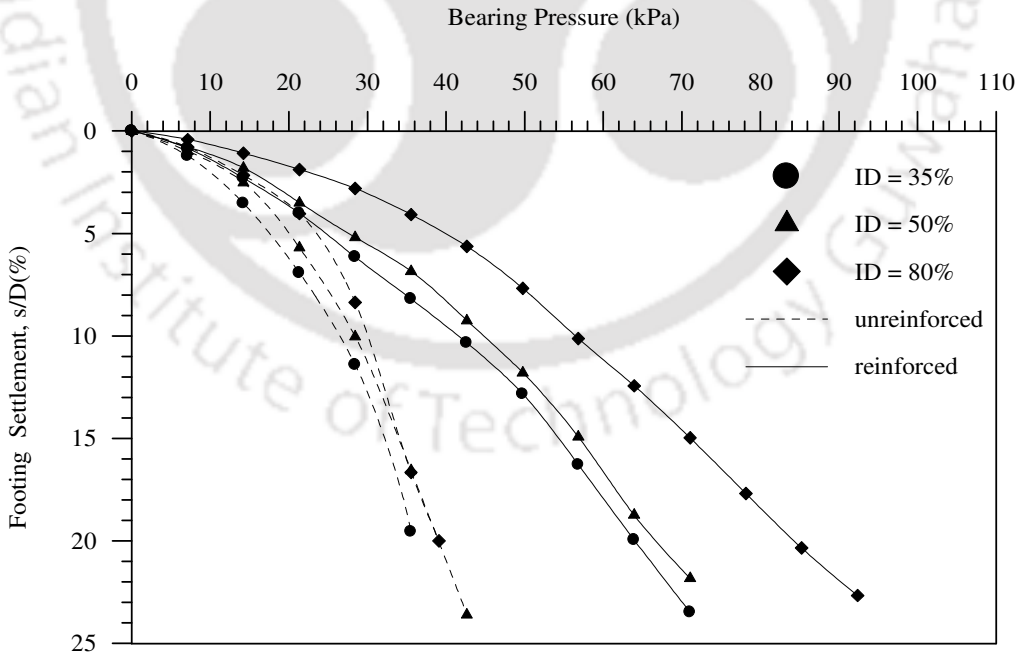

Fig. 5.66 Variation of bearing pressure with footing settlement for different relative densities (ID) of infill sand in geocells – Test Series A4, E1 to E3, h = 0.53D, d = 0.4D

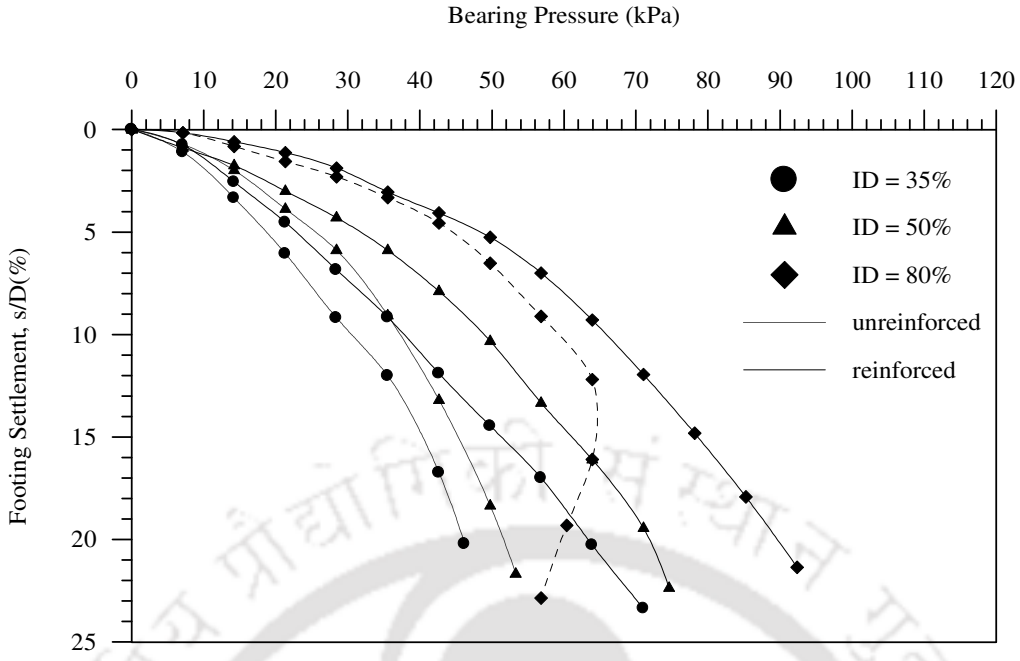

Fig. 5.67 Variation of bearing pressure with footing settlement for different relative densities (ID) of infill sand in geocells – Test Series A5, F1 to F3, h = 0.80D, d = 1.2D

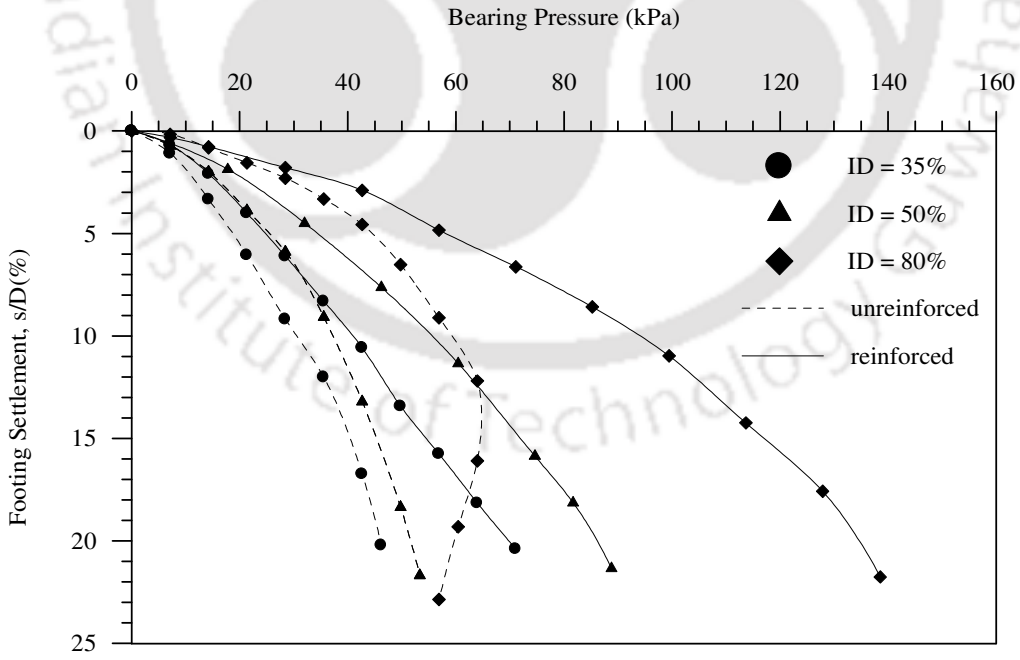

Fig. 5.68 Variation of bearing pressure with footing settlement for different relative densities (ID) of infill sand in geocells – Test Series A5, F1 to F3, h = 0.80D, d = 0.8D

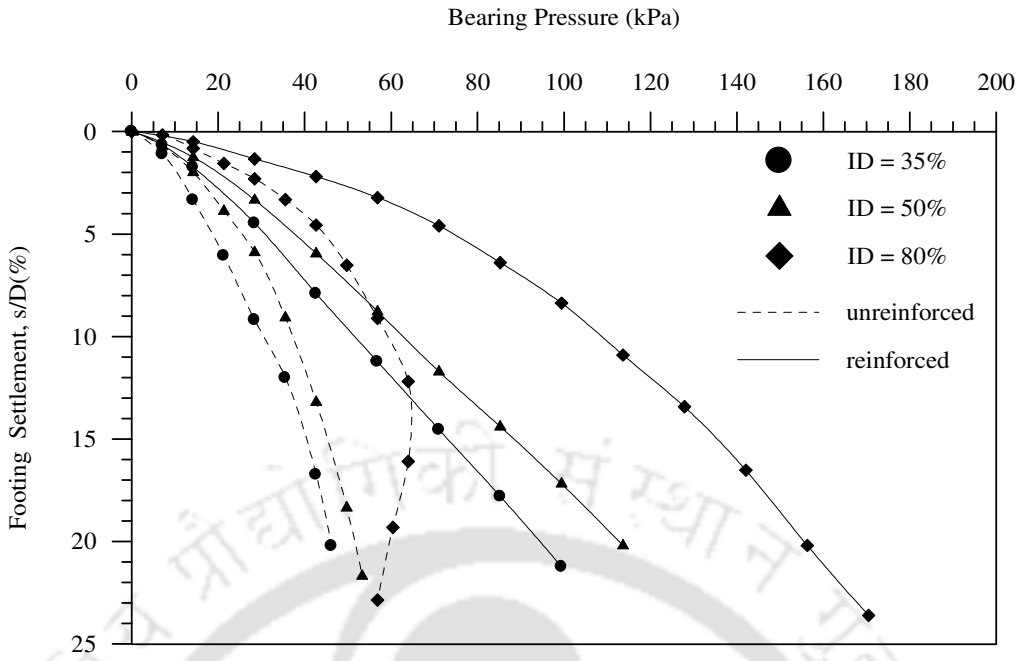

Fig. 5.69 Variation of bearing pressure with footing settlement for different relative densities (ID) of infill sand in geocells – Test Series A5, F1 to F3, h = 0.80D, d = 0.4D

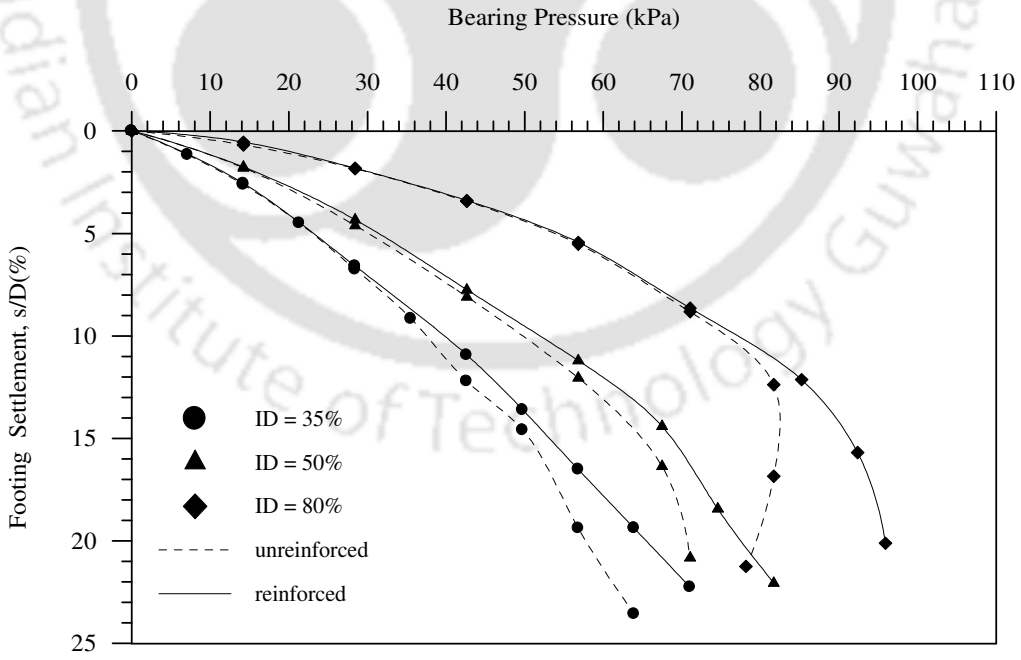

Fig. 5.70 Variation of bearing pressure with footing settlement for different relative densities (ID) of infill sand in geocells – Test Series A6, G1 to G3, h = 1.07D, d = 1.2D

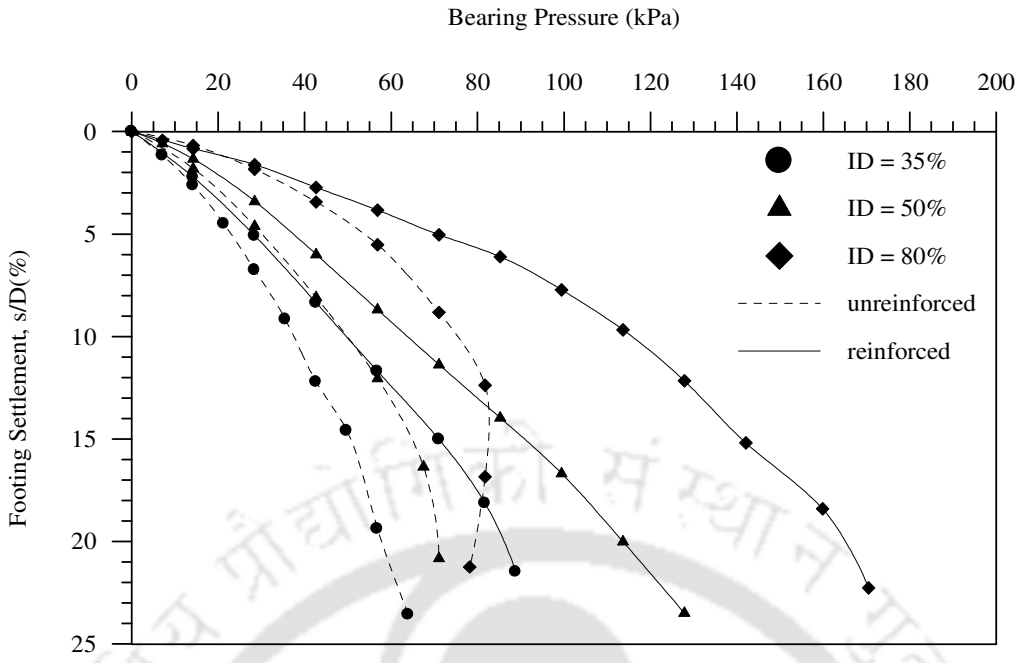

Fig. 5.71 Variation of bearing pressure with footing settlement for different relative densities (ID) of infill sand in geocells – Test Series A6, G1 to G3, h = 1.07D, d = 0.8D

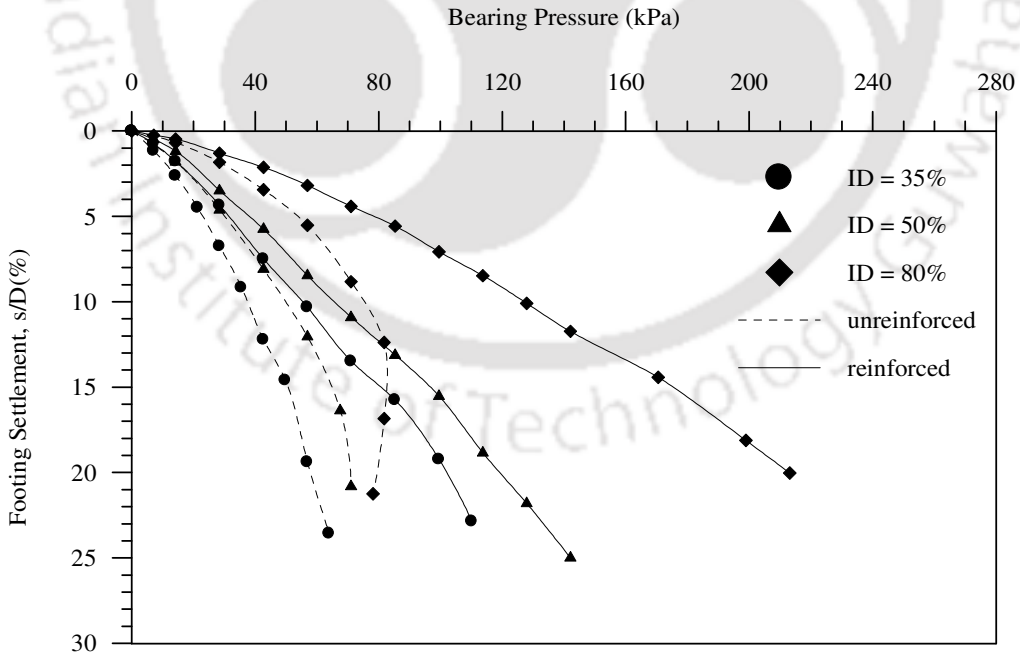

Fig. 5.72 Variation of bearing pressure with footing settlement for different relative densities (ID) of infill sand in geocells – Test Series A6, G1 to G3, h = 1.07D, d = 0.4D

heights (h = 0.8D, 1.07D; Tables 5.11, 5.12) of geocell mattress, greater benefit from reinforcement is derived with medium dense sand (ID = 50%). In case of smaller height (h = 0.27D and 0.53D) of geocell mattress, the sand under the footing overcomes the friction of the geocell wall and punches into the soft subgrade. Now the geocell cage sustains footing loading through mobilization of anchorage from the soil around. This anchorage increases with increased density of soil leading to higher mobilized benefit from the reinforcement. At higher height (h = 0.8D, 1.07D) the dense soil matrix through arching action itself supports a substantial portion of the applied loading that relatively less load is transmitted to the geocell reinforcement giving rise to reduced improvement factor (IF_{gc}). With very low density (ID = 35%), the infill soil is unable to provide adequate anchorage thereby the geocell reinforcement just settles down as a secondary footing under the applied loading leading to lower contribution of reinforcement and hence lower value of improvement factor. However for medium dense condition of infill sand (ID = 50%) the arching induced resistance being relatively low, the geocell reinforcement is subjected to loading and at the same time, the soil around too provide anchorage. As a result of which maximum deformation takes place in the reinforcement leading to maximum performance improvement (IF_{gc}). But for small pocket size (d = 0.4D), the dense sand being effectively held within the pockets of the geocell derives enhanced strength from geocell reinforcement through dilation induced volume expansion. Therefore, with reduced pocket size of geocells, dense sand tends to derive maximum reinforcing benefit. It is to be noted that it is the improvement in bearing pressure with respect to the unreinforced case i.e. IF_{gc} which decreases and not the total bearing pressure which continues to increase with increase in the relative density. It could also be observed that at a height of h = 1.07D and pocket size of d = 1.2D, the improvement factors (IF_{gc}) obtained are negligible for all densities of sand. This can be

explained through the pressure-settlement plot in Fig. 5.70 which shows that the unreinforced and reinforced responses are almost similar indicating that for higher heights, the stiffness of the sand layer itself is adequate to stand against the footing penetration and the influence of reinforcement is only marginal thereby resulting in low values of $IF_{gc.}$

Figs. 5.73 and 5.74 show that for shallow height (h = 0.27D) of geocell mattress, there is a substantial heave while for higher height (h = 1.07D), settlement prevails on geocell mattress surface. For shallow height, the punching of sand into the clay subgrade has induced high heaving. As with higher height, the soil is contained within the geocell and the mattress has settled as a composite body. This establishes the proposed mechanism.

Table 5.9 Summary of results in terms of bearing capacity improvement factor (IF_{gc}) showing the influence of relative density of sand at h = 0.27D, Test Series D1 to D3

Variable Parameter		Bearing capacity improvement factor (IF_{gc})				
		(s/D) 3%	(s/D) 5%	(s/D) 10%	(s/D) 15%	(s/D) 20%
(d/D)	(ID) %					
1.2	35	1.04	1.04	1.10	1.16	1.17
	50	1.08	1.10	1.12	1.18	1.24
	80	**1.29**	**1.29**	**1.31**	**1.32**	**1.34**
0.8	35	1.13	1.15	1.19	1.26	1.36
	50	1.09	1.14	1.27	1.35	1.46
	80	**1.37**	**1.47**	**1.62**	**1.70**	**1.79**
0.4	35	1.34	1.35	1.36	1.43	1.52
	50	1.23	1.24	1.33	1.42	1.54
	80	**1.59**	**1.66**	**1.82**	**1.92**	**1.96**

Table 5.10 Summary of results in terms of bearing capacity improvement factor (IF_{gc}) showing the influence of relative density of sand at h = 0.53D, Test Series E1 to E3

Variable Parameter		Bearing capacity improvement factor (IF_{gc})				
		(s/D) 3%	(s/D) 5%	(s/D) 10%	(s/D) 15%	(s/D) 20%
(d/D)	(ID) %					
1.2	35	1.11	1.16	1.18	1.24	1.35
	50	1.08	1.16	1.28	1.35	1.37
	80	**1.29**	**1.30**	**1.40**	**1.52**	**1.54**
0.8	35	1.21	1.22	1.25	1.40	1.57
	50	1.12	1.22	1.32	1.43	1.58
	80	**1.37**	**1.49**	**1.65**	**1.80**	**1.86**
0.4	35	1.34	1.41	1.57	1.69	1.79
	50	1.24	1.38	1.58	1.68	1.72
	80	**1.64**	**1.70**	**1.88**	**2.09**	**2.16**

Table 5.11 Summary of results in terms of bearing capacity improvement factor (IF_{gc}) showing the influence of relative density of sand at h = 0.80D, Test Series F1 to F3

Variable Parameter		Bearing capacity improvement factor (IF_{gc})				
		(s/D) 3%	(s/D) 5%	(s/D) 10%	(s/D) 15%	(s/D) 20%
(d/D)	(ID)%					
1.2	35	1.18	1.21	1.24	1.27	1.38
	50	**1.18**	**1.23**	**1.31**	**1.35**	1.39
	80	1.08	1.09	1.11	1.22	**1.50**
0.8	35	1.33	1.33	1.34	1.35	1.52
	50	**1.34**	**1.34**	1.49	1.59	1.67
	80	1.31	1.31	**1.58**	**1.81**	**2.25**
0.4	35	1.62	1.64	1.69	1.81	2.05
	50	1.45	1.47	1.69	1.94	2.19
	80	**1.62**	**1.67**	**1.82**	**2.10**	**2.60**

Table 5.12 Summary of results in terms of bearing capacity improvement factor (IF_{gc}) showing the influence of relative density of sand at h = 1.07D, Test Series G1 to G3

Variable Parameter		Bearing capacity improvement factor (IF_{gc})				
		(s/D) 3%	(s/D) 5%	(s/D) 10%	(s/D) 15%	(s/D) 20%
(d/D)	(ID)%					
1.2	35	1.03	1.03	1.06	1.06	1.13
	50	**1.04**	**1.05**	**1.05**	1.06	1.10
	80	1.01	1.01	1.01	**1.11**	**1.21**
0.8	35	1.17	1.23	1.32	1.41	1.49
	50	**1.23**	1.24	1.28	1.40	1.60
	80	1.19	**1.31**	**1.51**	**1.71**	**2.08**
0.4	35	1.36	1.38	1.48	1.60	1.76
	50	1.25	1.26	1.32	1.49	1.68
	80	**1.40**	**1.46**	**1.66**	**2.13**	**2.68**

The findings from the present study are contrary to the work of Dash et al. (2001a) who reported that in case of strip footing supported by geocell reinforced homogeneous sand bed, the bearing capacity improvement factor (IF_{gc}) continues to increase with increase in the relative density of sand. This disagreement can be attributed to the difference in the geometry of the two problems. In case of a homogeneous sand bed, the sand below the footing generally gets compressed under footing penetration. With increased density, the dilation induced resistance of the soil increases. Thus the benefit of higher order of geocell strength is mobilized in achieving higher load carrying capacity at higher density. However, in the present study, the geocell mattress being above the soft subgrade, the geocell-sand mattress visibly deflects downwards, under the application of load. This is resisted through the mobilization of the anchorage from soil in the adjacent region. When the sand is dense, the arching induced resistance is high enough to sustain substantial part of the applied load and a relatively less load is transferred to the reinforcement. This leads to decrease in the magnitude of the improvement factor (IF_{gc}).

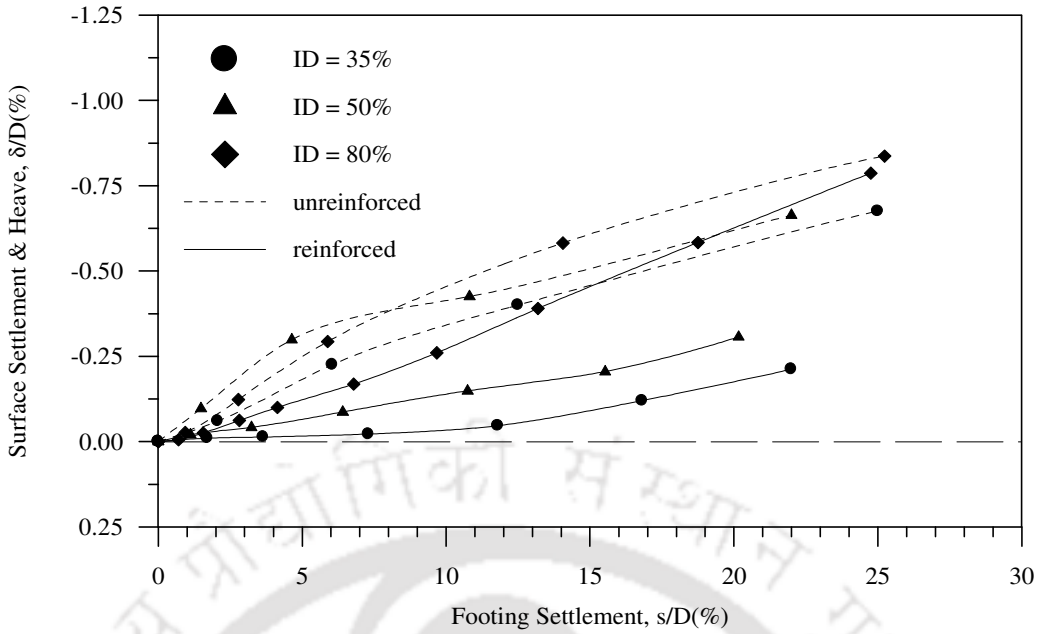

Fig. 5.73 Variation of average surface deformation with footing settlement at a distance x = 2D from the centre of the footing, for different relative densities (ID) of infill sand in geocells, Test Series A3, D1 to D3, d = 0.4D, h = 0.27D

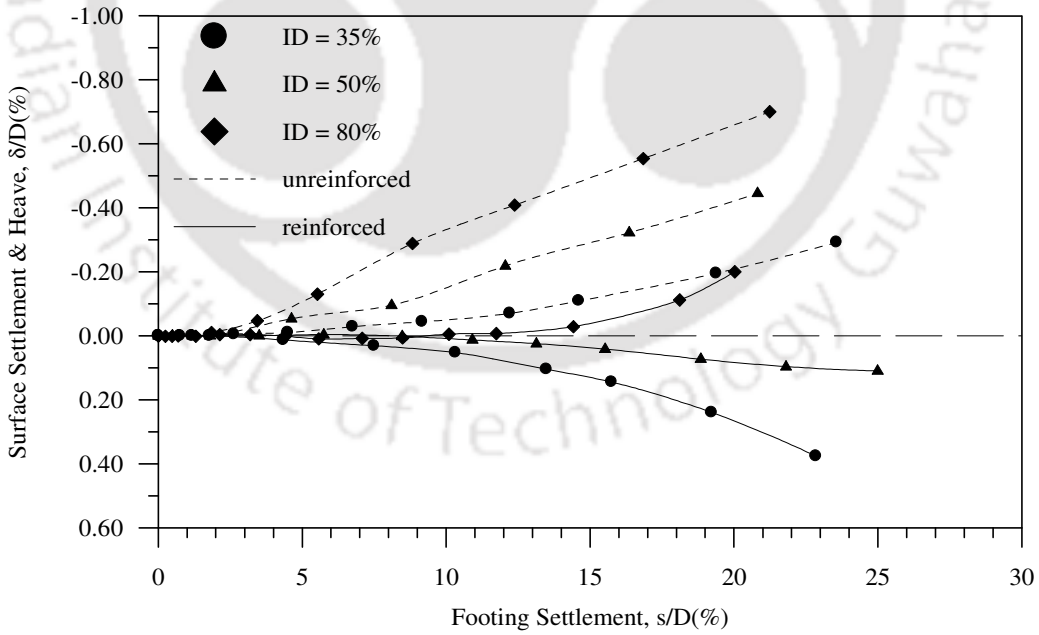

Fig. 5.74 Variation of average surface deformation with footing settlement at a distance x = 2D from the centre of the footing, for different relative densities (ID) of infill sand in geocells, Test Series A6, G1 to G3, d = 0.4D, h = 1.07D

From the above analysis it can be said that the relative density (ID) of infill sand at which the geocell reinforcement provides maximum performance improvement is dependent on the pocket size and height of the geocell mattress. For shallow height, the maximum benefit from the geocell reinforcement is obtained when the geocells are filled with dense sand. However, with geocells of larger pocket size and higher height, better performance improvement is observed with medium dense infill sand. While with smaller pocket size a dense soil matrix derives higher reinforcing efficacy from the geocells. Contrary to the dilation induced load transfer mechanism observed in case of homogeneous sand bed, it is the anchorage effect which predominantly governs the load transfer mechanism in the present case. It is however to be noted that the overall bearing capacity continues to increase with the increase in the relative density of the soil. Hence, in general, it is advantageous to fill the geocells with sand compacted to the densest state.

CHAPTER 6

GEOCELL - GEOGRID REINFORCED SAND LAYER OVERLYING CLAY SUBGRADE

6.1 INTRODUCTION

The test results in the previous chapter indicate a significant improvement in the bearing capacity due to the provision of geocell-sand mattress over the soft clay subgrade. It is, however, a common practice in the field to place the geocell mattress over a base of a planar geogrid layer. This basal geogrid serves twin purposes; while it acts as a platform for the construction of the geocell mattress, it also facilitates the movement of the construction equipments, over soft clay subgrades. It has also emerged from a review of literature in Chapter 2 that further improvement in bearing pressure could be obtained with the provision of an additional layer of geogrid below the geocell mattress. However the research in this area lacks a detailed investigation on the influence of various parameters pertaining to geocell-geogrid configuration on the behaviour of the composite structure. In view of this, another twelve series of tests (Test series H1 to K3) were conducted to investigate the behaviour of the composite geocell-geogrid system with varying parameters of geocells and infill sand (i.e. pocket size, height of geocells; relative density of infill sand). In doing so, the contribution of the additional geogrid layer to the overall performance improvement is suitably brought out. The details of the test series are presented in Table 3.4 (Chapter 3).

6.2 BEHAVIOUR OF GEOCELL-GEOGRID MATTRESS

A typical pressure-settlement response due to geocell reinforcement with and without a layer of geogrid at its base is shown in Fig. 6.1. It could be observed that the bearing pressure as well as the stiffness of the foundation bed further increases with the provision

of an additional layer of geogrid below the geocell mattress. The geocell-sand mattress over the clay bed behaves as a subgrade supported slab, which when loaded at the centre, deflects downwards. This downward movement is resisted by the geogrid layer at the base through mobilization of its membrane strength and anchorage provided by the soil. Thus a composite geocell-geogrid system provides a more coherent structure leading to higher bearing pressure and stiffness of the foundation bed.

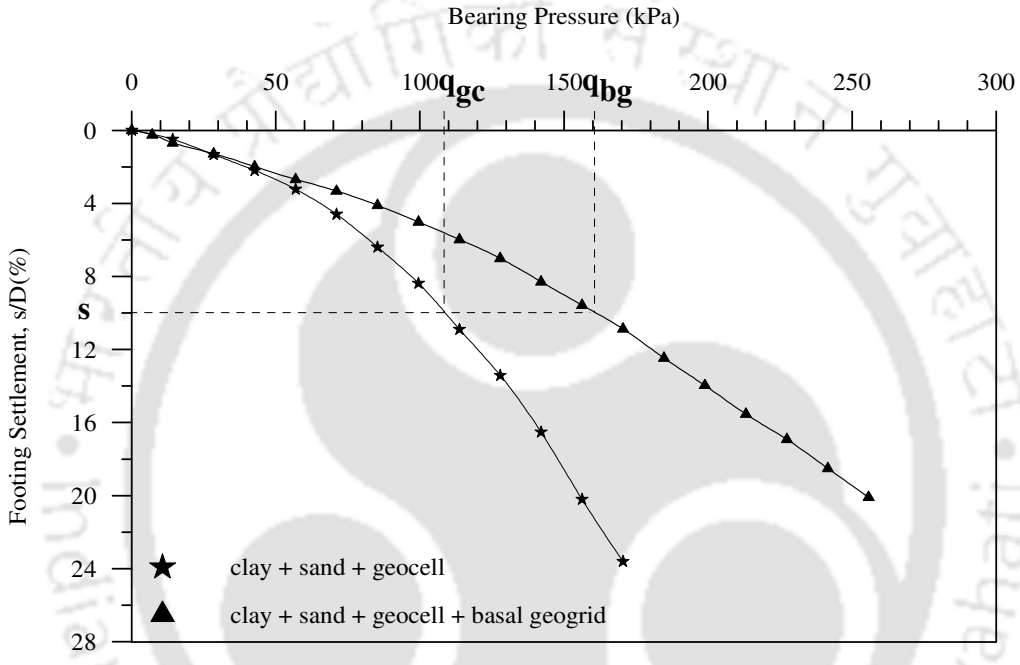

Fig. 6.1 Variation of bearing pressure with footing settlement for geocell mattress, with and without basal geogrid – Test Series F3, J3, u = 0.1D, h = 0.8D, d = 0.4D, ID = 80%

The performance improvement in bearing capacity due to the provision of the basal geogrid is quantified using a non dimensional factor, IF_{bg}, which is defined as the ratio of footing pressure (q_{bg}) with geocell and basal geogrid at a given settlement to the corresponding footing pressure (q_{gc}) of geocell mattress alone. It is observed from Fig. 6.1 that at a settlement of 10% of the footing diameter, the bearing pressure due to geocell reinforcement is about 110 kPa. With the inclusion of an additional geogrid layer at the base, the bearing pressure of the composite system is found to have increased to 160 kPa.

Thus, about 1.5 fold increase in bearing pressure is obtained with the provision of an additional basal geogrid. It was observed earlier (Fig. 5.1) that at this settlement the geocell-sand mattress increases the overall load carrying capacity of the clay subgrade by as much as six times ($IF_s \times IF_{gc} = 6$). When this improvement due to geocell-sand mattress is coupled with the present improvement due to the additional basal geogrid, the overall load carrying capacity of the clay subgrade is found to have increased by about nine times (i.e. $IF_s \times IF_{gc} \times IF_{bg} = 6 \times 1.5 = 9$).

For all tests in these series, geocells were formed in chevron pattern and depth of placement of geocell mattress (u) was kept at 0.1D. The parameters; pocket size (d) of geocells, height (h) of the geocell mattress and relative density (ID) of infill sand in the geocells, were varied and their influence on the pressure-settlement and surface deformation behaviour of the composite foundation system (geocell + base geogrid) are presented and discussed in the following sections.

6.2.1 Influence of pocket size of geocells

The bearing pressure versus settlement responses due to different pocket sizes (d = 1.2D, 0.8D and 0.4D) of geocells under varied conditions of geocell-geogrid reinforcement (i.e. height of geocell mattress and relative density of infill sand) are presented in Figs. 6.2 to 6.13. For the purpose of comparison, the corresponding pressure-settlement responses due to geocell reinforcement alone are also presented. It could be observed from these figures that the overall load carrying capacity of the geocell-geogrid composite bed increases with the reduction in the pocket size of the geocells. The influence of pocket size is more distinctly visible at higher relative density of sand (ID = 80%; Figs. 6.10 to 6.13) and will be discussed in more details in the next section.

The improvement in bearing pressure due to provision of an additional layer of basal geogrid (IF_{bg}) with relative densities of infill sand varying from 35% to 80% is summarized in Tables 6.1 to 6.3 respectively. It could be observed that, in general, the performance improvement due to basal geogrid is higher for geocells of larger pocket sizes (d = 1.2D). The deviation from this trend in some cases (h = 0.53D) is attributed to local effects. With geocells of larger pocket sizes, relatively more deformation is expected on the geocell mattress which in turn induces higher strain in the basal geogrid layer. At the same time, due to relatively less confinement at larger pocket sizes, the sand in the geocell pockets lying below the footing tends to move down under footing loading. However this downward movement of the soil mass is resisted through bearing resistance on the geogrid ribs. These two factors lead to higher mobilization of the strength of the basal geogrid thereby increasing its contribution to the overall performance improvement, in case of larger pocket openings.

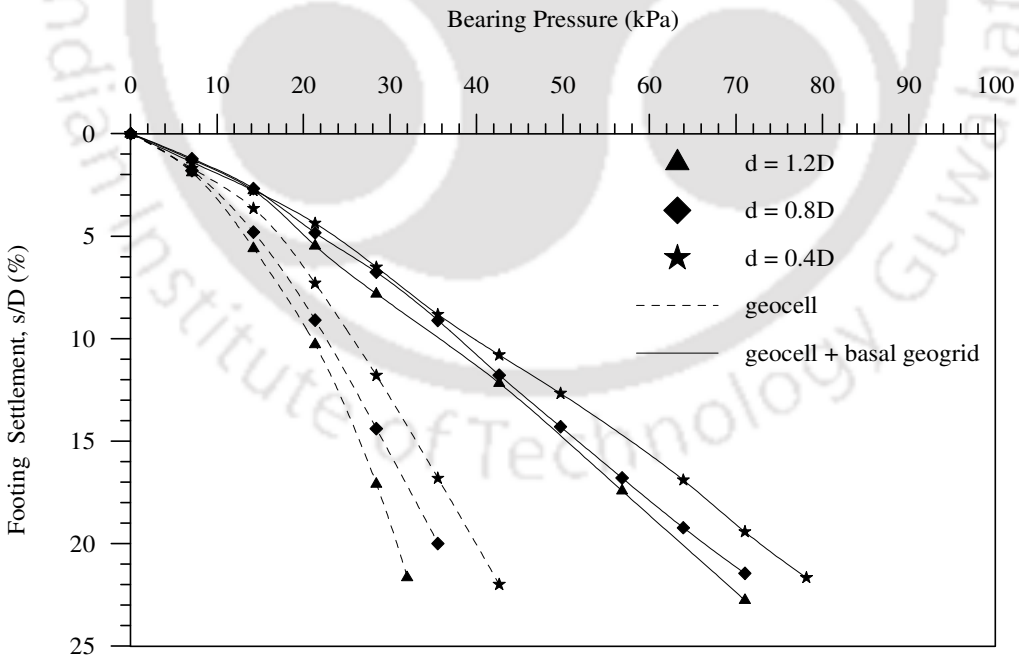

Fig. 6.2 Variation of bearing pressure with footing settlement for different pocket sizes (d) of geocell mattress, with and without basal geogrid – Test Series D1, H1, ID = 35%, h = 0.27D

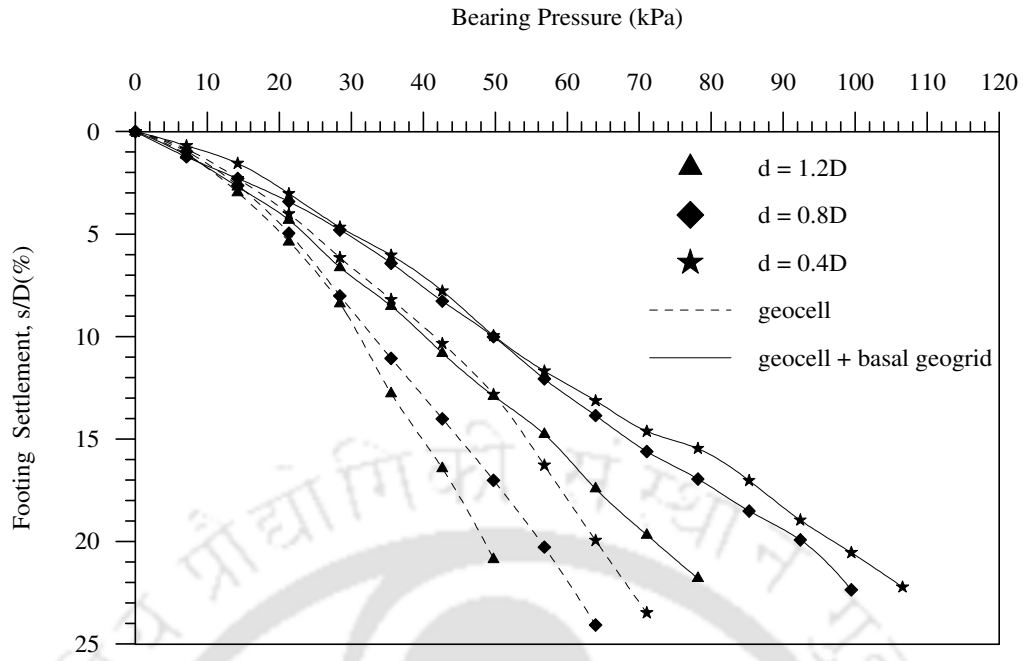

Fig. 6.3 Variation of bearing pressure with footing settlement for different pocket sizes (d) of geocell mattress, with and without basal geogrid – Test Series E1, I1, ID = 35%, h = 0.53D

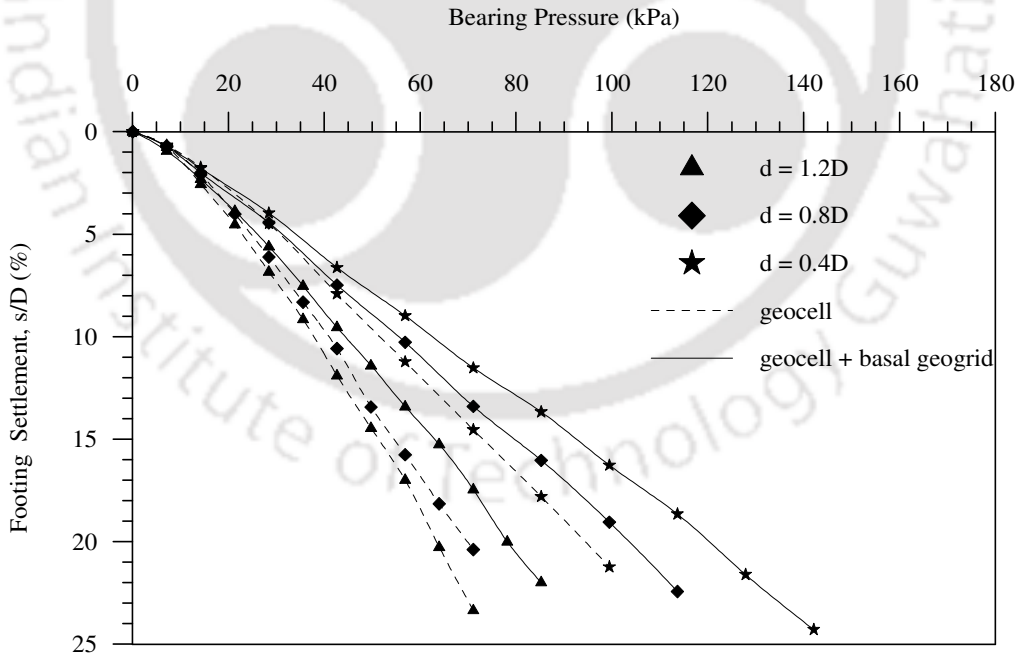

Fig. 6.4 Variation of bearing pressure with footing settlement for different pocket sizes (d) of geocell mattress, with and without basal geogrid – Test Series F1, J1, ID = 35%, h = 0.80D

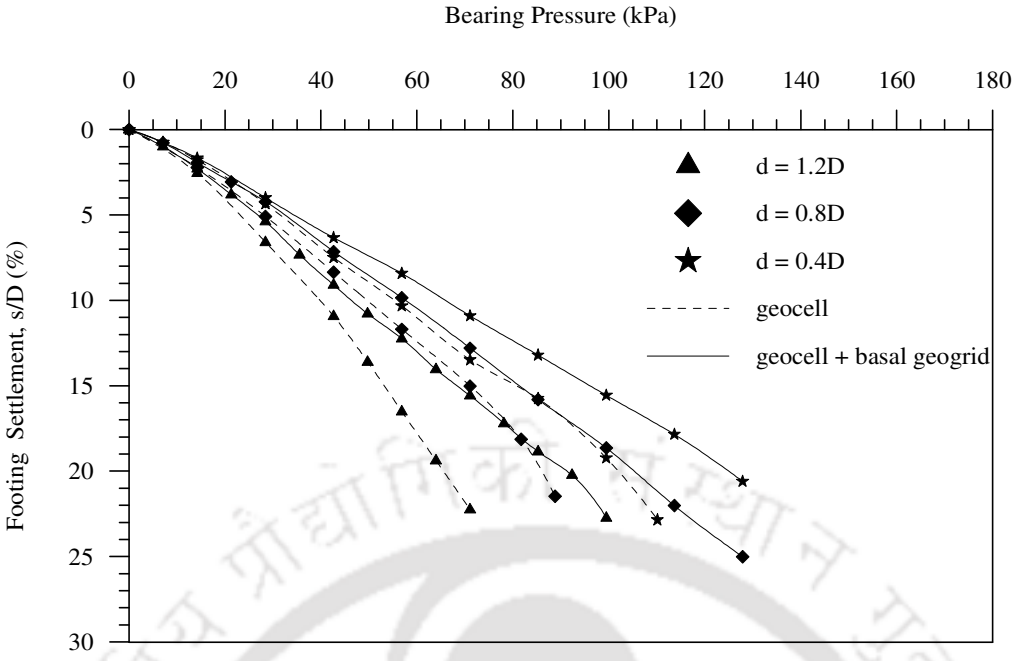

Fig. 6.5 Variation of bearing pressure with footing settlement for different pocket sizes (d) of geocell mattress, with and without basal geogrid – Test Series G1, K1, ID = 35%, h = 1.07D

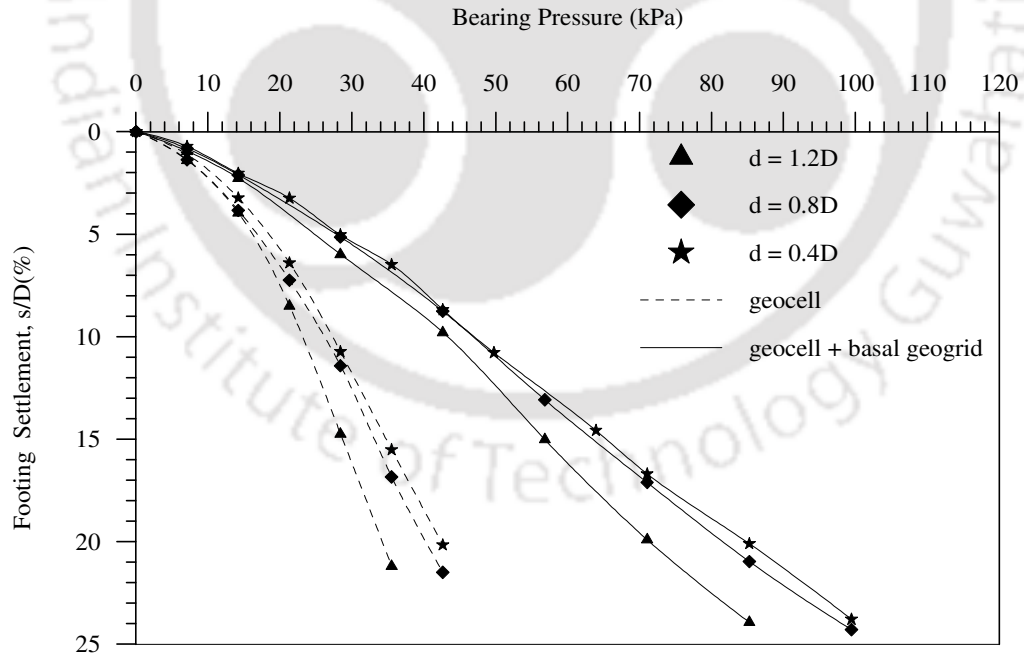

Fig. 6.6 Variation of bearing pressure with footing settlement for different pocket sizes (d) of geocell mattress, with and without basal geogrid –Test Series D2, H2, ID = 50%, h = 0.27D

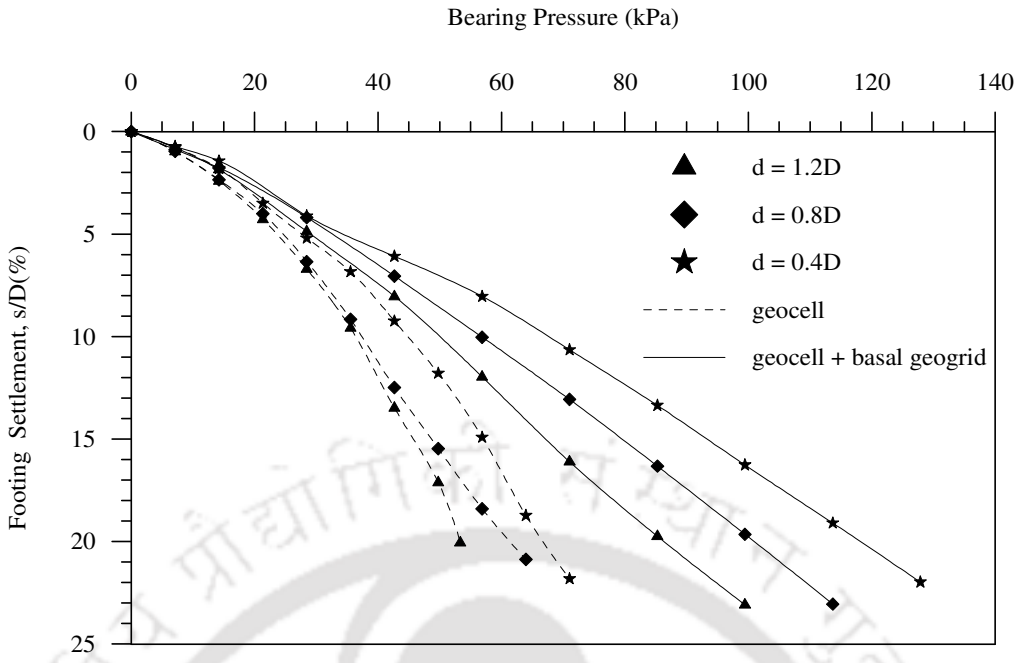

Fig. 6.7 Variation of bearing pressure with footing settlement for different pocket sizes (d) of geocell mattress, with and without basal geogrid – Test Series E2, I2, ID = 50%, h = 0.53D

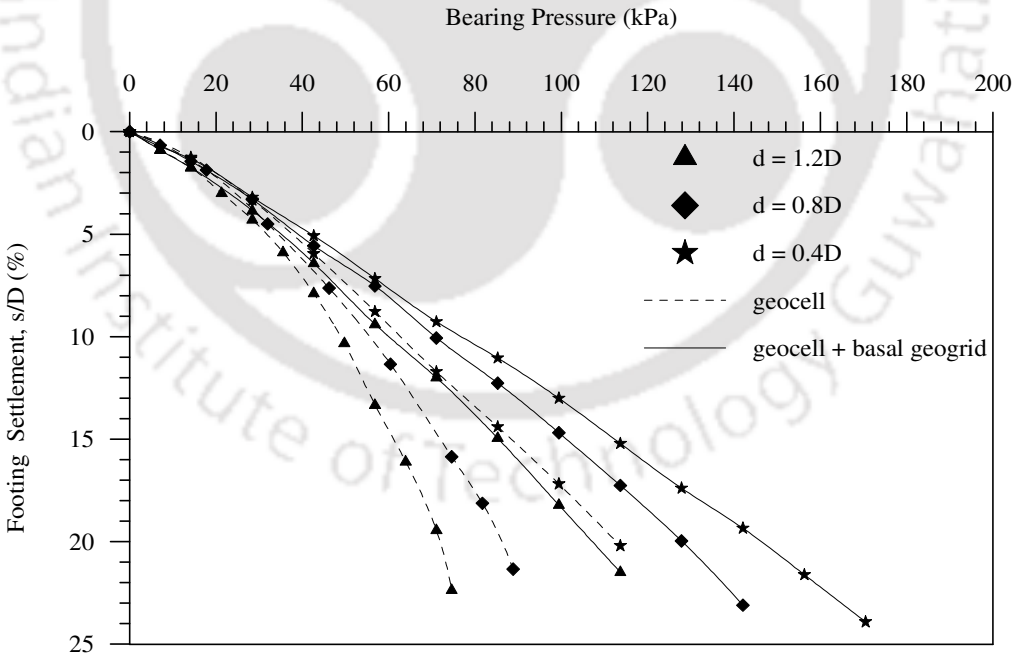

Fig. 6.8 Variation of bearing pressure with footing settlement for different pocket sizes (d) of geocell mattress, with and without basal geogrid – Test Series F2, J2, ID = 50%, h = 0.80D

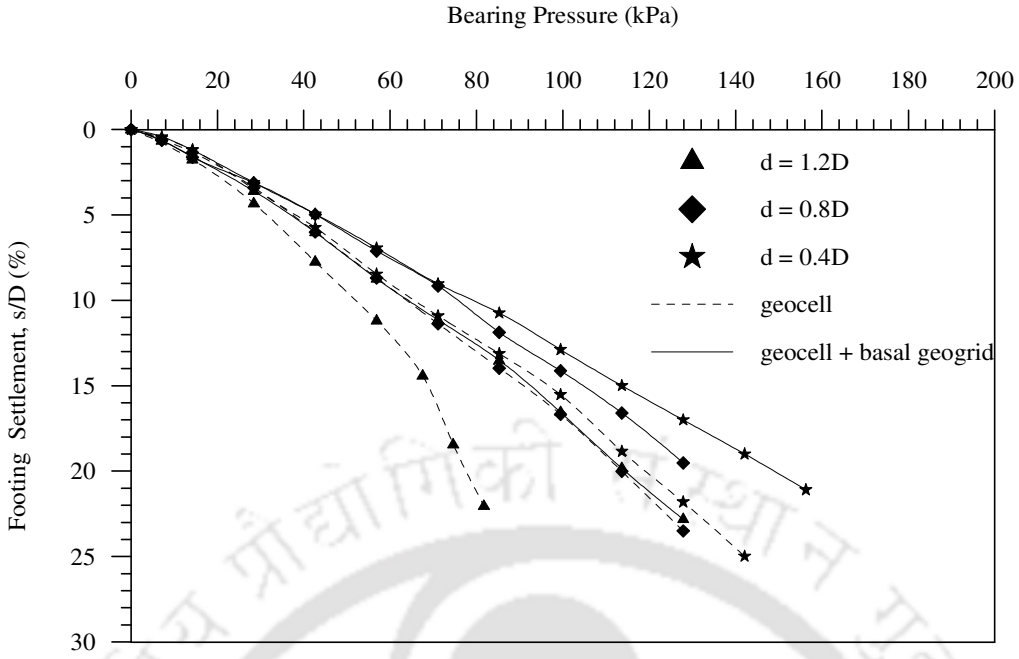

Fig. 6.9 Variation of bearing pressure with footing settlement for different pocket sizes (d) of geocell mattress, with and without basal geogrid – Test Series G2, K2, ID = 50%, h = 1.07D

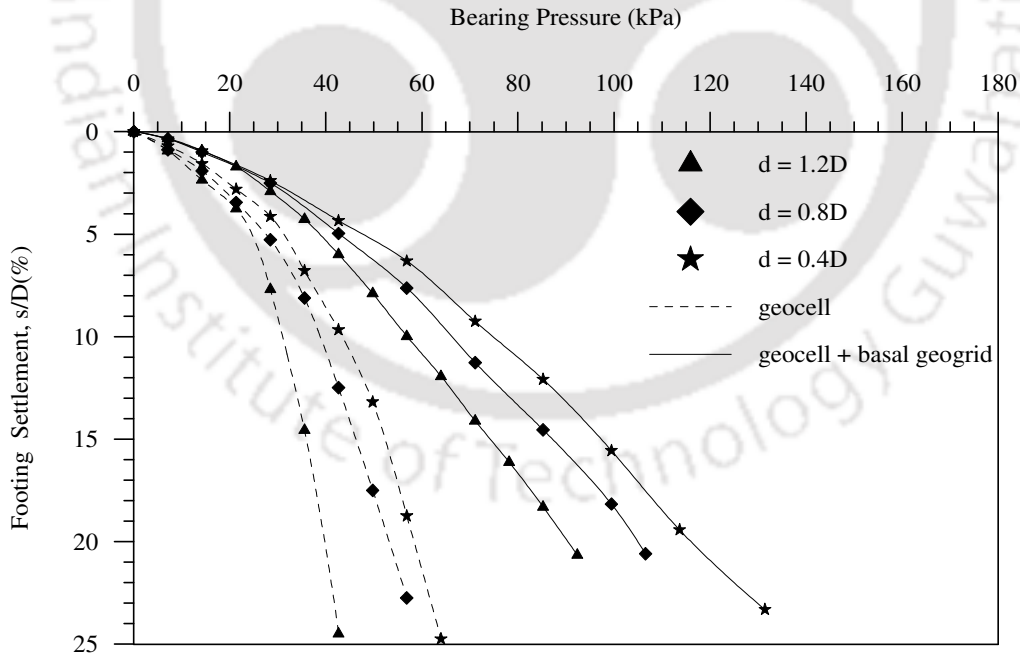

Fig. 6.10 Variation of bearing pressure with footing settlement for different pocket sizes (d) of geocell mattress, with and without basal geogrid – Test Series D3, H3, ID = 80%, h = 0.27D

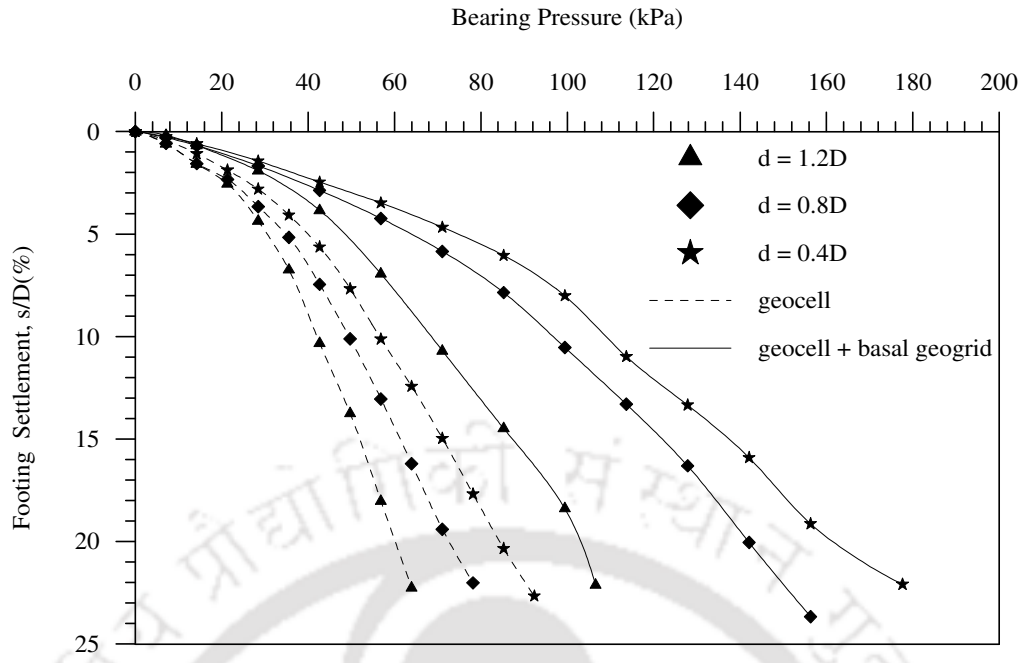

Fig. 6.11 Variation of bearing pressure with footing settlement for different pocket sizes (d) of geocell mattress, with and without basal geogrid – Test Series E3, I3, ID = 80%, h = 0.53D

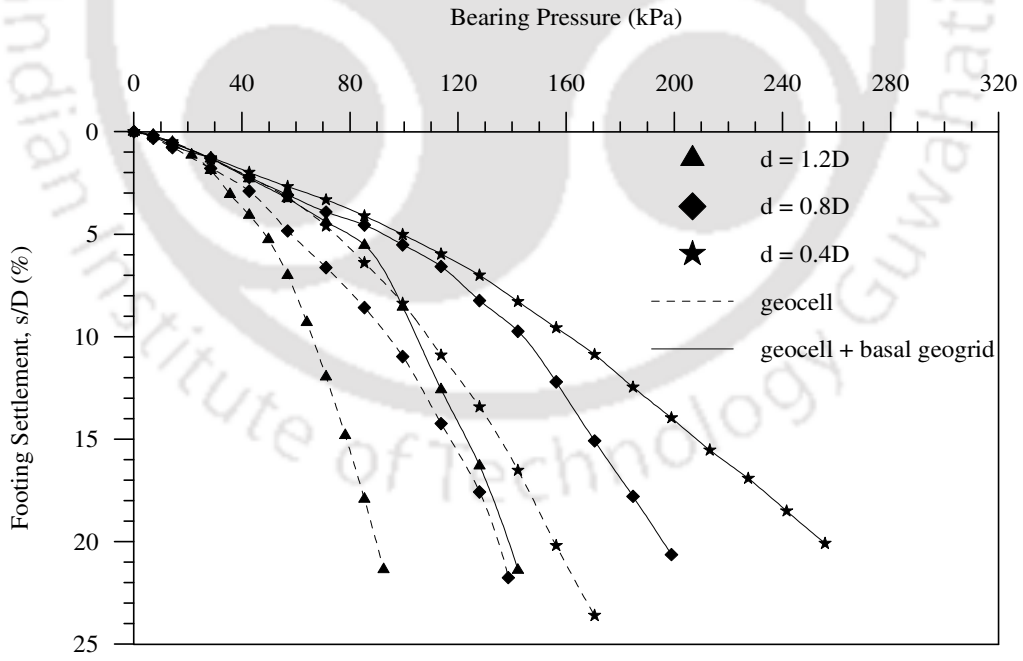

Fig. 6.12 Variation of bearing pressure with footing settlement for different pocket sizes (d) of geocell mattress, with and without basal geogrid – Test Series F3, J3, ID = 80%, h = 0.80D

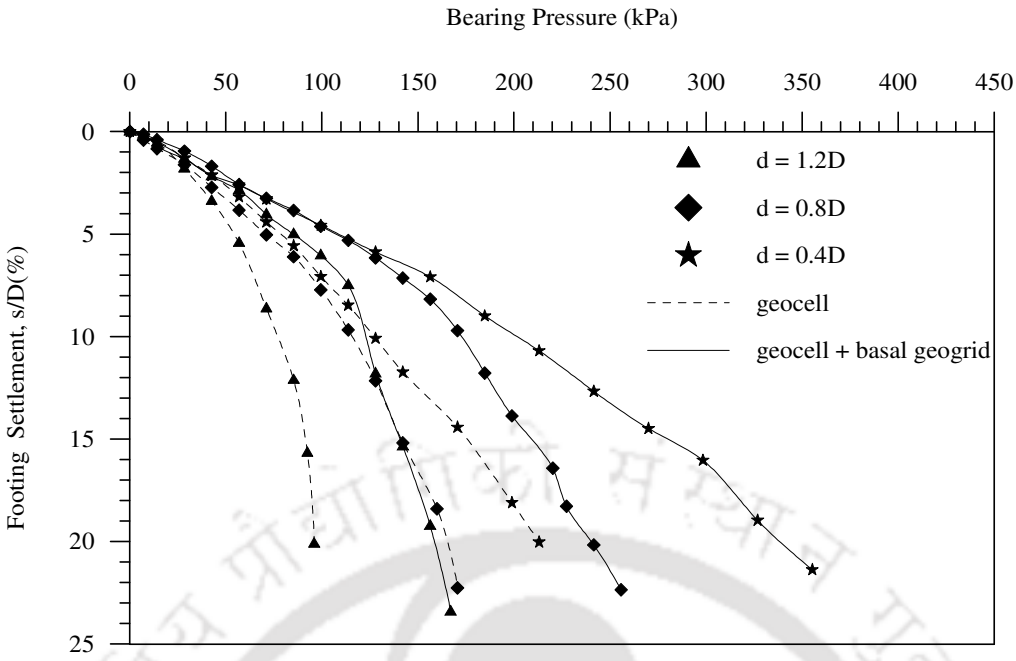

Fig. 6.13 Variation of bearing pressure with footing settlement for different pocket sizes (d) of geocell mattress, with and without basal geogrid – Test Series G3, K3, ID = 80%, h = 1.07D

Table 6.1 Summary of results in terms of bearing capacity improvement factor (IF_{bg}) showing the influence of pocket size (d) of geocells, ID = 35%

Variable Parameter		Bearing capacity improvement factor (IF_{bg})				
		(s/D) 3%	(s/D) 5%	(s/D) 10%	(s/D) 15%	(s/D) 20%
(h/D)	(d/D)					
0.27	**1.2**	**1.58**	**1.52**	**1.71**	**1.88**	**2.07**
	0.8	1.49	1.50	1.68	1.76	1.87
	0.4	1.25	1.37	1.53	1.75	1.82
0.53	1.2	1.09	1.15	1.29	1.44	1.49
	0.8	1.21	**1.37**	**1.51**	**1.52**	**1.65**
	0.4	**1.23**	1.22	1.20	1.36	1.51
0.80	1.2	1.10	1.15	1.17	1.23	1.23
	0.8	**1.14**	**1.25**	**1.36**	**1.46**	**1.48**
	0.4	1.06	1.11	1.21	1.27	1.27
1.07	**1.2**	1.09	**1.16**	**1.16**	**1.29**	**1.39**
	0.8	**1.14**	1.16	1.16	1.15	1.22
	0.4	1.06	1.09	1.19	1.19	1.23

Table 6.2 Summary of results in terms of bearing capacity improvement factor (IF_{bg}) showing the influence of pocket size (d) of geocells, ID = 50%

Variable Parameter		Bearing capacity improvement factor (IF_{bg})				
		(s/D) 3%	(s/D) 5%	(s/D) 10%	(s/D) 15%	(s/D) 20%
(h/D)	(d/D)					
0.27	**1.2**	1.44	1.53	**1.86**	**1.98**	**2.09**
	0.8	**1.54**	**1.65**	1.79	1.91	2.01
	0.4	1.47	1.53	1.72	1.86	2.00
0.53	1.2	1.19	1.25	1.37	1.47	1.62
	0.8	**1.28**	**1.33**	**1.51**	**1.64**	**1.65**
	0.4	1.17	1.24	1.51	1.64	1.77
0.80	**1.2**	**1.08**	**1.12**	**1.25**	**1.40**	**1.49**
	0.8	1.08	1.12	1.25	1.40	1.49
	0.4	1.03	1.12	1.22	1.27	1.30
1.07	**1.2**	**1.13**	**1.17**	**1.23**	**1.34**	**1.47**
	0.8	1.07	1.15	1.19	1.15	1.13
	0.4	1.06	1.13	1.20	1.17	1.25

Table 6.3 Summary of results in terms of bearing capacity improvement factor (IF_{bg}) showing the influence of pocket size (d) of geocells, ID = 80%

Variable Parameter		Bearing capacity improvement factor (IF_{bg})				
		(s/D) 3%	(s/D) 5%	(s/D) 10%	(s/D) 15%	(s/D) 20%
(h/D)	(d/D)					
0.27	**1.2**	1.59	**1.60**	**1.86**	**2.07**	**2.26**
	0.8	**1.63**	1.56	1.71	1.91	2.01
	0.4	1.47	1.53	1.72	1.86	2.00
0.53	1.2	1.60	1.59	1.63	1.68	1.71
	0.8	**1.78**	1.83	**1.96**	**1.99**	**1.96**
	0.4	1.70	**1.87**	1.93	1.93	1.91
0.80	**1.2**	**1.48**	**1.65**	**1.58**	**1.57**	1.55
	0.8	1.28	1.59	1.53	1.45	1.45
	0.4	1.18	1.33	1.48	1.54	**1.64**
1.07	**1.2**	**1.50**	**1.57**	**1.59**	1.54	**1.65**
	0.8	1.41	1.52	1.49	1.48	1.46
	0.4	1.19	1.39	1.59	**1.60**	1.59

Typical surface deformation responses near the footing region (i.e. x = D) for geocell mattress of heights, h = 0.27D and 1.07D, with and without a basal geogrid layer are shown in Figs. 6.14 and 6.15 respectively. It could be observed that, in general, the settlement on the surface of the composite foundation bed (geocell + base geogrid) is of lesser magnitude as compared to the corresponding settlement with geocell mattress alone. This is attributed to the increased rigidity of the geocell mattress due to the provision of basal geogrid. As a result of which the composite structure offers more resistance against the downwards deformation under footing penetration leading to relatively lesser settlement on the surface.

It was observed earlier that at smaller heights (h = 0.27D) of geocell mattress, the infill sand overcomes the frictional resistance of the geocell walls and moves downwards leading to surface heave. However with the provision of the geogrid layer at the base, the fill surface is found to settle instead of heaving (Fig. 6.14). This indicates that the geogrid layer at the base inhibits the downward movement of the soil through bearing over its ribs thereby effectively arresting the heave on the surface.

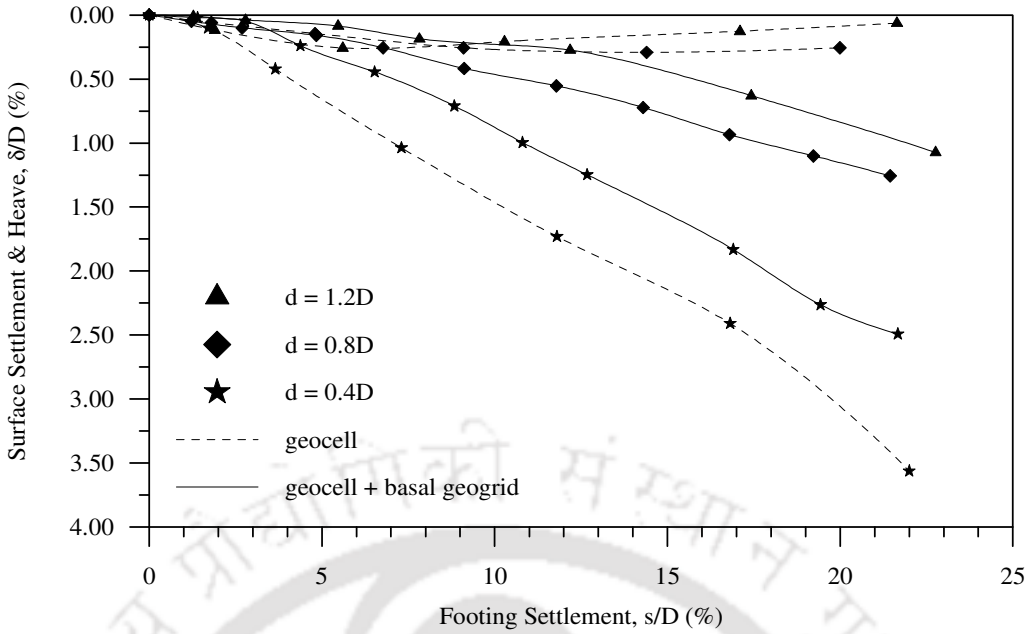

Fig. 6.14 Variation of average surface deformation with footing settlement at a distance of x = D from the centre of footing, for different pocket sizes (d) of geocell mattress, with and without basal geogrid – Test Series D1, H1, ID = 35%, h = 0.27D

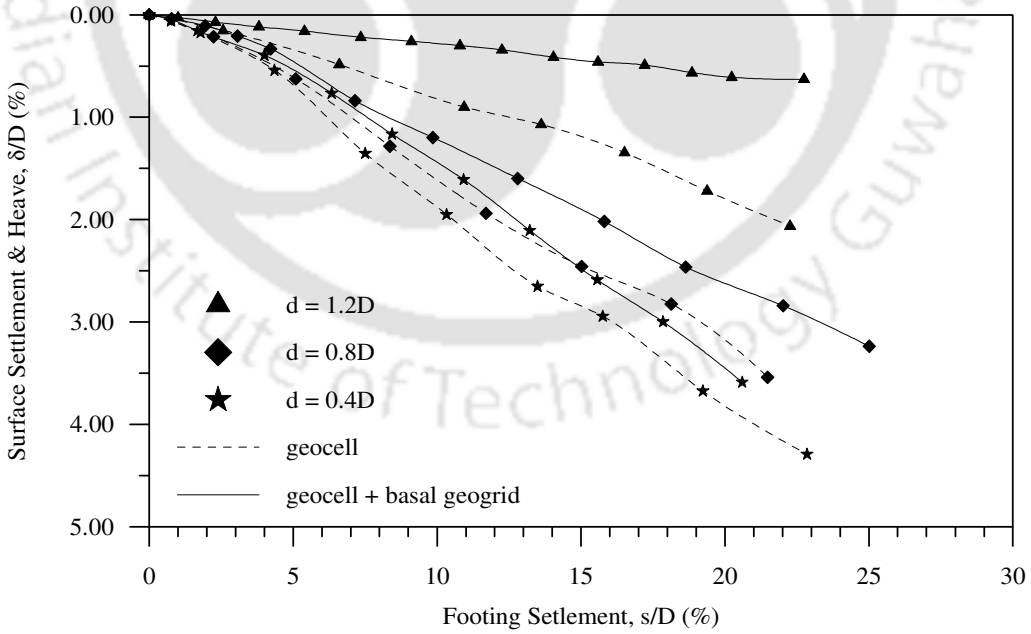

Fig. 6.15 Variation of average surface deformation with footing settlement at a distance of x = D from the centre of footing, for different pocket sizes (d) of geocell mattress, with and without basal geogrid – Test Series G1, K1, ID = 35%, h = 1.07D

6.2.2 Influence of height of geocell mattress

The pressure-settlement plots showing the influence of height of the geocell mattress on the overall performance of the geocell-geogrid composite structure are presented in Figs. 6.16 to 6.24. It could be observed that the pressure-settlement responses with geocell-geogrid reinforcement closely follow the earlier trend with geocell mattress alone (Figs. 5.42 to 5.50). The load carrying capacity of the composite structure increases with the increase in the height of the geocell mattress till a height of 0.8D, after which the improvement is marginal. The marginal improvement in performance of the composite structure beyond a height (h) of 0.8D could be attributed to the buckling of the geocell walls lying below the footing that reduce the effectiveness of load transfer to the basal geogrid layer. As much of the strength of the basal geogrid remains immobilized, the proportion of increase in the bearing pressure is relatively less.

The bearing pressure improvement factors (IF_{bg}), as obtained from Figs. 6.16 to 6.24, are reported in Tables 6.4 to 6.6. It could be observed that the beneficial effect of the basal geogrid, IF_{bg}, decreases with the increase in the height of the geocell mattress. This is because with increase in the height, the rigidity of the geocell mattress increases and the footing load is distributed within the geocell layer. Since relatively less load is transferred to the basal geogrid layer, it undergoes less deformation and subsequently lower membrane strength is mobilized. Hence, the contribution of basal geogrid to the overall performance improvement is reduced at higher heights of geocell mattress. The variation from the general trend noted in few cases (Table 6.6; d = 0.8D, 0.4D) is attributed to some local effects.

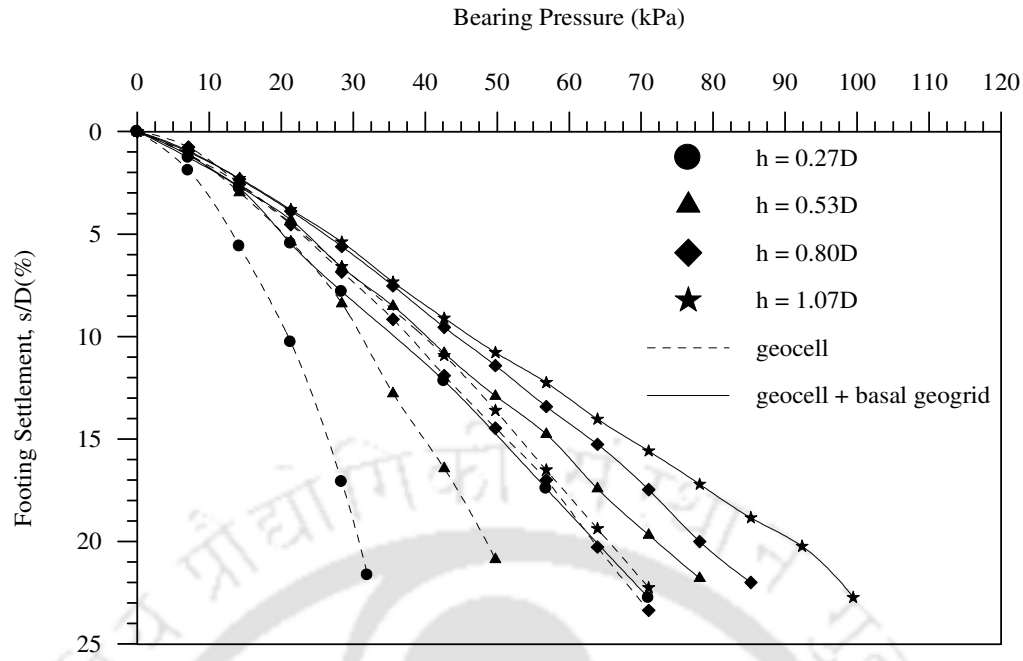

Fig. 6.16 Variation of bearing pressure with footing settlement for different heights (h) of geocell mattress, with and without basal geogrid – Test Series D1, E1, F1, G1, H1,I1, J1, K1, ID = 35%, d = 1.2D

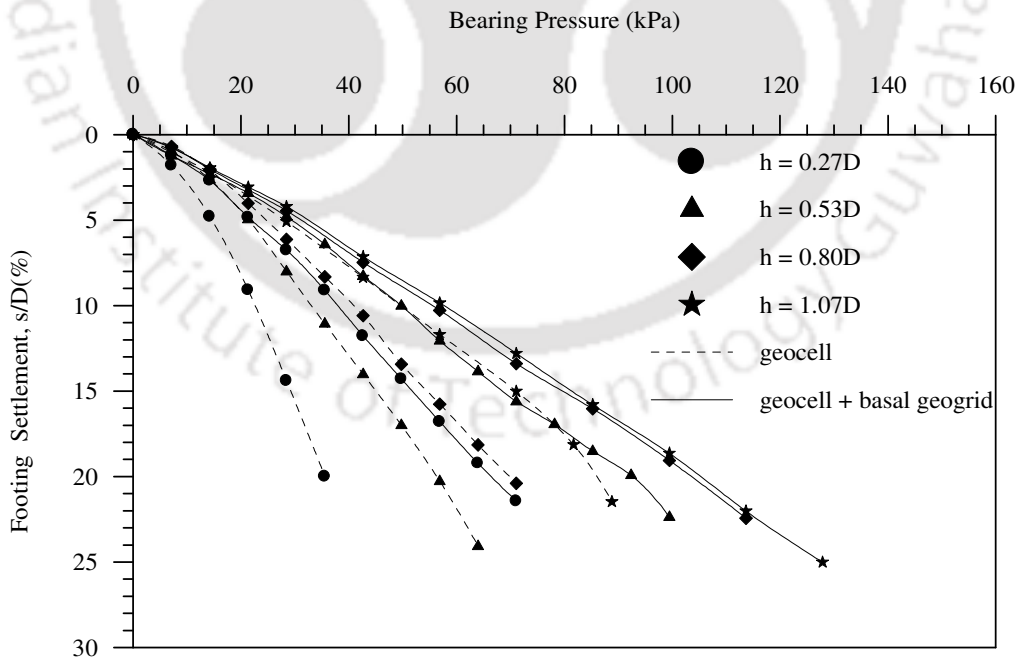

Fig. 6.17 Variation of bearing pressure with footing settlement for different heights (h) of geocell mattress, with and without basal geogrid – Test Series D1, E1, F1, G1, H1,I1, J1, K1, ID = 35%, d = 0.8D

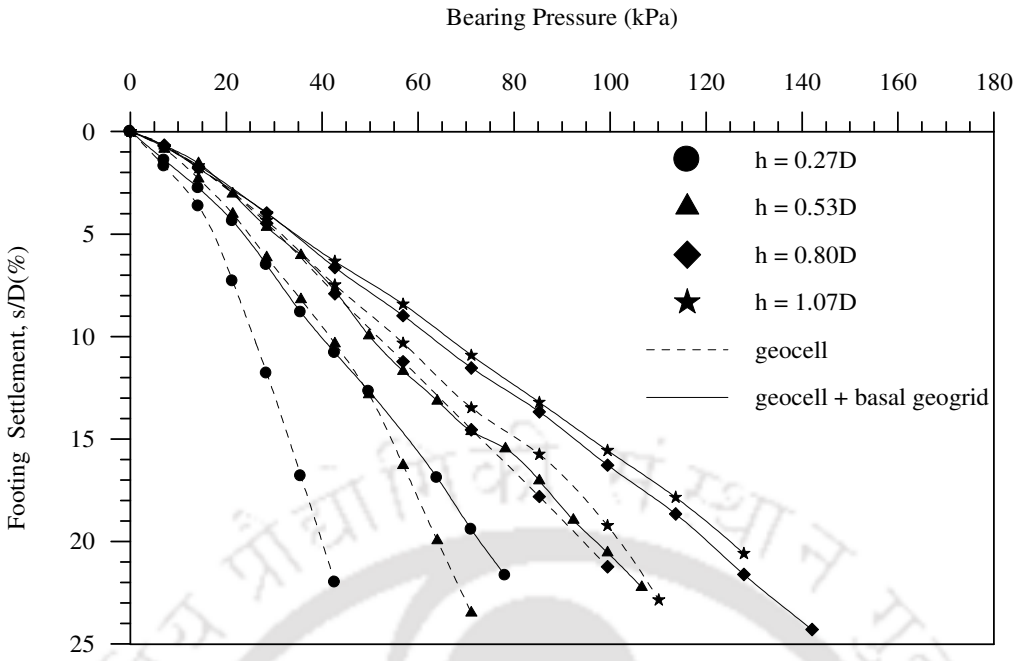

Fig. 6.18 Variation of bearing pressure with footing settlement for different heights (h) of geocell mattress, with and without basal geogrid – Test Series D1, E1, F1, G1, H1,I1, J1, K1, ID = 35%, d = 0.4D

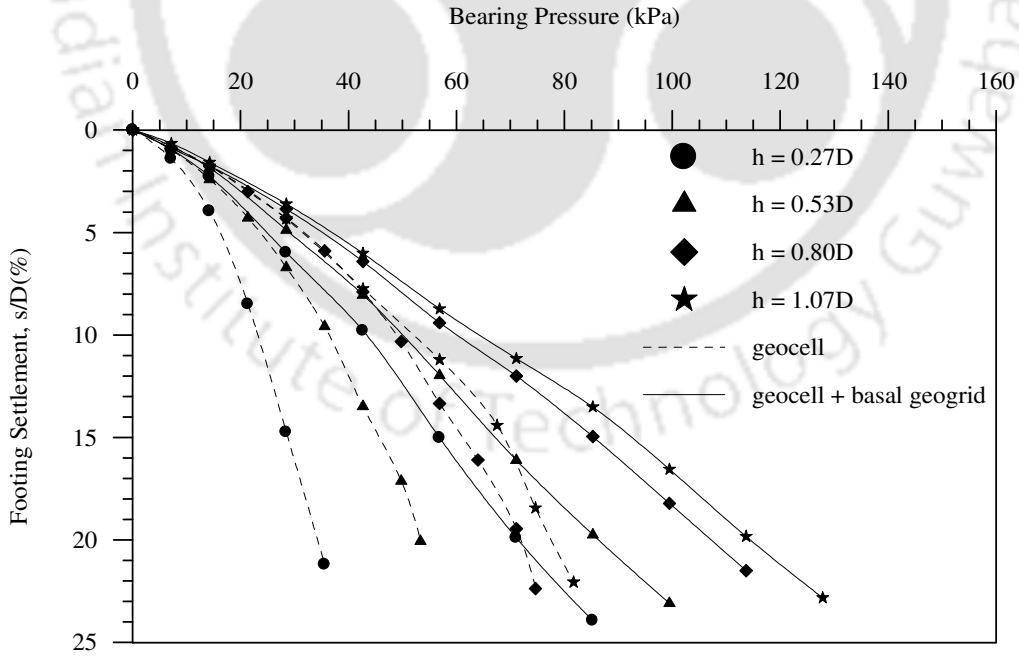

Fig. 6.19 Variation of bearing pressure with footing settlement for different heights (h) of geocell mattress, with and without basal geogrid – Test Series D2, E2, F2, G2, H2,I2, J2, K2, ID = 50%, d = 1.2D

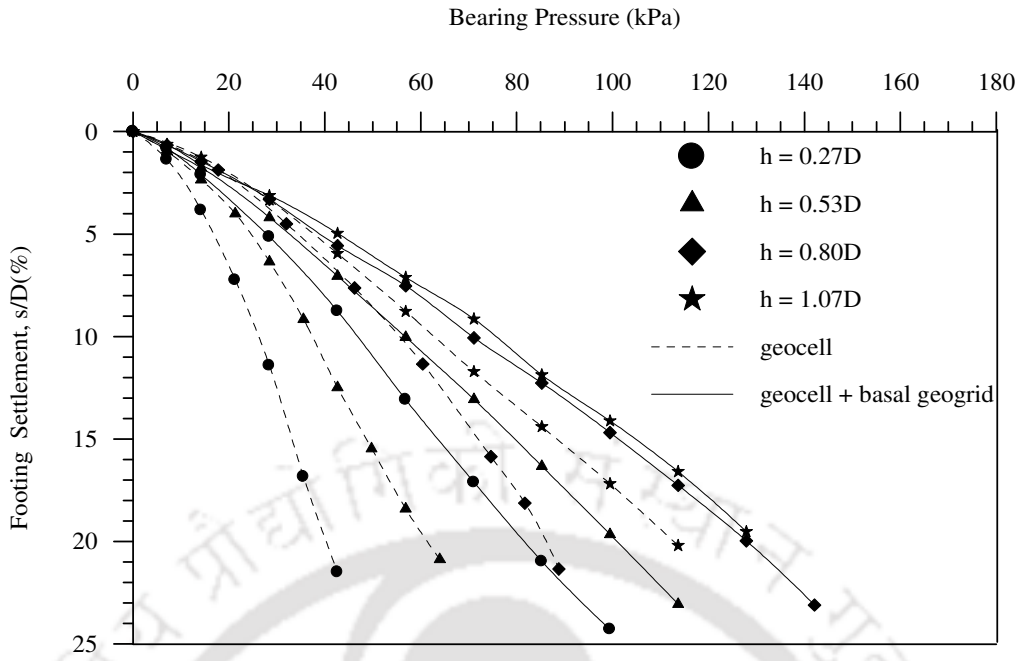

Fig. 6.20 Variation of bearing pressure with footing settlement for different heights (h) of geocell mattress, with and without basal geogrid – Test Series D2, E2, F2, G2, H2,I2, J2, K2, ID = 50%, d = 0.8D

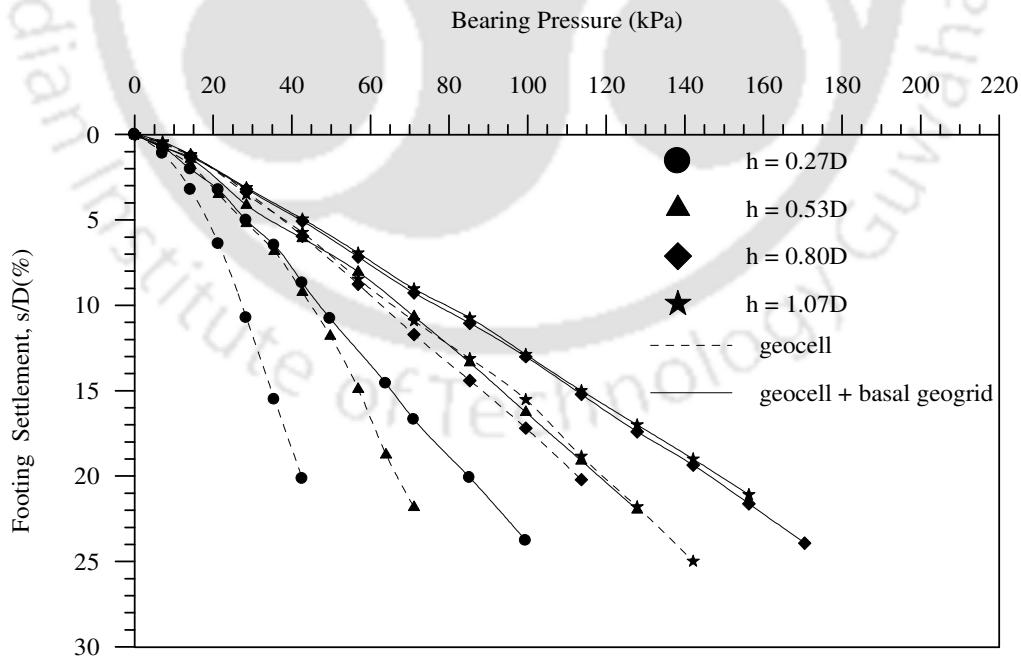

Fig. 6.21 Variation of bearing pressure with footing settlement for different heights (h) of geocell mattress, with and without basal geogrid – Test Series D2, E2, F2, G2, H2,I2, J2, K2, ID = 50%, d = 0.4D

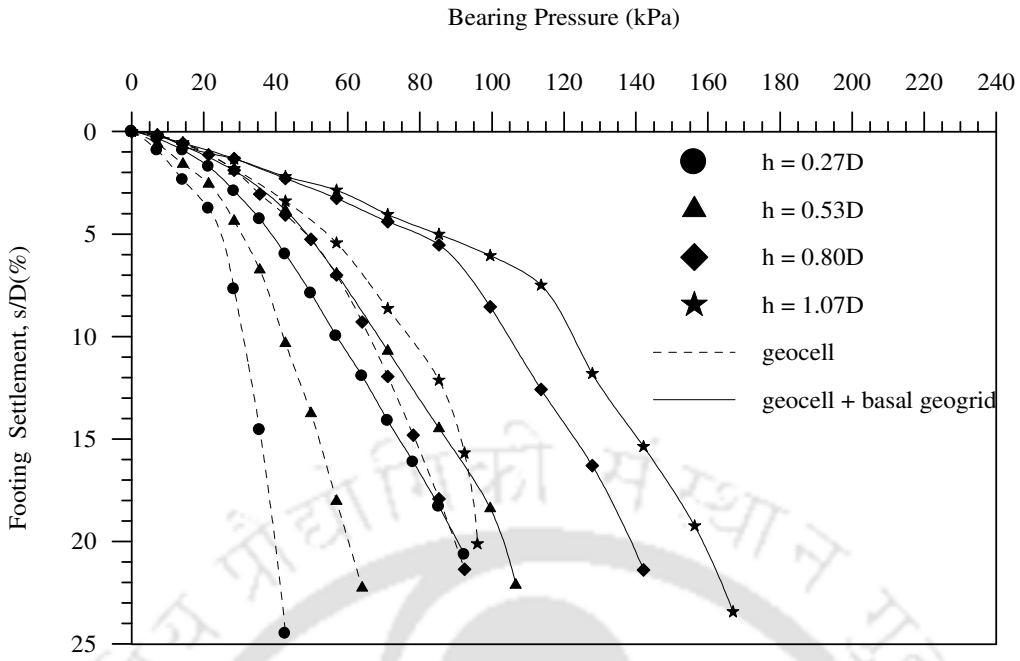

Fig. 6.22 Variation of bearing pressure with footing settlement for different heights (h) of geocell mattress, with and without basal geogrid – Test Series D3, E3, F3, G3, H3,I3, J3, K3, ID = 80%, d = 1.2D

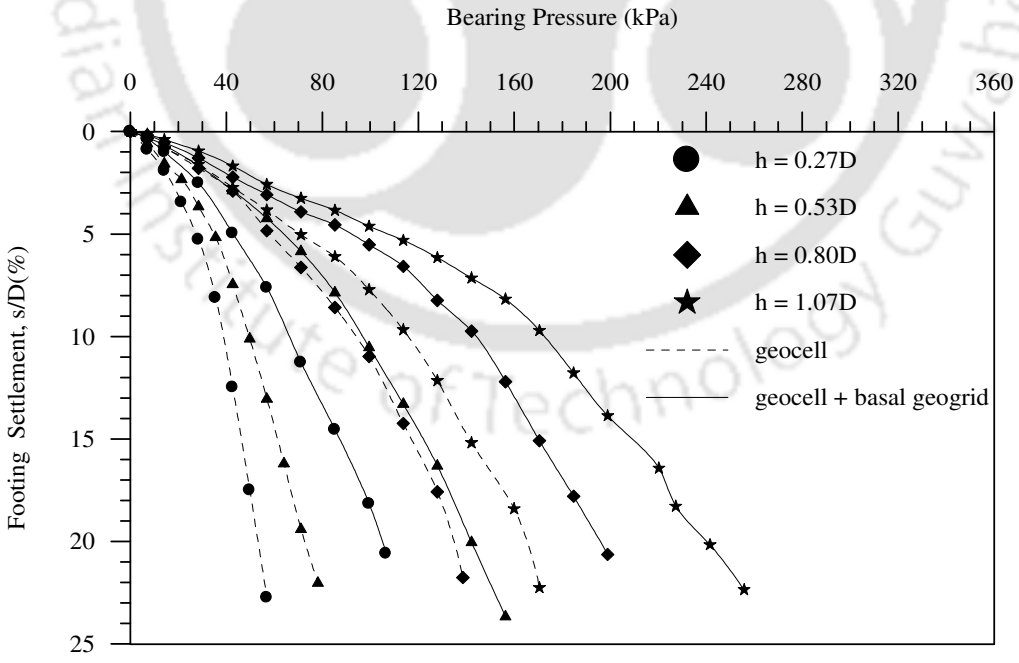

Fig. 6.23 Variation of bearing pressure with footing settlement for different heights (h) of geocell mattress, with and without basal geogrid – Test Series D3, E3, F3, G3, H3,I3, J3, K3, ID = 80%, d = 0.8D

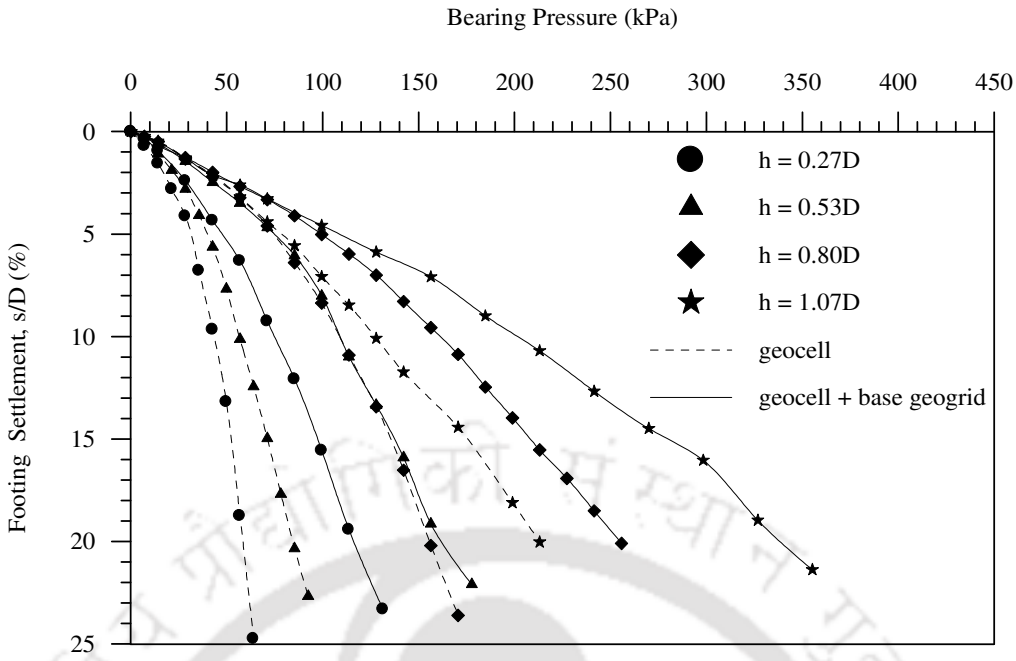

Fig. 6.24 Variation of bearing pressure with footing settlement for different heights (h) of geocell mattress, with and without basal geogrid – Test Series D3, E3, F3, G3, H3,I3, J3, K3, ID = 80%, d = 0.4D

Table 6.4 Summary of results in terms of bearing capacity improvement factor (IF_{bg}) showing the influence of height of geocell mattress, ID = 35%, Test Series H1, I1, J1, K1

Variable Parameter		Bearing capacity improvement factor (IF_{bg})				
		(s/D) 3%	(s/D) 5%	(s/D) 10%	(s/D) 15%	(s/D) 20%
(d/D)	(h/D)					
1.2	**0.27**	**1.58**	**1.52**	**1.71**	**1.88**	**2.07**
	0.53	1.09	1.15	1.29	1.44	1.49
	0.8	1.10	1.15	1.17	1.23	1.23
	1.07	1.09	1.16	1.16	1.29	1.39
0.8	**0.27**	**1.49**	**1.50**	**1.68**	**1.76**	**1.87**
	0.53	1.21	1.37	1.51	1.52	1.65
	0.8	1.14	1.25	1.36	1.46	1.48
	1.07	1.14	1.16	1.16	1.15	1.22
0.4	**0.27**	**1.25**	**1.37**	**1.53**	**1.75**	**1.82**
	0.53	1.23	1.22	1.20	1.36	1.51
	0.8	1.06	1.11	1.21	1.27	1.27
	1.07	1.06	1.09	1.19	1.19	1.23

Table 6.5 Summary of results in terms of bearing capacity improvement factor (IF_{bg}) showing the influence of height of geocell mattress, ID = 50%, Test Series H2, I2, J2, K2

Variable Parameter		Bearing capacity improvement factor (IF_{bg})				
		(s/D) 3%	(s/D) 5%	(s/D) 10%	(s/D) 15%	(s/D) 20%
(d/D)	(h/D)					
1.2	**0.27**	**1.44**	**1.53**	**1.86**	**1.98**	**2.09**
	0.53	1.19	1.25	1.37	1.47	1.62
	0.8	1.08	1.12	1.25	1.40	1.49
	1.07	1.13	1.17	1.23	1.34	1.47
0.8	**0.27**	**1.54**	**1.65**	**1.79**	**1.91**	**2.01**
	0.53	1.28	1.33	1.51	1.64	1.65
	0.8	1.08	1.12	1.25	1.40	1.49
	1.07	1.07	1.15	1.19	1.15	1.13
0.4	**0.27**	**1.47**	**1.53**	**1.72**	**1.86**	**2.00**
	0.53	1.17	1.24	1.51	1.64	1.77
	0.8	1.03	1.12	1.22	1.27	1.30
	1.07	1.06	1.13	1.20	1.17	1.25

Table 6.6 Summary of results in terms of bearing capacity improvement factor (IF_{bg}) showing the influence of height of geocell mattress, ID = 80%, Test Series H3, I3, J3, K3

Variable Parameter		Bearing capacity improvement factor (IF_{bg})				
		(s/D) 3%	(s/D) 5%	(s/D) 10%	(s/D) 15%	(s/D) 20%
(d/D)	(h/D)					
1.2	**0.27**	**1.59**	**1.60**	**1.86**	**2.07**	**2.26**
	0.53	1.60	1.59	1.63	1.68	1.71
	0.8	1.48	1.65	1.58	1.57	1.55
	1.07	1.50	1.57	1.59	1.54	1.65
0.8	0.27	1.63	1.56	1.71	1.91	**2.01**
	0.53	**1.78**	**1.83**	**1.96**	**1.99**	1.96
	0.8	1.28	1.59	1.53	1.45	1.45
	1.07	1.41	1.52	1.49	1.48	1.46
0.4	0.27	1.47	1.53	1.72	1.86	**2.00**
	0.53	**1.70**	**1.87**	**1.93**	**1.93**	1.91
	0.8	1.18	1.33	1.48	1.54	1.64
	1.07	1.19	1.39	1.59	1.60	1.59

Figs. 6.25, 6.26 and 6.27 show the influence of the basal geogrid with geocell mattress of different heights (h), on the surface deformation responses, at a distance of x = D, 2D and 3D from the centre of footing respectively. It could be observed that at x = D (Fig. 6.25) the contribution of basal geogrid layer in reducing the settlement on the fill surface decreases with increase in the height of the geocell mattress. This is because in case of higher heights of geocell mattress, the downwards movement of the soil is restricted due to mobilization of higher frictional resistance over a larger surface area of the geocell mattress. Thus a larger amount of the strength of the planar geogrid layer remains immobilized thereby decreasing its influence at higher heights. At x = 2D and 3D (Figs. 6.26 and 6.27), the composite foundation bed is observed to heave more than the corresponding geocell reinforced bed. With the geocell mattress getting restrained by the base geogrid against settlement under footing loading, its walls get locally compressed/buckled under the footing. The walls of geocells being continuous members, the central compression/buckling leads to lifting up in the region outside giving rise to induced heave on the fill surface.

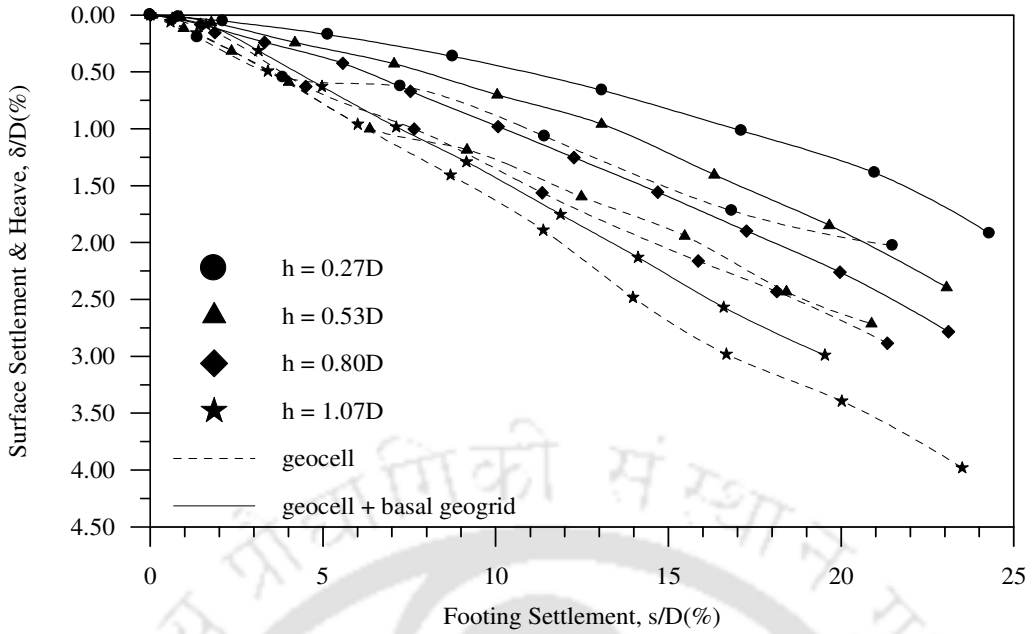

Fig. 6.25 Variation of average surface deformation with footing settlement at a distance of x = D from the centre of the footing, for different heights (h) of geocell mattress, with and without basal geogrid – Test Series D2, E2, F2, G2, H2,I2, J2, K2, ID = 50%, d = 0.8D

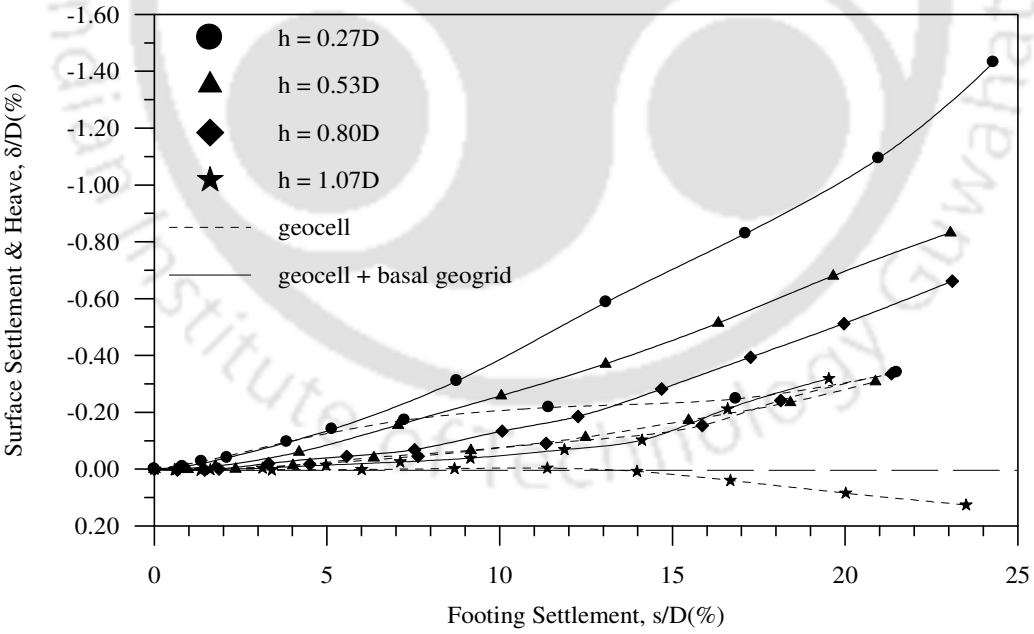

Fig. 6.26 Variation of average surface deformation with footing settlement at a distance of x = 2D from the centre of the footing, for different heights (h) of geocell mattress, with and without basal geogrid – Test Series D2, E2, F2, G2, H2,I2, J2, K2, ID = 50%, d = 0.8D

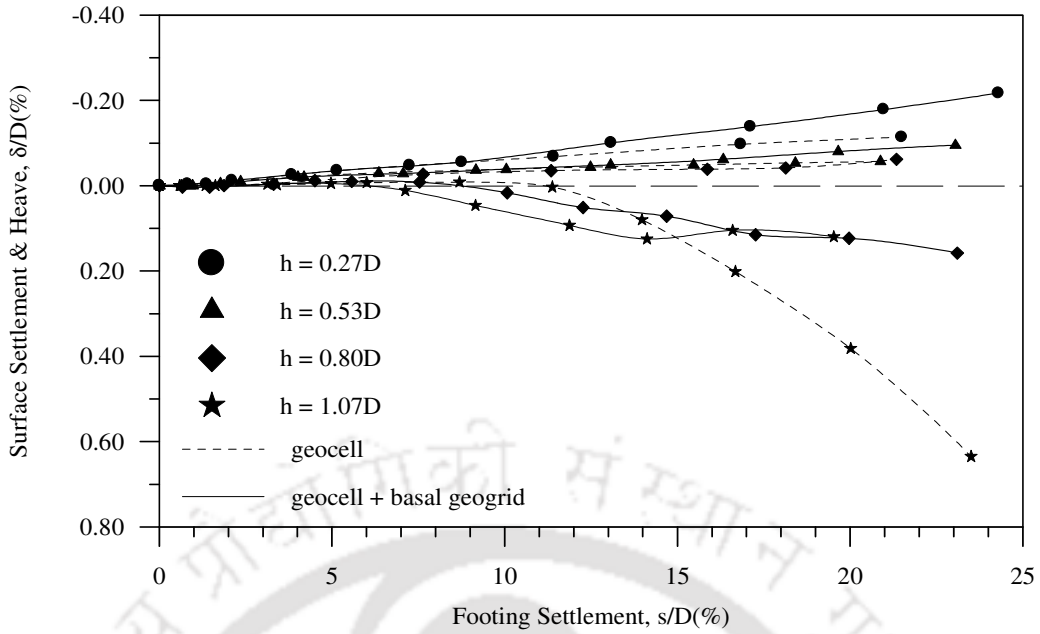

Fig. 6.27 Variation of average surface deformation with footing settlement at a distance of x = 3D from the centre of the footing, for different heights (h) of geocell mattress, with and without basal geogrid – Test Series D2, E2, F2, G2, H2,I2, J2, K2, ID = 50%, d = 0.8D

6.2.3 Influence of relative density of infill sand

The variation of bearing pressure with footing settlement with different relative densities of infill sand (ID = 35%, 50%, 80%) for various configurations of geocell-geogrid reinforcement, are presented in Figs. 6.28 to 6.39. A significant increase in the stiffness, as indicated by the steeper pressure-settlement response, could be observed with higher relative density (ID = 80%) of infill soil. This is due to enhanced confinement in case of dense infill soil in the geocells that relatively higher load is needed for small increment in settlement of the composite structure. The improvement in bearing pressure, due to the provision of a basal geogrid (IF_{bg}) with different heights of geocell mattress is summarized in Tables 6.7 to 6.10. It is observed that, in general, the maximum improvement in performance of the composite structure is obtained when the geocells are filled with dense sand (ID = 80%). When the composite structure with loose infill sand (ID = 35%, 50%) is loaded, the loose sand undergoes localized densification due to which

it is unable to transmit the footing pressure to the basal geogrid. As relatively less load is shared by the basal geogrid, it remains dormant leading to low performance improvement. On the other hand, in case of dense sand (ID = 80%) in the geocells, the infill sand has already reached the minimum level of compaction required to transmit pressure to the basal geogrid. On application of load, it will behave as a coherent composite structure which derives support of basal geogrid effectively. Typical surface deformation responses with different relative densities (ID) of sand, at a distance of x = D from the centre of footing, for geocell mattress with and without a geogrid layer at the base are presented in Fig. 6.40. Similar responses were observed with and without an additional layer of geogrid. However the magnitude of settlement in case of composite structure is much lesser than that with geocell mattress alone. This is attributed to the increased rigidity of the system due to the base geogrid as has been explained earlier.

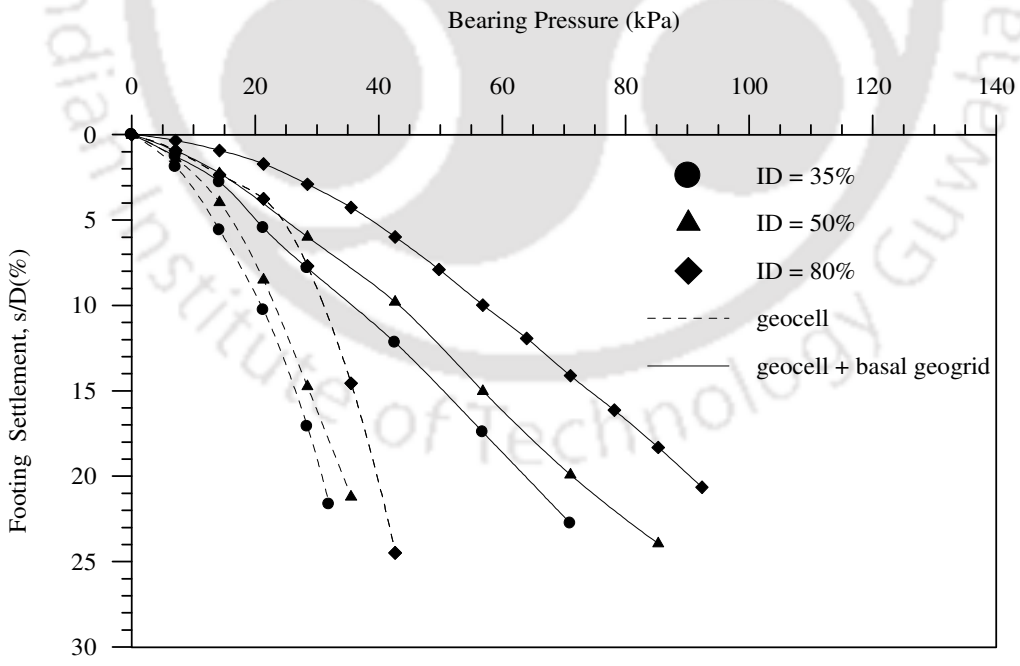

Fig. 6.28 Variation of bearing pressure with footing settlement for different relative densities (ID) of infill sand in geocells, with and without basal geogrid – Test Series D1, D2, D3, H1, H2, H3, h = 0.27D, d = 1.2D

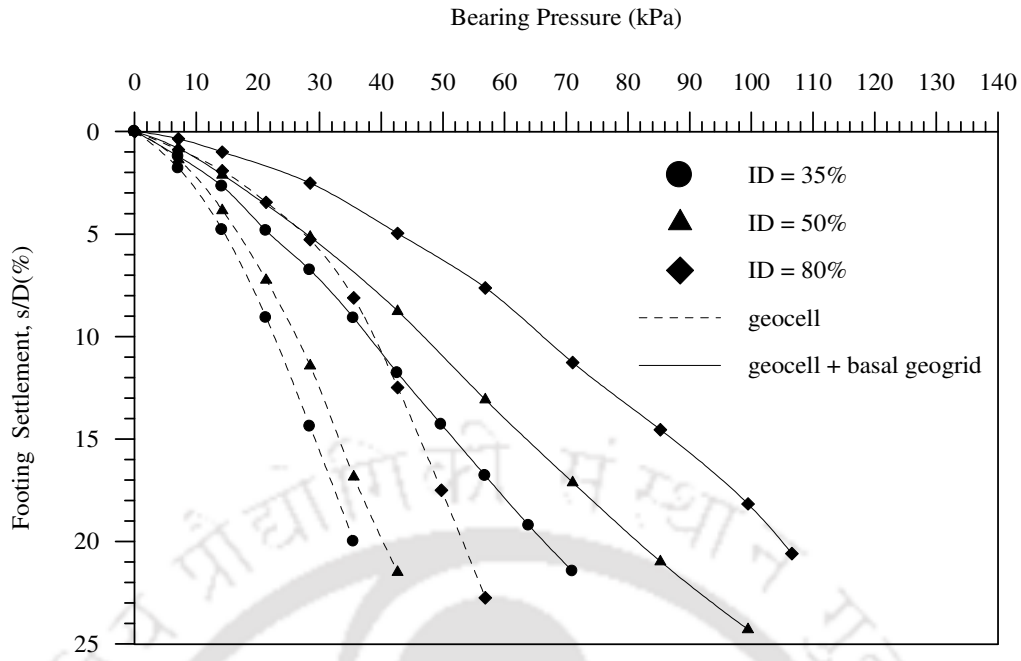

Fig. 6.29 Variation of bearing pressure with footing settlement for different relative densities (ID) of infill sand in geocells, with and without basal geogrid – Test Series D1, D2, D3, H1, H2, H3, h = 0.27D, d = 0.8D

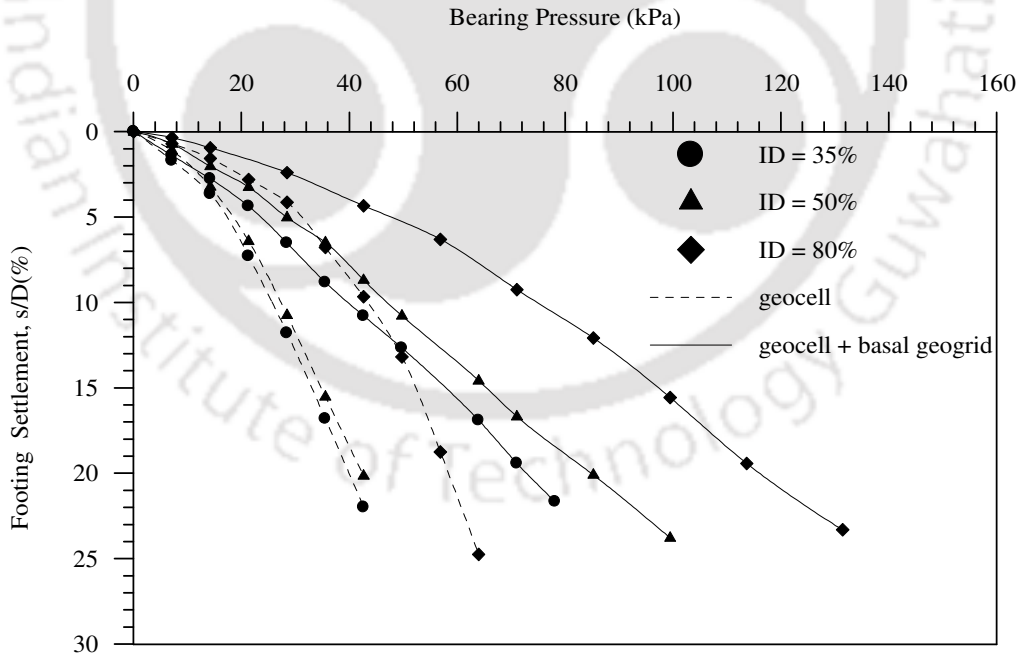

Fig. 6.30 Variation of bearing pressure with footing settlement for different relative densities (ID) of infill sand in geocells, with and without basal geogrid – Test Series D1, D2, D3, H1, H2, H3, h = 0.27D, d = 0.4D

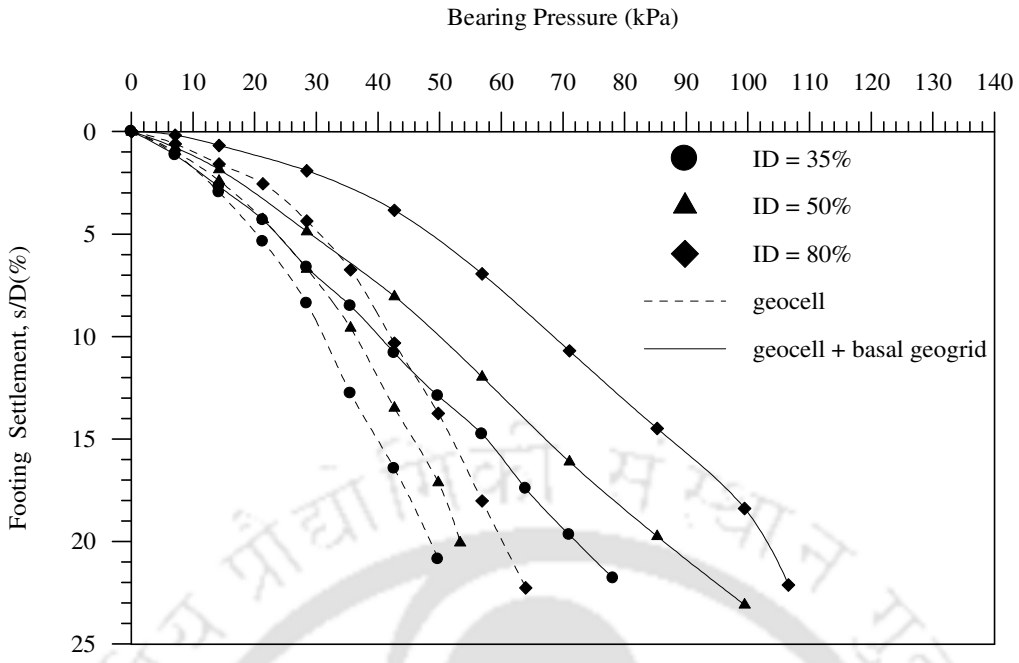

Fig. 6.31 Variation of bearing pressure with footing settlement for different relative densities (ID) of infill sand in geocells, with and without basal geogrid – Test Series E1, E2, E3, I1, I2, I3, h = 0.53D, d = 1.2D

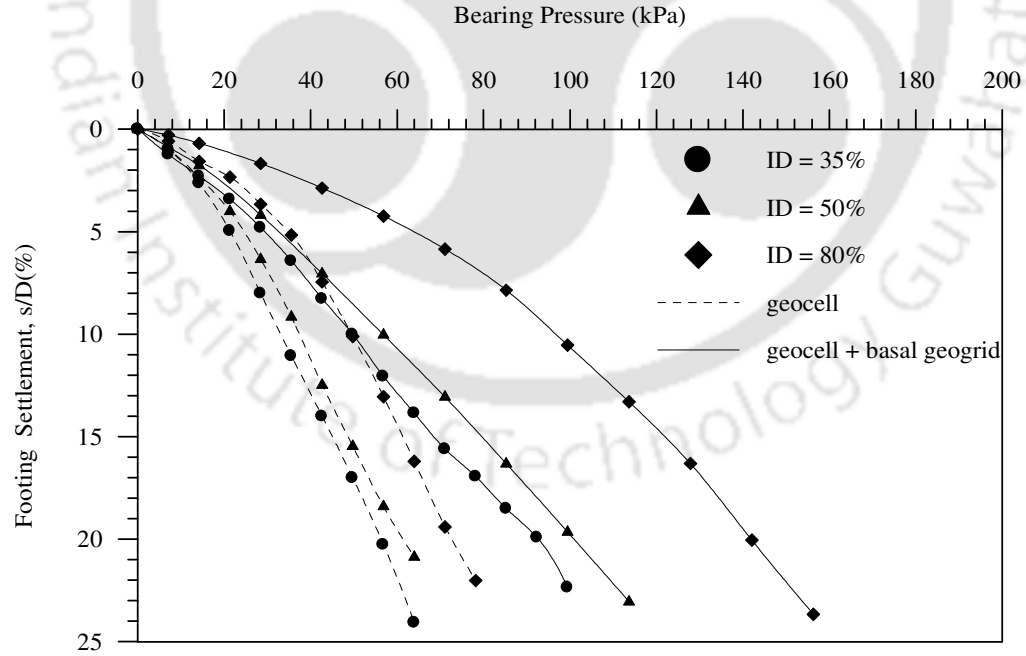

Fig. 6.32 Variation of bearing pressure with footing settlement for different relative densities (ID) of infill sand in geocells, with and without basal geogrid – Test Series E1, E2, E3, I1, I2, I3, h = 0.53D, d = 0.8D

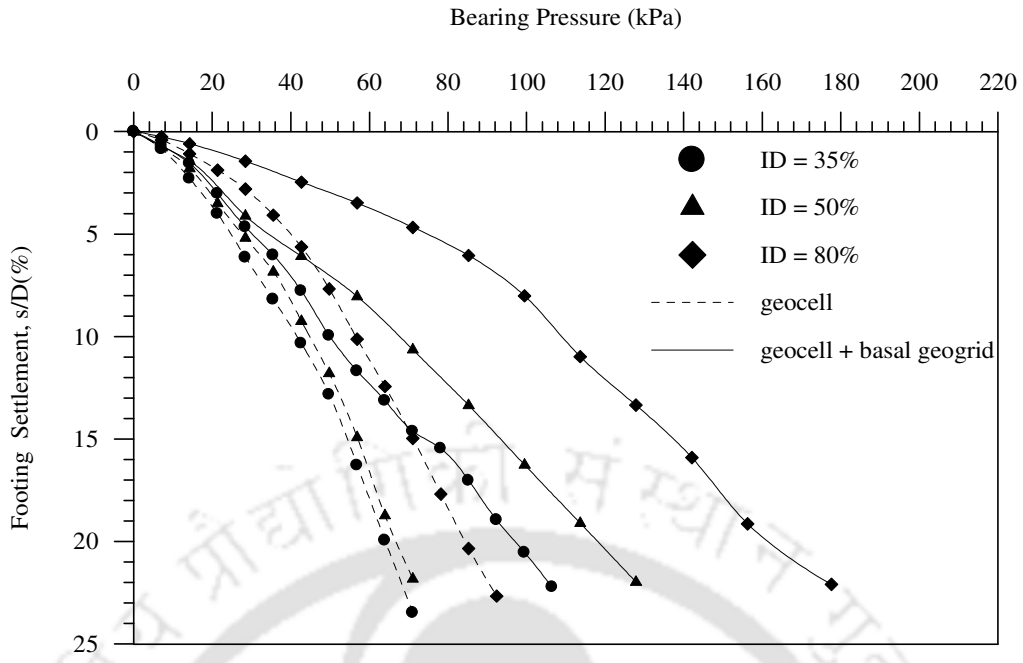

Fig. 6.33 Variation of bearing pressure with footing settlement for different relative densities (ID) of infill sand in geocells, with and without basal geogrid – Test Series E1, E2, E3, I1, I2, I3, h = 0.53D, d = 0.4D

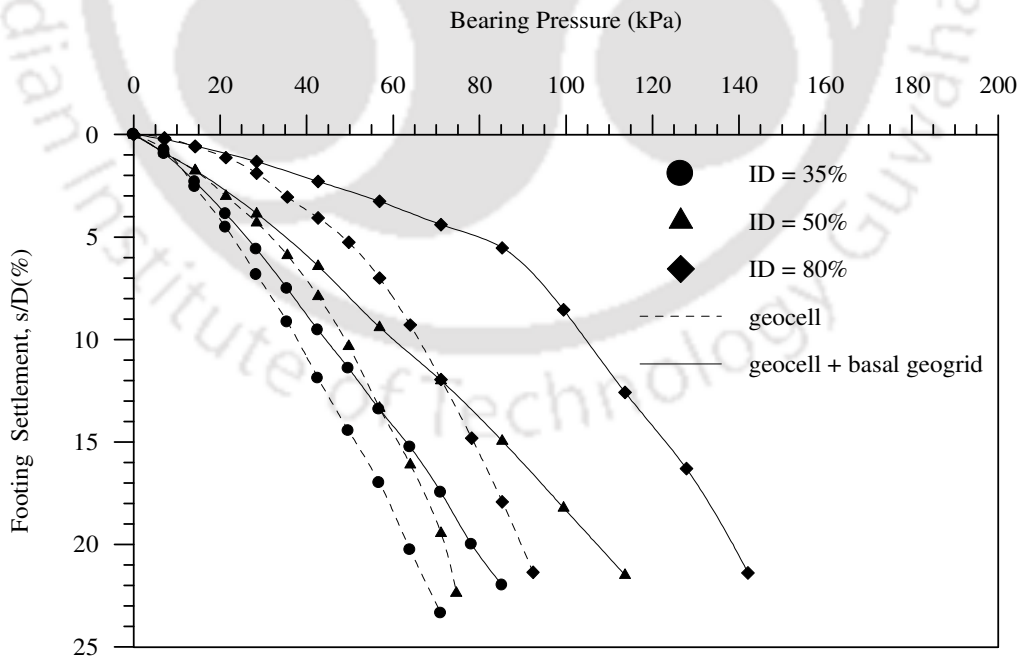

Fig. 6.34 Variation of bearing pressure with footing settlement for different relative densities (ID) of infill sand in geocells, with and without basal geogrid – Test Series F1, F2, F3, J1, J2, J3, h = 0.80D, d = 1.2D

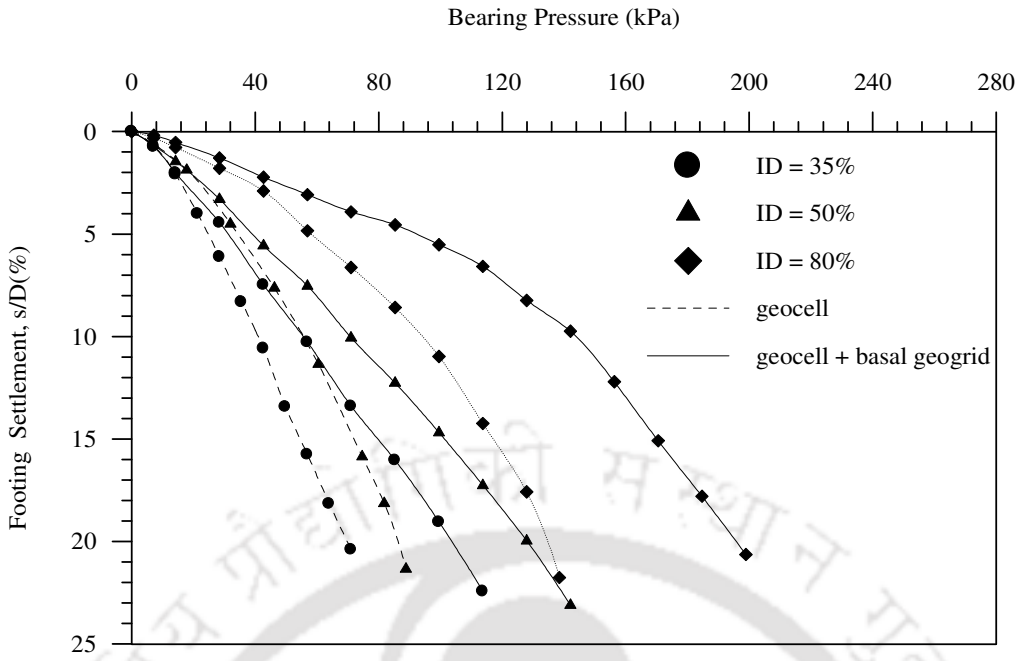

Fig. 6.35 Variation of bearing pressure with footing settlement for different relative densities (ID) of infill sand in geocells, with and without basal geogrid – Test Series F1, F2, F3, J1, J2, J3, h = 0.80D, d = 0.8D

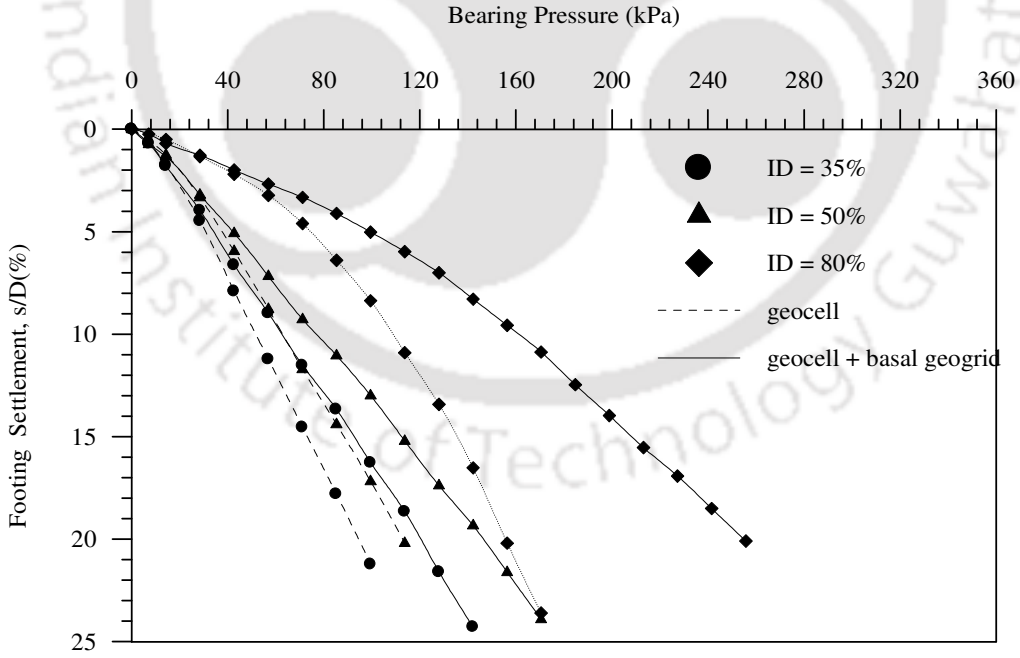

Fig. 6.36 Variation of bearing pressure with footing settlement for different relative densities (ID) of infill sand in geocells, with and without basal geogrid – Test Series F1, F2, F3, J1, J2, J3, h = 0.80D, d = 0.4D

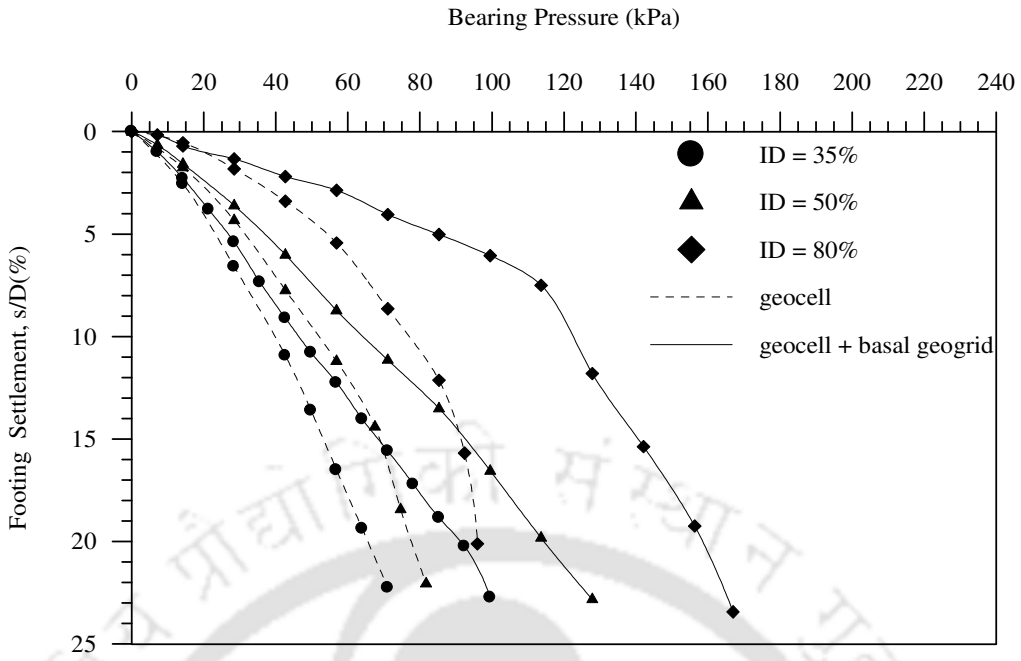

Fig. 6.37 Variation of bearing pressure with footing settlement for different relative densities (ID) of infill sand in geocells, with and without basal geogrid – Test Series G1, G2, G3, K1, K2, K3, h = 1.07D, d = 1.2D

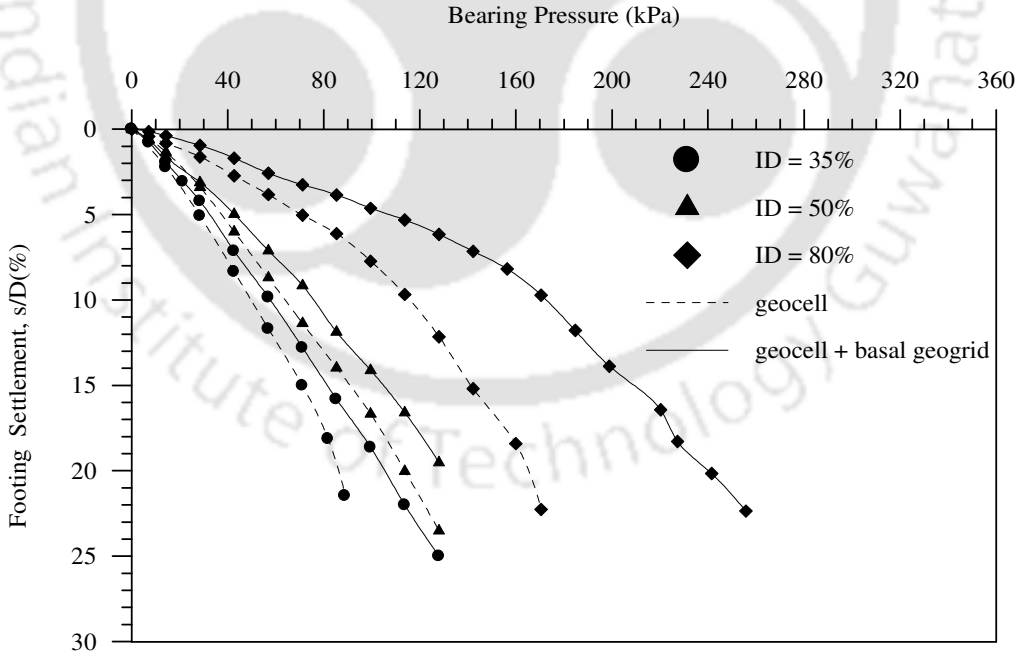

Fig. 6.38 Variation of bearing pressure with footing settlement for different relative densities (ID) of infill sand in geocells, with and without basal geogrid – Test Series G1, G2, G3, K1, K2, K3, h = 1.07D, d = 0.8D

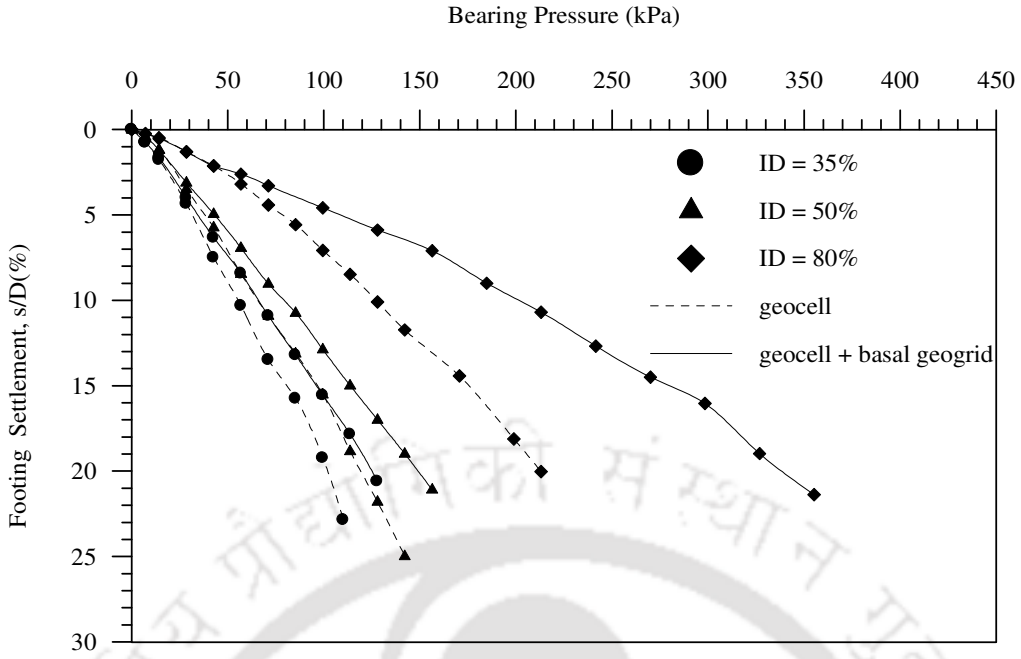

Fig. 6.39 Variation of bearing pressure with footing settlement for different relative densities (ID) of infill sand in geocells, with and without basal geogrid – Test Series G1, G2, G3, K1, K2, K3, h = 1.07D, d = 0.4D

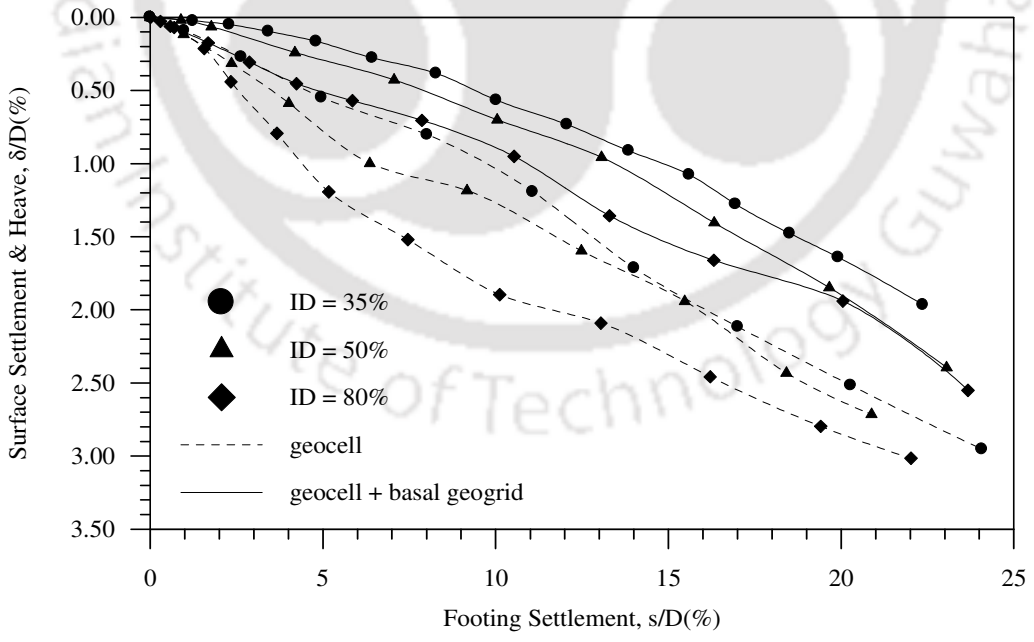

Fig. 6.40 Variation of average surface deformation with footing settlement at a distance of x = D from the centre of footing, for different relative densities (ID) of infill sand in the geocells, with and without basal geogrid – Test Series E1, E2, E3, I1, I2, I3, h = 0.53D, d = 0.8D

Table 6.7 Summary of results in terms of bearing capacity improvement factor (IF_{bg}) showing the influence of relative density (ID) of infill sand at h = 0.27D, Test Series H1 to H3

Variable Parameter		Bearing capacity improvement factor (IF_{bg})				
		(s/D) 3%	(s/D) 5%	(s/D) 10%	(s/D) 15%	(s/D) 20%
(d/D)	(ID) %					
1.2	35	1.58	1.52	1.71	1.88	2.07
	50	1.44	1.53	1.86	1.98	2.09
	80	**1.59**	**1.60**	**1.86**	**2.07**	**2.26**
0.8	35	1.49	1.50	1.68	1.76	1.87
	50	1.54	**1.65**	**1.79**	1.91	2.01
	80	**1.63**	1.56	1.71	**1.91**	**2.01**
0.4	35	1.25	1.37	1.53	1.75	1.82
	50	1.47	1.53	1.72	1.86	2.00
	80	**1.47**	**1.53**	**1.72**	**1.86**	**2.00**

Table 6.8 Summary of results in terms of bearing capacity improvement factor (IF_{bg}) showing the influence of relative density (ID) of infill sand at h = 0.53D, Test Series I1 to I3

Variable Parameter		Bearing capacity improvement factor (IF_{bg})				
		(s/D) 3%	(s/D) 5%	(s/D) 10%	(s/D) 15%	(s/D) 20%
(d/D)	(ID) %					
1.2	35	1.09	1.15	1.29	1.44	1.49
	50	1.19	1.25	1.37	1.47	1.62
	80	**1.60**	**1.59**	**1.63**	**1.68**	**1.71**
0.8	35	1.21	1.37	1.51	1.52	1.65
	50	1.28	1.33	1.51	1.64	1.65
	80	**1.78**	**1.83**	**1.96**	**1.99**	**1.96**
0.4	35	1.23	1.22	1.20	1.36	1.51
	50	1.17	1.24	1.51	1.64	1.77
	80	**1.70**	**1.87**	**1.93**	**1.93**	**1.91**

Table 6.9 Summary of results in terms of bearing capacity improvement factor (IF_{bg}) showing the influence of relative density (ID) of infill sand at h = 0.80D, Test Series J1 to J3

Variable Parameter		Bearing capacity improvement factor (IF_{bg})				
		(s/D) 3%	(s/D) 5%	(s/D) 10%	(s/D) 15%	(s/D) 20%
(d/D)	(ID) %					
1.2	35	1.10	1.15	1.17	1.23	1.23
	50	1.08	1.12	1.25	1.40	1.49
	80	**1.48**	**1.65**	**1.58**	**1.57**	**1.55**
0.8	35	1.14	1.25	1.36	**1.46**	**1.48**
	50	1.08	1.13	1.25	1.40	1.49
	80	**1.28**	**1.59**	**1.53**	1.45	1.45
0.4	35	1.06	1.11	1.21	1.27	1.27
	50	1.03	1.12	1.22	1.27	1.30
	80	**1.18**	**1.33**	**1.48**	**1.54**	**1.64**

Table 6.10 Summary of results in terms of bearing capacity improvement factor (IF_{bg}) showing the influence of relative density (ID) of infill sand at h = 1.07D, Test Series K1 to K3

Variable Parameter		Bearing capacity improvement factor (IF_{bg})				
		(s/D) 3%	(s/D) 5%	(s/D) 10%	(s/D) 15%	(s/D) 20%
(d/D)	(ID) %					
1.2	35	1.09	1.16	1.16	1.29	1.39
	50	1.13	1.17	1.23	1.34	1.47
	80	**1.50**	**1.57**	**1.59**	**1.54**	**1.65**
0.8	35	1.14	1.16	1.16	1.15	1.22
	50	1.07	1.15	1.19	1.15	1.13
	80	**1.41**	**1.52**	**1.49**	**1.48**	**1.46**
0.4	35	1.06	1.09	1.19	1.19	1.23
	50	1.06	1.13	1.20	1.17	1.25
	80	**1.19**	**1.39**	**1.59**	**1.60**	**1.59**

Based on the results obtained from the present investigation, it can be said that the inclusion of an additional layer of geogrid below the geocell mattress further enhances the load carrying capacity of the foundation bed. The effect of basal geogrid inclusion is found to be more pronounced for geocells with larger pocket sizes. The trend remains the same, irrespective of the height of the geocell mattress and relative density of the infill soil. The beneficial effect of the base geogrid layer, however, decreases with the increase in the height of the geocell mattress. Irrespective of the pocket size of geocells and height of the geocell mattress, a higher benefit from basal geogrid is derived when the geocells are filled with dense sand.

Indian Institute of Technology Guwahati

CHAPTER 7

REGRESSION MODEL AND DIMENSIONAL ANALYSIS

7.1 REGRESSION ANALYSIS

Regression analysis is a statistical tool for the investigation of relationship between dependent variable and independent variables. The influences of various parameters like depth of placement (u), pocket size (d), height (h), friction angle of sand (ϕ) and soil-geogrid interfacial friction angle (δ_s), on the bearing capacity of the foundation bed have already been established in the previous chapters. In this section, an attempt is made to develop a relationship to estimate the bearing capacity as a function of these influencing parameters. A multiple regression approach is chosen to develop a model on the basis of the experimental data, wherein, the bearing pressure is taken as the dependent (response) variable, while the rest of the parameters are considered as independent (predictor) variables.

7.1.1 Multiple regression analysis on geocell reinforced clay subgrade

The data for the regression analysis is obtained from the extensive model tests performed on geocell reinforced clay subgrade, the details of which have already described in the previous chapters. A total of 441 data points are considered for the analysis, out of which 117 number of data points are kept aside for the validation of the model. Through a series of trial and error, the following functional form (Eq. 7.1) is fitted to the data. Multiple regression analysis using the least square method is conducted and the obtained result is presented in Eq. 7.2.

$$q_{gc} = c_0 q_s^{\,c_1} * \left(\frac{s}{D}\right)^{c_2} * f^{c_3} * \left(\frac{h}{D}\right)^{c_4} * \left(\frac{d}{D}\right)^{c_5} * c_6^{\left(\frac{u}{D}\right)} \qquad (7.1)$$

Where, q_{gc} = bearing capacity of geocell reinforced bed (kN/m^2)

q_s = bearing capacity of unreinforced bed (kN/m^2)

f = friction angle ratio (δ_s /ϕ) i.e. ratio of soil-geogrid interfacial friction angle to peak angle of shear resistance of sand.

c_0, c_1, c_2, c_3, c_4, c_5 and c_6 = regression coefficients.

h = height of geocell mattress

d = pocket size

D = diameter of the footing

u = depth of placement of the geocell mattress from the base of the footing

$$q_{gc} = 2.514 q_s^{1.077} * \left(\frac{s}{D}\right)^{0.041} * f^{2.372} * \left(\frac{h}{D}\right)^{0.051} * \left(\frac{d}{D}\right)^{-0.222} * 0.790^{\left(\frac{u}{D}\right)} \quad (7.2)$$

Statistics for goodness of fit such as the multiple coefficient of determination R^2, adjusted value of R^2 (i.e. R_a^2) and standard error (E_s) are determined to check how well the model fits the experimental data. The model yielding the largest value of R^2, R_a^2 and the smallest value of E_s is considered the best fit model. The values of R^2, R_a^2 and E_s for the model, obtained from the regression analysis are given in Table 7.1. The proposed equation (Eq. 7.2) is validated by using the experimental data that were earlier not used for the regression analysis. Fig. 7.1 shows the comparison between the measured bearing capacity and estimated bearing capacity. It could be observed that there exists a good agreement (R^2 = 0.90) between the measured and estimated bearing capacity.

To determine the effectiveness of the entire model, significance tests of the overall model are performed. The overall significance of the model can be assessed by applying the F-test. The significance of individual regression coefficient in the multiple regression model

can be accessed through the t-test. The significance level α is set to be 0.05 in this study. The results of the Analysis of Variance (ANOVA) calculations are given in Table 7.2.

Table 7.1 Goodness of fit statistics for the non-linear model (geocell reinforced)

Regression Statistics	
Multiple R	0.9850
R Square	0.9703
Adjusted R Square	0.9697
Standard Error	0.0529
Observations	324

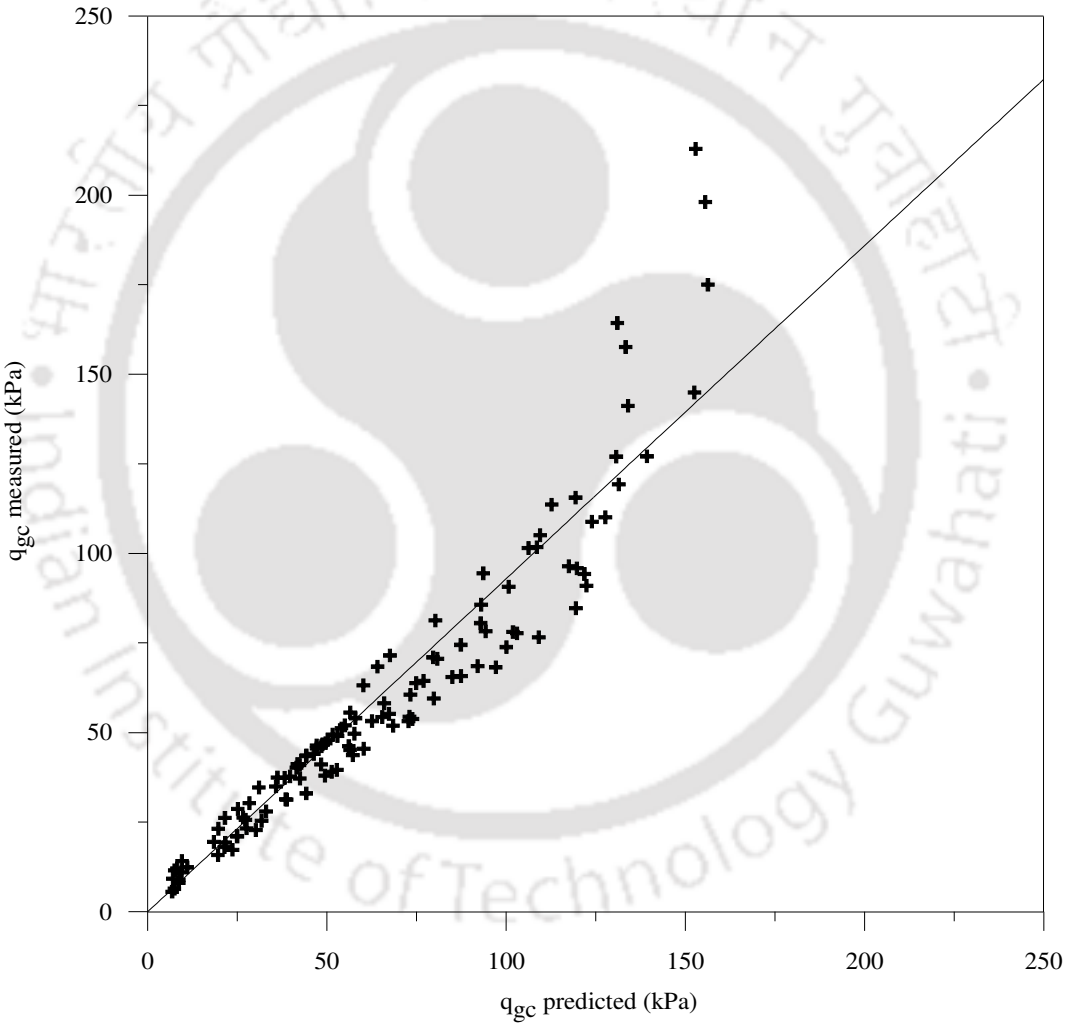

Fig. 7.1 Comparison between observed bearing capacity and estimated bearing capacity for geocell reinforced clay subgrade

Table 7.2 ANOVA table for the non-linear model (geocell reinforced)

	Degree of freedom (df)	Sum of squares	Mean Square	F	P-value
Regression	6	28.9760	4.8293	1726.6724	9.7647E-239
Residual	317	0.8866	0.0028		
Total	323	29.8627			

The null hypothesis for the F-test implies that none of the independent variables are related to the dependent variable. The alternate hypothesis suggests that atleast one of the independent variables is related to the dependent variable. From the F distribution table with $\alpha = 0.05$ and degrees of freedom, df = (6, 317), the critical values of F (i.e. F_{crt}) for the present study is found to be 2.0986. As the calculated value of F (i.e. $F_{cal} = 1726$; Table 7.2) is greater than F_{crt}, the null hypothesis is rejected, thus indicating that atleast one of the independent variables of Eq. 7.2 explains the variation of the dependent variable.

The summary of the t-values for various individual predictor parameters are given in Table 7.3. From the student's t-table, the critical value of t (i.e. t_{crt}) with $\alpha/2 = 0.025$ and df = 317, is found to be 1.959. The null hypothesis for t-test implies that the independent predictor variable (e.g. height, h) is not related to the dependent variable. The alternative hypothesis suggests that the individual predictor variable is related to the dependent variable. Similar hypothesis are assumed for all independent variables. From Table 7.2 it could be observed that the t values for all independent predictor variables lies in the range of:

$$(-)t_{crt} > t_{cal} > (+)t_{crt}$$

Hence the null hypothesis is rejected which means that all the independent variables are able to explain the variation in dependent variable. All of the above tests confirm that the proposed model is valid.

Table 7.3 Summary of t statistics for the non-linear model (geocell reinforced)

	Coefficients	Standard Error	t Stat	P-value
Intercept	0.4005	0.1950	2.0534	0.040850006
X Variable 1 (q_s)	1.0769	0.0342	31.5308	9.5177E-100
X Variable 2 (s)	0.0414	0.0202	2.04748	0.041434572
X Variable 3 (f)	2.3717	1.1723	2.0232	0.043895732
X Variable 4 (h)	0.0505	0.0225	2.2507	0.025091517
X Variable 5 (d)	-0.2224	0.0141	-15.8028	6.84147E-42
X Variable 6 (u)	-0.1027	0.0522	-1.9666	0.050103218

7.1.2 Multiple regression analysis on geocell-geogrid reinforced clay subgrade

Multiple regression analysis was carried out on the experimental data obtained for the composite geocell-geogrid clay subgrade and the result thus obtained is presented in Eq. 7.3. A total of 324 data points were evaluated out of which 231 was used for the regression analysis while the rest were used for validating the model.

$$q_{bg} = 16.6 q_{gc}^{0.907} * \left(\frac{s}{D}\right)^{0.160} * (0.038)^{f} * 1.052^{\left(\frac{d}{D}\right)} * 0.647^{\left(\frac{h}{D}\right)} \quad (7.3)$$

Where, q_{bg} = bearing capacity of geocell-geogrid reinforced bed (kN/m^2).

Statistics for goodness of fit (R^2, R_a^2 and E_s) presented in Table 7.4 suggest that the proposed model fits the observed data well. Fig. 7.2 indicates that a good correlation (R^2 = 0.95) exists between the measured bearing capacity and the bearing capacity estimated from the proposed equation.

Table 7.4 Goodness of fit statistics for the non-linear model (geocell-geogrid reinforced)

Regression Statistics	
Multiple R	0.9903
R Square	0.9808
Adjusted R Square	0.9803
Standard Error	0.0474
Observations	231

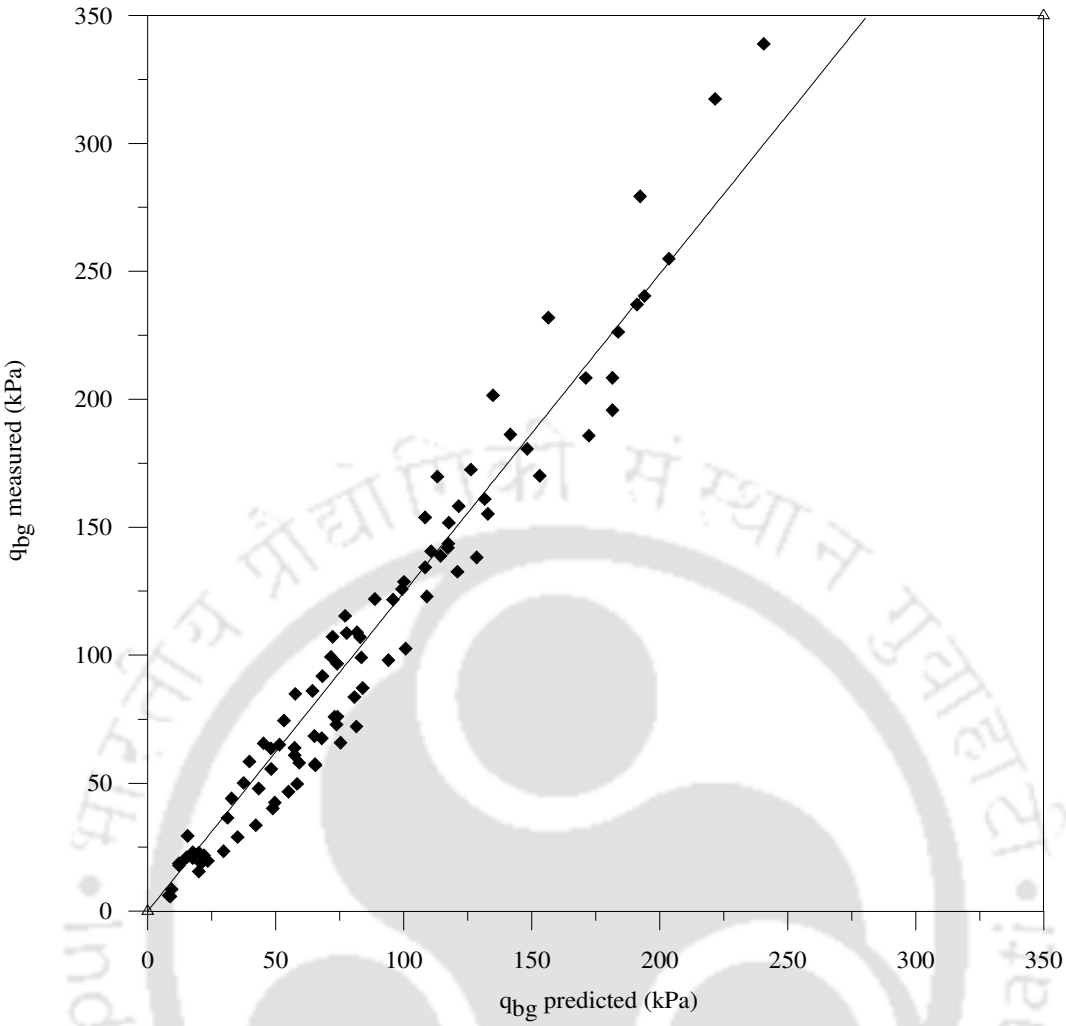

Fig. 7.2 Comparison between observed bearing capacity and estimated bearing capacity for geocell-geogrid reinforced clay subgrade

The significance tests (F-test and t-test) were carried out and the ANOVA results are presented in Tables 7.5 and 7.6 respectively. The significance level α is set to be 0.05. From the F distribution table with α = 0.05 and df = (5, 225) the critical values of F for the present study is found to be 2.2141. As $F_{cal} > F_{crt}$, the null hypothesis is rejected. From the student's t-table, with α/2 = 0.025 and df = 225, the critical value of t is found to be 1.960. As the individual t-values of independent variables satisfy the criteria i.e. $(-)t_{crt} > t_{cal} > (+)t_{crt}$, the null hypothesis is rejected in favour of the alternative hypothesis. All of the above analysis indicates that the proposed model is valid.

Table 7.5 ANOVA table for the non-linear model (geocell-geogrid reinforced)

	Degree of freedom (df)	Sum of squares	Mean Square	F	P-value
Regression	5	25.7525	5.1505	2293.0757	8.6608E-191
Residual	225	0.5054	0.0022		
Total	230	26.2579			

Table 7.6 Summary of t statistics for the non-linear model (geocell-geogrid reinforced)

	Coefficients	Standard Error	t Stat	P-value
Intercept	1.2222	0.4464	2.7378	0.006679822
X Variable 1 (q_{gc})	0.9073	0.0335	27.0889	9.08993E-73
X Variable 2 (s)	0.1599	0.0250	6.3986	8.98922E-10
X Variable 3 (f)	-1.4182	0.6432	-2.2048	0.028482583
X Variable 4 (d)	0.0218	0.0106	2.0502	0.041501812
X Variable 5 (h)	-0.1894	0.0158	-11.9554	7.93614E-26

7.2 DIMENSIONAL ANALYSIS

In an attempt to transfer the results of the model tests to the actual field conditions, dimensional analysis has been carried out. In the present study, the important parameters influencing the performance of the geocell reinforced foundation bed can be assumed to be: D, s, u, d, h b, S_t, G, γ, c_u, ϕ, δ_s, q_s, q_{gc}; where b is the width of geocell mattress, S_t is the stiffness of the reinforcement, G is the shear modulus of soil, γ is the unit weight of soil. The other symbols have already been defined. The function (f) that governs the system can be written as

$$f(D, s, u, d, h\ b, S_t, G, \gamma, c_u, \phi, \delta_s, q_s, q_{gc}) = 0 \quad (7.4)$$

The fourteen parameters in Eq. 7.4 have two fundamental dimensions (i.e. length and force). As per the theory of Langhaar (1951) this system can be studied by any complete

set of twelve (i.e. 14 – 2 = 12) independent parameters (i.e. π_1, π_1 π_1,….. π_{12}, Buckingham 1914). Hence Eq. 7.4 can be reduced to the following form

$g(\pi_1, \pi_1\ \pi_1, \ldots..\ \pi_{12}) =$

$$= g\left[\left(\frac{u}{D}\right),\left(\frac{d}{D}\right),\left(\frac{h}{D}\right),\left(\frac{h}{d}\right),\left(\frac{b}{D}\right),\left(\frac{s}{D}\right),\left(\frac{S_t\gamma}{G^2}\right),\left(\frac{G}{D\gamma}\right),\left(\frac{c_u}{D\gamma}\right),\left(\frac{q_{gc}}{q_s}\right),\phi,\delta_s\right] = 0 \qquad (7.5)$$

For a prototype footing (p) with diameter N times higher than the model (m)

$$\frac{D_p}{D_m} = N \qquad (7.6)$$

To achieve similarity between a model and prototype, all the corresponding π terms must be equated between the model and the prototype.

$$(\pi_8)_p = (\pi_8)_m \qquad (7.7)$$

$$\frac{G_p}{D_p\gamma_p} = \frac{G_m}{D_m\gamma_m} \qquad (7.8)$$

In the case of soils in the model and prototype to be of the same density Eq. 7.8 reduces to

$$\frac{G_p}{G_m} = \frac{D_p}{D_m} = N \qquad (7.9)$$

$$\text{Also, } (\pi_7)_p = (\pi_7)_m \qquad (7.10)$$

$$\frac{S_{tp}\gamma_p}{G_p^2} = \frac{S_{tm}\gamma_m}{G_m^2} \qquad (7.11)$$

$$\frac{S_{tp}}{S_{tm}} = \frac{G_p^2}{G_m^2} = N^2 \qquad (7.12)$$

The above analysis shows that while the geometric parameters of the geocell reinforcement have a linear variation, the strength varies in second order. Hence, for findings of the present study to be applicable in practice, the strength of the reinforcement in the prototype reinforced soil foundation bed should be N^2 times the strength of the reinforcement used in the model test, where N is the model scale. In the present model tests the strength and stiffness of the geocell joint is much lower compared to that of the geocell wall material (geogrid). Therefore the performance improvement due to geocell reinforcement will be proportionate to the strength and stiffness of the geocell joints rather than the strength of the geogrid used for making the geocells. Hence, for the results from the present study to be applicable in practice, the prototype geocell (both joint and geogrid) should have a minimum strength and stiffness of N^2 times the strength and stiffness of the geocell joint studied in the present model tests.

भारतीय प्रौद्योगिकी संस्थान गुवाहाटी
Indian Institute of Technology Guwahati

CHAPTER 8

SUMMARY AND CONCLUSIONS

8.1 SUMMARY

Construction of structures on soft soil often necessitates the utilization of ground improvement techniques. Among others, soil reinforcing techniques have proved to be a versatile, easy and cost effective alternative of improving the bearing capacity of soft soils. The conventional soil reinforcement techniques consisted of placing reinforcing elements in the form of grids, sheets and strips, horizontally in the ground. The latest advancement of this technique involves the use of geocell mattress. The geocell mattress consists of a series of interlocking cells constructed from polymer grid reinforcement, which contains and confines the soil within its pockets. The details of the construction of geocell mattress have been discussed in Chapter 1.

Although the benefits of using geocells have been reported by various investigators (Chapter 2), the influence of various key parameters on the overall performance and behaviour of geocell-sand mattress reinforced clay subgrade system are not well understood. Hence a detailed parametric study through a series of model load tests was conducted with the objective to develop an understanding of the behaviour of the soft clay supported geocell-sand mattress system under circular loading.

The model load tests have been carried out in a test bed-cum-loading frame assembly in the laboratory. The test pit was 2000 mm long, 2000 mm wide and 1500 mm deep. The model footing used was a rigid mild steel plate of 300 mm diameter and a thickness of 15 mm. For the preparation of the soft clay subgrade, the soil was placed in the tank, leveled out and compacted in layers till the desired depth in the tank was reached. The geocell

mattress was then placed on the soft clay subgrade and their pockets were filled with sand by raining technique.

A series of load tests were conducted on clay subgrade alone and with sand cushion of different thickness and relative density overlying the clay subgrade. Twenty-four series of tests were carried out by varying the depth of placement of the geocell mattress from the base of the footing (u), patterns of formation of the geocells, pocket size of geocells (d), height of the geocell mattress (h) and relative density of the infill sand (ID). Another twelve series of tests were conducted to find the influence of an additional planar geogrid layer below the geocell mattress. The parameters varied in these tests include pocket size of geocells, height of the geocell mattress and relative density of the infill sand. The influences of different parameters on the pressure-settlement and surface deformation behaviour of the foundation system were evaluated. The magnitude of the applied load was measured by a proving ring. The footing settlement and the surface deformations were recorded through the dial gauges. The details of the materials used, experimental setup, test programme and test procedure are discussed at length in Chapter 3.

In Chapter 4, the results of the tests done on clay subgrade alone and on sand layer overlying clay subgrade are presented and discussed. The load carrying capacity is found to increase with increase in relative density and thickness of the sand layer. The results obtained are used to compare and quantify the benefit of using geocell reinforcement.

The results of model load tests on geocell reinforced sand beds supported by soft clay subgrade are presented and discussed in Chapter 5. The parameters such as depth of placement of geocell mattress, pattern of formation, pocket size and height of geocells; relative density of infill sand in the geocells are found to have an influence on the performance of the reinforced structure. Based on the test results, the critical values of the

geocell-soil configuration giving the maximum bearing capacity improvement have been found out. With the provision of geocell mattress, the heaving on the surface was found to reduce and the fill surface settled instead. This indicates that the geocell-soil structure behaves as a composite unit that deflects like a centrally loaded slab under the footing, transmitting the pressure over a wider area giving rise to a much wider settlement zone.

The influence of the planar reinforcement on the performance of the geocell-geogrid composite foundation bed has been brought out in Chapter 6. The test results indicate that the bearing pressure as well as the stiffness of the geocell-geogrid composite system further increases with the provision of an additional layer of geogrid below the geocell mattress. Parameters such as pocket size, height of the geocell mattress and relative density of infill sand are found to have an influence on the load-settlement and surface deformation behaviour of the composite foundation bed. The fill surface was found to undergo less settlement with the provision of the basal geogrid layer.

Chapter 7 describes the regression analysis and dimensional analysis carried out on the experimental data obtained from the model load tests. Statistical analysis was conducted to develop an empirical equation to estimate the bearing capacity of the reinforced foundation as a function of various test parameters such as footing settlement (s), depth of placement (u), pocket size of geocells (d), height of the geocell mattress (h), friction angle of soil (ϕ) and soil-geogrid interfacial friction angle (δ_s). A multiple regression approach was adopted to develop the models wherein the bearing pressure of reinforced bed (q_{gc}/q_{bg}) is taken as the dependent variable while the rest of the parameters are considered as independent variables. In an attempt to use the results of the model study in actual field conditions, dimensional analysis using the Buckingham Pi theorem was carried out.

8.2 CONCLUSIONS

Based on the results obtained from the present investigation, the following major conclusions can be made on the behaviour of circular footing on geocell-reinforced soft clay subgrade.

1. The geocell reinforced foundation bed exhibits a much stronger and stiffer behaviour compared to the unreinforced cases. The pressure-settlement response of the clay subgrade shows large settlement with small change in footing pressure, a typical punching failure. But with the provision of geocell-sand mattress the pressure settlement response exhibits a nearly linear trend till large pressure and settlement as high as 20% of footing diameter, indicating that failure hasn't taken place.

2. The critical depth of placement (u_{cr}) of the geocell mattress giving maximum performance improvement is about 0.1D from the base of the footing. The pattern of formation, pocket size and height of the geocell mattress has little influence on the critical depth of placement of the geocell mattress.

3. The chevron pattern of formation gives a higher performance improvement as compared to the diamond pattern. This is true irrespective of the relative density of the infill soil, pocket size and height of the geocell mattress.

4. In general, the performance improvement in bearing pressure increases with reduction in the pocket size (d) of the geocells. However, when the footing size is larger than the geocell pocket size, the performance improvement is substantially high. Hence, for all practical applications, the geocell reinforcement and footing should be designed such that the footing completely covers atleast one geocell pocket opening.

5. The critical height (h_{cr}) of the geocell reinforcement giving maximum performance improvement depends on the relative density (ID) of the infill sand. It is about 0.8D

for low to medium dense sand and 0.53D for dense sand. However, for a given relative density of infill sand, the critical height (h_{cr}) is independent of the pocket size (d) of the geocells.

6. The relative density (ID) of infill sand at which the geocell reinforcement provides maximum performance improvement is dependent on the pocket size and height of the geocell mattress. For shallow height, the maximum benefit from the geocell reinforcement is obtained when the geocells are filled with dense sand. However, with geocells of larger pocket size and higher height, better performance improvement is observed with medium dense infill sand. While with smaller pocket size a dense soil matrix derives higher reinforcing efficacy from the geocells. It is however to be noted that the overall bearing capacity continues to increase with the increase in the relative density of the soil. Hence, in general, it is advantageous to fill the geocells with sand compacted to the densest state.
7. Contrary to the dilation induced load transfer mechanism observed in case of homogeneous sand bed, it is the anchorage effect which predominantly governs the load transfer mechanism in the present case with soft clay subgrade.
8. The inclusion of an additional layer of geogrid below the geocell mattress further enhances the load carrying capacity of the foundation bed.
9. The effect of basal geogrid inclusion is found to be more pronounced for geocells with larger pocket sizes. The trend remains the same, irrespective of the height of the geocell mattress and relative density of the infill soil.
10. The beneficial effect of the base geogrid layer decreases with the increase in the height of the geocell mattress.

11. Irrespective of the pocket size of geocells and height of the geocell mattress, a higher benefit from basal geogrid is derived when the geocells are filled with dense sand.

12. The quantification of the performance improvement indicates that with the provision of geocell reinforcement and basal geogrid in the granular soil layer overlying the soft clay subgrade, a four-fold improvement in performance ($IF_{gc} \times IF_{bg} = 2.68 \times 1.59 = 4.26$) could be obtained. When coupled with the improvement due to sand layer ($IF_s = 3.19$), the overall load carrying capacity of the footing increases by about fourteen times (i.e. $4.26 \times 3.19 = 13.59$), compared to the case of clay subgrade alone.

13. The performance of the geocell mattress of smaller height coupled with basal geogrid is comparable to that of geocell mattresses of higher heights. For example the performance improvement due to composite geocell-geogrid mattress of height 0.53D is equivalent to that of geocell mattress of height 0.8D. Hence with basal geogrid the cost of construction is expected to further reduce.

14. The proposed regression models are reasonably good in predicting the bearing capacity of the reinforced foundation bed under circular loading.

15. From dimensional analysis, it is observed that while the geometric parameters (depth of placement, pocket size, height, width) of the geocell mattress have a linear variation, the strength (geocell reinforcement and bodkin joints) varies in second order. Therefore, for the present test data to be valid in prototype case, the strength of geocells should be N^2 times the strength of geocells used in the present tests (i.e. 4.75 kN/m).

8.3 SCOPE FOR FURTHER RESEARCH

The scope of further investigation is suggested as below.

- In the present study, only one type of subgrade having a shear strength of 6kPa was used. Subgrade of varying strengths needs to be investigated so that a generalised model can be developed to predict the bearing capacity of a geocell reinforced subgrade.
- Behaviour of geocell reinforced foundation with different shape of the footing needs to be carried out in order to investigate the effect of shape of the footing on the performance of a geocell reinforced subgrade.
- An attempt can be made to develop a numerical model to simulate the behaviour of the geocell reinforced soft clay subgrade for various configurations of the geocell-soil system.
- Finite Element Modeling can be carried out to determine the equivalent elastic modulus of the composite layer (geocell mattress with sand) and clay subgrade of a two layer system or by combining the reinforced soil with the unreinforced soil as one layer and determining the equivalent elastic modulus of the system.

REFERENCES

1. **Adams, M.T.,** and **Collin, J.G.** (1997). "Large model spread footing load tests on geosynthetic reinforced soil foundations." *Journal of Geotechnical and Geoenvironmental Engineering*, ASCE, **123(1)**, 66-72.

2. **Akinmusuru, J.O.,** and **Akinbolade, J.A.** (1981). "Stability of loaded footing on reinforced soil." *Journal of Geotechnical Engineering*, ASCE, **107(6)**, 819-827.

3. **Alawaji, H.A.** (2001). "Settlement and bearing capacity of geogrid-reinforced sand over collapsible soil." *Geotextiles and Geomembranes*, **19(2)**, 75-88.

4. **ASTM standard D 0854**, 2006. Standard test methods for specific gravity of soil solids by water pycnometer. ASTM International, West Conshohocken, PA, 2006, Vol. 04.09.

5. **ASTM standard D2487**, 2006(e1). Standard practice for classification of soils for engineering purposes (Unified Soil Classification System). ASTM International, West Conshohocken, PA, 2006, Vol. 04.08.

6. **ASTM standard D2850,** 2003 (2007). Standard test method for unconsolidated-undrained triaxial compression test on cohesive soils. ASTM International, West Conshohocken, PA, 2007, Vol. 04.08.

7. **ASTM standard D4221**, 1999 (2005). Standard test method for dispersive characteristics of clay soil by double hydrometer. ASTM International, West Conshohocken, PA, 2005, Vol. 04.08.

8. **ASTM standard D4253**, 2000 (2006). Standard test methods for maximum index density and unit weight of soils and calculation of relative density. ASTM International, West Conshohocken, PA, 2006, Vol. 04.08.

9. **ASTM standard D4254,** 2000 (2006). Standard test methods for minimum index density and unit weight of soils and calculation of relative density. ASTM International, West Conshohocken, PA, 2006, Vol. 04.08.

10. **ASTM standard D4318,** 2005. Standard Test Methods for Liquid Limit, Plastic Limit, and Plasticity Index of Soil. ASTM International, West Conshohocken, PA, 2005, Vol. 04.08.

11. **ASTM standard D5311**, 1992 (2004e1). Standard test method for load controlled cyclic triaxial strength of soil. ASTM International, West Conshohocken, PA, 2004, Vol. 04.08.

12. **ASTM standard D4884**, 2009. Standard test method for strength of sewn or thermally bonded seams of geotextiles. ASTM International, West Conshohocken, PA, 2009, Vol. 04.13.

13. **ASTM standard D6528**, 2007. Standard test method for consolidated undrained direct simple shear testing of cohesive soils. ASTM International, West Conshohocken, PA, 2007, Vol. 04.09.

14. **ASTM standard D6637**, 2001 (2009). Standard test method for determining tensile properties of geogrids by the single or multi-rib tensile test method. ASTM International, West Conshohocken, PA, 2009, Vol. 04.13.

15. **ASTM standard D6706**, 2001 (2007). Standard test method for measuring geosynthetic pullout resistance in soil. ASTM International, West Conshohocken, PA, 2007, Vol. 04.13.

16. **ASTM standard D6913**, 2004(e2). Standard test methods for particle-size distribution (gradation) of soils using sieve analysis. ASTM International, West Conshohocken, PA, 2004, Vol. 04.09.

17. **Bathurst, R.J.,** and **Jarrett, P.M.** (1988). "Large scale model tests of geocomposite mattresses over peat subgrades." *Transportation Research Record*, Transportation Research Board, Washington, D.C, **1188,** 28-36.

18. **Bathurst, R.J.,** and **Karpurapu, R.** (1993). "Large-scale triaxial compression testing of geocell-reinforced granular soils." *Geotechnical Testing Journal*, **16(3)**, 296-303.

19. **Bathurst, R.J.,** and **Knight, M.A.** (1998). "Analysis of geocell reinforced-soil covers over large span conduits." Computers and Geotechnics, **22 (3/4),** 205-219.

20. **Binquet, J.,** and **Lee, K.L.** (1975). "Bearing capacity tests on reinforced earth slabs." *Journal of Geotechnical Engineering Division*, ASCE, **101(12)**, 1241-1255.

21. **Buckingham, E.** (1914). "On physically similar systems; illustrations of the use of dimensional equations." *Physics Review,* **4**, 345-376.

22. **Bush, D.I., Jenner, C.G.,** and **Bassett, R.H.** (1990). "The design and construction of geocell foundation mattress supporting embankments over soft ground." *Geotextiles and Geomembranes*, **9(1)**, 83-98.

23. **Carroll Jr, R.G.,** and **Curtis, V.C.** (1990). "Geogrid connections." *Geotextiles and Geomembranes*, **9(4-6)**, 515-530.

24. **Chummar, A.V.** (1972). "Bearing capacity theory from experimental results." *Journal of the Soil Mechanics and Foundations Division,* ASCE, **98(12)**, 1311-1324.

25. **Cowland, J.W.,** and **Wong, S.C.K.** (1993). "Performance of a road embankment on soft clay supported on a geocell mattress foundation." *Geotextiles and Geomembranes*, **12(8)**, 687-705.

26. **Das, B.M.,** and **Omar, M.T.** (1994). "The effects of foundation width on model tests for the bearing capacity of sand with geogrid reinforcement." *Geotechnical and Geological Engineering*, **12(3)**, 133-141.

27. **Das, B.M.,** and **Khing, K.H.** (1994). "Foundation on layered soil with geogrid reinforcement – effect of a void." *Geotextiles and Geomembranes*, **13(8)**, 545-553.

28. **Dash, S.K., Krishnaswamy, N.R.,** and **Rajagopal, K.** (2001a). "Bearing Capacity of Strip Footings Supported on Geocell-Reinforced Sand." *Geotextiles and Geomembranes*, **19(4)**, 235-256.

29. **Dash, S.K., Rajagopal, K.,** and **Krishnaswamy, N.R.** (2001b). "Strip footing on geocell reinforced sand beds with additional planar reinforcement." *Geotextiles and Geomembranes,* **19(8),** 529-538.

30. **Dash, S.K., Sireesh, S.,** and **Sitharam, T.G.** (2003a). "Model Studies on Circular Footing Supported on Geocell Reinforced Sand Underlain by Soft Clay." *Geotextiles and Geomembranes*, **21(4)**, 197-219.

31. **Dash, S.K., Sireesh, S.,** and **Sitharam, T.G.** (2003b). "Behaviour of Geocell Reinforced Sand Beds Under Circular Footing." *Ground Improvement*, **7(3)**, 111-115.

32. **Dash, S.K., Rajagopal, K.,** and **Krishnaswamy, N.R.** (2004). "Performance of different geosynthetic reinforcement materials in sand foundations." *Geosynthetics International,* **11(1),** 35-42.

33. **Dash, S.K., Reddy, P.D.,** and **Raghukanth, T.G.** (2008). "Subgrade modulus of geocell-reinforced sand foundation" *Ground Improvement,* **161(12),** 79-87.

34. **De Garidel, R.,** and **Morel, G.** (1986). "New strengthening techniques by textile elements for low-volume roads." *Proceedings of 3rd International Conference on Geotextiles,* Vienna, Austria, 1027-1032**.**

35. **Emersleben, A.,** and **Meyer, N.** (2008). "The use of geocells in road construction over soft soil: Vertical stress and falling weight deflectometer measurements." *EuroGeo4,* Paper number **132**, 1-8.

36. **Forsman, J., Slunga, E.,** and **Lahtinen, P.** (1998). "Geogrid and Geocell Reinforced Secondary Road over Deep Peat Deposit." *Proceedings of the 6th International Conference on Geosynthetics,* Atlanta, **2,** 773-778.

37. **Fragaszy, R.J.,** and **Lawton, E.** (1984). "Bearing capacity of reinforced sand subgrades." *Journal of Geotechnical Engineering,* ASCE, **110(10)**, 1500-1507.

38. **Gibson, R.E.** (1953). "Experimental Determination of the True Cohesion and True Angle of Internal Friction in Clays." *Proceedings of the 3rd International Conference on Soil Mechanics and Foundation Engineering*, Zurich, **1,** 126-130.

39. **Guido, V.A., Chang, D.K.,** and **Sweeny, M.A.** (1986). "Comparison of geogrid and geotextile reinforced slabs." *Canadian Geotechnical Journal*, **23(1)**, 435-440.

40. **Gupta, A.,** and **Somnath, B.** (1994). "Bearing Capacity improvement using geogrids." *Civil Engineering and Construction Review*, **7**, 12-13.

41. **Hendricker, A.T., Fredianelli, K.H., Kavazanjiam, E. Jr.,** and **McKelvey III, J.A.** (1998). "Reinforcement requirements at a hazardous waste site." *Proceedings of the 6th International Conference on Geosynthetics*, Atlanta, **1**, 465-468.

42. **Henkel, D.J.,** and **Gilbert, G.D.** (1952). "The effect of rubber membranes on the measured triaxial compression strength of clay samples." *Geotechnique,* **3(1)**, 20-29.

43. **Huang, C.C.,** and **Tatsuoka, F.** (1990). "Bearing capacity of reinforced horizontal sandy ground." *Geotextiles and Geomembranes,* **9(1)**, 51-82.

44. **Johnson, J. E.** (1982). "Bridge and Tidal Waters." *Municipal Engineer,* **109**, 104-107.

45. **Kawalec, J., Golos, M.,** and **Urbanski, P.** (2006). "Stiff geogrids for road engineering structures used in the latest applications in Poland." *Geosynthetics and Plastics in geotechnical engineering and construction engineering*, Scientific and Technical Conference, Czestochowa.

46. **Kazerani, B.,** and **Jamnejad, G. H.** (1987). "Polymer grid cell reinforcement in construction of pavement structures." *Geosynthetic* Conference, IFAI, USA. **1**, 58-68.

47. **Khay, M.,** and **Perrier, H.** (1990). "Sand confinement by geotextiles in road construction." *4th Inernational Conference on Geotextiles, Geomembranes and other Related Products,* 255.

48. **Khing, K.H., Das, B.M., Puri, V.K., Cook, E.E.,** and **Yen, S.C.** (1993). "The bearing capacity of a strip foundation on geogrid-reinforced sand." *Geotextiles and Geomembranes*, **12(4)**, 351-361.

49. **Khing, K.H., Das, B.M., Puri, V.K., Yen, S.C.,** and **Cook, E.E.** (1994). "Foundation on strong sand underlain by weak clay with geogrid at the interface." *Geotextiles and Geomembranes*, **13(3)**, 199-206.

50. **Kim, S.I.,** and **Cho, S.D.** (1988). "An experimental study on the contribution of geotextiles to bearing capacity of footings on weak clays." *Proceedings of International Geotechnical Symposium on Theory and Practice of Earth Reinforcement*, Fukuoka, Japan, 215-220.

51. **Koerner, R.M.** (1997) *Designing with geosynthetics,* 3rd edition, Prentice Hall Inc., New Jersey, USA.

52. **Kong, A.L.L**. (2005). "Reinforced soil structures with geosynthetics." *Jurutera,* The Institute of Engineers, Malaysia, **6,** 56-57.

53. **Langhaar, H.L.** (1951). "Dimensional analysis and theory of models". John Wiley & Sons Inc., New York.

54. **Latha, G.M** and **Murthy, V.S.** (2007). "Effects of reinforcement form on the behaviour of geosynthetic reinforced sand." *Geotextiles and Geomembranes,* **25(1)**, 23-32.

55. **Lau, A., Edil, T., Benson, C.,** and **Tanyu, B.** (2001). "Use of Geocells in Flexible Pavements over Poor Subgrades." Geo Engineering Report No.**01-05**. Department of Civil and Environmental Engineering, University of Wisconsin-Madison, Madison,W.I, USA.

56. **Love, J.P., Burd, H.J., Milligan, G.W.E.,** and **Houlsby, G.T.** (1987). "Analytical and model studies of reinforcement of a layer of granular fill on soft clay subgrade." *Canadian Geotechnical Journal*, 2**4(4)**, 611-622.

57. **Mandal, J.N.,** and **Sah, H.S.** (1992). "Bearing capacity tests on Geogrid-Reinforced clay." *Geotextiles and Geomembranes,* **11(3)**, 327-333.

58. **Mandal, J.N.,** and **Gupta, P.** (1994). "Stability of geocell-reinforced soil." *Construction and Building Materials*, **8**, 55-62.

59. **Mengelt, M., Edil, T.B.,** and **Benson, C.H.** (2006). "Resilient modulus and plastic deformation of soil confined in geocell." *Geosynthetics International*, **13(5)**, 195-205.

60. **Mhaiskar, S.Y.,** and **Mandal, J.N.** (1996). "Soft clay subgrade stabilization using geocells." *Construction and Building Materials*, **10(4)**, 281-286.

61. **Mitchell, J.K., Kao, T.C.,** and **Kavazanjiam, E.Jr.** (1979). "Analysis of grid cell reinforced pavement bases." Technical Report **GL-79–8,** US Army Engineers Waterways Experiment Station, Vicksburg, VA.

62. **Omar, M.T., Das, B.M., Yen, S.C., Puri, V.K.,** and **Cook, E.E.** (1993). "Ultimate bearing capacity of rectangular foundations on geogrid-reinforced sand." *Geotechnical Testing Journal*, ASTM, **16(2)**, 246-252.

63. **Panda, B.C.** (2000). **"**Structural behaviour of concrete block pavement." PhD Thesis, Department of Civil Engineering, Indian Institute of Technology Kharagpur, India.

64. **Rajagopal, K., Krishnaswamy, N.R.,** and **Latha, G.M.** (1999). "Behaviour of sand confined with single and multiple geocells." *Geotextiles and Geomembranes*, **17(3)**, 171-184.

65. **Rea, C.,** and **Mitchell, J. K.,** (1978). "Sand reinforcement using paper grid cells, Reprint 3130, ASCE spring convention and exhibit. Pittsburgh, PA, 24-28.

66. **Robertson, J.,** and **Gilchrist, A. J. T.** (1987). "Design and construction of a reinforced embankment across soft lakebed deposits." *Proceedings of the International Conference on Foundations and Tunnels,* London, M. C. Forde. Engineering Technics Press, Edinburgh**, 2**, 84-92.

67. **Samatani, N. C.,** and **Sonpal, R. C.** (1989). "Laboratory tests of strip footing on reinforced cohesive soil." *Journal of Geotechnical Engineering*. ASCE, **115(9),** 1326-1330.

68. **Shimizu, M.,** and **Inui, T. (**1990). "Increase in the bearing capacity of ground with geotextile wall frame." *Proceedings of the 4th International Conference on Geotextiles Geomembranes and Related Products*, Hague, Netherlands, **1**, 254.

69. **Shin, E.C., Das. B.M., Puri. V.K., Yen, S.C.,** and **Cook, E.E.** (1993). "Bearing Capacity of Strip Foundation on Geogrid Reinforced Clay." *Geotechnical Testing Journal*, **16(4)**, 534-541.

70. **Simac, M.R.** (1990). "Connections for geogrid systems." *Geotextiles and Geomembranes*, **9(4-6)**, 537-546.

71. **Sireesh, S., Sitharam, T.G.,** and **Dash, S.K.** (2009). "Bearing capacity of circular footing on geocell–sand mattress overlying clay bed with void." *Geotextiles and Geomembranes*, **27**, 89-98.

72. **Sitharam, T.G., Sireesh, S.,** and **Dash, S.K.** (2007). "Performance of surface footing on geocell-reinforced soft clay beds." *Geotechnical and Geological Engineering,* **25**, 509-524.

73. **Terzaghi, K.** (1943). *Theoretical Soil Mechanics,* John Willey and Sons Inc., New York, U.S.A.

74. **Vidal, H.** (1969). "The Principle of reinforced earth." *Highway Research Record*, **282**, Washington, D.C.

75. **Webster, S.L.,** and **Alford, S.J.** (1978). "Investigation of Construction Concepts for Pavements across Soft Ground." Technical Report **S-78-6**, United States Army Corps of Engineers, Waterways Experiment Station, Mississippi, USA.

76. **Webster, S. L.,** and **Watkins, J. E.** (1977). "Investigation of Construction Techniques for Tactical Bridge Approach Roads across Soft Ground." Technical Report **S-77-1**, United States Army Corps of Engineers, Waterways Experiment Station, Mississippi, USA.

77. **Wesseloo, J., Vissar, A.T.,** and **Rust, E.,** (2009). "The stress-strain behaviour of multiple cell geocell packs." *Geotextiles and Geomembranes,* **27(1)**, 31-38.

78. **Yetimoglu, T., Wu, J.T.H.,** and **Saglamer, A.** (1994). "Bearing capacity of rectangular footings on geogrid-reinforced sand." *Journal of Geotechnical Engineering,* ASCE, **120(12)**, 2083-2099.

79. **Zhou, H.,** and **Wen, X.** (2008). "Model studies on geogrid or geocell-reinforced sand cushion on soft soil." *Geotextiles and Geomembranes*, **26(3)**, 231-238.

APPENDIX – A1

SURFACE DEFORMATION PLOTS

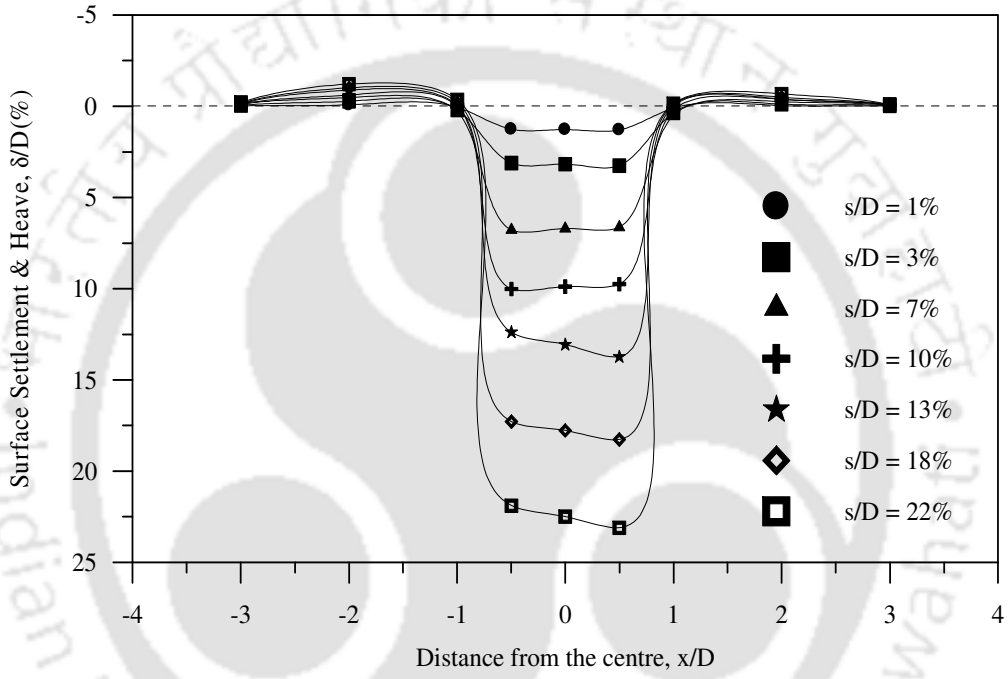

Fig. A1.1 Surface deformation profiles with geocell reinforcement – Test Series B1, chevron, u/D = 0, d = 1.6D

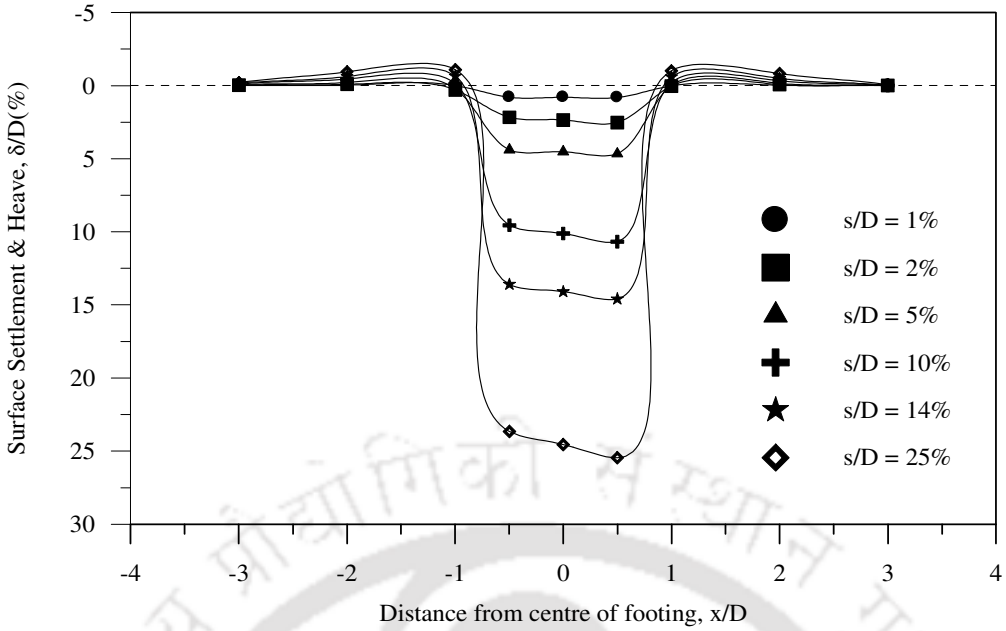

Fig. A1.2 Surface deformation profiles with geocell reinforcement – Test Series B2, chevron, u/D = 0.1, d = 1.6D

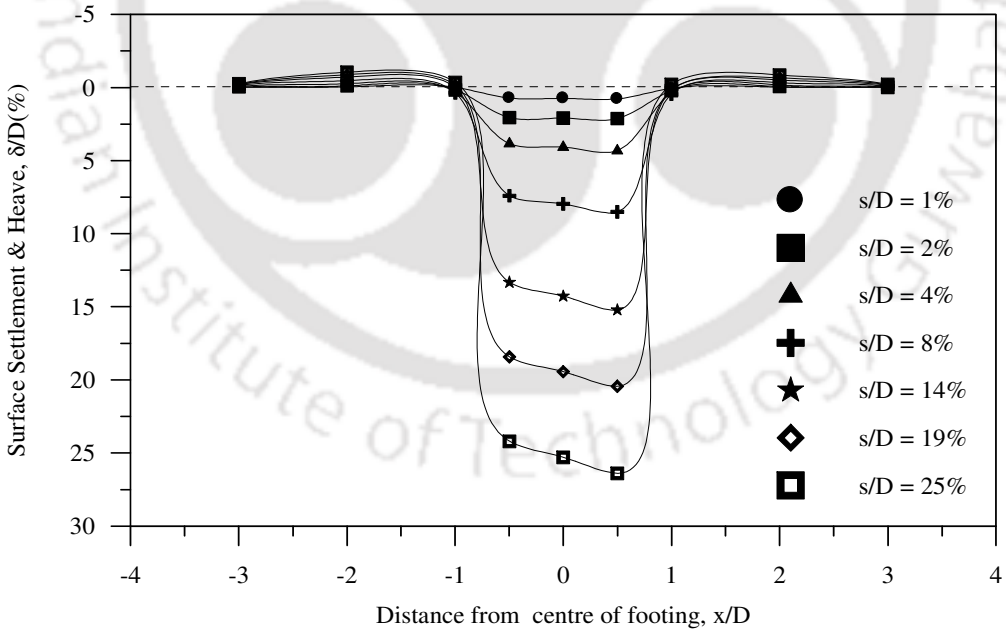

Fig. A1.3 Surface deformation profiles with geocell reinforcement – Test Series B3, chevron, u/D = 0.25, d = 1.6D

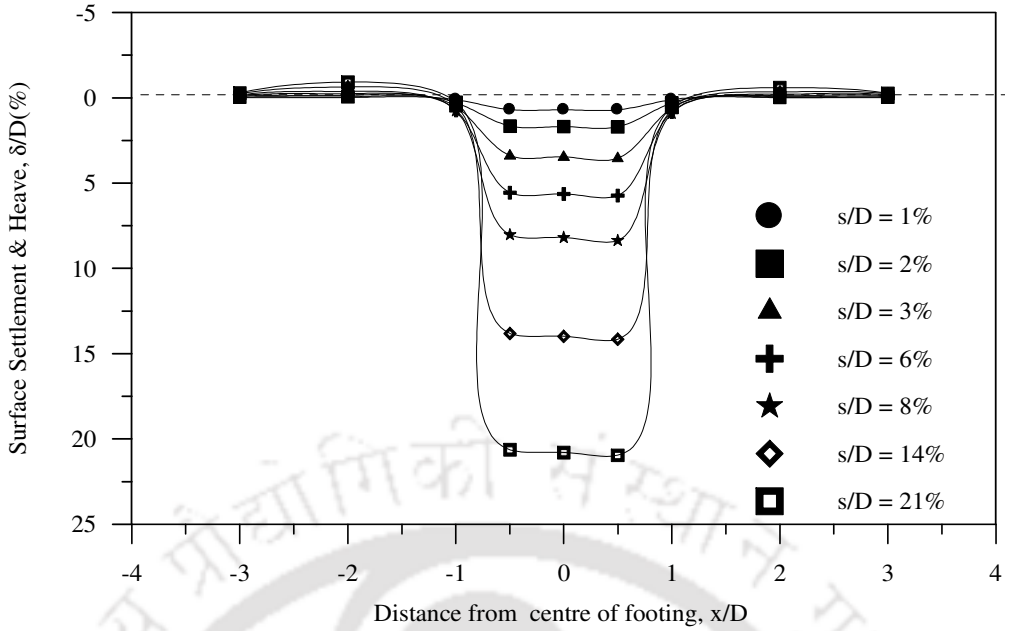

Fig. A1.4 Surface deformation profiles with geocell reinforcement – Test Series B4, chevron, u/D = 0.5, d = 1.6D

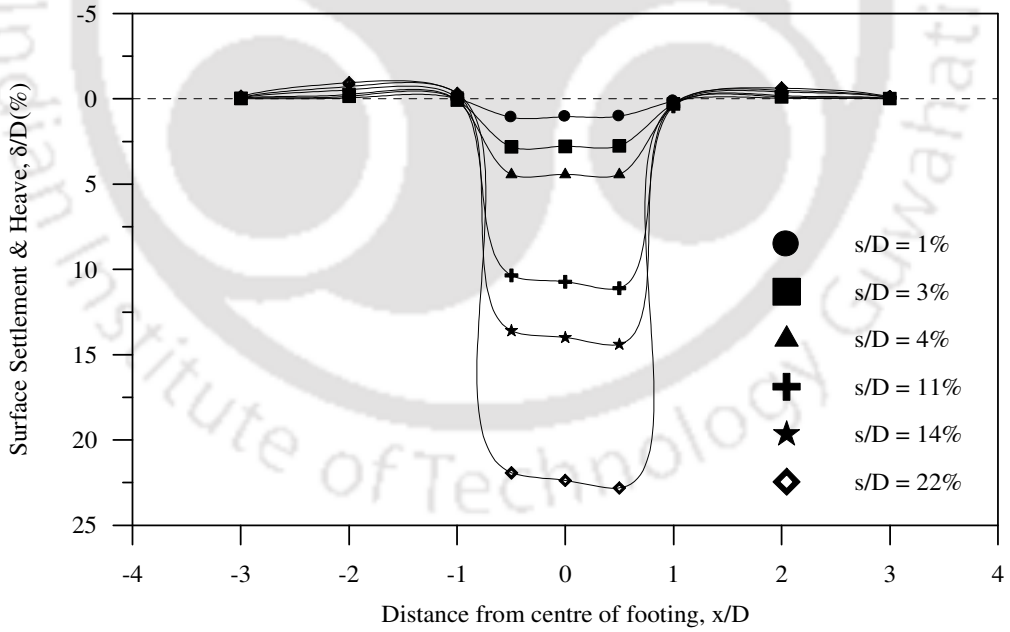

Fig. A1.5 Surface deformation profiles with geocell reinforcement – Test Series B1, chevron, u/D = 0, d = 1.2D

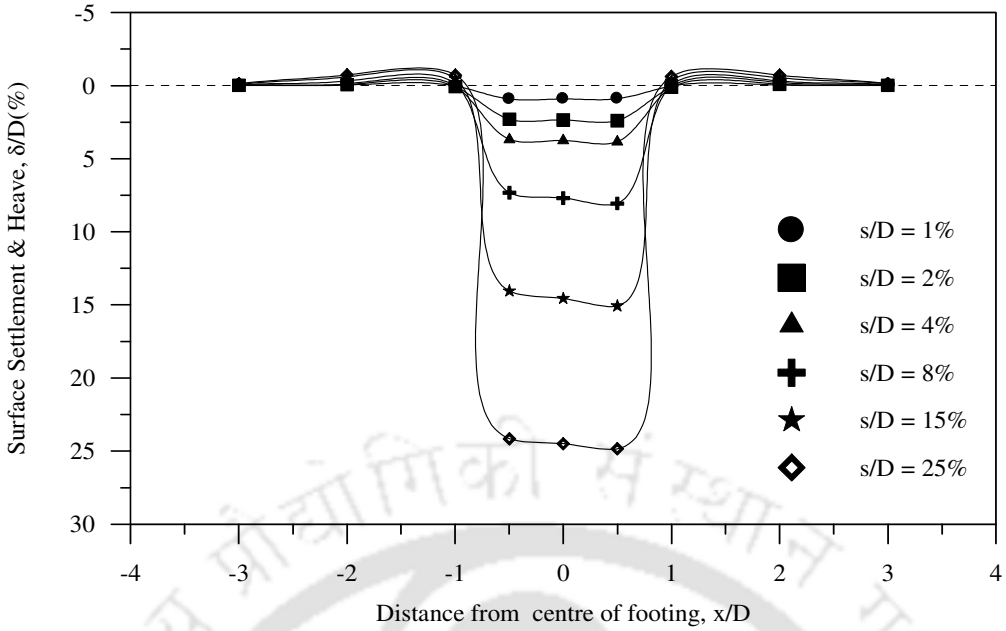

Fig. A1.6 Surface deformation profiles with geocell reinforcement – Test Series B2, chevron, u/D = 0.1, d = 1.2D

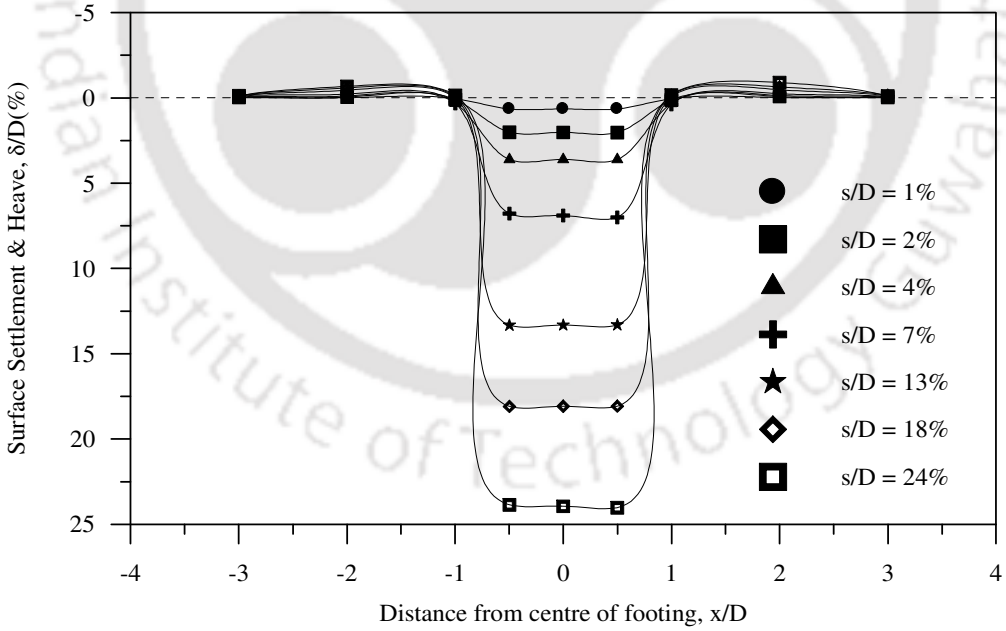

Fig. A1.7 Surface deformation profiles with geocell reinforcement – Test Series B3, chevron, u/D = 0.25, d = 1.2D

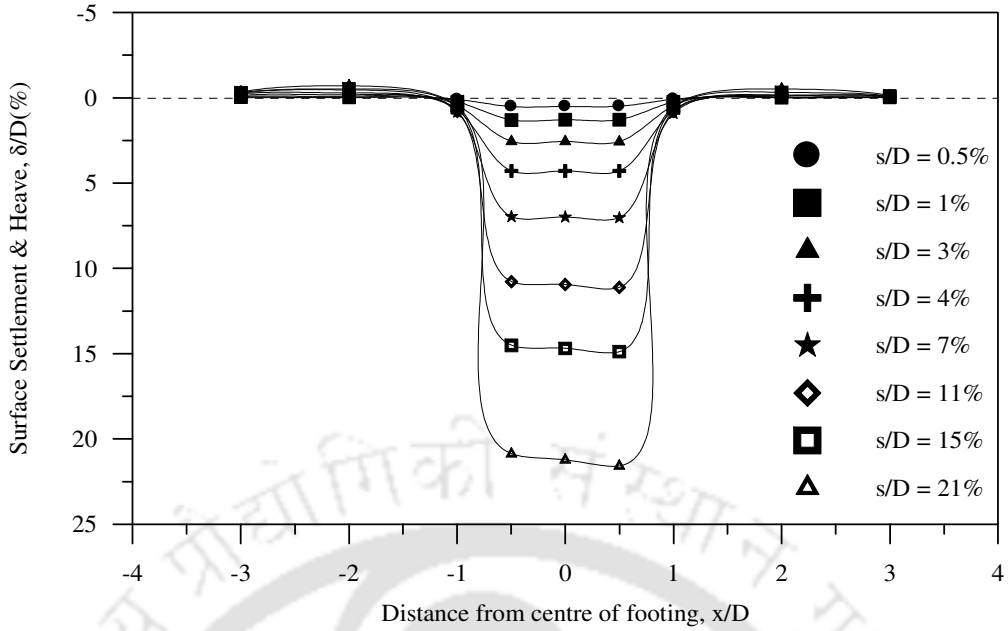

Fig. A1.8 Surface deformation profiles with geocell reinforcement – Test Series B4, chevron, u/D = 0.5, d = 1.2D

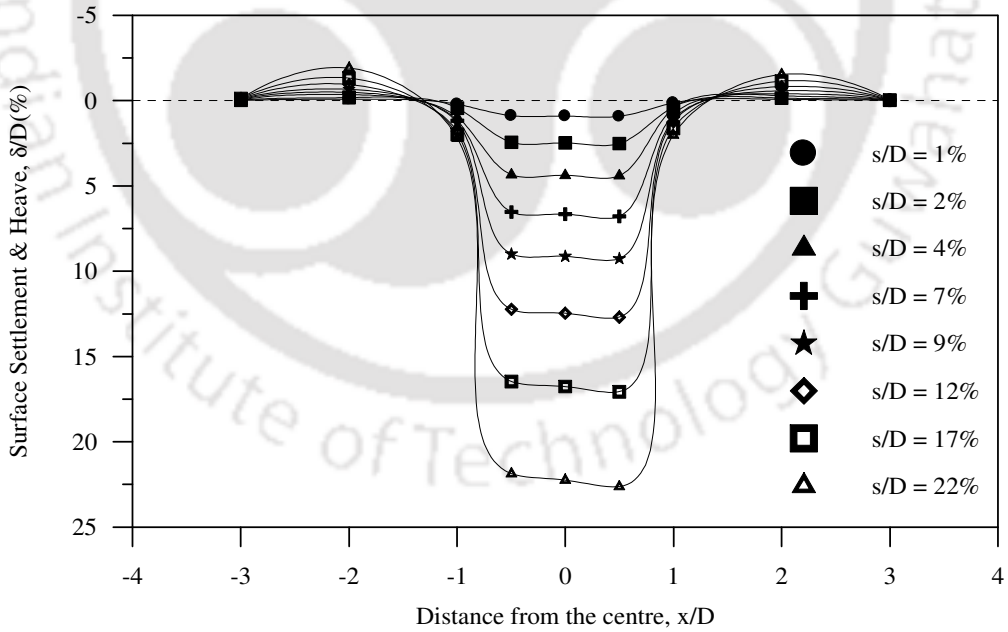

Fig. A1.9 Surface deformation profiles with geocell reinforcement – Test Series B1, chevron, u/D = 0, d = 0.4D

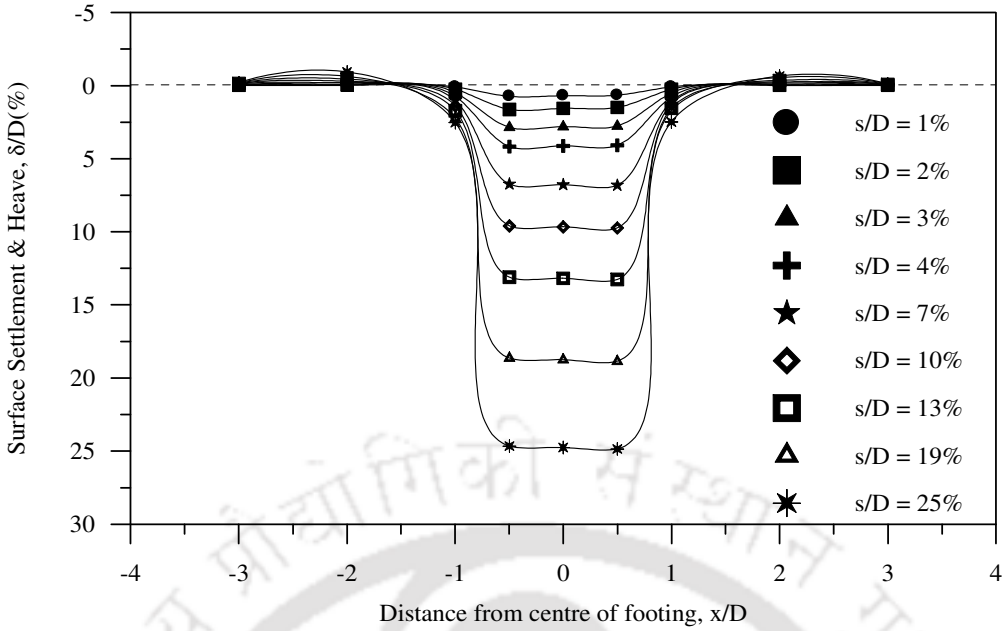

Fig. A1.10 Surface deformation profiles with geocell reinforcement – Test Series B2, chevron, u/D = 0.1, d = 0.4D

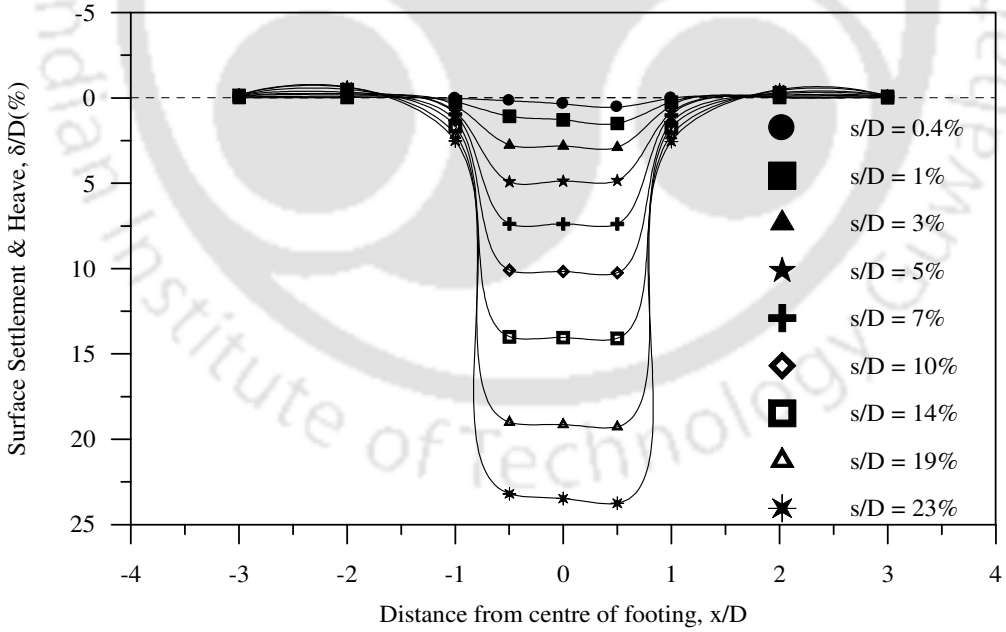

Fig. A1.11 Surface deformation profiles with geocell reinforcement – Test Series B3, chevron, u/D = 0.25, d = 0.4D

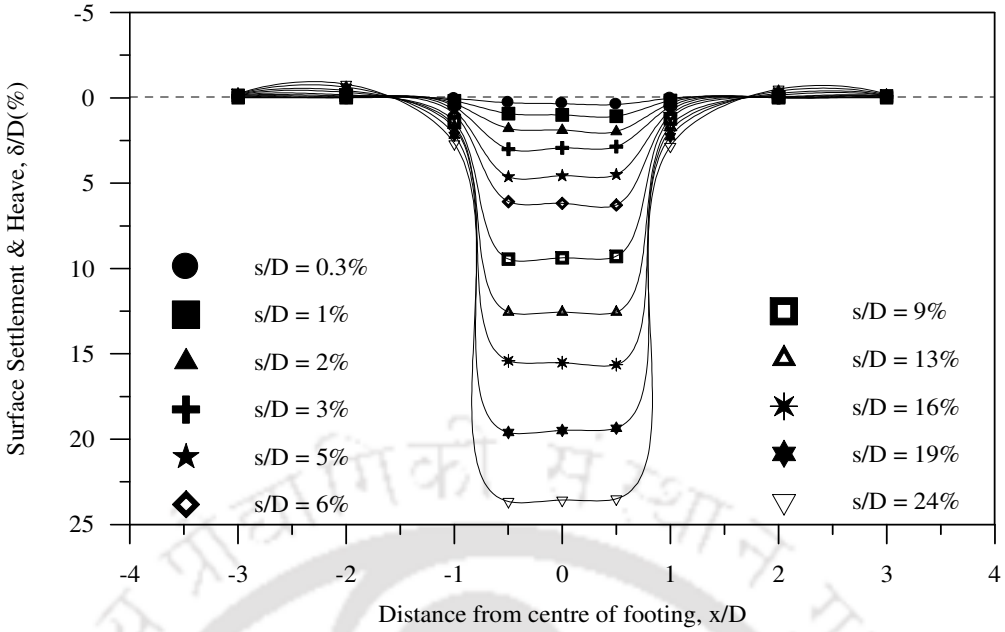

Fig. A1.12 Surface deformation profiles with geocell reinforcement – Test Series B4, chevron, u/D = 0.5, d = 0.4D

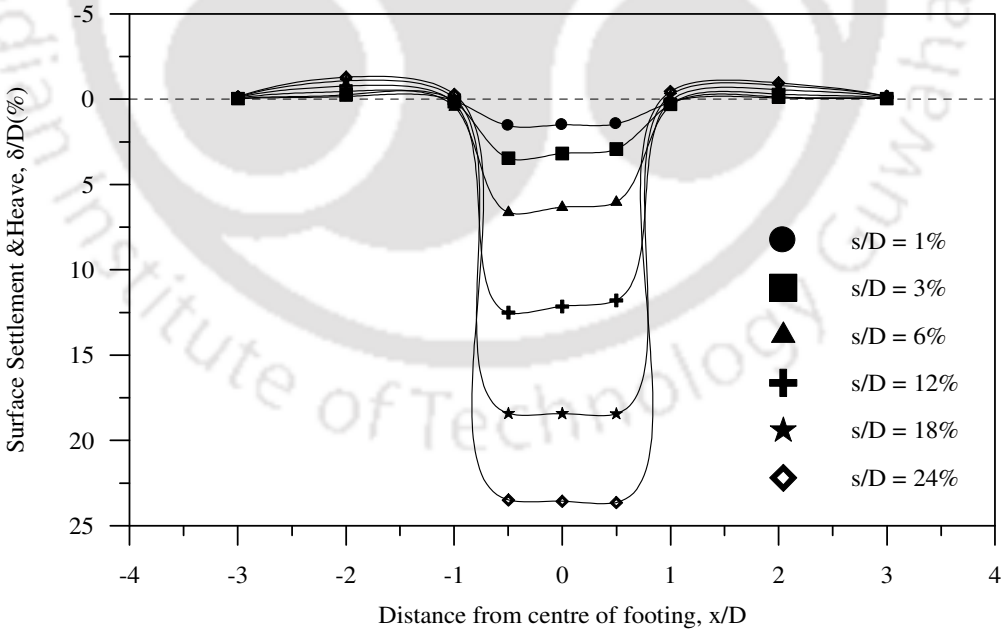

Fig. A1.13 Surface deformation profiles with geocell reinforcement – Test Series C1, diamond, u/D = 0, d = 1.6D

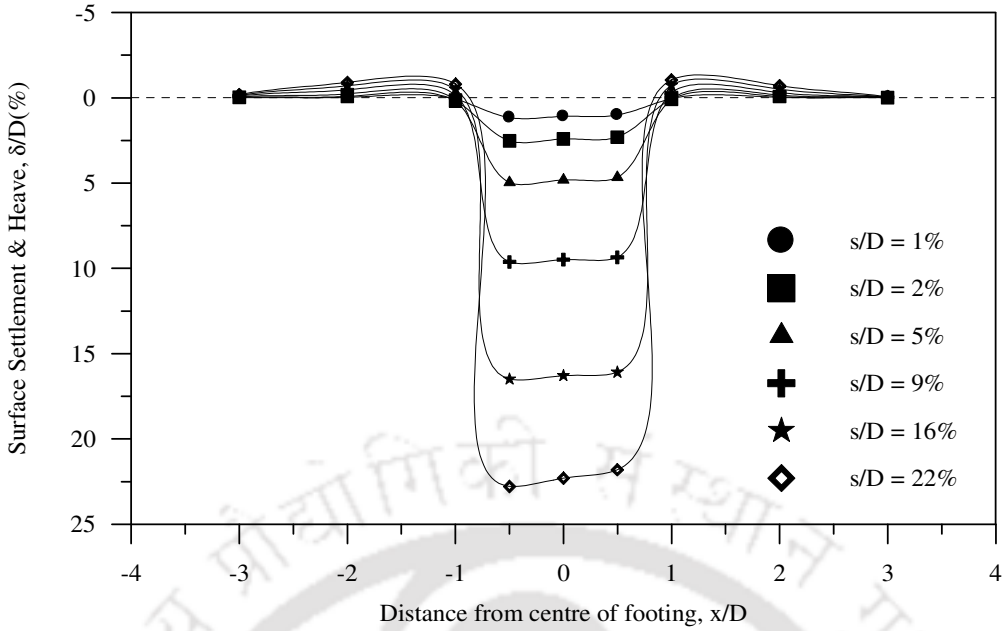

Fig. A1.14 Surface deformation profiles with geocell reinforcement – Test Series C1, diamond, u/D = 0.1, d = 1.6D

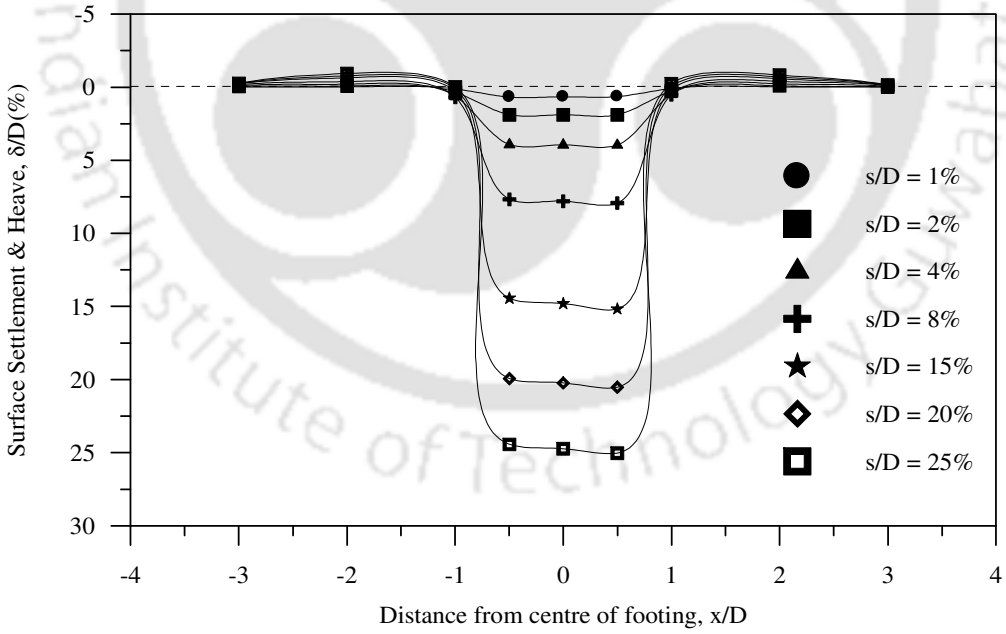

Fig. A1.15 Surface deformation profiles with geocell reinforcement – Test Series C3, diamond, u/D = 0.25, d = 1.6D

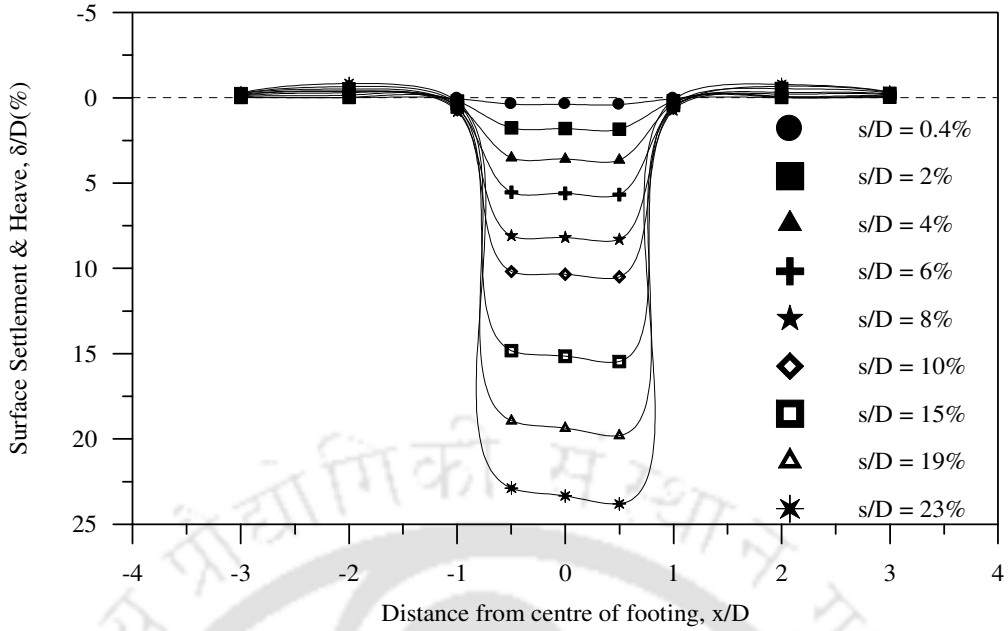

Fig. A1.16 Surface deformation profiles with geocell reinforcement – Test Series C4, diamond, u/D = 0.5, d = 1.6D

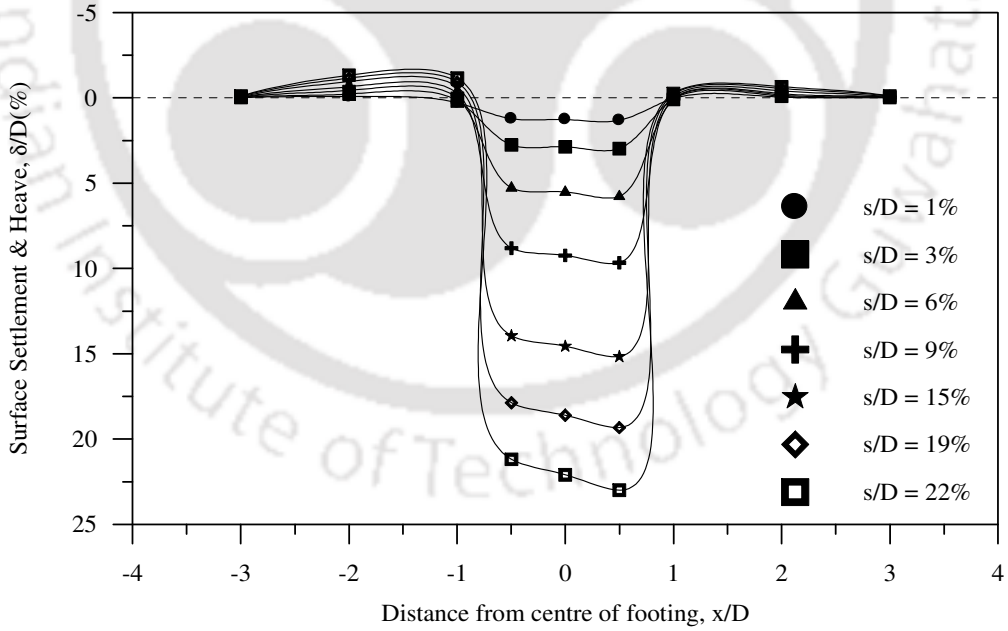

Fig. A1.17 Surface deformation profiles with geocell reinforcement – Test Series C1, diamond, u/D = 0, d = 1.2D

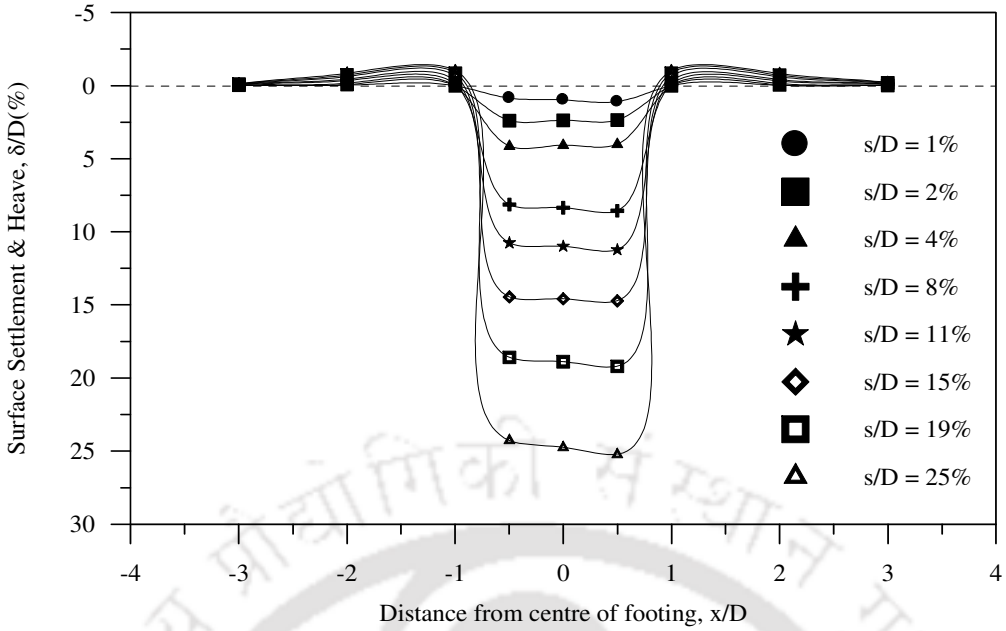

Fig. A1.18 Surface deformation profiles with geocell reinforcement – Test Series C2, diamond, u/D = 0.1, d = 1.2D

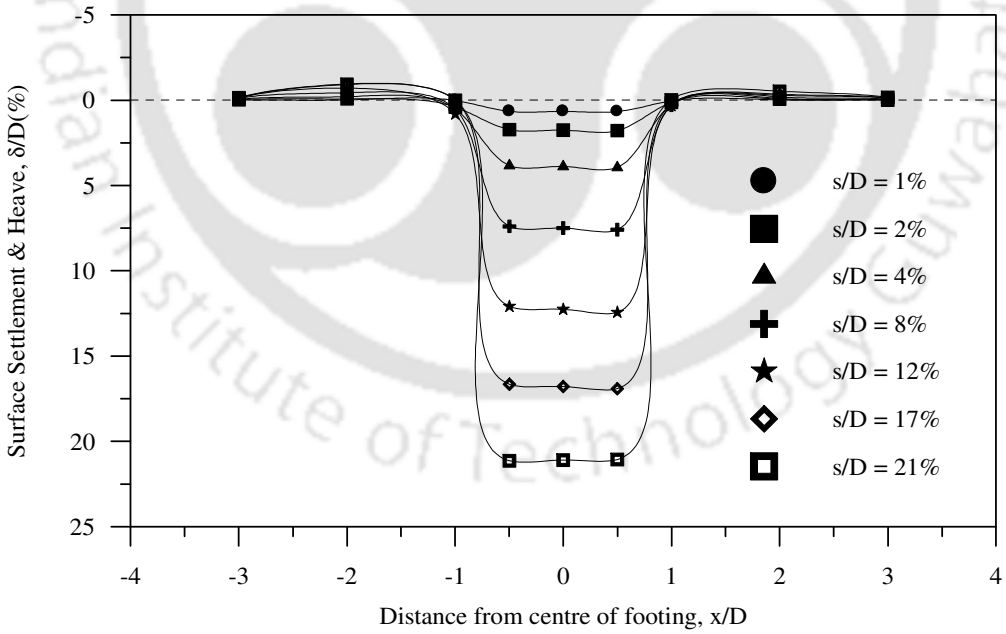

Fig. A1.19 Surface deformation profiles with geocell reinforcement – Test Series C3, diamond, u/D = 0.25, d = 1.2D

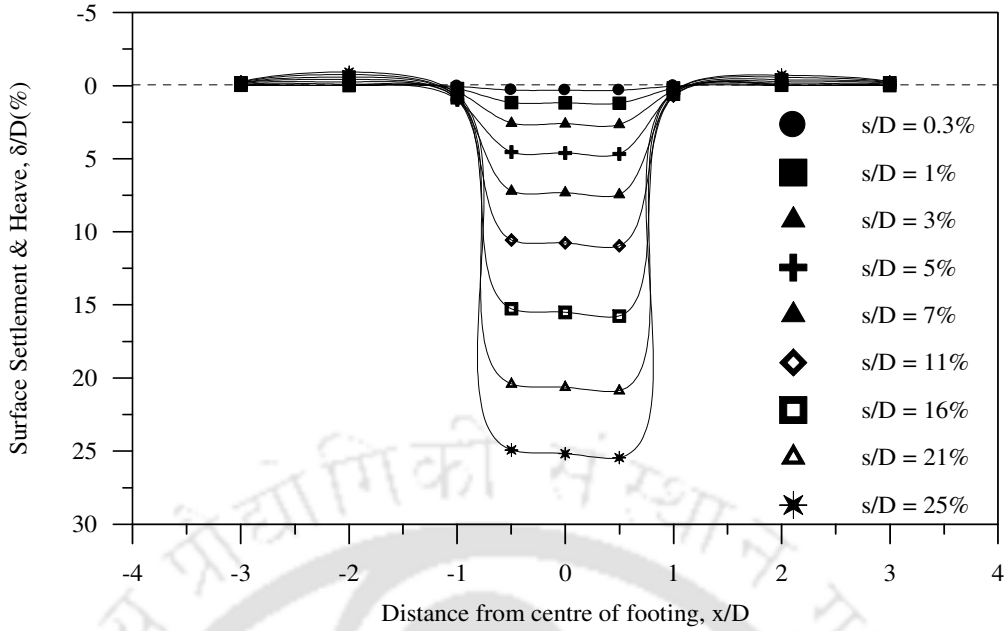

Fig. A1.20 Surface deformation profiles with geocell reinforcement – Test Series C4, diamond, u/D = 0.5, d = 1.2D

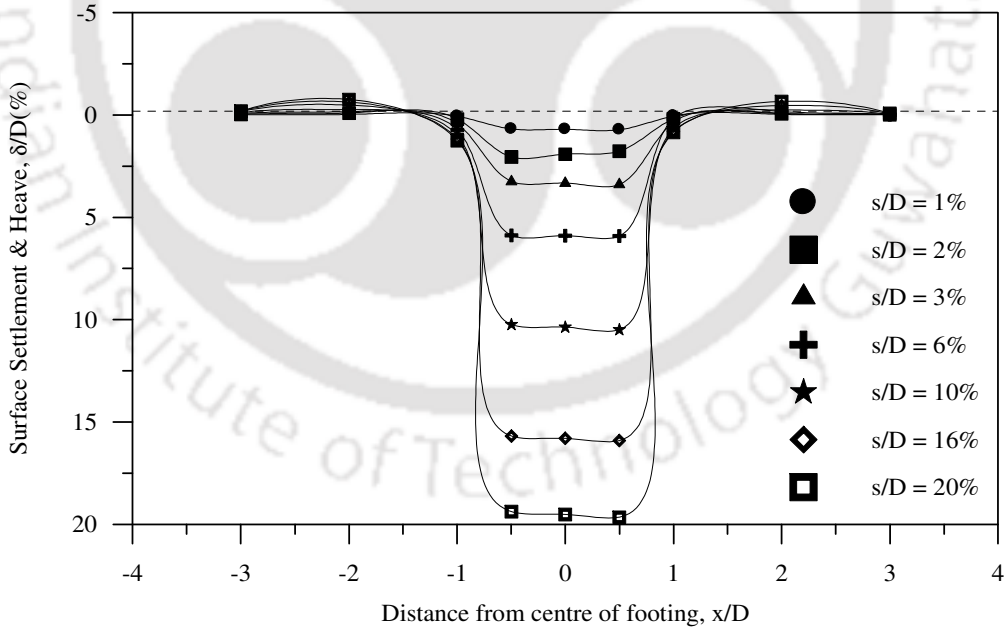

Fig. A1.21 Surface deformation profiles with geocell reinforcement – Test Series C2, diamond, u/D = 0.1, d = 0.8D

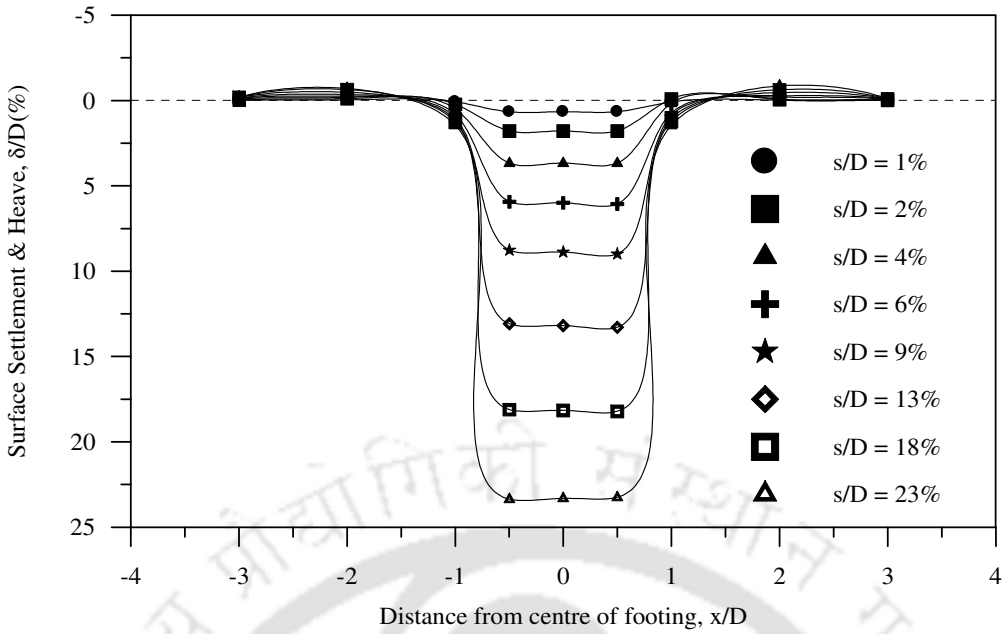

Fig. A1.22 Surface deformation profiles with geocell reinforcement – Test Series C3, diamond, u/D = 0.25, d = 0.8D

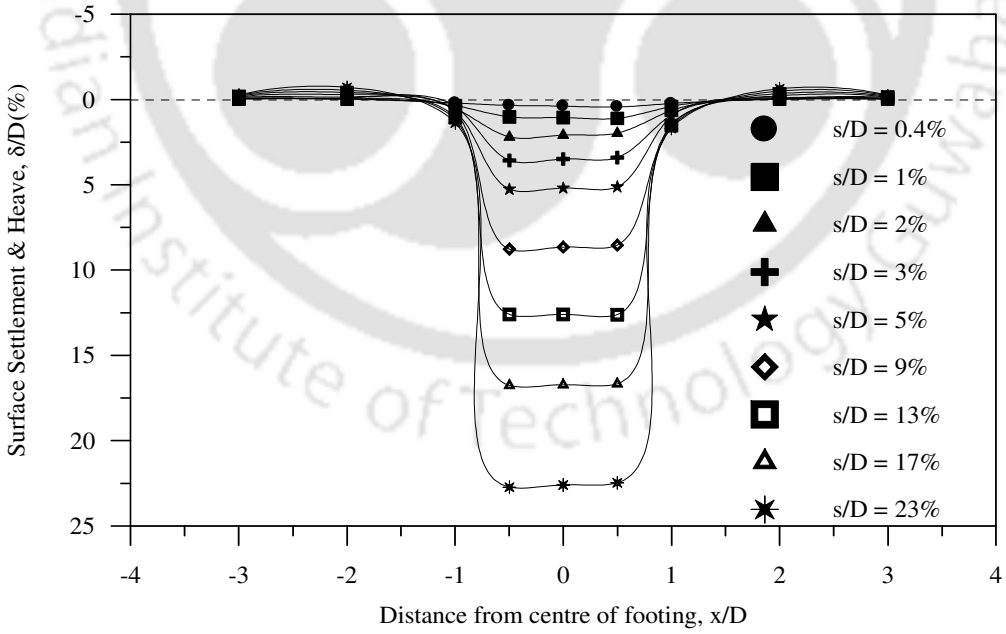

Fig. A1.23 Surface deformation profiles with geocell reinforcement – Test Series C4, diamond, u/D = 0.5, d = 0.8D

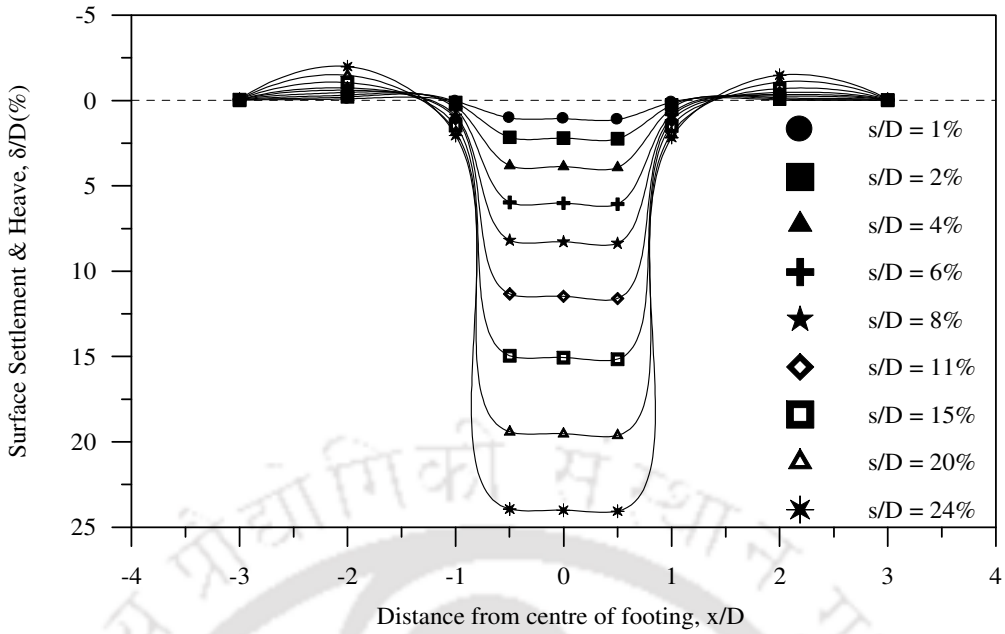

Fig. A1.24 Surface deformation profiles with geocell reinforcement – Test Series C1, diamond, u/D = 0, d = 0.4D

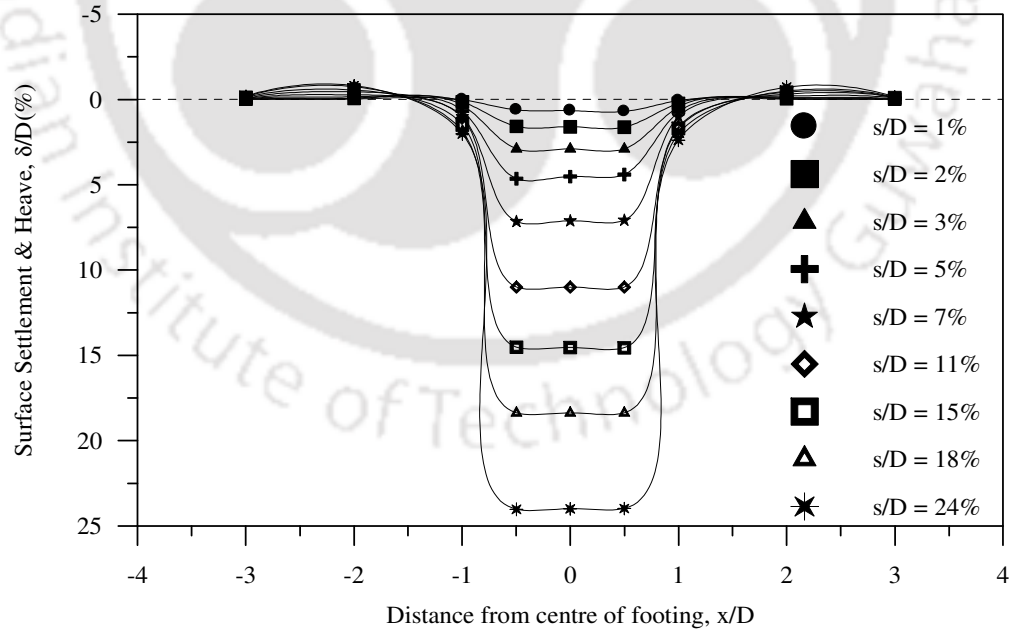

Fig. A1.25 Surface deformation profiles with geocell reinforcement – Test Series C2, diamond, u/D = 0.1, d = 0.4D

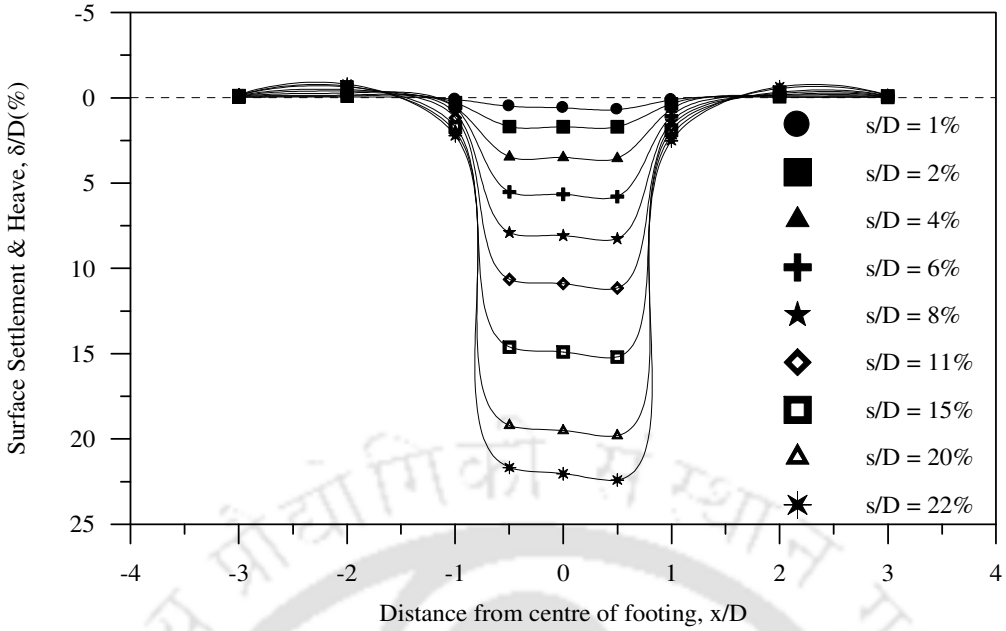

Fig. A1.26 Surface deformation profiles with geocell reinforcement – Test Series C3, diamond, u/D = 0.25, d = 0.4D

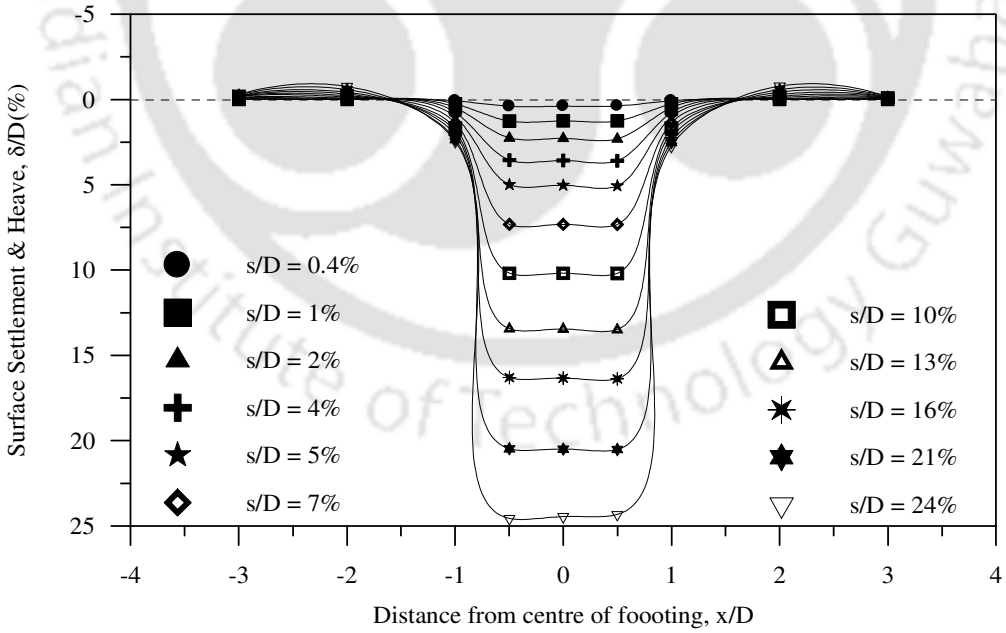

Fig. A1.27 Surface deformation profiles with geocell reinforcement – Test Series C4, diamond, u/D = 0.5, d = 0.4D

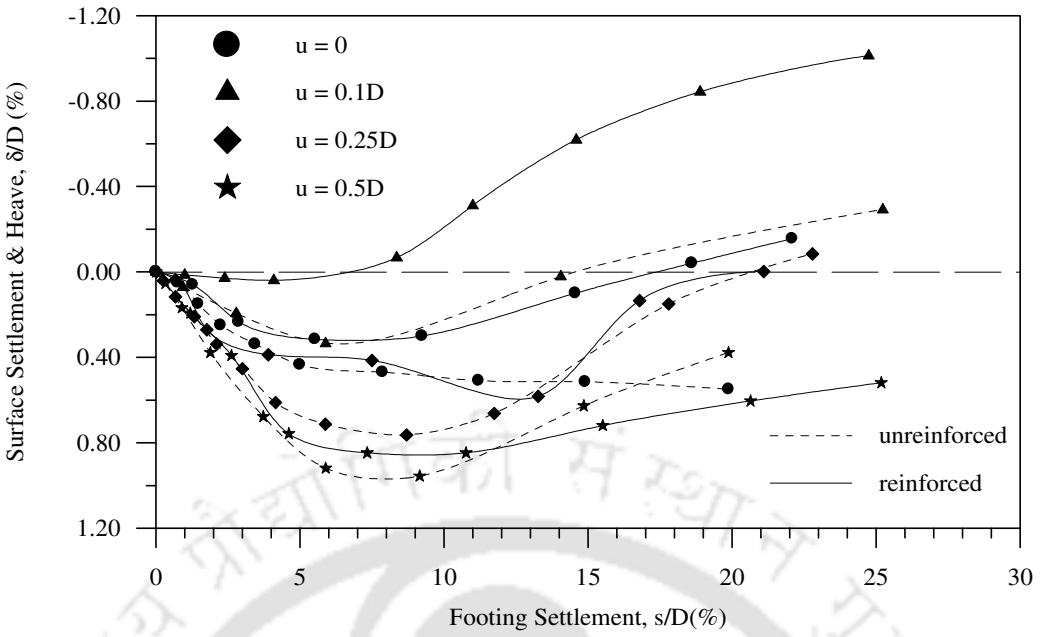

Fig. A1.28 Variation of average surface deformation with footing settlement at a distance x = D from the centre of footing, for different depth of placement (u) of geocell mattress. Test Series A2, C1- C4, h = 0.27D, diamond, d = 1.2D

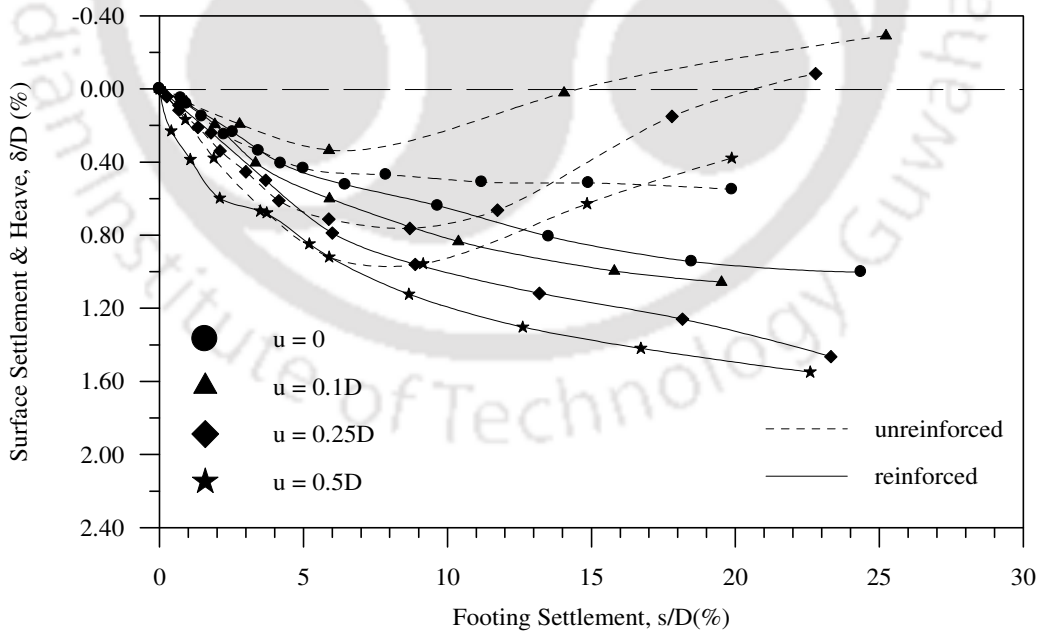

Fig. A1.29 Variation of average surface deformation with footing settlement at a distance x = D from the centre of footing, for different depth of placement (u) of geocell mattress. Test Series A2, C1- C4, h = 0.27D, diamond, d = 0.8D

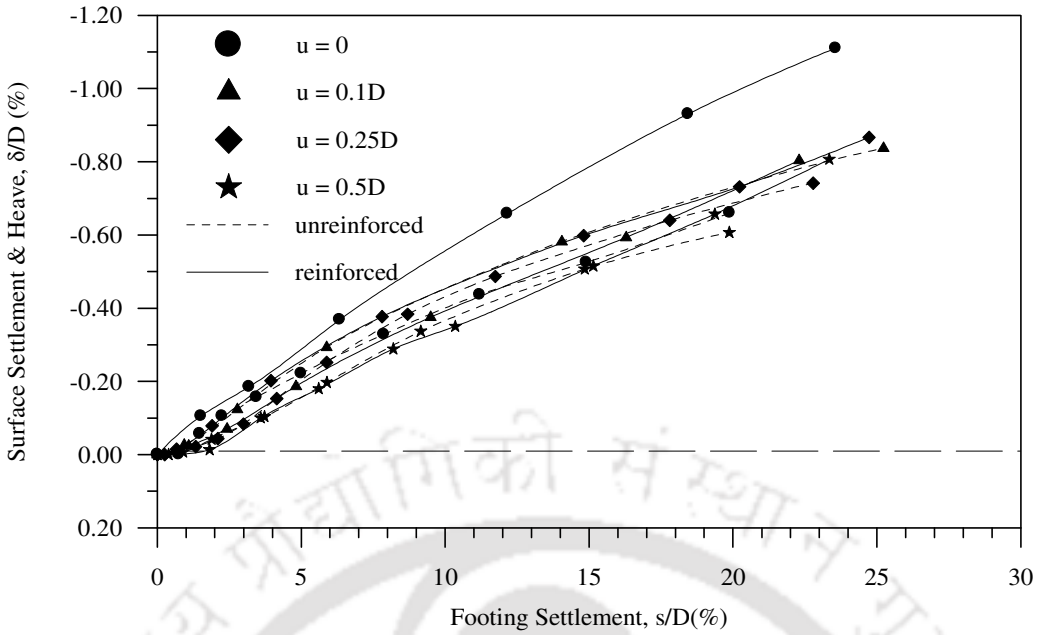

Fig. A1.30 Variation of average surface deformation with footing settlement at a distance x = 2D from the centre of footing, for different depth of placement (u) of geocell mattress. Test Series A2, C1- C4, h = 0.27D, diamond, d = 1.6D

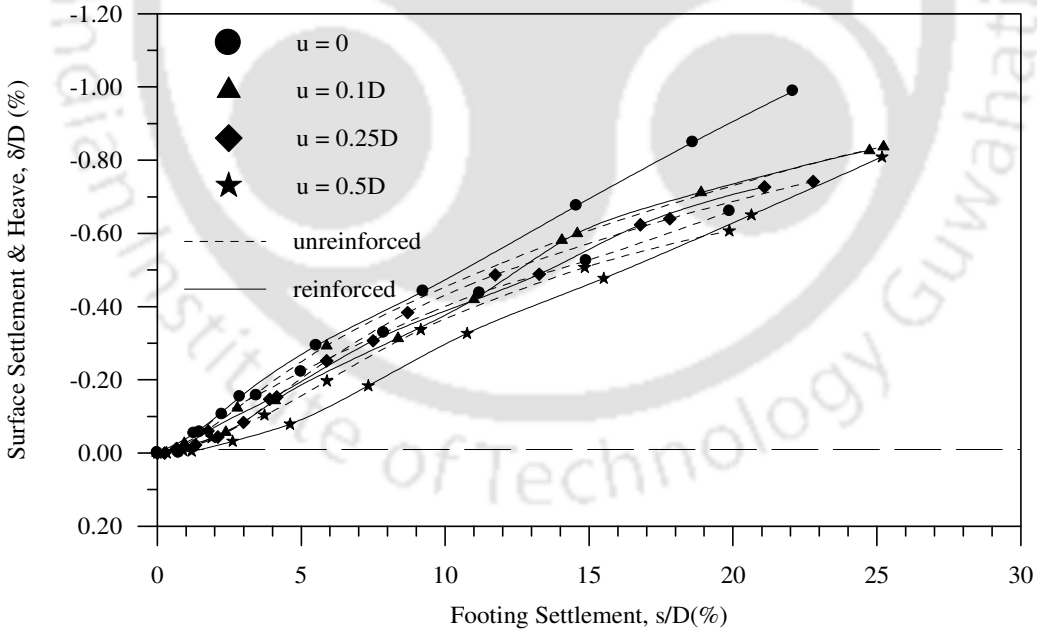

Fig. A1.31 Variation of average surface deformation with footing settlement at a distance x = 2D from the centre of footing, for different depth of placement (u) of geocell mattress. Test Series A2, C1- C4, h = 0.27D, diamond, d = 1.2D

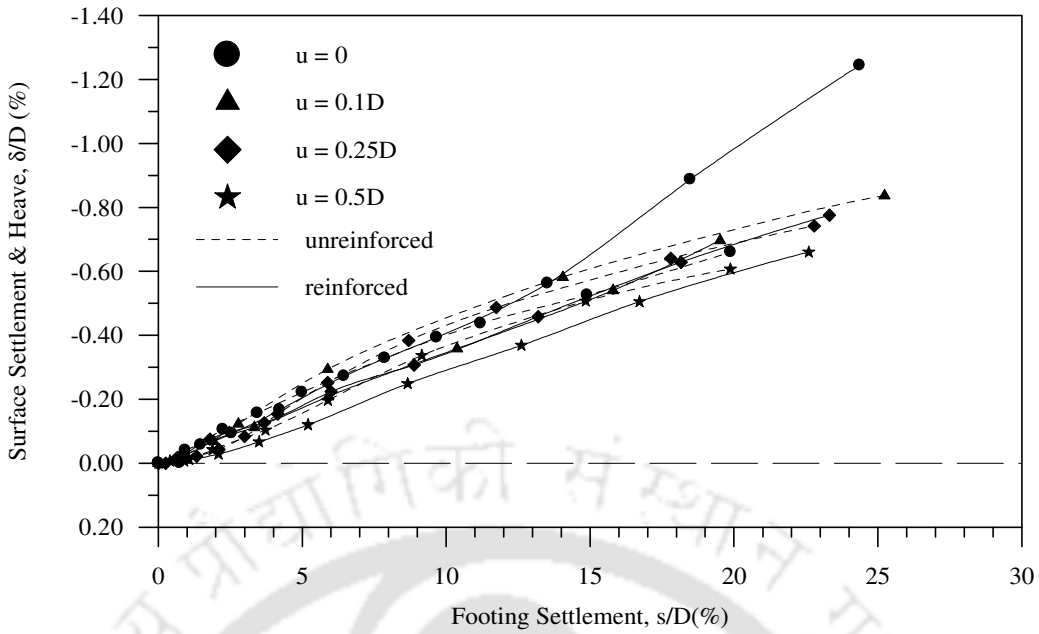

Fig. A1.32 Variation of average surface deformation with footing settlement at a distance x = 2D from the centre of footing, for different depth of placement (u) of geocell mattress. Test Series A2, C1- C4, h = 0.27D, diamond, d = 0.8D

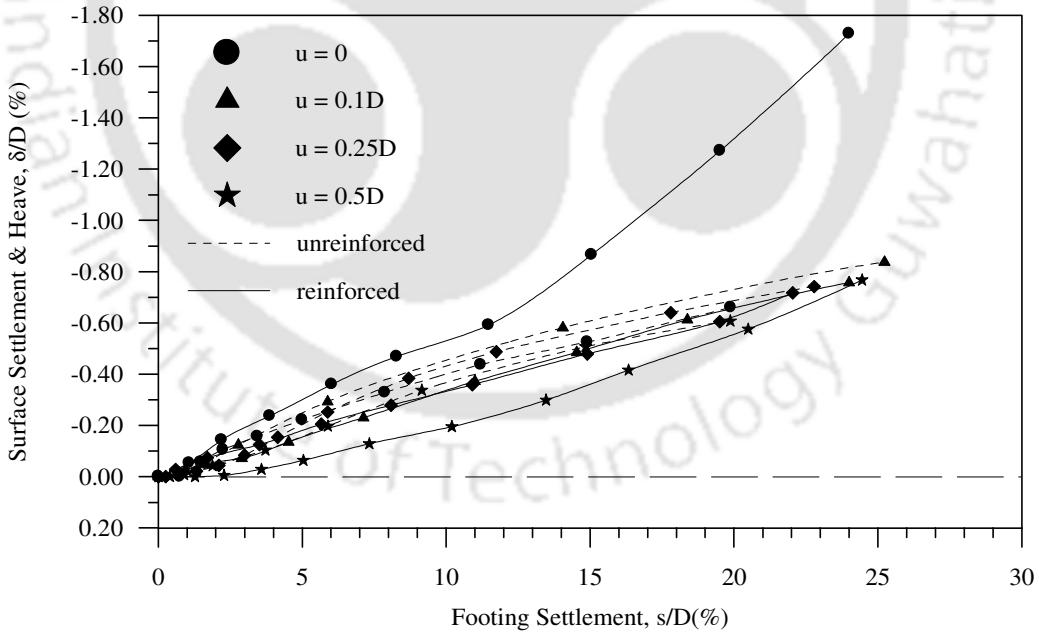

Fig. A1.33 Variation of average surface deformation with footing settlement at a distance x = 2D from the centre of footing, for different depth of placement (u) of geocell mattress. Test Series A2, C1- C4, h = 0.27D, diamond, d = 0.4D

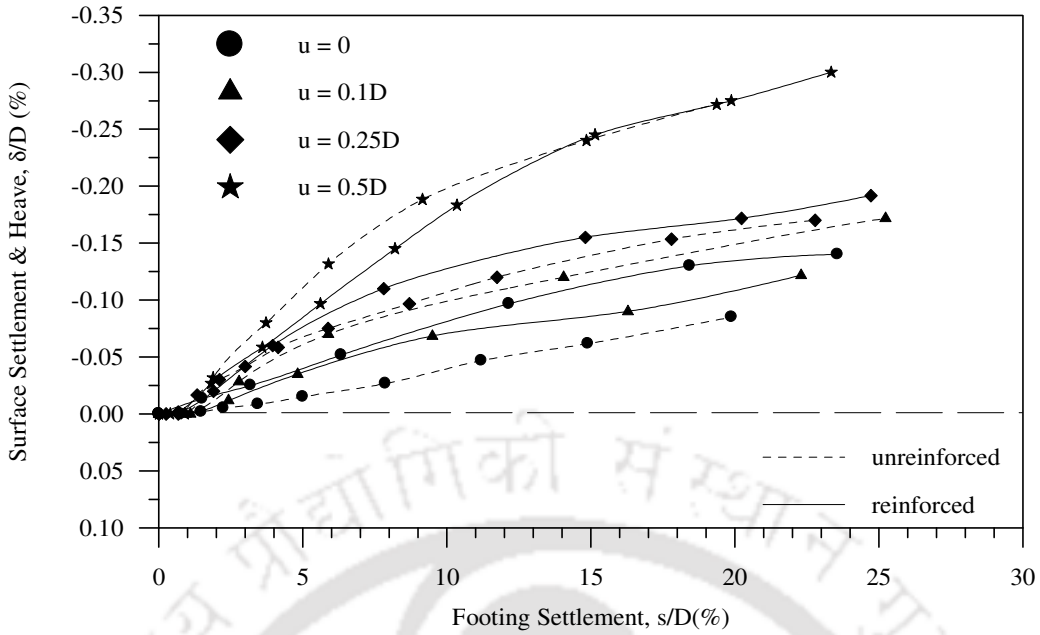

Fig. A1.34 Variation of average surface deformation with footing settlement at a distance x = 3D from the centre of footing, for different depth of placement (u) of geocell mattress. Test Series A2, C1- C4, h = 0.27D, diamond, d = 1.6D

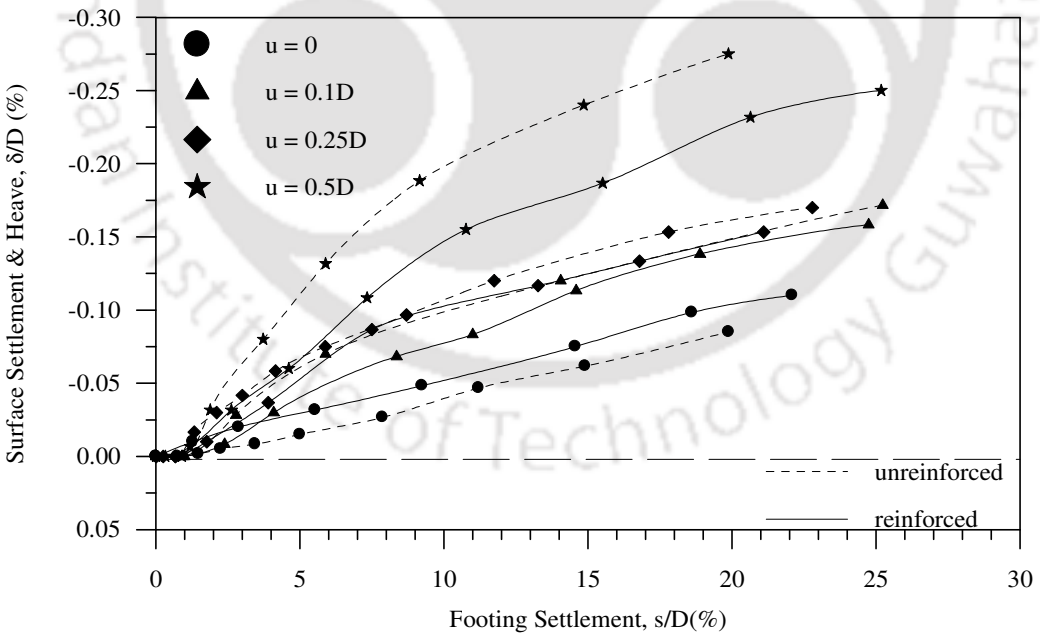

Fig. A1.35 Variation of average surface deformation with footing settlement at a distance x = 3D from the centre of footing, for different depth of placement (u) of geocell mattress. Test Series A2, C1- C4, h = 0.27D, diamond, d = 1.2D

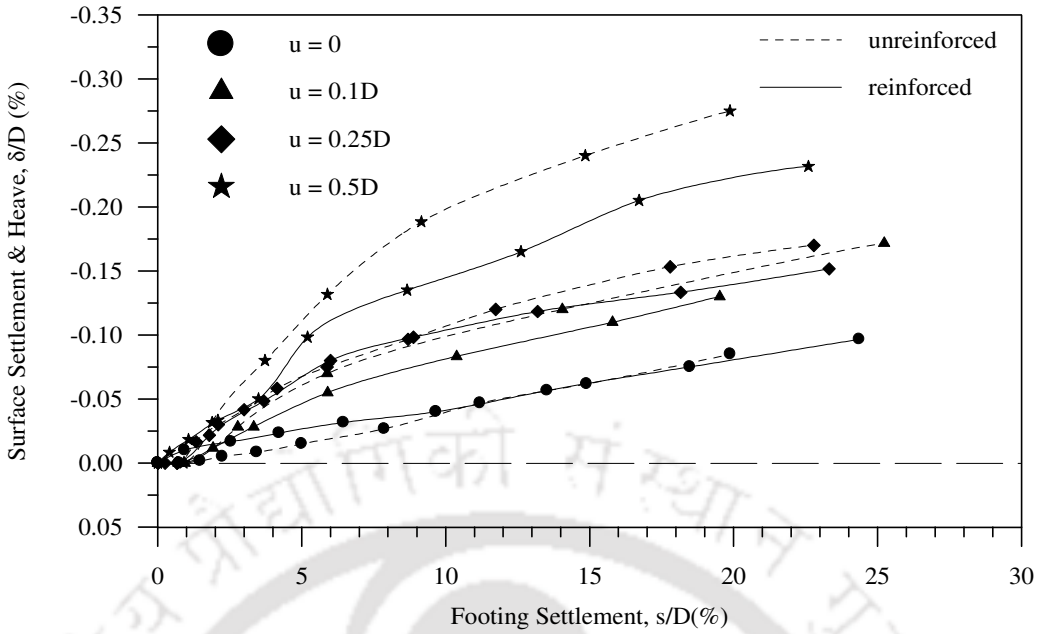

Fig. A1.36 Variation of average surface deformation with footing settlement at a distance x = 3D from the centre of footing, for different depth of placement (u) of geocell mattress. Test Series A2, C1- C4, h = 0.27D, diamond, d = 0.8D

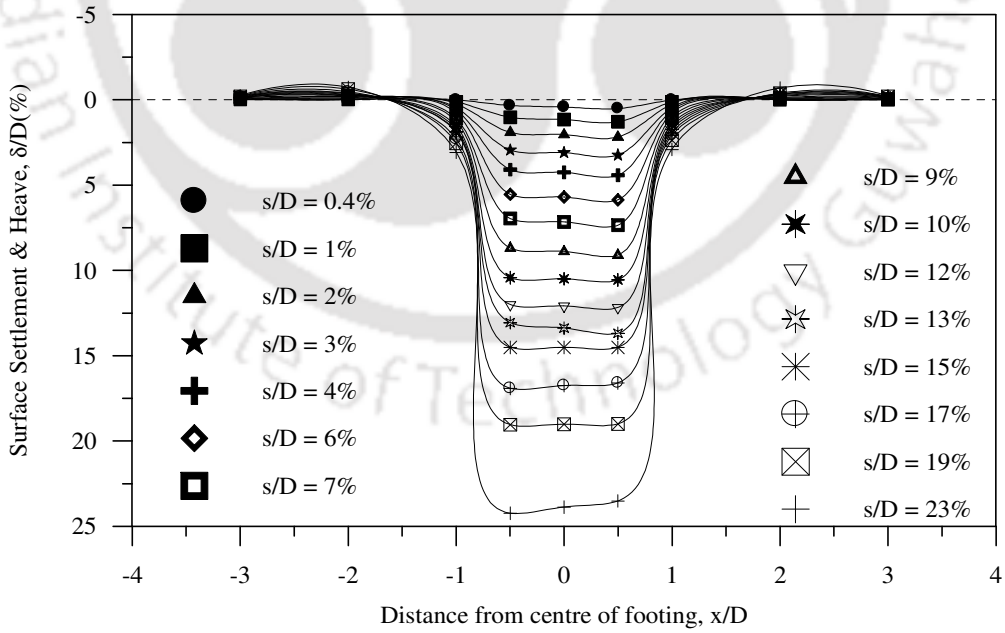

Fig. A1.37 Surface deformation profiles with geocell reinforcement – Test Series B5, h = 0.8D, d = 0.8D, u/D = 0

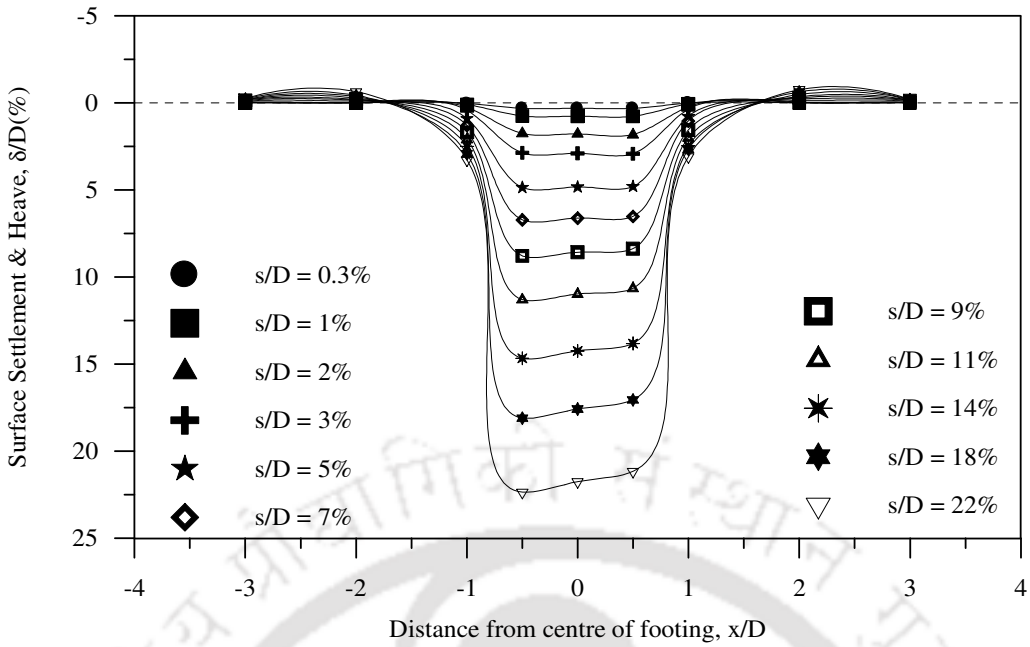

Fig. A1.38 Surface deformation profiles with geocell reinforcement – Test Series B5, h = 0.8D, d = 0.8D, u/D = 0.1

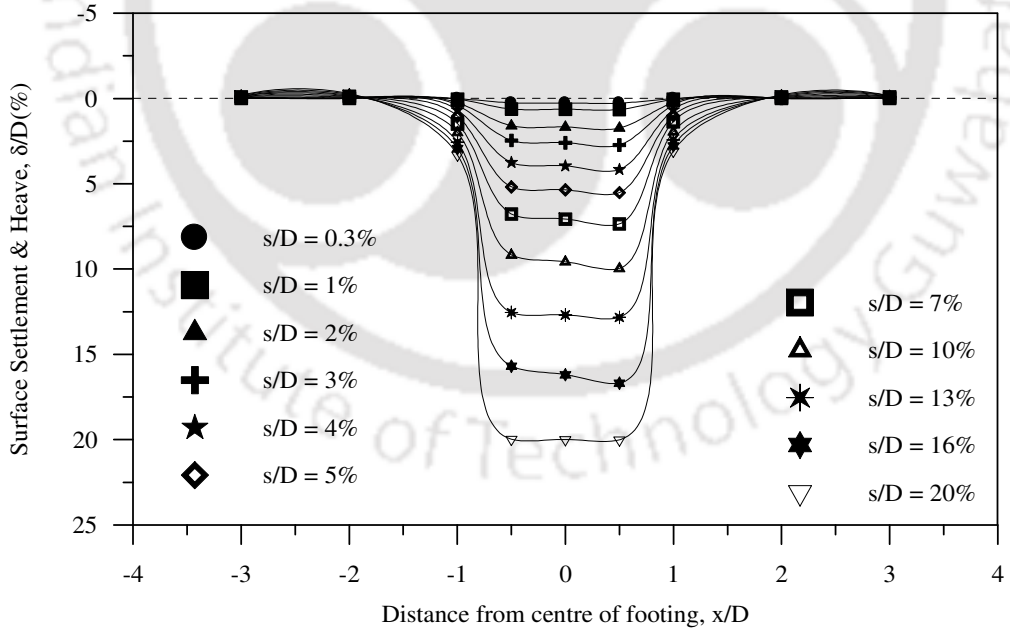

Fig. A1.39 Surface deformation profiles with geocell reinforcement – Test Series B5, h = 0.8D, d = 0.8D, u/D = 0.25

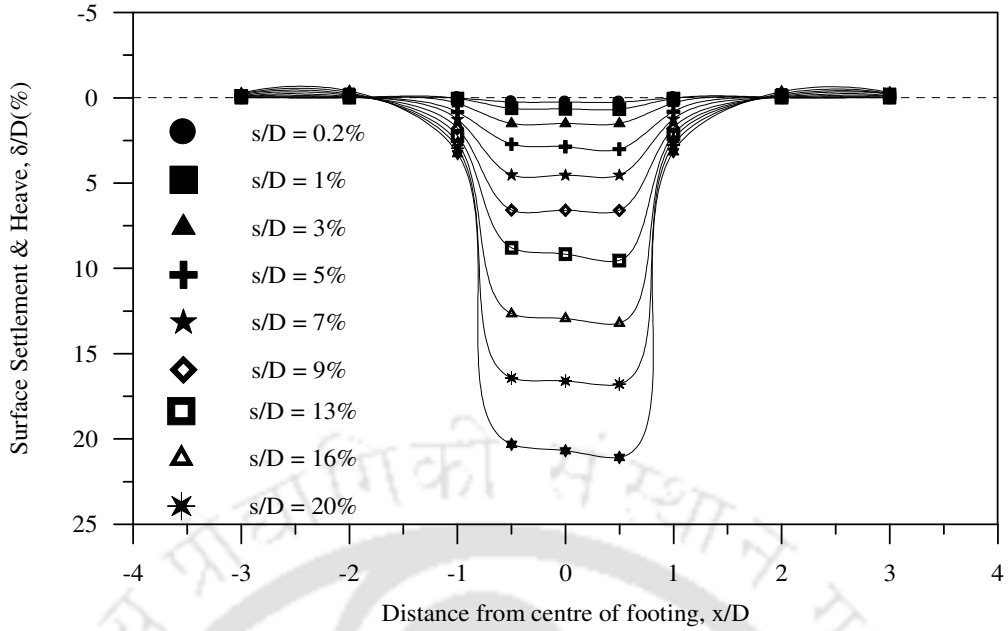

Fig. A1.40 Surface deformation profiles with geocell reinforcement – Test Series B5, h = 0.8D, d = 0.8D, u/D = 0.5

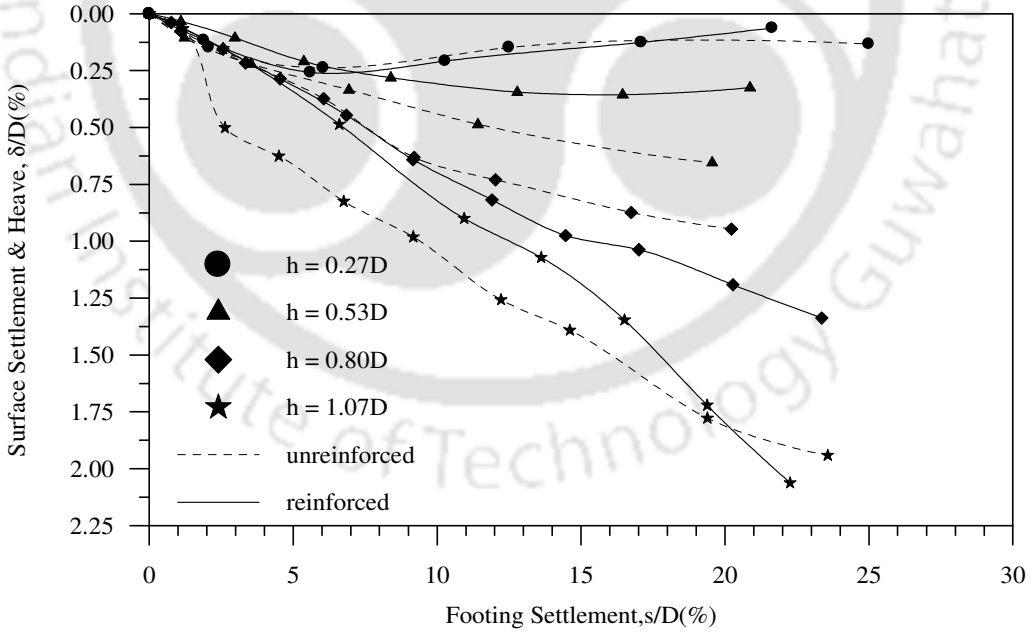

Fig. A1.41 Variation of average surface deformation with footing settlement at a distance x = D from the centre of the footing, for different for different heights (h) of geocell mattress –Test Series A2 - A5, D1, E1, F1, G1, ID = 35%, d = 1.2D

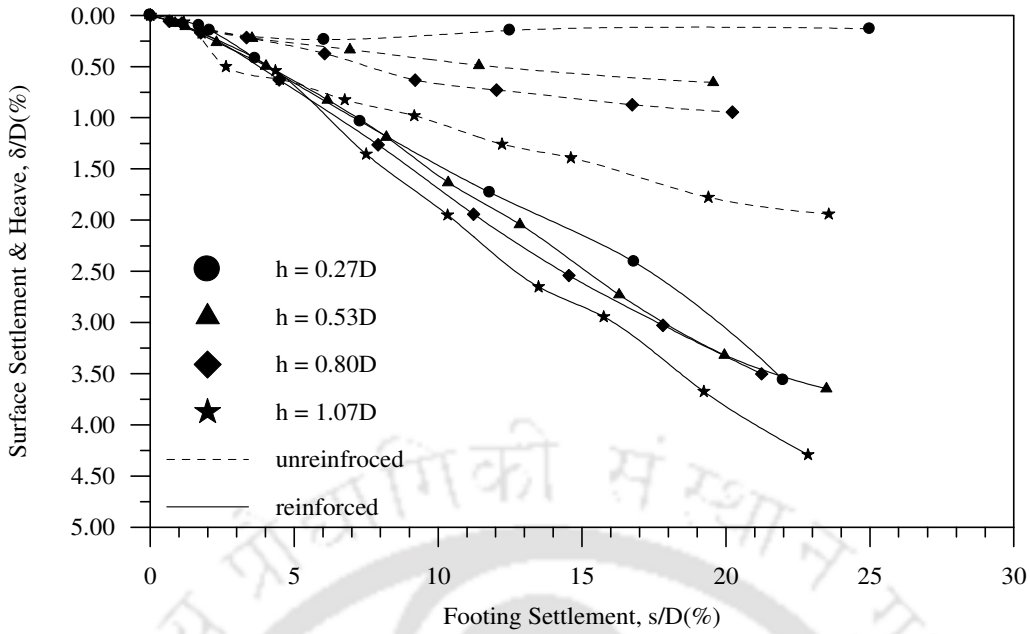

Fig. A1.42 Variation of average surface deformation with footing settlement at a distance x = D from the centre of the footing, for different for different heights (h) of geocell mattress – Test Series A2 - A5, D1, E1, F1, G1, ID = 35%, d = 0.4D

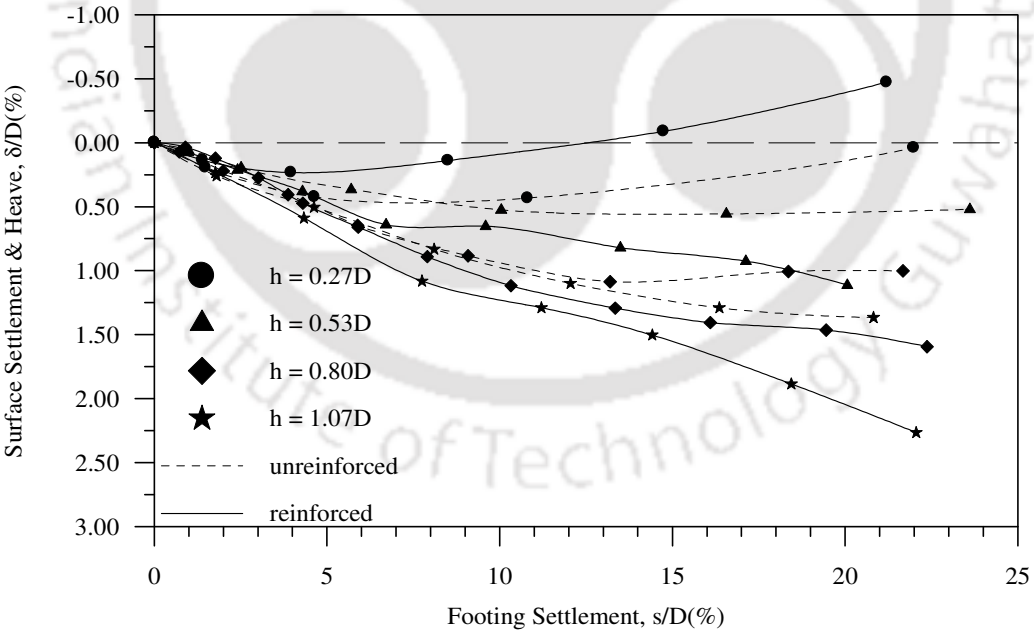

Fig. A1.43 Variation of average surface deformation with footing settlement at a distance x = D from the centre of the footing, for different for different heights (h) of geocell mattress – Test Series A2 - A5, D2, E2, F2, G2, ID = 50%, d = 1.2D

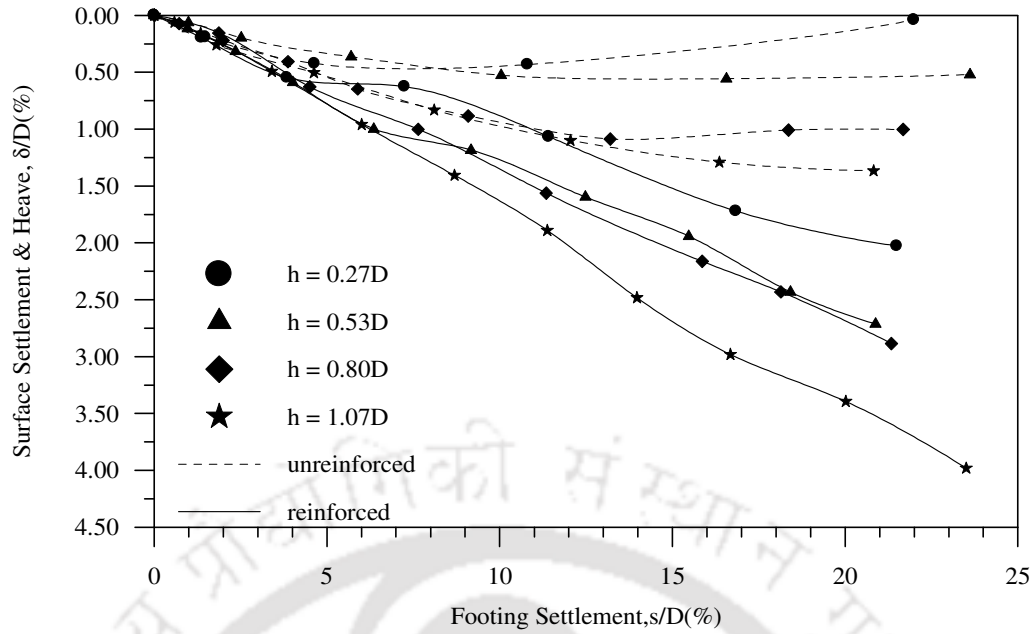

Fig. A1.44 Variation of average surface deformation with footing settlement at a distance x = D from the centre of the footing, for different for different heights (h) of geocell mattress – Test Series A2 - A5, D2, E2, F2, G2, ID = 50%, d = 0.8D

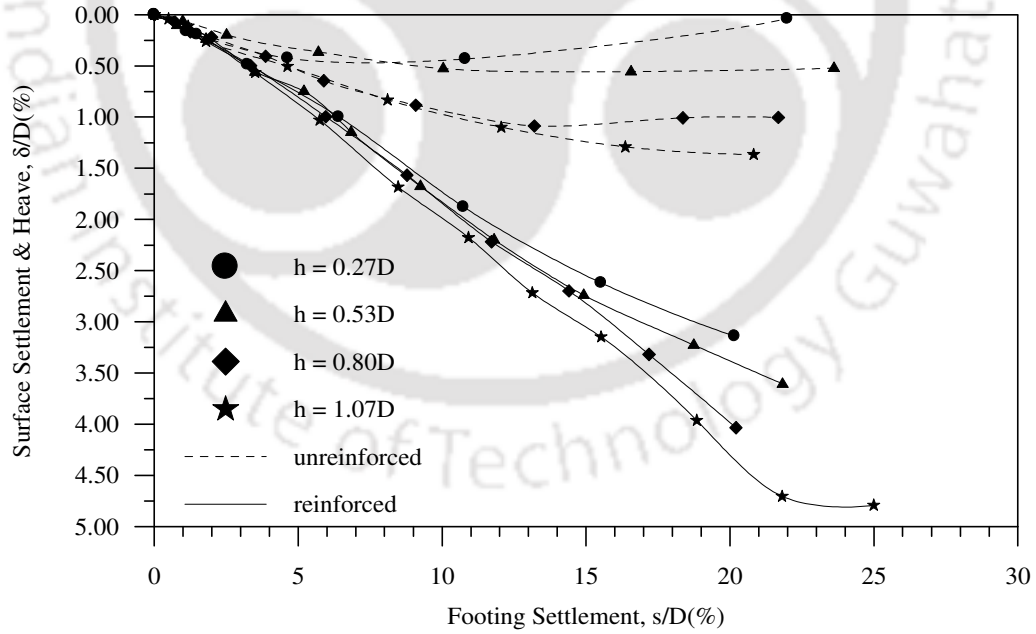

Fig. A1.45 Variation of average surface deformation with footing settlement at a distance x = D from the centre of the footing, for different for different heights (h) of geocell mattress – Test Series A2 - A5, D2, E2, F2, G2, ID = 50%, d = 0.4D

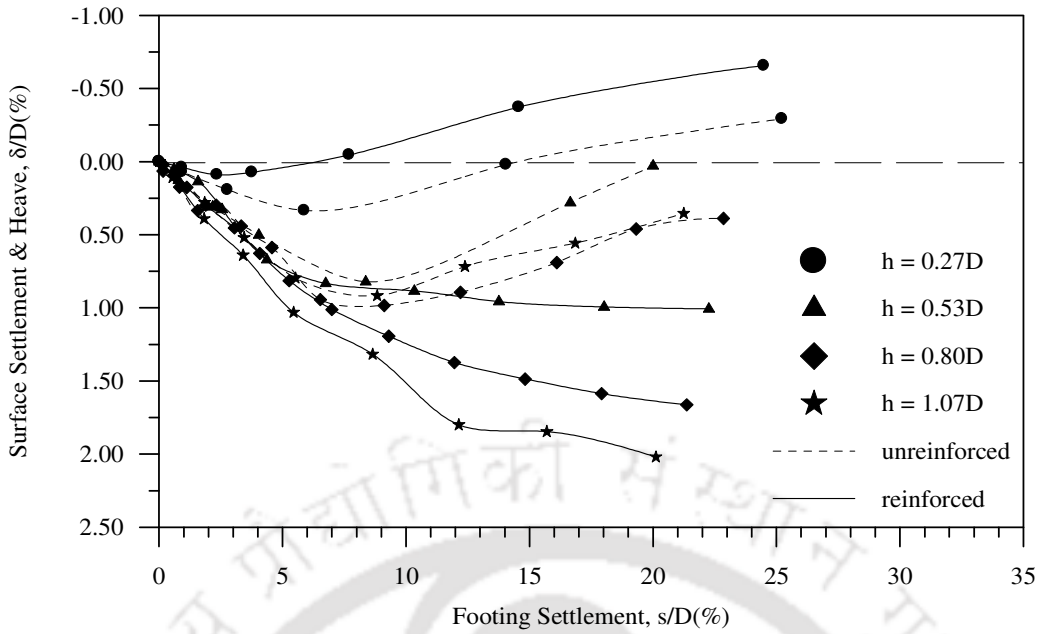

Fig. A1.46 Variation of average surface deformation with footing settlement at a distance x = D from the centre of the footing, for different for different heights (h) of geocell mattress - Test Series A2 – A5, D3, E3, F3, G3, ID = 80%, d = 1.2D

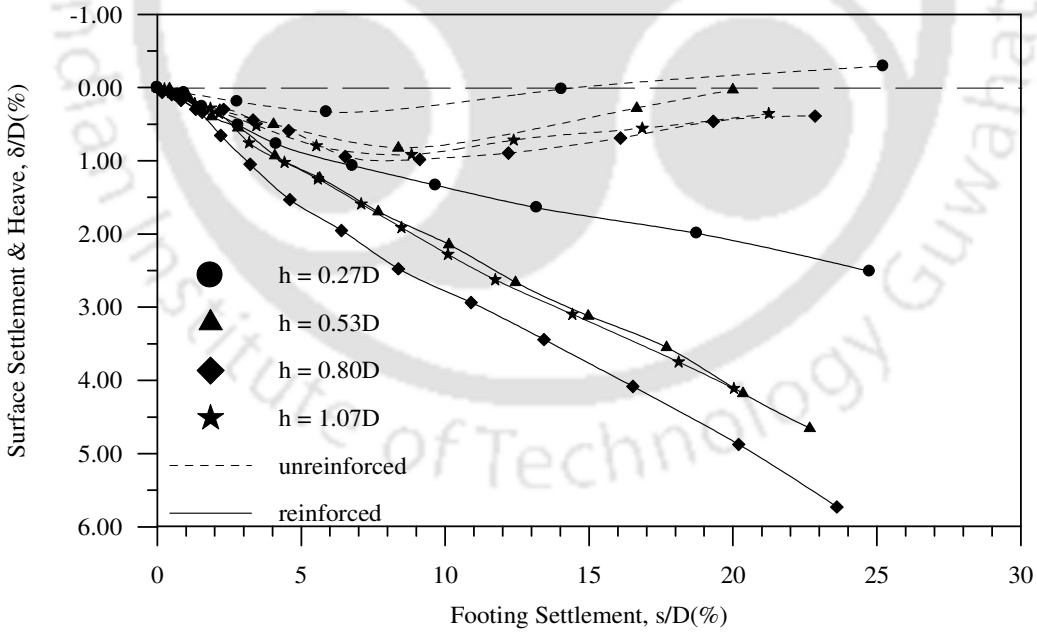

Fig. A1.47 Variation of average surface deformation with footing settlement at a distance x = D from the centre of the footing, for different for different heights (h) of geocell mattress – Test Series A2 – A5, D3, E3, F3, G3, ID = 80%, d = 0.4D

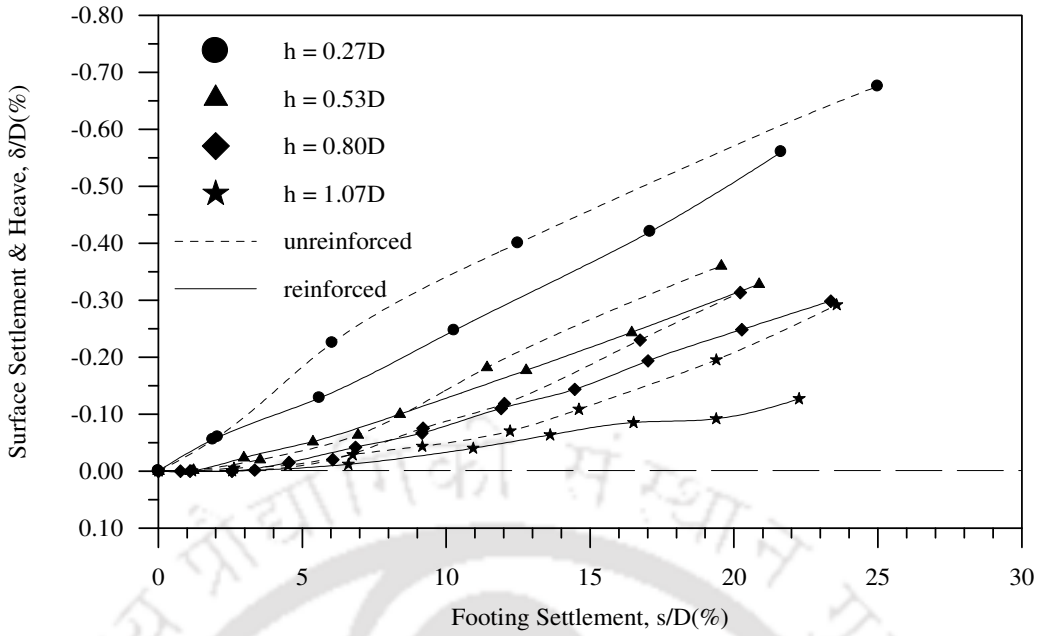

Fig. A1.48 Variation of average surface deformation with footing settlement at a distance x = 2D from the centre of the footing, for different for different heights (h) of geocell mattress – Test Series A2 - A5, D1, E1, F1, G1, ID = 35%, d = 1.2D

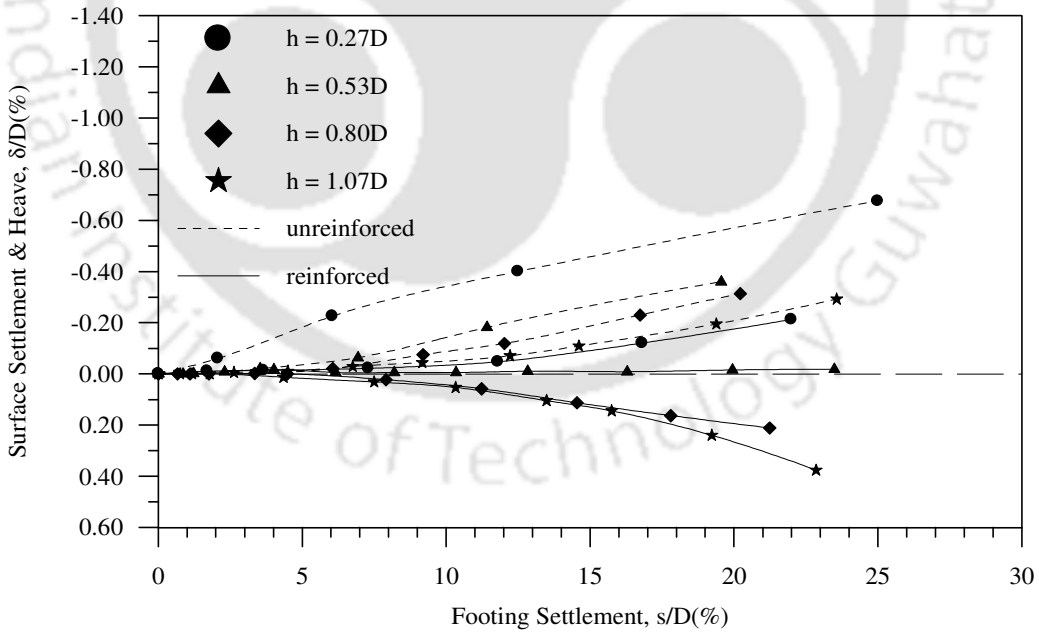

Fig. A1.49 Variation of average surface deformation with footing settlement at a distance x = 2D from the centre of the footing, for different for different heights (h) of geocell mattress – Test Series A2 - A5, D1, E1, F1, G1, ID = 35%, d = 0.4D

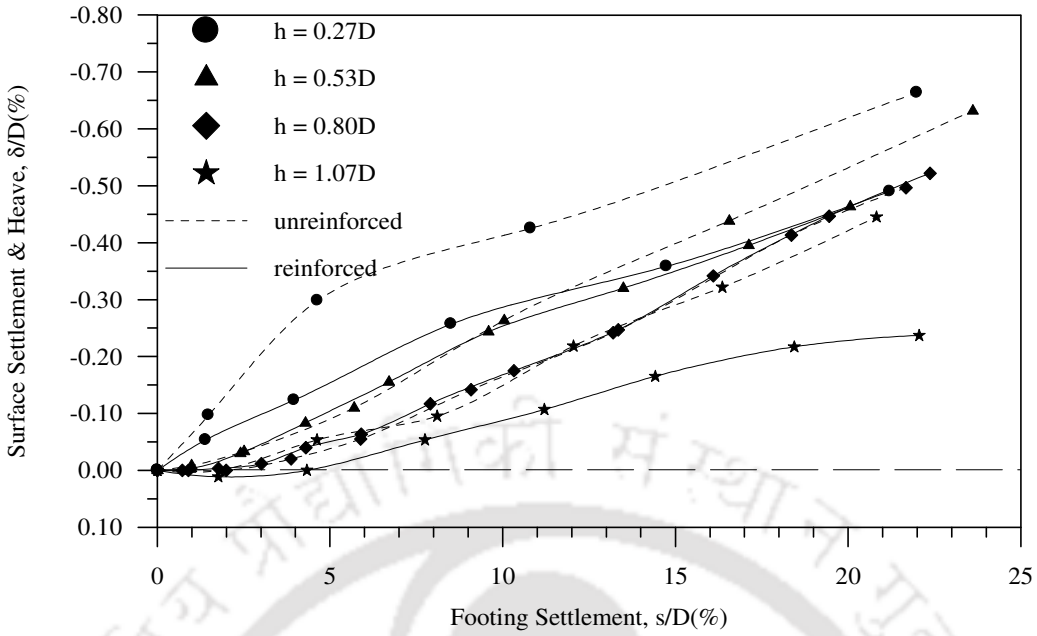

Fig. A1.50 Variation of average surface deformation with footing settlement at a distance x = 2D from the centre of the footing, for different for different heights (h) of geocell mattress – Test Series A2 - A5, D2, E2, F2, G2, ID = 50%, d = 1.2D

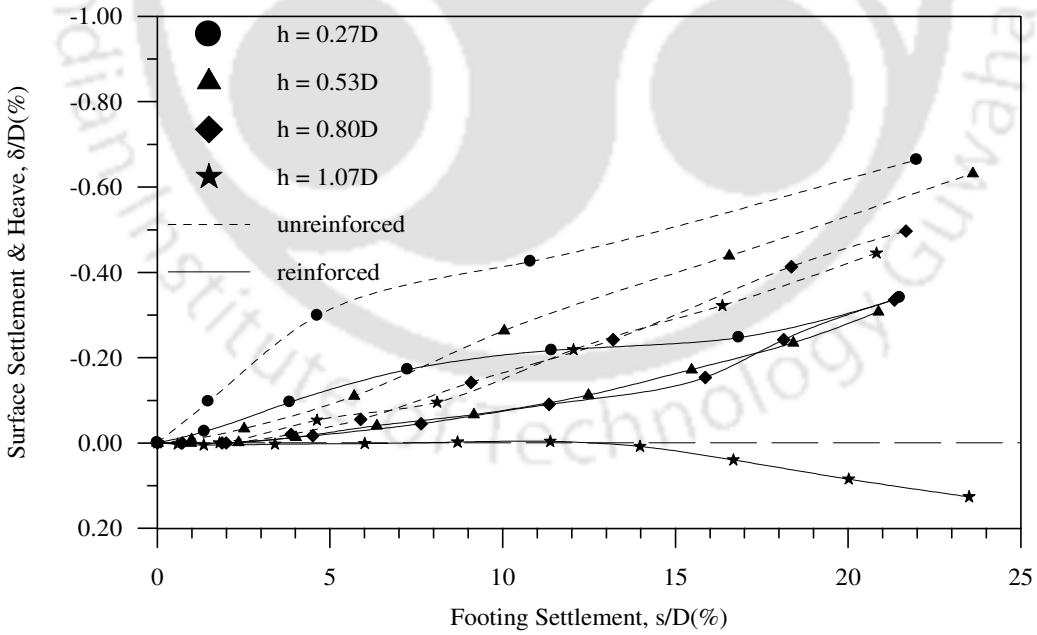

Fig. A1.51 Variation of average surface deformation with footing settlement at a distance x = 2D from the centre of the footing, for different for different heights (h) of geocell mattress – Test Series A2 - A5, D2, E2, F2, G2, ID = 50%, d = 0.8D

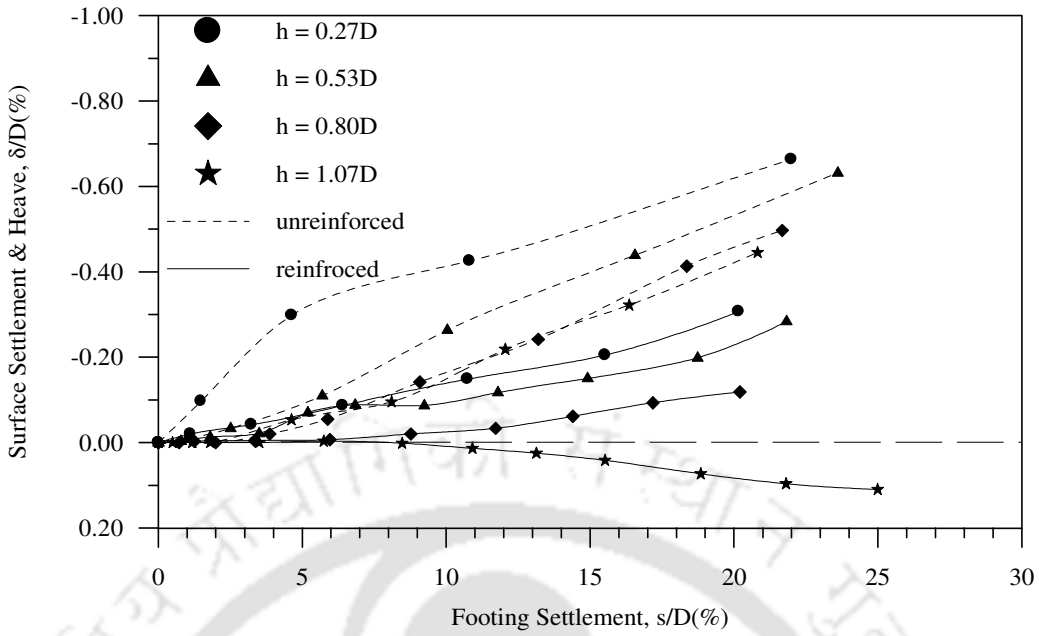

Fig. A1.52 Variation of average surface deformation with footing settlement at a distance x = 2D from the centre of the footing, for different for different heights (h) of geocell mattress – Test Series A2 - A5, D2, E2, F2, G2, ID = 50%, d = 0.4D

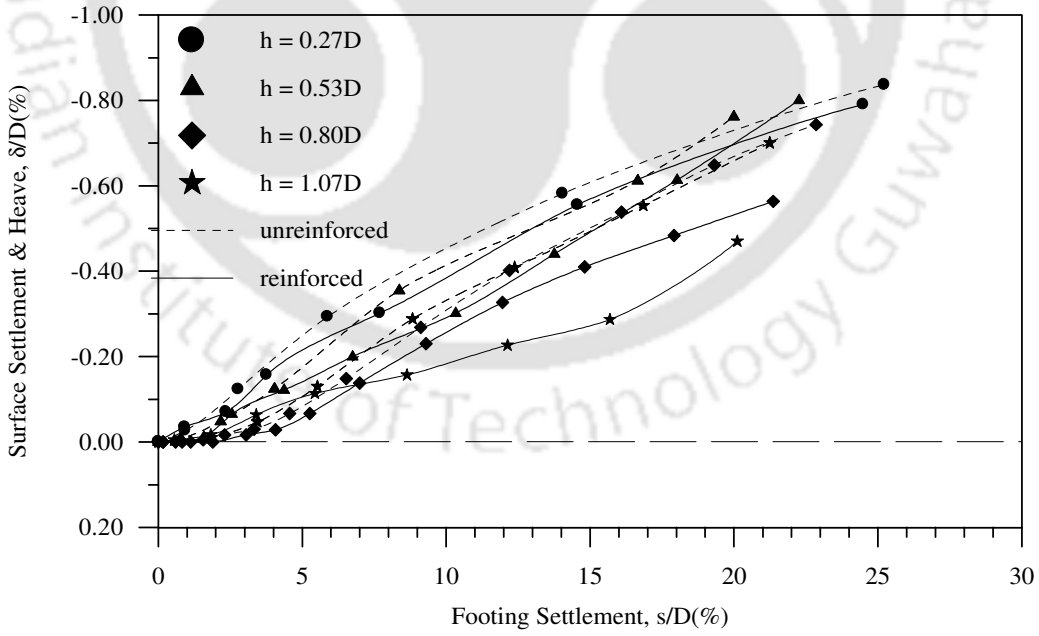

Fig. A1.53 Variation of average surface deformation with footing settlement at a distance x = 2D from the centre of the footing, for different for different heights (h) of geocell mattress – Test Series A2 - A5, D3, E3, F3, G3, ID = 80%, d = 1.2D

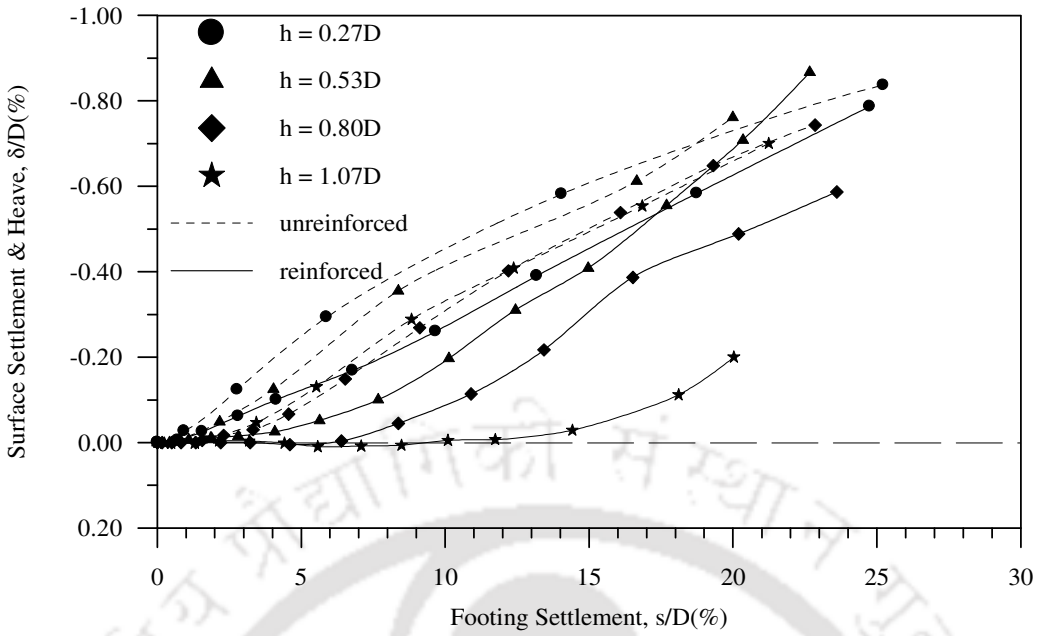

Fig. A1.54 Variation of average surface deformation with footing settlement at a distance x = 2D from the centre of the footing, for different for different heights (h) of geocell mattress – Test Series A2 - A5, D3, E3, F3, G3, ID = 80%, d = 0.4D

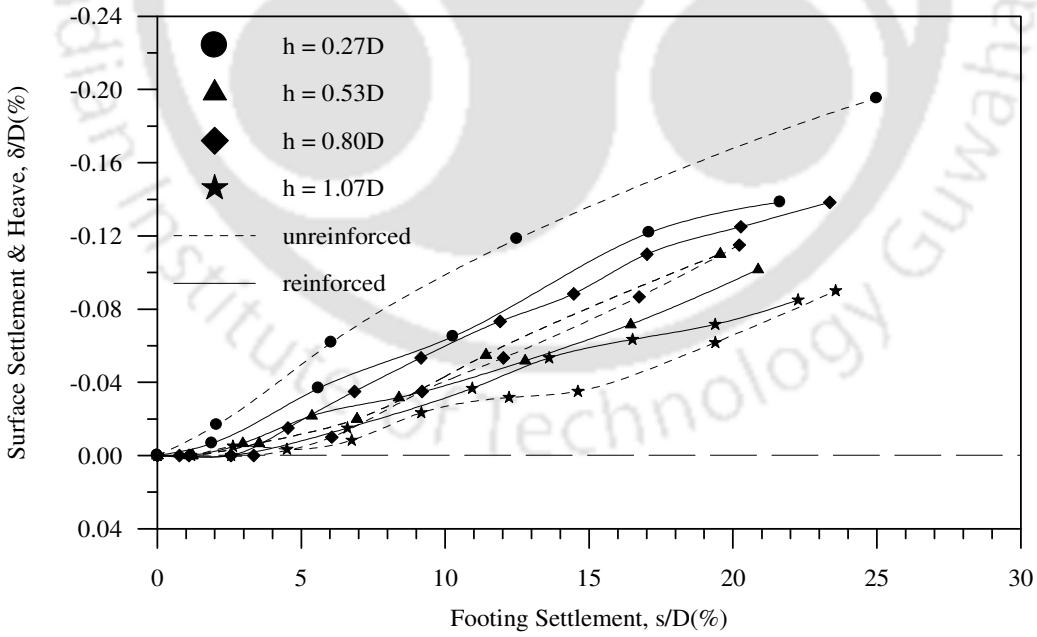

Fig. A1.55 Variation of average surface deformation with footing settlement at a distance x = 3D from the centre of the footing, for different for different heights (h) of geocell mattress – Test Series A2 - A5, D1, E1, F1, G1, ID = 35%, d = 1.2D

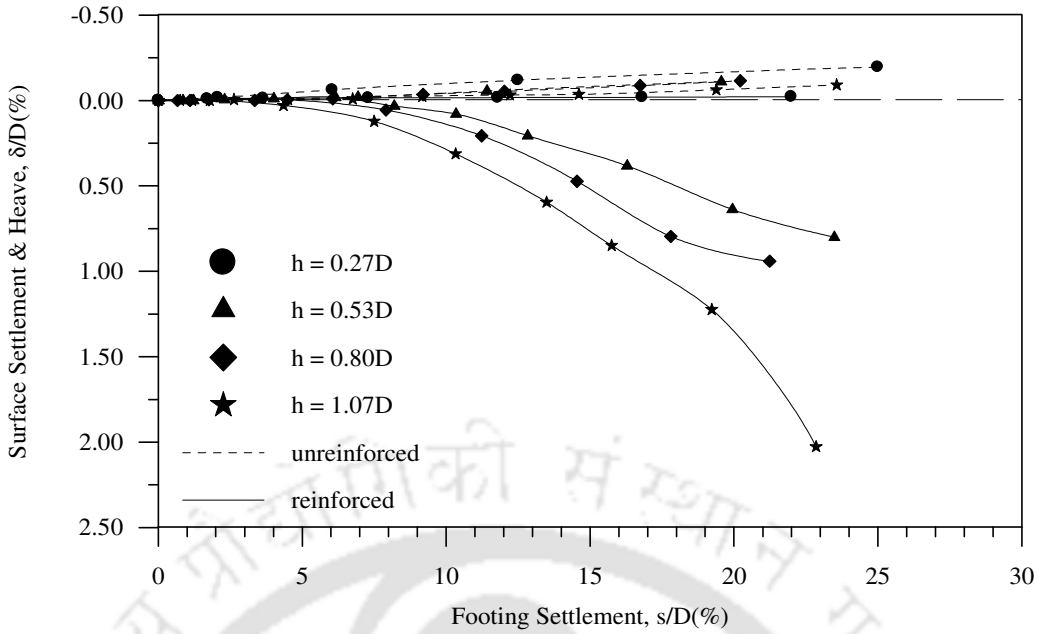

Fig. A1.56 Variation of average surface deformation with footing settlement at a distance x = 3D from the centre of the footing, for different for different heights (h) of geocell mattress –Test Series A2 - A5, D1, E1, F1, G1, ID = 35%, d = 0.4D

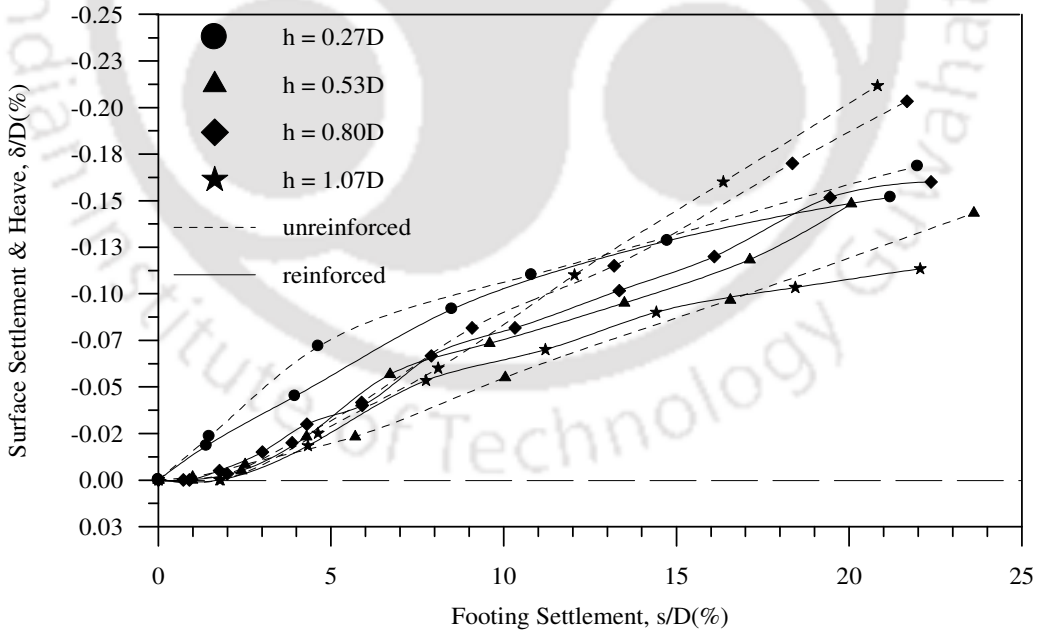

Fig. A1.57 Variation of average surface deformation with footing settlement at a distance x = 3D from the centre of the footing, for different for different heights (h) of geocell mattress –Test Series A2 - A5, D2, E2, F2, G2, ID = 50%, d = 1.2D

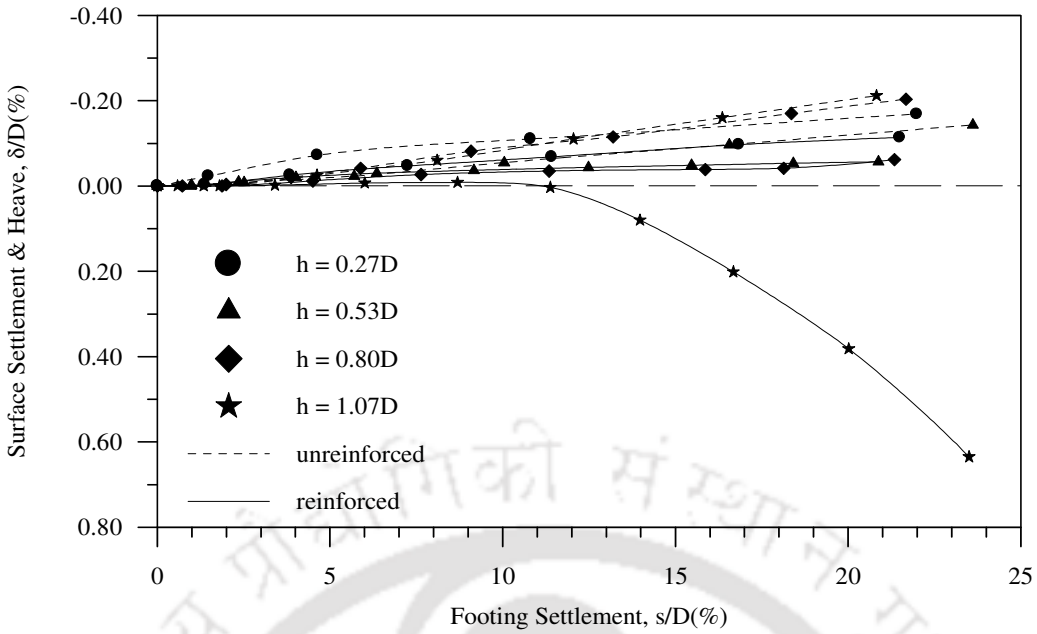

Fig. A1.58 Variation of average surface deformation with footing settlement at a distance x = 3D from the centre of the footing, for different heights (h) of geocell mattress – Test Series A2 - A5, D2, E2, F2, G2, ID = 50%, d = 0.8D

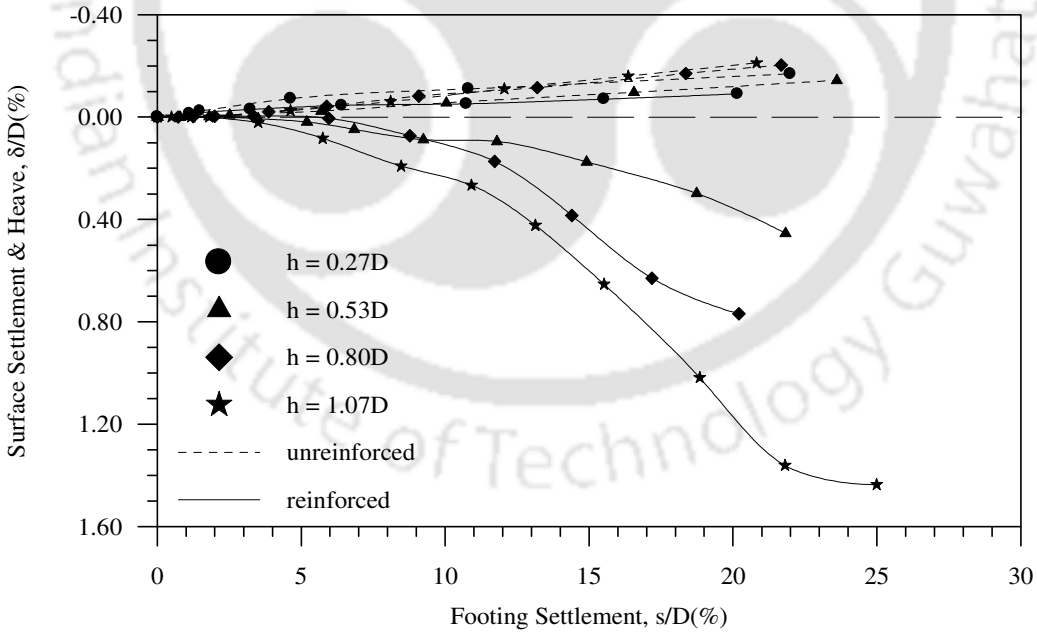

Fig. A1.59 Variation of average surface deformation with footing settlement at a distance x = 3D from the centre of the footing, for different for different heights (h) of geocell mattress –Test Series A2 - A5, D2, E2, F2, G2, ID = 50%, d = 0.4D

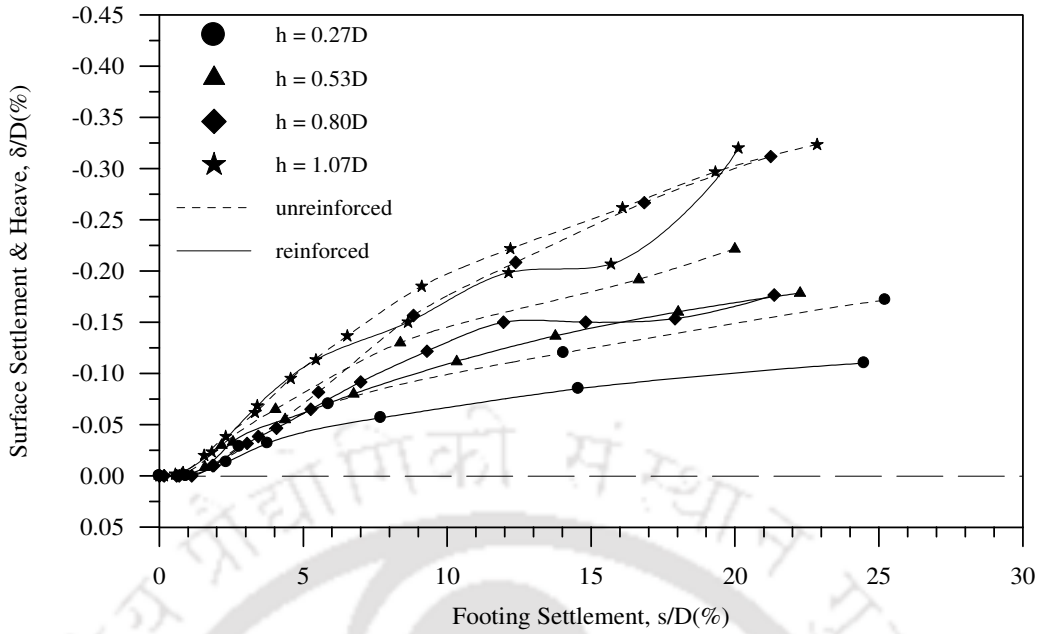

Fig. A1.60 Variation of average surface deformation with footing settlement at a distance x = 3D from the centre of the footing, for different for different heights (h) of geocell mattress - Test Series A2 – A5, D3, E3, F3, G3, ID = 80%, d = 1.2D

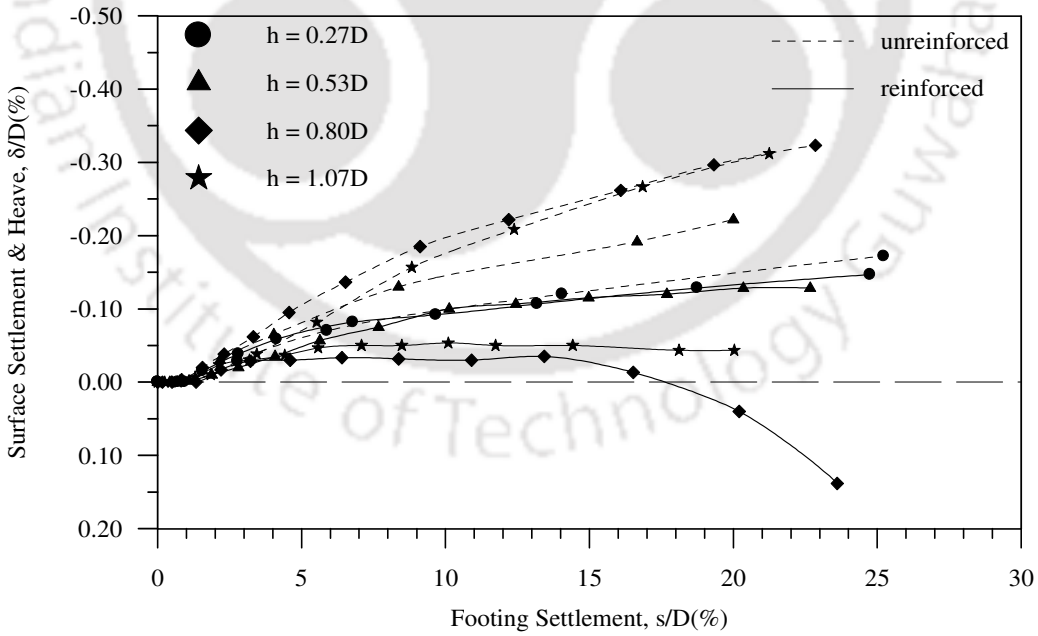

Fig. A1.61 Variation of average surface deformation with footing settlement at a distance x = 3D from the centre of the footing, for different for different heights (h) of geocell mattress - Test Series A2 – A5, D3, E3, F3, G3, ID = 80%, d = 0.4D

APPENDIX - A2

The test for significance in the case of multiple linear regression analysis is carried out using the analysis of variance (ANOVA). A typical ANOVA table is shown in Fig. A2.1. The explanations of all the statistical terms in the table are presented in this section.

Table A2.1 Typical ANOVA table for regression.

Regression Statistics					
Multiple R	0.9827				
R Square	0.9657				
Adjusted R Square	0.9656				
Standard Error	0.0608				
Observations (n)	325				
ANOVA	*Df (degree of Freedom)*	*SS(sum of squares)*	*MS(Mean Squares)*	*F*	*P-value*
Regression	k	SSR	MSR	F=MSR/MSE	
Residual	n-k-1	SSE	MSE		
Total	n-1	SST			
	Coefficients	*Standard Error*	*t Stat*	*P-value*	
Intercept	-0.039574804	0.015362295	-2.5760997	0.010436	
X Variable 1	1.021242247	0.010704826	95.4001703	1.1E-238	
X Variable 2	1.021242247	0.010704826	95.4001703	1.1E-238	

Where, n = number of observations in a sample, k = number of variables.

Sum of squares due to regression

$$SSR = \sum_{i}^{i=n} (\hat{y}_i - \bar{y})^2$$

Sum of squares due to error

$$SSE = \sum_{i}^{i=n} (y_i - \hat{y}_i)^2$$

Total some of squares

$$SST = \sum_{i}^{i=n} (y_i - \bar{y})^2$$

Where, $\hat{y}_i$ are the predicted values, $\bar{y}$ is the mean of the dependent variables.

Further, there exists a relationship between the sums of squares: $SST = SSR + SSE$

Mean square due to regression

$$MSR = \frac{SSR}{k}$$

Mean square due to error

$$MSE = \frac{SSE}{n-k-1}$$

Goodness of Fit Statistics

A measure of how well the regression model fits the data can be expressed through multiple coefficient of determination (R^2) which is expressed as

$$R^2 = 1 - \frac{SSE}{SST}$$

The value of R^2 ranges from 0 to 1. The closer the value is to 1, the better the fit. Sometimes the value of R^2 can be increased simply by adding more independent variables. This shortcoming can be overcome by using the adjusted R^2, a version of R^2 which attempts to reduce the inflation in R^2 by taking into account the number of independent variables.

The adjusted R^2 can be expressed as

$$R_a^2 = 1 - \frac{MSE}{MST}$$

The Standard Error (E_s) of a regression is a measure of its variability. The smaller the value of the standard error, the better is the fit. The estimate of the standard deviation of the regression model is given by

$$E_s = \sqrt{\frac{SSE}{n-k-1}} = \sqrt{MSE}$$

Tests of Significance

The F-test is carried out to test the overall significance of the regression model. It determines if at least one of the independent variable is able to explain the variation of dependent variable. The null hypothesis (H_O) for the F test is that all the regression coefficients c_1, c_2.....c_k are equal to zero, i.e. H_O: c_1, c_2.....c_k = 0. The alternative hypothesis (H_A) states that at least one of the values of c_i is non zero i.e. H_A: at least one $c_i \neq 0$. The calculated value of F is the ratio of mean square of regression to mean square of error.

$$F_{cal} = \frac{MSR}{MSE}$$

The decision rule for F test is

Accept H_O if $F_{cal} \leq F_{crt(k, n-k-1)}$

Reject H_O if $F_{cal} > F_{crt(k, n-k-1)}$

Where, F_{crt} can be obtained from the statistical table for a given degree of freedom (k, n-k-1) and level of significance 'α'. The acceptance of a null hypothesis (H_O) means that none of the independent variables are able to explain the variation in dependent variable.

The alternate hypothesis (H_A) suggests that at least one of the independent variables is able to explain the variation in dependent variable.

The t-test is used to check the significance of individual regression coefficients in the regression model. The hypothesis statements to test the significance of an individual regression coefficient, c_i, are null hypothesis, H_O: $c_i = 0$ and alternative hypothesis, H_A: $c_i \neq 0$. For the analysis, the t value can be calculated as

$$t_i = \frac{c_{i-0}}{E_{si}}$$

The decision rule for t test is

Accept H_O if $\quad - t_{crt(n-k-1)} \leq t_{cal} \leq t_{crt(n-k-1)}$

Reject H_O if $\quad t_{cal} > t_{crt\ (n-k-1)}$ or $t_{cal} < - t_{crt(n-k-1)}$

Where, t_{crt} can be obtained from the statistical table for a given degree of freedom (n-k-1) and level of significance 'α/2'. The null hypothesis for a t-test implies that the independent predictor variable is not related to the response variable. The rejection of the null hypothesis means that all the predictor variables are related to the response variable.

The significance level of a statistical hypothesis test is a fixed probability of wrongly rejecting the null hypothesis H_0, if it is in fact true. It is usually denoted by the symbol 'α'.

The P-value, attempts to provide a measure of the strength of the results of a test. The smaller it is, the more convincing is the rejection of the null hypothesis. It indicates the strength of evidence for say, rejecting the null hypothesis H_O, rather than simply concluding 'reject H_O' or 'do not reject H_O'. One may combine the P-value with the significance level (α) to make decision on a given test of hypothesis. In such a case, if the P-value is less than 'α' then you reject the null hypothesis.